Characterisation of Quiescin-Sulfhydryl Oxidase and Nematode Astacin mutants using functional studies in *Caenorhabditis elegans.*

Andrew J. Birnie

Institute of Comparative Medicine,
Faculty of Veterinary Medicine,
University of Glasgow.

Submitted for degree of Doctor of Philosophy at the University of Glasgow

December 2007

Declaration

The work presented in this thesis was performed entirely by the author except where indicated. This thesis contains unique work and will not be submitted for any other degree, diploma or qualification at any other university.

Andrew J. Birnie, December 2007

Acknowledgments

Firstly I wish to thank my supervisor, Tony Page, for his enthusiasm, encouragement, honesty, guidance, ideas and above all his untiring patience, and who gave me the chance to undertake this project. Tony, thank you.

The following people are thanked for their kind provision of reagents and materials: M. Wayne Davis for the pWD100.4 construct, Iain Johnstone for the anti-DPY-7 antibodies and staged cDNA samples, Andy Fire for the pPD series of vectors, the CGC for nematode strains and Julie Ahringer for the RNAi library. NBP Japan is also thanked for provision of mutant nematode strains. In addition, thank you to Gillian McCormack for her screening of the deletion library and isolation of the *qsox-1* mutant strain. Thanks also go to John Gilleard for providing the trichostrongylid parasites used during the course of this project.

I would also like to thank my assessors, Sylvain Eschenlauer and Colette Britton, for their stimulating discussions, reassurance and fervour. Thanks must also go to those people who have made my time in the lab very enjoyable; Alan, who proof read this thesis, always had time to answer my questions and who is a good man, Gill, Mel, Gillian, Victoria and to all the people who used to work on level 3 of the WCMP and to the Vet school staff and students. I don't think I will meet a better group of people for some time, thank you.

And to my friends, however distant now, Davie, Graham, Chris, Michael, Dave and the unstoppable Billy thank you. You all know me, and yet you remained humorous, dependable and above all people I could trust which means more to me than words on a page can convey. A special thank you must also be given to the Murphy family, who have always treated Fiona and I far better than we deserved, thank you.

And finally to my family Gran, Gramdpa, Mum and Fiona, my long suffering proof reading girlfriend who I love deeply, without whose support I could never have managed to get to where I am today. Above all the people thanked one has been my greatest supporter, given so much and asked so little in return and I'm sure has done more for me than I will ever know, my Mother, to whom I dedicate this thesis, thanks Mum.

Table of Contents

List of Tables

List of Figures

Abstract

Nematodes, both free-living and parasitic, are dependant upon their Extra Cellular Matrix (ECM) for multiple aspects of functionality. Two distinct ECMs are present in *Caenorhabditis elegans*, the basement membrane and the cuticle. The cuticle of *C. elegans,* like other nematodes is composed largely of collagen-like proteins, with the trimeric collagenous proteins forming approximately 80% of the cuticle. Cuticle collagens are believed to be highly processed in a manner similar to vertebrate collagen maturation, with collagens being; co-translationanly modified, folded into triple helices and proteolytically cleaved at the C- and N- termini. Cross-linking of mature triple helical collagens into higher order structures leads to the generation of a flexible yet robust cuticle. Disulphide bonding is crucial in the formation of the cuticle, with cysteine cross-linking mutants having been shown to produce severely disrupted cuticles and associated lethal phenotypes. During the life cycle, *C. elegans* progresses through four moults during which a new cuticle is synthesised and the old cuticle is shed. Moulting occurs by proteolytic digestion and shedding of an anterior cuticular cap which provides an opening for the nematode to escape the previous stage cuticle. Both free-living and parasitic nematodes shed and exsheath their cuticles in this manner.

Two distinct phases of cuticle processing become apparent: cuticle synthesis and cuticle degradation. Of the enzymes involved with processing of cuticular collagens, the quiescin sulfhydryl oxidases (QSOX), and the nematode astacins (NAS) are of particular interest with regard to cuticle synthesis and proteolytic cleavage of cuticular collagens respectively. QSOX have been shown to be linked directly to the generation of disulphide bonds, and have also been shown to associate with other essential proteins of cuticle formation, namely the protein disulphide isomerases. There are three distinct QSOX family members found within the *C. elegans* genome, which have been shown to temporally coincide with *lethargus* (cuticle synthesis) and have been proven to spatially localise to the *C. elegans* hypodermis, the tissue responsible for cuticle secretion. Characterisation of *qsox* mutants reveals weak cuticular phenotypes when disrupted singly; but, in combination, silencing of *qsox-1* and *qsox-2* resulted in blistered cuticles and lethality, by RNA mediated interference and double knockouts respectively. This demonstrates the essential nature of the cuticle associated QSOX enzymes, and to my knowledge represents the first loss-of-function mutant in a QSOX enzyme.

Investigation of the NAS enzymes focused on the group V astacins, members of which exhibit the only notable defects associated with disruption of *C. elegans nas* genes, namely: dumpy body shape, *nas-35/dpy-31*; hatching, *nas-34/hch-1*; and moult defects, *nas-36* and *37*. With regard to proteolytic degradation of cuticular components, NAS-36 and NAS-37 were of specific interest as mutants resulted in moult defective nematodes unable to digest and fully escape their previous stage cuticles; in addition, spatial expression illustrated an association of these gene products with regions of cuticle attachment and degradation. *C. elegans* NAS-36 and NAS-37 were also shown to digest isolated L3(2M) trichostrongylid cuticles of parasites of veterinary importance, suggesting that the metalloprotease and cuticle substrates involved in exsheathment is conserved between trichostrongylid and free-living nematodes. Conservation is poor between ecdysozoan and non-moulting organisms, meaning that proteins such as NAS-36 and 37 could become specific novel targets for anti-nematode drug development.

List of Abbreviations

ALR	augmenter of liver regeneration
Arg	arginine
Asn	asparagine
Bli	blister
Bmd	body morphology defect
BMP	bone morphogenic protein
Ca^{2+}	calcium
COL	collagen
Cys	cysteine
DIC	differential interference contrast
DNA	deoxyribonucleic acid
Dpy	dumpy
ds	double stranded
DUOX	dual oxidase
ECM	extracellular matrix
EGF	epidermal growth factor
Egl	egg laying defective
Eml	embryonic lethal
EMS	ethyl methanesulphonate
ER	endoplasmic reticulum
EST	expressed sequence tag
F1	first filial
FACIT	fibril-associated collagens with interrupted triple helices
GFP	green fluorescent protein
Gly	glycine
H_2O_2	hydrogen peroxide
His	histidine
HPX	animal haem peroxidase
HSP	heat shock protein
Let	lethal
Lon	long
Lvl	larval lethal
Mlt	moult defect
mRNA	messenger ribonucleic acid
NAS	nematode astacin
NHR	nuclear hormone receptor
OD	optical density
PAGE	polyacrylamide gel electrophoresis
PCP	pro-collagen C-proteinase
PCR	polymerase chain reaction
PDI	protein disulphide isomerase
PHY/P4H	prolyl 4-hyroxlylase
PPI	peptidyl prolyl *cis-trans* isomerase
QSOX	quiescin-sulfhydryl oxidase
RNA	ribonucleic acid
RNAi	RNAi-mediated interference
Rol	roller
ROS	reactive oxygen species
RT-PCR	reverse transcription polymerase chain reaction

SEM	scanning electron microscopy
SL	splice leader
Sma	small
SNP	single nucleotide polymorphism
Sqt	squat
ss	single stranded
Tet	tetracycline
TEM	transmission electon microscopy
TGase	transglutaminase
TGF-β	transforming growth factor-β
ts	temperature sensitive
TSP	thrombospondin
Tyr	tyrosine
Unc	uncoordinated
UV	ultraviolet
YAC	yeast artificial chromosome
Zn^{2+}	zinc

Measurements

bp	base pair
cm	centimetre
kb	kilobase
kDa	kilodalton
Mb	megabase
mg	milligram
µg	microgram
ng	nanogram
mm	millimetre
µm	micrometer
nm	nanometer
L	litre
ml	millilitre
µl	microlitre
M	molar
mM	millimolar
µM	micromolar
nM	nanomolar
µmol	micromoles
nmol	nanomoles
pmol	picomoles
nm	nanometer
V	volts
rpm	revolutions per minute
g	acceleration due to gravity
Gy	greys

Chapter 1: General Introduction.

1.1 *Caenorhabditis elegans* as a model organism

Caenorhabditis elegans belongs to the phylum Nematoda, or round worms, a large and diverse group of organisms. Estimates of between 100,000 to 1 million described species (Parkinson *et al.,* 2004) place the nematodes as one of the most species rich phyla in the Kingdom Animalia. Nematodes are recognised as perhaps the most significant metazoan parasite associated with humans. Of the species defined approximately 15,000 have been found to be parasitic; however, most nematodes are free-living, not parasitic, and cover a wide range of aquatic (marine and freshwater) and terrestrial habitats. The marine habitat hosts the largest known nematode *Placentonemea gigantissima,* a parasite of the sperm whale placenta which measure approximately 8m in length and 2.5cm in diameter.

Many free-living nematodes are detritivores or decomposers, others, such as *C. elegans,* are bacteriovores and most are useful in recycling chemicals and organic nutrients. However, many are not beneficial with plant parasites able to wipe out entire crops in a single season. Nematodes are also able to infect almost all phyla of animals, the effects of which can be far from advantageous. These parasitic nematodes can be difficult to study *in vitro* due to the lack of suitable host strains. As such *C. elegans* with its ease of *in vitro* culture is becoming adopted as a model organism for parasitology (Gilleard, 2004; Britton and Murray, 2006; Murray *et al.,* 2007). Phylogenetic classification, using small subunit ribosomal RNA (SSU rRNA) sequences (Parkinson *et al.,* 2004), places *C. elegans* within the family Rhabditidae; clade V of the cladogram which represents the nematode species, see Figure 1.1. Clade V also contains many veterinary important parasites, for example: *Haemonchus contortus*, *Teladorsagia circumcincta*; and the human infective hookworms *Necator americanus* and *Ancylostoma ceylanicum*. Thus *C. elegans* is phylogenetically well placed as a model organism for such important parasites, assuming that members of the same clade are relatively well conserved.

C. elegans is a free-living nematode, with a typically vermiform structure and a life cycle which involves the transition through a number of larval stages, see Figure 1.2. In conditions of abundant food and low population numbers *C. elegans* develops through four larval stages (L1- L4) without pause, and mature into the adult form following the larval stages; however, a specialised alternate L3 life cycle stage termed dauer also exists. Dauer animals are particularly resilient and can survive for prolonged times without aging.

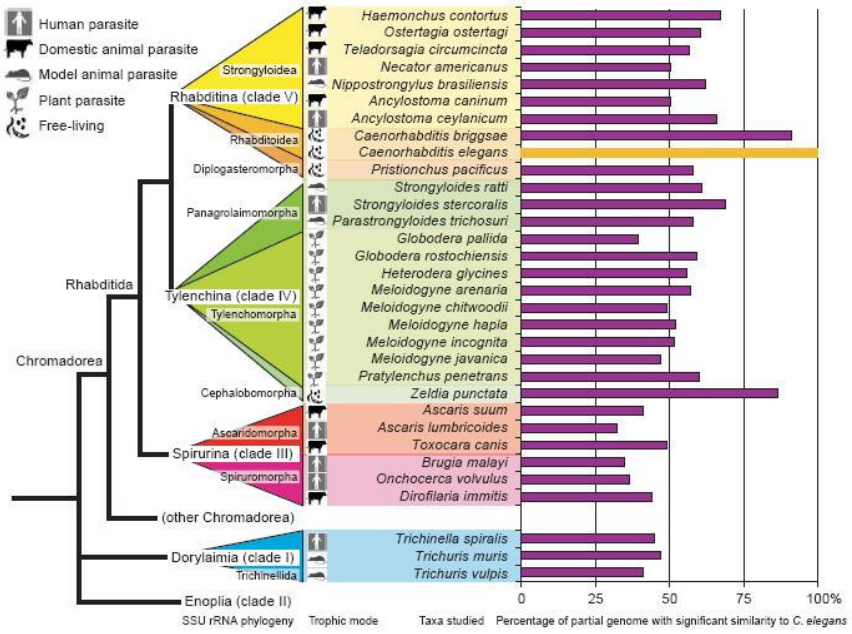

Figure 1.1: Phylogenetic map of selected nematode species showing the clade to which they belong (grouped by SSU rRNA sequence), tropic distribution and comparative similarity to the fully sequenced genome of *C. elegans*. Taken from (Parkinson *et al.,* 2004).

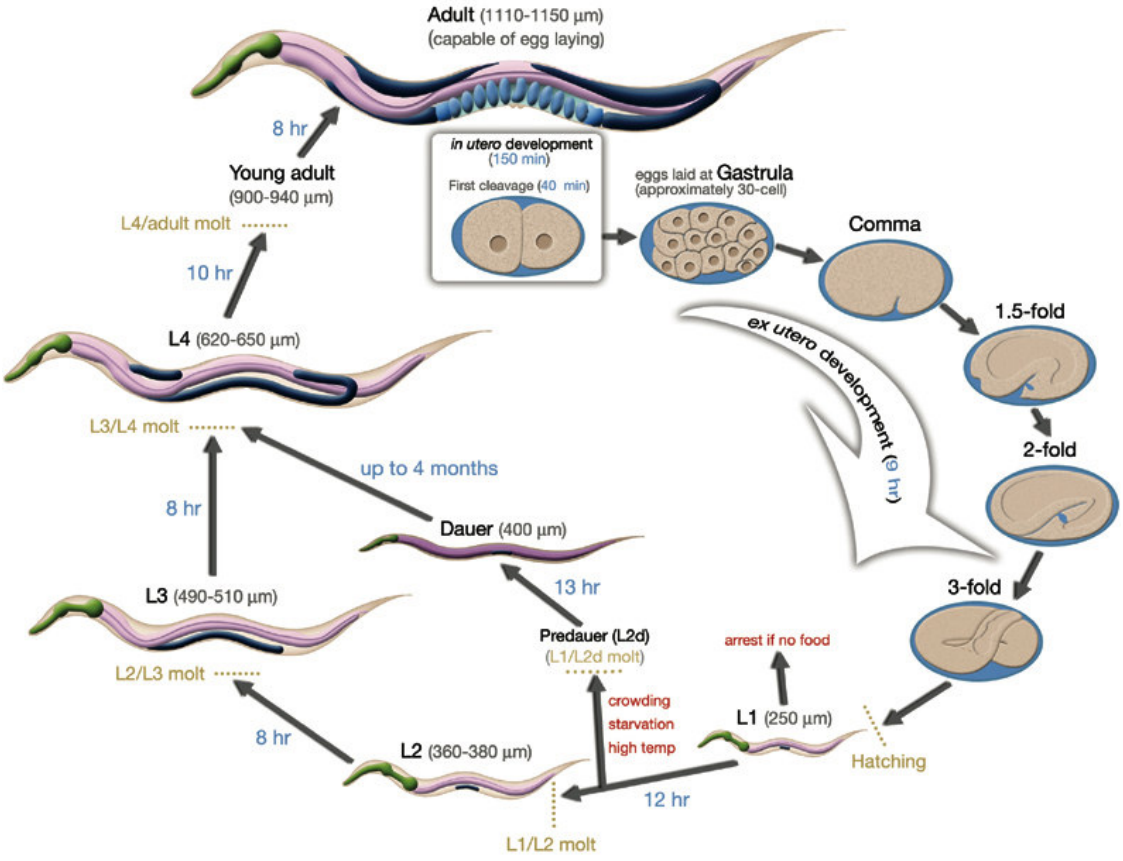

Figure 1.2: Diagrammatic representation of the *C. elegans* life cycle at 22ºC. Taken from http://www.wormatlas.org.

Triggers of the dauer stage include over population and shortage of a food source, inverse of these conditions will direct the dauer back to the normal life cycle, re-entering as an L4. Transitions from each stage are marked by moults, characteristic features of the Ecdysozoans and all nematodes. The Ecdysozoan clade was defined by the ability to moult and includes all animals that shed their exoskeleton such as the arthropods, tardigrades, onychophorans, nematodes, nematomorphs, kinorhynchs and priapulids (Aguinaldo *et al.,* 1997). Given constant temperatures and a ready supply of food timing of the moults is invariant.

C. elegans has a number of biological systems in common with higher eukaryotes such as: a nervous system, programmed cell death and a defined developmental body plan with a defined cell lineage (Sulston and Horvitz, 1977), *C. elegans* hermaphrodites and males containing an invariant number of somatic cells, 959 and 1031 respectively. Other useful traits of *C. elegans* which make it a suitable model organism include: a short three day life cycle; small overall size, adults are approximately 1mm in length; self fertilisation, allowing for large populations of genetically identical progeny to be produced from one animal; transparency; ease of growth, *C. elegans* being able to be grown in either liquid or solid medium when supplied with an *E. coli* food source; freeze tolerance; easily mutable, by treatment with chemicals or ionising radiation; relative ease of transgenic line generation, by microinjection (Mello *et al.,* 1991); ease of crossing (Brenner, 1974); and a fully sequenced and annotated genome (Consortium, 1998), available through www.wormbase.org. The genome contains 100Mb of sequence and roughly 20,000 genes dispersed over five pairs of autosomes and one pair of sex chromosomes (XX for hermaphrodites and XO for males). Of these genes ~40% have been shown to have high homology with both parasites and humans (Hashmi *et al.,* 2001; Kamath *et al.,* 2003; Parkinson *et al.,* 2004).

Publishing of the genome has resulted in many other resources becoming available such as: yeast artificial chromosomes (YACs) covering the entire genome, detailed single nucleotide polymorphism (SNP) maps (Swan *et al.,* 2002), an expressed sequence tag (EST) database, a bank of multiple alleles of mutant strains (*C. elegans* genetics centre) and two knockout consortia (the *C. elegans* Gene Knockout Consortium and the National Bioresource Project, Japan). These resources have allowed for comparative analysis of genomes, characterisation of single and double knockout mutants, identification of gene families by homology (e.g., the collagens) and functional genomic microarray experiments (Kim *et al.,* 2001). Access to the *C. elegans* genome has also simplified PCR primer design and construct generation (reporter, rescue, protein expression and RNAi for example).

RNA mediatated interference (RNAi) has become a cornerstone of research performed in *C. elegans*, by allowing for the specific targeting and silencing of a particular gene product (Fire *et al.,* 1998). RNAi is a fast and easy method of gene silencing; as such it has been used in many high-throughput screens (Maeda *et al.,* 2001; Kamath *et al.,* 2003; Simmer *et al.,* 2003). Silencing can be achieved by feeding, soaking, electroporation or injection of dsRNA, of these techniques injection is the most effective. A library of RNAi bacterial constructs representing 86% of the genome is available (Kamath *et al.,* 2003), and has been used in many screens with N2 and the RNAi hypersensitive *(rrf-3)* mutant strain (Kamath *et al.,* 2003; Simmer *et al.,* 2003). Targeted screens have also been performed seeking to find genes which have particular relevance to a specific process such as cell division (Gönczy *et al.,* 2000), increased life span (Lee *et al.,* 2003), embryogenesis (Sonnichsen *et al.,* 2005), altered genome stability (Pothof *et al.,* 2003) and moulting (Frand *et al.,* 2005). These screens have led to the isolation of key genes involved with many different essential developmental processes in *C. elegans.* Similarly in this project, RNAi was used to isolate candidate enzymes associated with cuticle synthesis and degradation. The enzymes involved in biogenesis, modification (co- and post-translational), cross-linking and cleavage of *C. elegans* cuticle components, such as collagen, have been repeatedly shown to be essential (Novelli *et al.,* 2004; Winter *et al.,* 2007; Winter *et al.,* 2007b) and conserved between other nematodes and vertebrates alike (Johnstone *et al.,* 1996b; Eschenlauer and Page, 2003).

1.2 Structure and function of the nematode extracellular matrix (ECM)

C. elegans has two distinct ECMs (Kramer, 1994): the hypodermally-secreted cuticle, and the basement membrane, which is secreted by muscles and organs (the basement membrane is discussed further in section 1.16). Together, these two ECMs define the borders of the two concentric tubes that make up the basic vermiform body structure.

The cuticle of the nematode is a complex matrix of proteins that covers the outermost surface of nematode hypodermal cells, pharynx and rectum (Cox *et al.,* 1981b; White, 1988; Kramer, 1994). The most abundant cuticle proteins are the collagens, which make up 80% of the cuticle (Cox *et al.,* 1981), and the non-collagenous cuticlins (Sebastiano *et al.,* 1991; Kramer, 1997). There are 175 collagen genes found in the *C. elegans* genome (Myllyharju and Kivirikko, 2004) and with the three-stranded nature of the mature collagen unit the potential for interactions between individual collagens exists. The

importance of individual collagens varies from non-essential to essential, for example, COL-19 and SQT-3 respectively (Thein *et al.,* 2003; Novelli *et al.,* 2006); thus, the correct processing of the essential collagens carries an inherently non-trivial burden

The nematode cuticular ECM is synthesised five times, once per life cycle stage with the synthesis phase being termed *lethargus,* due to the inactivity of the worm at this time. As the synthesis of a new cuticle takes place beneath an existing one, with the outer most cuticular layers being synthesised first and the inner layers last, there must also be an associated shedding of the previous overlying cuticle; this is termed *ecdysis*, and it occurs four times in the life cycle, see section 1.12 for more detail on moulting.

The structure of all nematode cuticles appears similar with regard to composition and overall structure, the most extensive characterisation being performed in *C. elegans* (Cox *et al.,* 1981). The cuticle is a multi-layered structure comprised of six discernable regions, from internal to external; basal layer, an amorphous layer overlying the hypodermal cells; two fibril layers, each fibre layer is in opposite orientation spiralling around the length of the worm; the medial layer, which is adult specific, fluid filled and contains the struts; the internal and external cortical layers, internal layer has no regular structure and is bounded by the external; and the outermost epicuticle (Cox *et al.,* 1981), Figure 1.3. The epicuticle is lipid-rich and this in turn is overlaid by a glycoprotein-rich surface coat (Page and Winter, 2003). Collagens form the basal, fibre, internal cortical layers and struts of the *C. elegans* cuticle. Cuticlin is located within the external cortical layer and a limited amount is found within the internal cortical layer (Cox *et al.,* 1981b). The non-collagenous cuticlin component is an insoluble, collagenase resistant material which endures following exposure of the cuticle to strong reducing agents and detergents (Cox *et al.,* 1981b). Cuticlin is found in all stages of larval development but is particularly a feature of the robust dauer stage (Cox *et al.,* 1981), which may contribute to the strength of this cuticle. Notable external features of the cuticle include the annulae, annular furrows and the lateral alae. Each annulus is a circumferential band (1.2µm wide) around the worm, with intervening annular furrows between each annulus, the furrows being caused by underlying actin bundles, see section 1.4. The lateral alae are stage specific structures which are only present in the L1, dauer and adult stages resembling symmetrical longitudinal ridges that run almost the entire length of the animal overlying the lateral hypodermal seam cells.

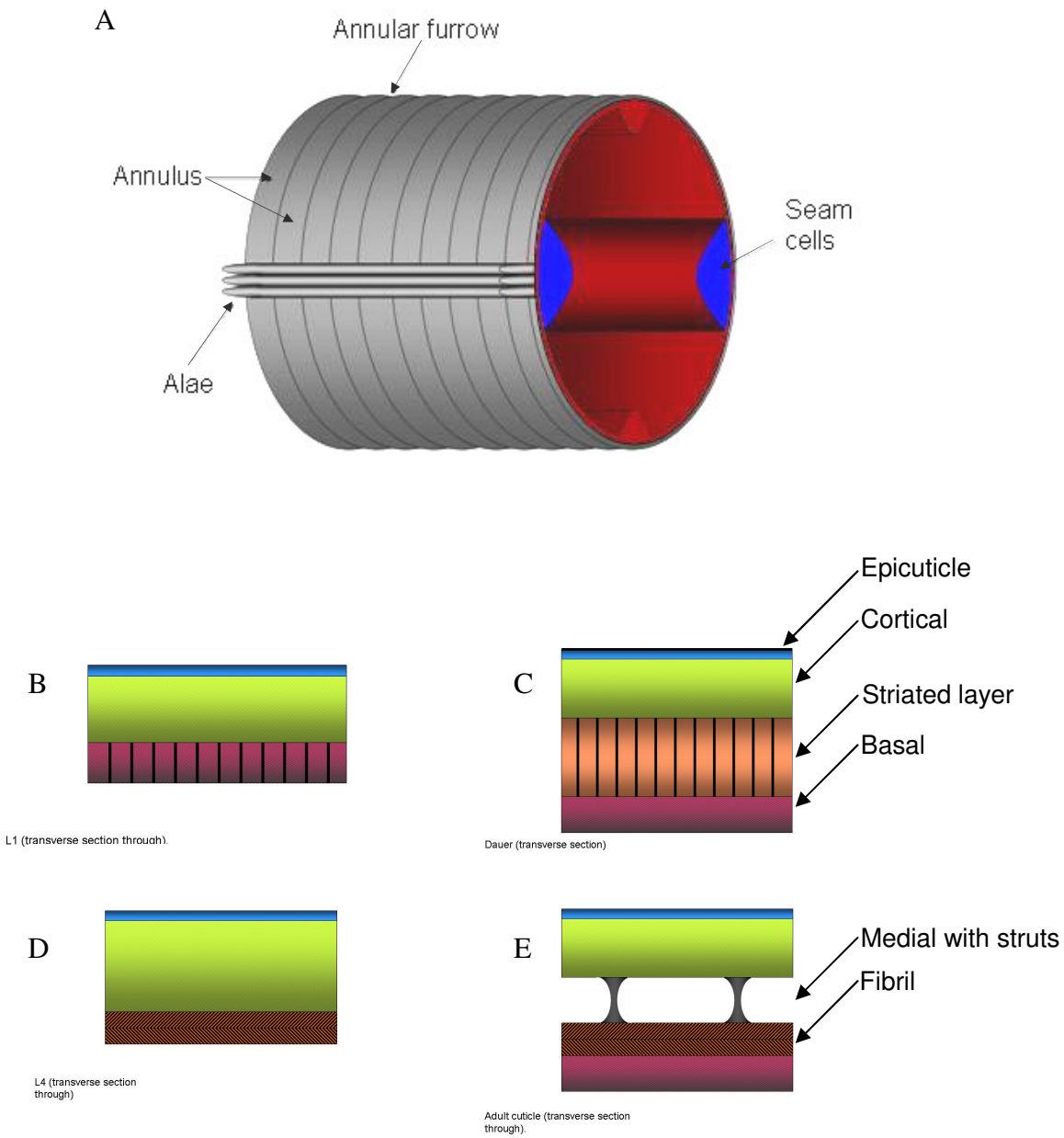

Figure 1.3: Diagrammatic representation of the *C. elegans* cuticle. (A) Shows a transverse section through an adult *C. elegans* cuticle. Visible are the annuli, the annular furrows the lateral alae and the underlying seam cells responsible for the lateral alae formation. (B, C, D and E) Show the differences between the various stages (L1, dauer, L4 and adult respectively) of *C. elegans* development and the associated differences of those particular stage cuticles. (D) The L4 cuticle is also representative of the L2 and L3 stages of development.

The L1 lateral alae adopts a tri-foil mushroom structure, the dauer a five fold and the adult a three fold structure (Singh and Sulston, 1978; Cox *et al.,* 1981b). The cuticular layers are also noted to vary in thickness and presence depending upon the developmental stage of the worm. For example, the medial layer is only found in adult worms, and the dauer and L1 stages have a striated layer, characterized by darkly staining bands of about 18nm periodicity, in place of a fibre layer. The dauer cuticle is also much thicker in relation to body length when compared to all other life cycle stages (Cox *et al.,* 1981b). L2, L3 and L4 cuticles are very similar in structure and are represented in Figure 1.3, by the L4 cuticle. The collagenous component of the cuticle is also variable with life cycle stage, *col-2* and *col-19* only being expressed in the dauer and adult specific stages respectively (Kramer *et al.,* 1985; Liu *et al.,* 1995).

Since the cuticle is the most external surface of the nematode its role is multipurpose. The tough but flexible nature of the cuticle maintains body shape, provides a protective barrier from, and a point of interaction with, the environment and permits motility as it is the point of muscle attachment (Kramer, 1994b; Johnstone, 2000; Davies *et al.,* 2001). In parasitic nematodes these interactions with the environment can be with the hosts' own immune system, for example, *Brugia malayi,* a filarial parasitic nematode responsible for lymphatic filariasis in over 120 million people in 80 countries, which can be found within the lymph nodes of infected individuals.

1.3 *C. elegans* hypodermis

The single cell thick hypodermis of *C. elegans* is responsible for the secretion of the cuticle, establishment of the vermiform animal and the phagocytotic uptake of apoptotic bodies.

The hypodermis is comprised of multi-nucleated syncytial regions which form by cell fusion during development (Sulston *et al.,* 1983). Specialised hypodermal cells cover the major opening of the worm including: the arcade cells and buccal epithelium, duct and pore cell, vulval epithelium, rectal epithelial cells and the sensory socket and sheath cells (Altun, 2005). The apical surfaces of the hypodermis are bound by the cuticle and the basal regions are covered by the basal lamina (Altun, 2005). The main body hypodermis is a large hyp7 syncitium, with the head and tail comprised of distinct hypodermal cells denoted hyp1 to hyp11 (hyp13 in males) (Nguyen *et al.,* 1999). Various hypodermal tissues fuse with and become hyp7 tissue as the worm progresses through development, hyp6, for example, fuses to hyp7 at mid-L3 stage (Yochem *et al.,* 1998). Hyp13 also fuses

to hyp7, at different developmental stages respective to sex, the hermaphrodites hyp13 fusing to hyp7 during elongation with males not fusing until late L4 (Yochem *et al.,* 1998).

The pharynx of *C. elegans* is comprised of rings of hypodermal cells. The lips have three concentric rings of hypodermis; hyp1, the inner most ring; hyp2, and hyp3, the outermost ring which connect with hyp4. Posterior to hyp3 lie three more rings of hypodermal syncytial cells, hyp4, hyp5 and hyp6, with hyp6 fusing to hyp7 as described above (Yochem *et al.,* 1998; Altun, 2005).

The tail of *C. elegans* is comprised of four hypodermal cells, hyp8 to hyp11. Fusion events that occur in the tail are sex specific, with the male's two celled hyp10 fusing to hyp8, hyp9 and hyp11 between the 1.5- and 3-fold stages of embryogenesis, where as the hermaphrodite hyp8, hyp9, hyp10 and hyp11 remain distinct hypodermal tissues (Nguyen *et al.,* 1999).

L1 (post-hatching) *C. elegans* possess 12 unfused ventral epidermal cells, P1/2 to P11/12. These are positioned as two parallel rows of six, with each cell confronting its bilateral homologue. These cells divide and the anterior daughter cells detach from the epithelium and become neuroblast cells (Sulston and Horvitz, 1977). The remaining posterior daughters of P1, P2, P9 and P12 fuse to the main body syncytial hyp7 at the end of L1. P3 to P8 divide again at L3 and their daughters fuse with hyp7 also. The remaining unfused cells become vulval precursor cells.

Seam cells are classified as specialised epithelial cells, and are located along the lateral midline of the worm running most of the length of the worm. These specialised cells are responsible for the generation and secretion of the lateral alae of the L1, dauer and adult stages of development (Silhankova *et al.,* 2005). No alae are present at L2, L3 or L4. The seam cells also produce neurons of the lumber ganglion, tail spike neurons, phasmid support cells and notably the male tail (Altun, 2005). The seam cells vary in girth respective to the position along there long axis. Centrally the seam cells are at their thickest to accommodate the cell body, and if a transverse section is viewed at this point it could be seen that the seam cells will reach further into the centre of the worm than the syncytial hypodermis (Altun, 2005). The seam cell then tapers from its midpoint to the periphery, where if a transverse section was taken the seam cell would be covered over by the single cell thick syncytial hypodermis. Seam cells are attached apically to the hypodermis by small adherens junctions which run the full length of the worm, and by gap junction on

their lateral membranes (Altun, 2005). Thus the apical face of the seam cells are in contact with the cuticle exactly underlying the lateral alae (Singh and Sulston, 1978).

L1 *C. elegans* has two rows of 10 seam cells embedded laterally in the hyp7 syncytium. At each stage during maturation of the larval worm the seam cells divide, except the most anterior seam cell, H0, which does not divide. The posterior daughter of these dividing seam cells (H1, H2, V1-6 and T) becomes a new seam cell and the anterior daughter apicaly detaches and fuses to the hyp7 syncytium (Podbilewicz and White, 1994). The new seam cells then elongate to meet their neighbouring seam cells and another row is generated. This cycle of division, hyp7 fusion and elongation occurs in all larval stages until mid-L4, leading to a total production of 98 syncytial hypodermal cell nuclei. At mid-L4 the 15 newly generated seam cells (15 per side, 30 in total) elongate laterally and fuse with each other and H0, leading to the formation of two continuous lateral seam cell syncytia (Podbilewicz and White, 1994; Altun, 2005). These are the last fusion events to occur in post-embryonic *C. elegans* development (Podbilewicz and White, 1994). Schematic representation of L1 and adult seam cells can be seen in chapter 5 Figure 5.6.

Sex specific hypodermal remodelling also occurs with V5, V6 and T, the three most posterior lateral seam cells in L1 worms producing the sensory rays of the male tail, as opposed to secreting alae in hermaphrodites (Sutherlin and Emmons, 1994). Another sex specific event to occur in hypodermal development is the process of male tail remodelling, which results in the generation of a male tail central/ventral syncytium at the L4-adult transition. The process can be divided into five stages (Nguyen *et al.,* 1999) with breaking of cell boundaries and fusion events processing in an anterior to posterior manner. The fusions of the male tail hypodermal cell types leads to the generation of this syncytium, which then migrates into the body cavity at the midline leading to the generation of a strip of central hypodermis.

1.4 Actin filaments are required for elongation during embryogenesis

The cylindrical body architecture of the worm is initially dictated by the hypodermis with the vermiform body plan established by the process of elongation; during which, circumferential actin bundles form at regular intervals along the apical membrane of all epidermal cells. This cytoskeletal arrangement of actin bundles is however only a transient feature with actin filaments appearing unordered in epidermal cells one hour before and

after elongation (Mei *et al.,* 2004). Contraction of this circumferential array of actin microfilaments results in a decrease in diameter, with an associated lengthening of the longitudinal axis. Treatment of embryos with cytochalasin-D disrupts the organisation of their actin microfilament bundles and prevents elongation (Piekny and Mains, 2003; Mei *et al.,* 2004), illustrating their importance to the elongation process.

The regular positioning of the actin bundles and their contraction during elongation gives rise to the regular arrangement of indentations termed the annular furrows (Priess and Hirsh, 1986). These indentations of the cuticle allow room for growth between each moult and freedom of motion (Costa *et al.,* 1997). The mechanism behind the positioning and formation of these actin bundles in the epidermis is as yet unknown (Mei *et al.,* 2004); however, a physical attachment between the membrane and actin filaments is likely, allowing for the position of the actin bundles to be translated into the cuticle furrows (McMahon *et al.,* 2003). The actin filaments required for embryonic elongation become disorganised following completion of elongation, needing to reform circumferentially prior to each larval stage transition (Costa *et al.,* 1997; Mei *et al.,* 2004).

As discussed the cuticle of *C. elegans* is secreted by the hypodermal cells, with patterning of the cuticle and elongation affected by the underlying cytoskeletal arrangement of the transient actin filaments. Following I will discuss the process of cuticle synthesis, an enzyme catalysed multi-step process, which based on homology to the extensively characterised vertebrate system, was used as a model for nematode cuticle collagen biosynthesis.

1.5 Structure of vertebrate collagens

The collagens are a closely related family with multiple distinct members. Collagens are defined by the repeat sequence Gly-X-Y, where Gly is a glycine residue and X and Y can be any other residue but are most often proline and 4-hydroxyproline respectively. Collagen subunits combine to form triple helical structures which fold along a common long axis. This helical conformation adopted by the collagens is afforded by having glycine, the amino acid with the smallest side chain, as every third residue within the Gly-X-Y repeat regions. 4-hydroxyproline, most often found at the Y position, adds thermal stability to the collagen molecules and is also a source for hydrogen bonds which stabilise the molecule (Kivirikko *et al.,* 1992).

Nematode collagens are most closely related to vertebrate fibril-associated collagens with interrupted triple helices (FACIT) type collagens; however, the nematode collagens are smaller, *C. elegans* collagens having a molecular weight of between 26-35kDa, than their vertebrate counterparts which can weigh over 150kDa (Cox, 1992). There are 43 unique vertebrate collagen monomers which are sub-divided into 28 collagen types (I-XXVIII) (Khoshnoodi *et al.,* 2006). The FACIT type collagens differ from other vertebrate collagens by having more than one helical Gly-X-Y repeat region, FACIT collagens include collagen types IX, XII, XIV, XVI, XIX, XX, XXI, and XXII (Khoshnoodi *et al.,* 2006). The FACIT collagens localise to the surface of fibrils and are thought to be important molecular bridges required for the organisation and stability of the ECM (Shaw and Olsen, 1991). Vertebrate collagens have been shown to homotrimerise, heterotrimerise or associate two collagen chains of one type with one chain of another type (Myllyharju and Kivirikko, 2001). It has not yet been determined whether *C. elegans* collagens form homotrimers or heterotrimers during cuticle biosynthesis, genetic evidence exists which suggests the presence of more than one type of collagen within a triple helix (Kramer and Johnson, 1993; Levy *et al.,* 1993; Nyström *et al.,* 2002); this has not yet been confirmed. It may also be possible that these proposed associations are actually higher order associations of triple helical strands or larger complexes. To date SQT-3 is the only collagen which has been shown to homotrimerise (Prof A. Page, personal communication).

1.6 Vertebrate collagen biosynthesis

The study of collagen biosynthesis has been most thoroughly studied in the vertebrate system (Engel and Prockop, 1991; Myllyharju and Kivirikko, 2004). This provides a model on which to base the nematode process of collagen biosynthesis.

In vertebrates a number of modification events occur prior to production of a mature collagen, see Figure 1.4. As synthesis takes place hydroxylation occurs at a number of sites. Collagen hydroxylation occurs by the modification of peptide-bound residues, not by the incorporation of hydroxylated amino acids. Prolyl 4-hydroxylase (P4H) and Lysyl hydroxylase (LH) enzymes are involved with the hydroxylation of Y-position proline and lysine residues respectively. Proline found at the X position of the Gly-X-Y repeat can also become hydroxylated by 3-hydroxyproline, exclusively within the natural collagen sequence Gly-3Hyp-4Hyp (Kivirikko *et al.,* 1992; Jenkins *et al.,* 2003). Hydroxylysine and certain asparagine residues can also be glycosylated by the addition of galactose or glucose. Following hydroxylation and glycosylation, association of three

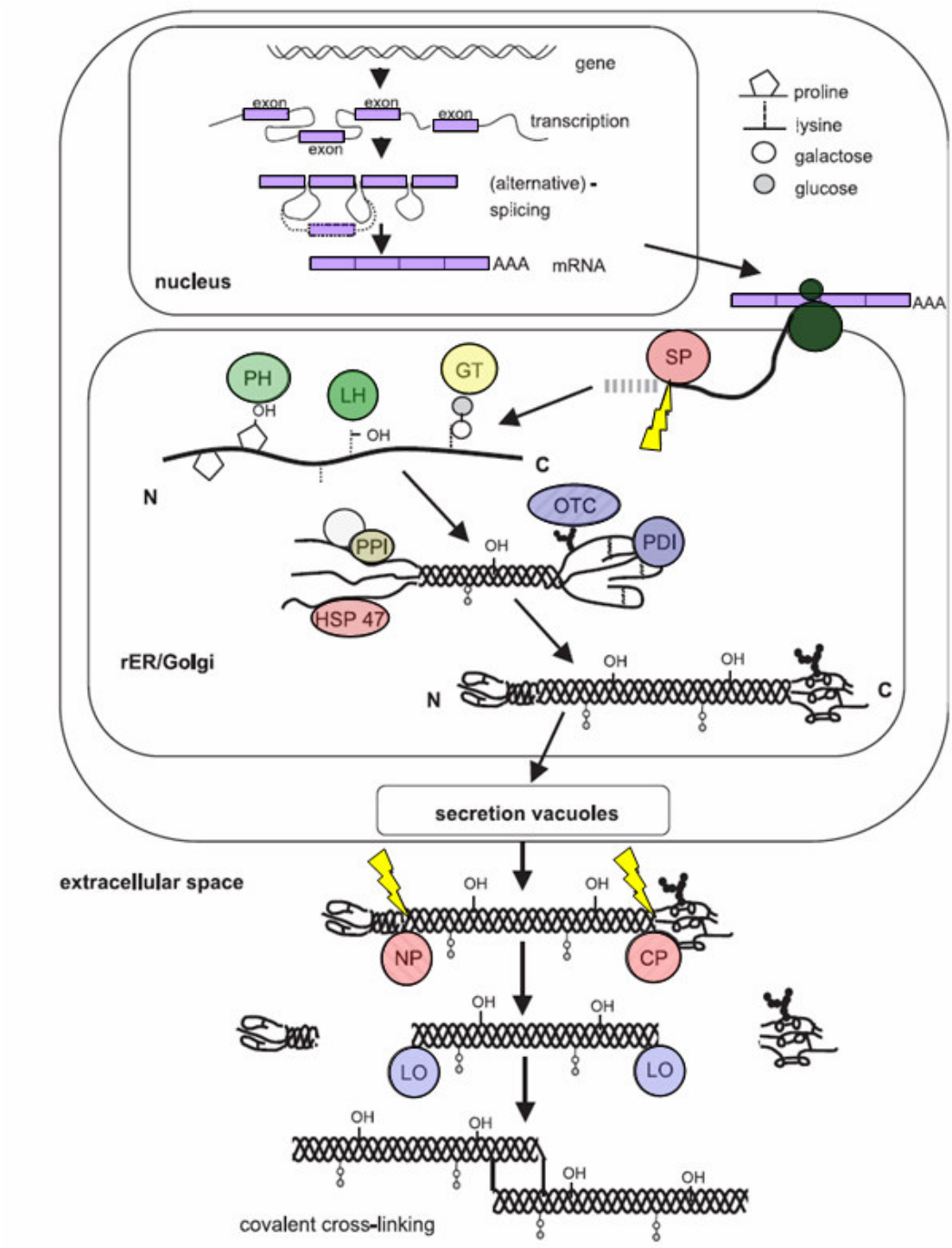

Figure 1.4: Schematic representation of collagen synthesis starting from the nuclear transcription of the collagen genes, mRNA processing, ribosomal protein synthesis (translation) and post-translational modifications, secretion and the final steps of fibril formation. (SP: signal peptidase; GT: hydroxylysyl galactosyltransferase and galactosylhydroxylysyl glucosyltransferase; LH: lysyl hydroxylase; PH: prolyl hydroxylase; OTC: oligosaccharyl transferase complex; PDI: protein disulphide isomerase; PPI: peptidyl-prolyl cis-trans-isomerase; NP: procollagen N-proteinase; CP: procollagen C-proteinase; LO: lysyl oxidase; HSP47: heat shock protein 47 A.K.A colligin1). Taken from (Gelse *et al.,* 2003).

monomer strands occurs and in many vertebrate collagens this association is directed by the C-terminal non-collagen like domain, and is associated with the generation of both inter- and intra-chain disulphide bonds mediated by protein disulphide isomerase (PDI). The association of the three monomers generates a triple helical region which propagates in a C- to N-terminal direction, the rate of which is directed by the slow *cis-trans* isomerisation of peptidyl proline bonds, see section 1.9.2. After assembly of the three collagen monomers into one triple helical structure, proteolytic cleavage by specific peptidases occurs removing the non-collagen like C- and N-terminal domains. Not all vertebrate collagens require proteolytic cleavage, as some are synthesised without the non-collagenous terminal domains. FACIT collagens for example are synthesised without the non-collagenous extensions, and associate by the spontaneous triple helical folding of no fewer than two Gly-Pro-Hyp sequences (Khoshnoodi *et al.,* 2006). Disulphide bonds can subsequently form due to the proximity of the C-termini, which *via* lateral interactions have been held proximal to each other (McLaughlin and Bulleid, 1998). After cleavage the final stage of vertebrate fibril collagen assembly occurs, this involves the cross-linking of molecules by lysyl oxidase (LO). Folding of collagens also requires the use of chaperones such as P4H, PDI and Hsp47 (Walmsley *et al.,* 1999; Nagai *et al.,* 2000). Hsp47 is an essential protein in vertebrate collagen assembly, its knockout in mice proving to be embryonic lethal (Nagai *et al.,* 2000). No Hsp47 homologue has been identified in *C. elegans*, as such P4H (which contains a PDI-2 subunit) may be acting as a *C. elegans* collagen specific chaperone (Norman and Moerman, 2000).

Vertebrate collagen biosynthesis as a general model for collagen assembly is useful; however, exceptions to the model must be noted. For example, many non-fibrilar vertebrate collagens, although having an N- and C-terminal non-collagenous extension, are not proteolyticaly cleaved (Khoshnoodi *et al.,* 2006), and the transmembrane vertebrate collagen (types XIII, XVII, XXIII and XXV) do not associate *via* their C-termini like all other collagen types, instead they associate *via* their N-termini with helical propagation occurring in the N- to C-terminal direction, the opposite of all other collagen classes. FACIT collagens also deviate from the vertebrate model as described above.

1.7 *C. elegans* cuticle collagens

Deviations from the vertebrate model for collagen synthesis are noted with regard to *C. elegans* collagen assembly. For instance, no nematode species has been found, thus far, to contain a homologue to the chaperone Hsp47. Also, importantly, hydroxylysine derived

cross-linking in *C. elegans* cuticles is restricted to dauer cuticles (Cox *et al.,* 1981b). This is interesting since these are the predominant intermolecular bonds in vertebrate collagens (Bornstein, 2003), consequently the cross-links formed in nematode collagens are predominantly not the lysine based cross-links seen in vertebrate collagens; instead, di-, tri-, and/or isotyrosine cross-links are found in nematodes (Fetterer *et al.,* 1993), see section 1.10.2.

C. elegans collagens are numerous with approximately 175 collagens identified, the majority of which are believed to be cuticular (Myllyharju and Kivirikko, 2004). Characteristically, nematode collagens are small, and the genes which encode them are typically less than 2kbps and contain few (1-3) intronic regions. *C. elegans* collagens have two Gly-X-Y repeat domains which are flanked by highly conserved cysteines. The number of repeats in the N-terminal Gly-X-Y domain is less than the C-terminal domain, ~8-10 and 40-42 repeats respectively. The larger C-terminal Gly-X-Y domain also tends to have one or two interrupting non Gly-X-Y regions, these intervening sequences vary in size and position between molecules. The *C. elegans* collagens also contain N- and C-terminal non-collagenous domains which are variable in size. The N-terminal domain contains the signal peptide, which directs the collagens through the endoplasmic reticulum (ER), and a proposed subtilisin site, which is involved with the processing of the pro-collagen to its mature form (Yang and Kramer, 1999). The C-terminal non-collagenous domains are also variable in size, often being very short, for example 14 residues for COL-19 (Thein *et al.,* 2003); in contrast however, is that of BLI-1 which has a 400 residue C-terminal non-collagenous domain (Crew and Kramer, personal communication). The N- and C-terminal domains are proposed to be cleaved by the proteolytic enzymes BLI-4 and DPY-31/NAS-35, a *C. elegans* homologue of the vertebrate pro-collagen protease BMP-1, respectively (Novelli *et al.,* 2004; Page *et al.,* 2006). *bli-4,* a Kex2/subtilisin class pro-protein convertase encoding gene, is essential for post-embryonic viability in *C. elegans* (Peters et al., 1991). All cuticle collagens possess a highly conserved N-terminal cleavage site for BLI-4, which was demonstrated as essential for processing by site directed mutagenesis experiments with ROL-6 and SQT-1 collagens (Yang and Kramer, 1994). A C-terminal cleavage site has similarly been shown to be conserved in all 49 members of the collagen family represented by SQT-3 (Novelli *et al.,* 2004). Mutations which affect this C-terminal cleavage site are dominant and result in cuticle defects, abnormal morphology, and embryonic lethality. Novelli *et al.* (2004) showed that DPY-31 is responsible for these defects and the C-terminal proteolytic processing of SQT-3 collagen,

and could therefore be considered a structural and functional homologue of vertebrate BMP-1 (a vertebrate pro-collagen convertase, see section 1.15.2).

The number, positioning and spacing of the conserved cysteines flanking the Gly-X-Y repeats are used for the characterisation/classification of nematode collagens, the results of which lead to the generation of six *C. elegans* collagen families: 1, 1A, 2, 3, *dpy-7* and *dpy-2* (Johnstone, 2000). Similar groupings were generated when N- and C-terminal non-collagenous components were analysed (Johnstone, 2000). The high degree of conservation noted in the collagens across the nematode phylum highlights the importance of the proteins and therefore the enzymes associated with their processing (Kingston, 1991; Johnstone *et al.,* 1996b).

1.8 Collagen expression profiling

Examination of the levels of specific collagen gene transcripts throughout post-embryonic development by RT-PCR on staged samples has shown that a precise expression pattern of individual genes is repeated during the synthesis of each new cuticle (Johnstone and Barry, 1996). Collagen gene transcripts were found at specific intervals during the period between moults when the new cuticle is synthesised, and can be classified as early (4hrs pre-moult), intermediate (2hrs pre-moult) and late (coincidental with the moults) collagens (Johnstone and Barry, 1996). The specific timing of expression within a moult for each gene is invariably repeated at every life cycle stage. This temporal control of collagen gene expression provides a possible mechanism through which association of collagen trimer partners could occur (Johnstone and Barry, 1996). As discussed earlier, it is not currently known whether nematode collagen trimers are composed of homo- or heterotrimers. However, if only relatively similar collagens are assumed to associate, then expression of similar collagens at the same time would support the interactions of correct partners (Johnstone and Barry, 1996). The timing of expression of these cuticular components may also reflect their localisation within the final cuticle with early expressed collagens possibly forming the most exterior layers and late expressed components the inner layers. The number of possible interactions between collagen monomers would also be reduced if only temporally coexisting molecules could associate.

1.9 Collagen modifying enzymes of *C. elegans*

There are many enzyme catalysed steps associated with the generation of a mature collagen molecule. The following section will discuss these enzymes and the reactions they catalyse.

1.9.1 Prolyl 4-hydroxylase and its PDI subunit

One of the first major modifications to occur in the process of *C. elegans* collagen maturation involves the hydroxylation of proline residues of the Y position, catalysed by prolyl 4-hydroxylase. This co-translational modification allows the proper folding of the collagen into a thermally-stable form (Kivirikko and Pihlajaniemi, 1998). The structure of *C. elegans* P4H was derived from vertebrate P4H, which showed a tetrameric enzyme comprising of two α subunits and two β subunits (Vuori *et al.,* 1992; Annunen *et al.,* 1997). The two *C. elegans* α subunits being the catalytically active PHY-1(*dpy-18*) and PHY-2 proteins, and the two β subunits being protein disulphide isomerase (Winter and Page, 2000; Myllyharju *et al.,* 2002). Although three PDI enzymes are found in *C. elegans* only PDI-2 has been shown to complex with the PHY α subunits to generate active P4H (Myllyharju *et al.,* 2002). Also dimers of PHY-1 and PDI have also been shown to exist in *C. elegans*, and have been shown to possess P4H activity (Veijola *et al.,* 1994). Association of P4H with collagen modification has been exploited in the *in vitro* synthesis of collagens, with co-expression (in insect cells or yeast) of P4H and collagens resulting in an increased production of thermally stable collagen trimers (Lamberg *et al.,* 1996). Insect and yeast cells having extremely low levels of endogenous P4H activity (Lamberg *et al.,* 1996).

The modular nature of the P4H enzyme allows for the generation of active hybrid enzymes which contain α subunits from one organism and β subunits from another (Veijola *et al.,* 1996b). Human PDI has been shown to be extremely adaptable accepting α subunits from *D. melanogaster*, *C. elegans*, and mouse (Veijola *et al.,* 1994; Helaakoski *et al.,* 1995; Annunen *et al.,* 1999). *C. elegans* PDI can also form an active tetramer with human α subunits (Veijola *et al.,* 1996b). P4H has also been identified in the parasitic nematode *Onchocerca volvulus,* where co-expression of its α subunit and β subunit in a baculovirus system resulted in the production of enzymatically active P4H (Merriweather *et al.,* 2001).

Enzymatic activity of P4H requires the presence of the co-factors Fe^{2+}, 2-oxoglutarate, O_2 and ascorbate. The O_2 molecule is split with one oxygen molecule being incorporated into the accompanying 2-oxoglutarate and the other forming the hydroxyl group in the proline residue. CO_2 is then resolved by the decarboxylation of 2-oxyglutarate (Kivirikko and Myllyharju, 1998b) ultimately yielding a CO_2, 4-hydroxylated proline and a succinate molecule for each O_2 used in this P4H catalysed reaction (Kivirikko and Myllyharju, 1998b).

The PDI β subunit of P4H is a multi-functional enzyme with chaperone and disulphide bond functions within the ER (Winter *et al.,* 2007). PDIs are modular proteins consisting of four domains: a, b, b′, a′ and an acidic C-terminal extension, c, which contains an ER retention signal. The a/a′ domains contain the catalytic motif CGHC and show similarities with thioredoxin. The b/b′ domains do not contain the catalytic motif and show no sequence similarity with thioredoxin; however, the b domains do fold like thioredoxins (Tian *et al.,* 2006). The C-terminal c domain is not required for function but is essential for maintaining P4H in the ER (Vuori *et al.,* 1992). The PDI enzymatic activity is not required for function as a P4H subunit in humans, as demonstrated when PDI with either one or both of the catalytic sequences mutated, formed fully active tetramers when co-expressed with α subunits in insect cells (Vuori *et al.,* 1992). The function of PDI in the P4H enzyme is to stop the aggregation of the PHY (α subunits) and maintain the P4H in an active conformation (John *et al.,* 1993; Veijola *et al.,* 1996).

Mutants of P4H have cuticle associated defects. Disruption to PHY-1(*dpy-18*) produce medium dumpy (Dpy) worms which exhibit reduced hydroxyproline content (Winter and Page, 2000; Winter *et al.,* 2007c). Disruption of the PHY-2 subunit however does not produce any notable cuticular defects, as an increase in PHY-1 is able to compensate for the loss (Winter *et al.,* 2007). However, combinational knockout or knockdown of both PHY-1 and PHY-2 subunits, by crossing of mutant strains (Friedman *et al.,* 2000) and RNAi (Winter and Page, 2000) respectively, results in embryonic lethality. Similarly embryonic lethality is evident when the β subunit is disrupted (Winter and Page, 2000; Winter *et al.,* 2007). The lethality associated with disruption of the subunits that comprise the P4H enzyme demonstrates the importance of proline hydroxylation in collagen maturation.

Aside from association with the PHY subunits in the generation of active P4H, PDI-2 also acts as a chaperone, both with and without PHY, retaining non-helical and non-hydroxylated collagens in the ER (Walmsley *et al.,* 1999; Wilson *et al.,* 1998) . PDI-2

may also catalyse the formation of inter- and intra-chain disulphide bonds through its thioredoxin-like activity (Eschenlauer and Page, 2003; Winter *et al.,* 2007), PDI-1 and PDI-3 may also share these additional functions.

1.9.2 Peptidyl prolyl cis-trans isomerase

The propagation of registered collagen trimers is rate limited by slow *cis-trans* proline isomerisation, and requires the catalytic activity of the peptidyl prolyl *cis-trans* isomerase (PPIase) enzymes of the cyclophilin (CYP) and FK506 binding protein (FKB) class (Winter *et al.,* 2007b). Peptide bound proline residues must be in the *trans* form in the native collagen triple helix, therefore the *cis* sequences of Gly-Pro-Y and Gly-Pro-4Hyp must be isomerised to *trans* peptide bonds, a reaction catalysed by the enzyme peptidyl prolyl *cis-trans* isomerase (PPIase).

The PPIase families are large and exhibit redundancy between family members. For example, there are 26 PPIases (Page *et al.,* 1996; Page and Winter, 2003) 18 CYPs and eight FKBs (of which FKB-3, 4 and 5 have dual PPI domains, signal peptides and ER retention signals), singly mutants FKB-3, 4 and 5 exhibit no phenotype; however, combined triple mutants arrest at 12ºC but develop normally at 15-25ºC (Winter *et al.,* 2007b). Cuticle collagen expression (DPY-7), moulting and the cuticular ECM were also affected in these cold sensitive mutants. CYP-9, which is found to be polycistronic along with PDI-1, similarly does not exhibit any cuticular defects when silenced (Page and Winter, 2003), although its expression profile is noted to be cyclical with cuticle collagens, and localised with regions associated with collagen production, reinforcing the redundant nature of this apparently essential class of enzymes.

1.10 Collagen cross-links; and the enzymes responsible

Collagen biosynthesis ultimately generates large cross-linked molecules which are comprised of many individual collagen subunits. These collagen building blocks must be held together by an adhesive force; in *C. elegans,* and other nematodes, these forces include intermolecular disulphide (Myllyharju and Kivirikko, 2004), tyrosine (Fujimoto, 1975; Fujimoto *et al.,* 1981) and glutamine derived bonds (Mehta *et al.,* 1990). There are differences noted in the properties of these bonds, notably in their response to detergents and reducing agents. The disulphide bonds, which are formed by thioredoxins, are soluble in detergent and β-mercaptoethanol containing solutions, (Cox *et al.,* 1981b; Cox, 1992),

while the tyrosine- and glutamate derived covalent cross-links are unaffected by detergent or β-mercaptoethanol treatment. As would be expected there are developmental stage specific responses to treatment with reducing agents, which suggests stage specific dependence upon certain types of bonding in the cuticles. The dauer cuticles, in particular, are the least susceptible to reduction which can be explained by their relatively high proportion of covalent cross-links (Cox *et al.,* 1981c). While tyrosine-derived bonds are formed by the catalytic action of animal-haem peroxidases in the presence of H_2O_2 (Cariello *et al.,* 1990; Edens *et al.,* 2001), transglutaminases (TGase) catalyse the formation of glutamate derived bonds (Greenberg *et al.,* 1991). The glutamate derived bonds are like the tyrosine bonds non-reducible; however, they are also resistant to proteolysis, only being destroyed upon the complete degradation of the peptide chain containing these bonds (Greenberg *et al.,* 1991). The disulphide, glutamate and tyrosine derived cross-links are not the principal form of cross-links associated with vertebrate collagens, vertebrate collagens instead being predominately cross-linked by hydroxylysine derived bonds (Takaluoma *et al.,* 2007). Hydroxylysine bonding is found within *C. elegans,* but only in the dauer stage (Cox *et al.,* 1981b). Tyrosine derived cross-linking is not found in vertebrate collagens; however, they have been identified in the lens of vertebrate eyes with cataracts (Garciacastineiras *et al.,* 1978; Fetterer and Rhoads, 1990). This is an interesting point to note as the quiescin-sulfhydryl oxidases (QSOX, see section 1.11), a potential source of H_2O_2 for tyrosine cross-linking, has also been found in the vertebrate eye (Tury *et al.,* 2006). The different types of bonds observed in vertebrates and nematodes may reflect the differing structures that they form; the majority of vertebrate collagens form fibrils unlike the non-fibrillar, cuticular *C. elegans* collagens.

The dependence of nematodes upon these cross-links is clearly demonstrated by the severe mutant/lethal phenotypes associated with disruption of the enzymes which catalyse their formation. For example, mild blister to lethal phenotypes are observed in *C. elegans* when certain animal haem-peroxidase enzymes (DUOX) are mutated or ablated (Edens *et al.,* 2001). Pleiotropic mutants, including Dpy, are also associated with the absence of or mutations in thioredoxins and thioredoxin homologue containing proteins (Ko and Chow, 2002; Winter *et al.,* 2007). In vertebrates TGase enzymes have been shown to be essential, with TGase deficiency in mice resulting in neonatal death (Matsuki *et al.,* 1998).

1.10.1 Disulphide bonding mediated by thioredoxins

Thioredoxins catalyse various thiol-disulphide exchange reactions. Several endoplasmic reticulum proteins (ERp), PDIs and the quiescin sulfhydryl oxidase family (QSOX) are

members of the thioredoxin superfamily, based upon them all pocessing at least one homologous thioredoxin domain and a redox-active thiol/disulphide CxxC site. Cuticle collagens contain many intra- and inter-chain disulphide bonds, as described in Section 1.7, and as such are dependant upon the enzymes which catalyse their synthesis (Winter *et al.,* 2007). The *C. elegans dpy-11* mutant has been shown to encode a novel thioredoxin comprising 256 amino acids with a signal peptide, thioredoxin-, transmembrane- and C-terminal domain. All of which are essential as transgenic rescue constructs lacking these regions were not able to recover the associated Dpy mutant phenotype (Ko and Chow, 2002). *dpy-11* is a hypodermally expressed gene and is active from early embryogenesis and throughout larval development. The sub-cellular localisation of DPY-11 illustrates a possible association with the ER; however, no definitive substrate has been identified for *dpy-11* although its tissue and sub-cellular localisation, enzymatic activity and altered body morphology when mutated point strongly towards a role in modifying components of the *C. elegans* cuticle (Ko and Chow, 2002). It was also shown that the thioredoxins may be mediating cuticular morphology by acting on signalling molecules rather than directly associating with the cuticle collagens, demonstrated when *dpy-11* mutants were shown to suppress signalling molecule mutants (Ko and Chow, 2002). The proposed substrates for DPY-11 are the collagens *dpy-2, 7, 10* and *13*, of these collagens *dpy-2* and *10* mutants (which exhibited phenocopy of *dpy-11* mutants) could suppress the mutants associated with signalling defects in *mup-1* and *glp-1* (Nishiwaki and Miwa, 1998; Ko and Chow, 2002). *dpy-11* mutants were shown to suppress the mutations associated with these signalling molecules through interaction with the collagen molecules *dpy-2* and *10*, thus demonstrating a potential epistatic control of *dpy-11* over these signalling molecules and potential collagen substrates (Nishiwaki and Miwa, 1998).

The partial loss-of-function mutant *dpy-11(e224)* exhibits a Dpy phenotype at the mid-body and tail region with bifurcated and branched alae (Thein *et al.,* 2003). The null mutant allele *dpy-11(e1180)* causes a more severe Dpy and slow growth. Both mutant alleles *e224* and *e1180* have male tail defects, but retain breeding capability (Ko and Chow, 2002). Vertebrate systems have also been shown to rely upon thioredoxin proteins; this is exemplified in mice, in which a knockout of their one thioredoxin gene results in embryonic lethality (Matsui *et al.,* 1996).

Disruption to a novel gene, *lon-8*, has recently been shown to affect body length and male tail morphology, *via* interaction with *dpy-11*, to mediate body length independently of the Small/Male abnormal (Sma/Mab) pathway (for a review of this signalling pathway see (Savage, 2005)) (Soete *et al.,* 2007). *lon-8* appears to be genetically interacting with the

cuticle collagen modifying enzymes *dpy-11* and *dpy-18/phy-1*, this is unlike other isolated *lon* genes which associate with the Sma/Mab pathway. Therefore thioredoxin enzymes may also be mediators of body length and male tail morphology independent of the Sma/Mab signalling pathway under the control of *lon-8* (Soete *et al.,* 2007), and may be eliciting these effects through direct association with cuticle collagens or by proxy through signalling molecule interaction. *lon-8* encodes a secreted product of the hypodermis that is highly conserved in rhabditid nematodes (Soete *et al.,* 2007).

1.10.2 Tyrosine derived cross-links mediated by peroxidases

Although *C. elegans* cuticle collagens are comparatively small when cuticle extracts are made under reducing conditions high molecular weight products of over 200kDa can be found (Cox *et al.,* 1981). This demonstrated that the higher order collagen structures contained, at least in part, non-reducible covalent cross-links in addition to disulphide bridges. The di-, tri- and isotri-tyrosine cross-links in the *C. elegans* cuticle are biphenyl linkages of tyrosine molecules (Fujimoto, 1975). The di- and tri-tyrosine cross-links have been identified in a number of structural proteins in at least three phyla (arthropoda, nematoda and vertebrate) (Fujimoto, 1975), with the isotri-tyrosine cross-links having only been shown to be present in cuticles of nematodes (Fetterer and Rhoads, 1990). Tyrosine derived cross-links have been found in the cuticles of the human and pig ascarid parasites *Ascaris lumbricoides* (in the cuticlins) and *Ascaris summ* respectively (Fujimoto *et al.,* 1981; Sakura and Fujimoto, 1984; Fetterer *et al.,* 1993). The retained second stage cuticle sheaths of L3 *Haemoncus contortus* have also been shown to contain such cross-links (Fetterer and Rhoads, 1990).

Tyrosine derived cross-linking by peroxidases was initially demonstrated following inhibitor studies in *Ascaris suum* (Fetterer *et al.,* 1993). To date, a large amount of the work regarding tyrosine cross-linking enzymes has centred on the cross-linking of cuticulins, which are highly cross-linked alae residing components (Parise and Bazzicalupo, 1997; Sapio *et al.,* 2005). Lassandro *et al.,* 1994, demonstrated *in vitro* that horseradish peroxidase can insert di-tyrosyl cross-links into the *C. elegans* cuticlin protein CUT-2 in the presence of H_2O_2, leading to the generation of high molecular weight tyrosyl cross-linked complexes.

The tyrosine derived cross-links of the *C. elegans* cuticle have been shown to be catalysed by two dual oxidase (DUOX) gene products. Disruption of either or both of these genes produces severe defects consistent with a role in cuticle component modification, and can

cause lethality (Edens *et al.,* 2001). The DUOX enzymes of humans and *C. elegans* contain two catalytic domains: an N-terminal NADPH-oxidase domain (homologue of gp91 *phox*) and a C-terminal domain with homology to animal haem peroxidases. The C-terminal domain by analysis of recombinant protein is itself sufficient to catalyse the formation of tyrosine derived cross-links in 3,3′,5,5′-tetramethylbenzidine (TMB), a well-characterized peroxidase synthetic substrate, and the N-terminal NADPH-oxidase domain is presumed to be the source of the hydrogen peroxide (H_2O_2) required for the reaction (Edens *et al.,* 2001). The *duox* genes isolated in *C. elegans* are *bli-3* and *hpx-1* (*hpx-1* contains only the heam peroxidase domain and is presumed to be reliant upon an external H_2O_2 source) (Unpublished data from Melanie Thein University of Glasgow)

1.10.3 Glutamate derived cross-links mediated by a transglutaminase like thioredoxin containing enzyme

Transglutaminases (TGases) catalyse the formation of non-reducible covalent ε-(γ-glutamyl)lysine cross-links in substrates such as fibrinogen, actin, myosin, fibronectin, laminin and vertebrate and invertebrate collagens (Griffin *et al.,* 2002) where these bonds contribute to the insoluble cuticle component. TGases activity and enzymatic products were identified in nematodes through inhibitor studies in parasites (Mehta *et al.,* 1990; Mehta *et al.,* 1992; Lustigman *et al.,* 1995). Chemical inhibitors of TGases caused developmental and survival defects in the filarial nematodes *B. malayi* (Rao *et al.,* 1991; Mehta *et al.,* 1992); and L3 larvae of *Onchocerca volvulus* treated with TGase inhibitors displayed moulting defects at the transition to L4 with a thinning of the L4 cuticle (Lustigman *et al.,* 1995). Localisation of TGase modified components within the larval cuticles illustrated presence of glutamate derived bonds at the boundary between the new epicuticle and the basal layer of the previous stage cuticle, which is the region where separation between the old and new cuticles occurs (Lustigman *et al.,* 1995).

TGase activity has been noted in other parasites besides *B. malayi* and *O. volvulus,* such as the dog filarial heartworm nematode *Dirofilaria immitis* (Singh *et al.,* 1995). In which a 56kDa protein shares similarities with the *B. malayi* TGase (Singh and Mehta, 1994) but both are distinct from the mammalian form of the enzyme. Isolation, cloning and sequencing of the *D. immitis* TGase enzyme revealed that it had no sequence homology to other known TGase enzymes; however, it was similar to PDI and PDI-like ER proteins ERp60s (Chandrashekar *et al.,* 1998). Similar to *O. volvulus*, moult defects were noted in *D. immitis* subjected to TGase inhibition (Chandrashekar *et al.,* 2002).

Although no designated TGase enzymes have been identified from *C. elegans,* PDI-3 has been shown to possess TGase activity as well as disulphide bond generating and chaperone activity (Eschenlauer and Page, 2003). PDI-3 is a homologue of the mammalian TGase enzyme ERp60 (Blasko *et al.,* 2003; Eschenlauer and Page, 2003). The thioredoxin motif (CxxC) of PDI-3 has been shown to be involved with TGase activity and the second cysteine of this motif has been shown by site directed mutagenesis to be essential for activity (Blasko *et al.,* 2003). This motif can be more stringently characterised by inclusion of tryptophan, glycine and histidine residues to make a wCghC TGase motif. This motif is shared by all of the PDI family members, although PDI-3 has the greatest TGase activity (Eschenlauer and Page, 2003). This TGase motif is also found within the thioredoxin domain of two out of the three QSOX enzymes. Disruption of PDI-3 has no effect upon moulting; only exhibiting a slight Dpy phenotype, however, when PDI-3 is combined with select cuticle mutants, such as *dpy-18* and *sqt-3* which singly result in weakened cuticles, various severe morphological defects become apparent (Eschenlauer and Page, 2003). An explanation for this is that PDI-3 may be required for the proper maintenance of post-embryonic body shape in strains with weakened cuticles, perhaps through ECM stabilisation *via* TGase cross-linking activity, protein disulfide isomerase activity, chaperone activity, or *via* a combination of these events (Eschenlauer and Page, 2003).

1.11 The Quiescin-Sulfhydryl Oxidases (QSOX) enzymes

Eukaryotic flavin-dependant sulfhydryl oxidases catalyse oxidative protein folding with the generation of disulphides and the reduction of molecular oxygen to the reactive oxygen species (ROS) hydrogen peroxide (H_2O_2). The quiescin-sulfhydryl oxidases (QSOX) are found in multiple copies within multicellular organisms, and singly within a number of protozoan parasites. However, only recently, after their initial discovery some 30 years ago (Janolino and Swaisgood, 1975), have they attracted attention, which was brought about following the isolation of a QSOX enzyme in chicken egg white which shared 64% identity to the human enzyme quiescin Q6. These findings defined the new class of flavin-linked sulfhydryl oxidases termed QSOX (Hoober *et al.,* 1996; Hoober *et al.,* 1999b).

The QSOX family of enzymes are characterised by an N-terminal thioredoxin domain (similar to that found in the PDI enzymes) and a downstream ERV1/ALR domain; ERV, denotes ER vesicle protein; and ALR, augmenter of liver regeneration. Thioredoxins are themselves small disulphide containing proteins found in all kingdoms of living organisms

and serve as general protein disulphide oxidoreductases (Holmgren, 1989), see section 1.10.1, with Erv1p, Erv2p and ALR (the proteins which define the ERV1/ALR family) having also been shown to be FAD-dependant sulfhydryl oxidases (Coppock and Thorpe, 2006). Thus the QSOX family are a fusion of both of these distinct disulphide bond generating moieties (Raje and Thorpe, 2003), resulting in enzymes which catalyse the net generation of disulphide bonds at the expense of molecular oxygen (see diagram below) (Thorpe *et al.,* 2002; Coppock and Thorpe, 2006). Organisms, such as yeast, which lack QSOX enzymes have been shown to associate distinct PDI (Pdi-1p) and ERV (Erv2p) subunits to facilitate disulphide bonding (Sevier *et al.,* 2001).

$$2P\text{-}SH + O_2 \longrightarrow P\text{-}S\text{-}S\text{-}P + H_2O_2$$

From this reaction it can be seen that the ROS H_2O_2 is produced as a by-product of QSOX mediated disulphide bond generation, thus the QSOX enzymes are also a possible source of H_2O_2 which could be utilised in the afore-mentioned tyrosyl cross-linking process.

The process of disulphide bond generation involves a series of disulphide exchanges beginning with the oxidation of a dithiol substrate by an oxidising disulphide (CxxC) found in the QSOX N-terminal thioredoxin domain. The initial substrate-QSOX mixed disulphide is likely to be between the most N-terminal of the cysteines in the thioredoxin CxxC motif (Coppock and Thorpe, 2006). Following resolution of this mixed disulphide bond a series of internal disulphide exchanges occur, the first of which sees the transfer of reducing equivalents from the most N-terminal CxxC motif of the thioredoxin domain, to the most C-terminaly located CxxC motif of the ERV1/ALR domain (Gross *et al.,* 2002). The ERV1/ALR domain itself contains two CxxC motifs, the most N-terminal of which is called the proximal disulphide, and an FAD binding domain. Reduction of the proximal disulphide generates a cysteine thiolate which has a low pK and is involved in a strong charge-transfer interaction with the electron deficient flavin (Coppock and Thorpe, 2006). The nucleophilic thiolate then generates a bond between the flavin C4(a) atom and the cysteine, this bond is often termed the C(4a) adduct. This ultimately yields the generation of reduced flavin and the reformation of the disulphide bond in the proximal disulphide (Thorpe *et al.,* 2002). Catalysis is completed by the passing of the reducing equivalents from reduced flavin onto molecular oxygen, which occurs *via* electron transfer and generation of the C(4a)-hydroperoxyflavin intermediate ultimately yielding oxidised flavin and H_2O_2 (Massey, 1994). Such reactions require sufficient space and a suitably polar local flavin environment, which has been identified in Erv2p (Gross *et al.,* 2002).

The proposed substrate of the QSOX enzymes is not well understood. Currently avian QSOX1 is the only enzyme for which detailed enzymological studies have been performed. The preferred substrates of avian QSOX1 are not small mono-thiols but instead are an apparently unlimited array of reduced proteins and peptides (Hoober *et al.,* 1999). A particularly interesting association is the cooperation of avian QSOX and PDI in the generation and rearrangement of native disulphide bonds *in vivo* (Hoober *et al.,* 1999). When both avian PDI and QSOX are exposed to reduced RNase A correct refolding occurs more quickly and accurately than is achieved be either protein alone (Hoober *et al.,* 1999). It was also noted that reduced avian PDI was a substrate for avian QSOX (Hoober *et al.,* 1999), with avain PDI being reoxidised, and therefore ready to generate disulphide bonds, by avain QSOX, a process which in yeast has been attributed to Ero-1(endoplasmic reticulum oxidase 1) (Chakravarthi *et al.,* 2006; Sevier and Kaiser, 2006). This association of QSOX with PDI needs to be tested with a wider range of substrates, such as *C. elegans* QSOX and PDI where an association of this nature would prove very interesting with regard to cuticle synthesis.

The spatial distribution of the QSOX enzymes has illustrated that they are associated with regions of high secretory load. For example, in rats QSOX enzymes have been isolated in; seminiferous tubules of the reproductive system, the skin, the eye, and the islets of langerhans in the pancreas (Tury *et al.,* 2006). In humans QSOX enzymes have been found at high levels in; the islets of langerhans (where their production of H_2O_2 is proposed as a contributing factor of type II *diabetes mellitus* (Coppock and Thorpe, 2006)), the placenta and the parotid gland (Coppock and Thorpe, 2006). QSOX enzymes have also been localised to avian egg white (Hoober *et al.,* 1996) and in the male accessory glands of *Drosophila* (Arbeitman *et al.,* 2004). It was first noted that the QSOX enzymes were to be found extracellularly; however, QSOX enzymes are also found intracellularly in the ER, Golgi, secretory granules (Lee *et al.,* 2000; Thorpe *et al.,* 2002; Tury *et al.,* 2004) and dense core granules of the pituitary gland (Tury *et al.,* 2004). The QSOX enzymes can thus be found in a range of locales in diverse cell types and tissues, most of which have a high secretory load and the products of which require disulphide bonding.

Phylogenetic analysis shows that at least one QSOX can be found in all metazoans with higher plants also being found to contain QSOX enzymes. Several important human protozoan parasites have a single QSOX-like gene including *Plasmodium falciparum, Trypanosoma brucei, Leishmania major* and *Cryptosporidium parvum* (Coppock and Thorpe, 2006). The metazoans, it would appear, have undergone gene duplication several times with regard to their *qsox* genes, as the *Drosophila* and *C. elegans* paralogues more

closely resemble those of the same species than others. Similarly a duplication event, which predated the division of the bony fish from what became the current day mammals and birds, has given rise to the two QSOX noted in the vertebrate clades (Coppock and Thorpe, 2006).

To the best of my knowledge, no loss-of-function mutants exist in the QSOX of vertebrates, and no gross morphological defects have been reported concerning the loss of any QSOX enzymes. Work presented here illustrates a cuticle defective Bli mutant and lethality associated with combined loss of two *C. elegans* QSOX enzymes.

1.12 Moulting in nematodes

Moulting is a hallmark of the Ecdysozoan clade; however, neither the endocrine control of moulting *via* size, stage and nutritional inputs nor the enzyme catalysed synthesis and release of the ECM is well understood (Frand *et al.,* 2005). Genome wide screening by RNAi in *C. elegans* has identified 159 genes that when disrupted caused moult defects (Frand *et al.,* 2005), these included peroxidases, megalin-like receptors, transcription factors, proteases and protease inhibitors (Frand *et al.,* 2005). The identification of proteases is of importance to the subject matter in this thesis.

1.12.1 Moulting in Caenorhabditis elegans

As previously stated *C. elegans* moults four times, the timings of which are invariant given a constant temperature and a sufficient food source. Moulting can be broken down into three distinct phases (Singh and Sulston, 1978): apolysis, the separation of the cuticle connections between the old cuticle and the hypodermis; late lethargus, formation of the new cuticle underlying the existing cuticle; and ecdysis, the shedding of the old cuticle. Prior to apolysis pharyngeal pumping stops and the animal enters lethergus (Singh and Sulston, 1978). Lethargus can be divided into two phases; the first of which is characterised by loosening of the cuticle around the lips, tail and buccal cavity, locomotion also ceases. During the second phase of lethargus the animal “flips” repeatedly along its long axis, further loosening the old cuticle from the hypodermis (Singh and Sulston, 1978). About 30 minutes pre-ecdysis the terminal bulb begins to twitch spasmodically, spontaneous body movement begins and large refractile granules accumulate in the pharyngeal gland cell bodies. Ten mintues before ecdysis the granules move forward through the gland cell processes and the entire pharynx begins to contract spasmodically

(Singh and Sulston, 1978). The cuticular lining of the pharynx breaks and the animal pulls back from it repeatedly, in so doing it detaches the entire pharyngeal cuticle which is expelled by shuddering movements of the pharynx (Singh and Sulston, 1978). At this point a cuticle cap is detached from the anterior of the animal, through the action of proteases (Davis *et al.,* 2004), and feeding begins immediately, the animal then crawls out of the old cuticle (Singh and Sulston, 1978).

Proteolytic activity is thus an important aspect of moulting, as demonstrated by the moult defects noted when proteolytic enzymes are disrupted; NAS-37 (Davis *et al.,* 2004), CPL-1 (Britton and Murray, 2002) and BLI-4 (Frand *et al.,* 2005) for example. These proteases also exhibit cuticle morphology defects reflecting their multiple roles during development. The nematode astacin (NAS) proteases (also termed M12A) are discussed distinctly in section 1.14.

The cysteine proteases were first linked to moulting on the basis of assays using specific protease inhibitors in *D. immitis* (Richer *et al.,* 1993). Since their identification in parasites cathepsin-L (CPL) and Z-like (CPZ) proteins have been characterised and their activities attributed to embryogenesis and moulting. CPLs have been cloned in *C. elegans* and characterised in *Onchocerca volvulus*, *Brugia malayi* and *Brugia pahangi* all have localisations, temporal expression patterns, and RNAi/inhibitor phenotypes consistent with their role in moulting (Hashmi *et al.,* 2002; Guiliano *et al.,* 2004). Localisation of CPL-1 has been shown in embryonic yolk vesicles where it has been linked to the essential role of this protease in embryonic development (yolk processing) (Britton and Murray, 2002; Hashmi *et al.,* 2002). RNAi of *cpl-1* is embryonic lethal indicating that this is its primary role (Britton and Murray, 2002). These results, complemented with the fact that *cpl-1*, when expressed four hours prior to the moult, becomes localised to both the old and new cuticles, indicate that CPL-1 has roles in moulting and embryonic development (Hashmi *et al.,* 2002).

Two *C. elegans* cathepsin Z proteins are found in the genome, with *cpz-1* being expressed concurrently with each moult (Hashmi *et al.,* 2004). *cpz-1* RNAi treated animals have moult defects and some degree of embryonic lethality; and additionally, have abnormal head, tail and gonad morphology, these morphological disruptions implicate CPZ-1 as also having a role in cuticle synthesis. Such a role, distinct from the moult, is consistent with the adult expression of a *Toxocara canis* homologue and the function that human forms of this protease have in tumour progression (Hashmi *et al.,* 2004).

1.12.2 Moulting in trichostrongylid parasites

Moulting in trichostrongylid parasites is poorly understood, although sharing similarities with *C. elegans* moulting, described above. However, a distinct deviation from the *C. elegans* system of moulting occurs at the L2 to L3 transition. At this stage the moulting process is not completed, and ecdysis does not immediately follow late lethargus. L3 animals instead are retained within the protective sheath of the L2 cuticle, termed L3(2M), and await the correct, species-specific, cues to exsheath from the retained L2 cuticle. Exsheathment occurs in L3(2M) nematodes by the proteolytic digestion of the retained L2 cuticle by a component of the exsheathment fluid (EF). Isolated L3(2M) cuticles exposed to EF form refractile rings (Ozerol and Silverma.Ph, 1972; Gamble *et al.,* 1989b), these denote the points at which the cuticle degrades and burst open to release the cuticle cap and the sheathed animal (Ozerol and Silverma.Ph, 1972). The refractile rings of *Haemonchus contortus* occur at two invariant points on the cuticle; the first occurs 20µm from the anterior tip of the worm and the second 9µm from the anterior tip of the worm (Ozerol and Silverma.Ph, 1972). In *H. contortus* exsheathment has been attributed to an unknown 44kDa Zn^{2+} metalloprotease, and the EF of *H. contortus* has been shown to cross-react and induce exsheathment in other clade V trichostrongylid parasites including; *O. ostertagi*, *C. oncophora* and *H. placei* (Gamble *et al.,* 1989), thus demonstrating a conservation of substrate and enzymology between these trichostrongylid parasites. An aim of this thesis was to determine if such conservation was noted between *C. elegans* moulting enzymes and the process of exsheathment in trichostronglids, see chapter 7, as such enzymes could become potential anti-nematode drug targets.

1.13 Control of cuticle component gene expression and moulting

The factors controlling cuticle component expression, and the site of cuticle biosynthetic enzyme activity, localise within hypodermal tissues (Page and Winter, 2003).

1.13.1 Nuclear hormone receptors

Nuclear hormone receptors (NHR) are a class of ligand-regulated transcription factors, members of which have been shown to be associated with the correct synthesis and ecdysis of the *C. elegans* cuticle (Lam *et al.,* 1997; Gissendanner and Sluder, 2000; Frand *et al.,* 2005). *C. elegans* has an expansive family of *nhrs* with 284 of these transcription factors

found within the genome, approximately 20 of which have been genetically analysed with most having homologues within other metazoans (Mooijaart *et al.,* 2005). The *C. elegans nhrs* have been shown to associate with the processes of sex determination, life span, cuticle formation, developmental timing, diapause, and moulting (Asahina *et al.,* 2000; Gissendanner and Sluder, 2000; Mooijaart *et al.,* 2005; Silhankova *et al.,* 2005). Two such *nhr* which are associated with the process of moulting are *nhr-23* and *nhr-25*. A *Drosophila melanogaster* steroid hormone controled homologue of *nhr-23* termed *DHR3* has similarly been shown to be involved in ecdysis (Lam *et al.,* 1997; White *et al.,* 1997). Expression of *C. elegans nhr-23* has been noted in hypodermal cells throughout development (Kostrouchova *et al.,* 2001), and has been found to be involved with the expression of genes including *mlt-7, mlt-9, mlt-10, mlt-11, nas-37, acn-1* and the cuticle collagen *dpy-7*, which cause moult (all except *dpy-7*) and cuticular defects by RNAi (Frand *et al.,* 2005). *nhr-25* also has a *D. melanogaster* homologue in βFTZ-F1, which is regulated by DHR3, and in which disruption leads to ecdysis defects (Lam *et al.,* 1997; White *et al.,* 1997). Knockouts of *nhr-25* in *C. elegans* were embryonic lethal, with embryos failing in the epidermally controlled process of elongation (Asahina *et al.,* 2000). RNAi of *nhr-25* caused larval lethality, morphological and moult defects. *nhr-25* like *nhr-23* also exhibited hypodermal expression throughout development (Silhankova *et al.,* 2005).

The NHRs required for proper moulting might be responding to, or producing, the hormonal cues to moult, mediated by the expression of zinc-finger transcription factors which could be controlling the production of proteases such as NAS-37 (Frand *et al.,* 2005). The data gathered regarding NHRs involvement with the moulting process provides evidence, for a hormonal cue to moulting (Kurzchalia and Ward, 2003).

1.13.2 Megalin-like receptor

Megalin is a mammalian protein associated with the uptake of cholesterol, of which LRP-1 is a *C. elegans* homologue. *lrp-1* mutants exhibit; moulting defects, larval arrest and slight dumpyness (Yochem *et al.,* 1999). The moult defects noted in *lrp-1* disrupted worms are identical to the phenotype noted when worms are grown in media lacking cholesterol; however, the moult defective phenotype takes two generations to become evident in worms grown in presumably cholesterol-free conditions compared with the *lrp-1* mutants which did not show a time-lag in expressing the mutant phenotype (Kurzchalia and Ward, 2003). This time-lag associated with the sterol deprived worms can be somewhat explained by noting the quantities of cholesterol required for wild type moulting in *C. elegans*. Standard

growth conditions contain 2000 times more (5 µg/ml) cholesterol than is required to reverse sterol deprived arrest and allow wild type transitions between life cycle stages (Merris *et al.,* 2003). Also, flow of cholesterol has been noted from adult into oocytes by yolk proteins known as vitellogenins (Matyash *et al.,* 2001). This may provide sufficient quantities of exogenous cholesterol for the synthesis of ecdysones in the first generation. The small quantities of cholesterol required by *C. elegans* preclude it as a component of the ECM, and instead direct it as a signalling molecule (Kurzchalia and Ward, 2003).

Based on the similarity of LRP-1 to megalin, its localisation on the apical surface of hyp7 cells (Yochem *et al.,* 1999) and phenocopy of cholesterol deprived worms, it would appear that LRP-1 is involved with the uptake of essential exogenous cholesterol (Kurzchalia and Ward, 2003). This dependency upon cholesterol suggests that moulting is an ecdysoan controlled system, a claim supported by the moult defective phenotypes noted in *nhr-23* and *-25* disrupted worms. However, no steroid hormones or ecdysones have been isolated in nematodes, a peculiarity considering the number of nuclear hormone receptors found in the *C. elegans* genome, many of which have steroid-binding receptor homologues in other organisms (Sluder *et al.,* 1999). Additionally, synthesis of ecdysteroids from cholesterol in nematodes has not been demonstrated with *C. elegans* appearing not to have homologs of the *Drosophila* ecdysone receptor complex genes (Kurzchalia and Ward, 2003). Ecdysteroid signalling in insects is mediated by the ecdysone receptor complex that is composed of a heterodimer of the ecdysone receptor (EcR) and ultraspiracle (UsP, which is the *Drosophila* homologue of the vertebrate RXRs, the receptors for 9-*cis* retinoic acid) proteins (Vogtli *et al.,* 1998). EcR and UsP are both members of the *nhr* superfamily and interact with steroid hormone 20-hydroxyecdysone which controls a hierarchical response ultimately controlling the development of both larval and imaginal tissues in moulting and metamorphosis in *Drosophila* (Vogtli *et al.,* 1998).

1.13.3 Heterochronic genes

A family of genes have been identified in *C. elegans* that appear to act, almost exclusively, in the control of the relative timing of stage-specific events, and are termed heterochronic genes. Heterochronic genes, which include *lin-4*, *lin-14*, *lin-28*, and *lin-29*, cause precocious or retarded development of certain cell lineages, leading to, for example, larvae with adult tissues or adults with larval tissues. The heterochronic gene *lin-29* has been shown to regulate the expression of collagen genes (Liu *et al.,* 1995). The product of the *lin-29* gene is a zinc-finger transcription factor that has been shown to affect expression of stage-specific collagen genes such as COL-19, an adult specific collagen (Liu *et al.,* 1995;

Newman *et al.,* 2000). In a *lin-29* loss-of-function mutant the worm enters a cycle of synthesis and shedding of the L4 cuticle (Liu *et al.,* 1995; Page and Winter, 2003), thus *lin-29* is a member of the heterochronic regulatory pathway and has an action associated with termination of the moulting cycle. As stated previously NHRs may be controlling the moulting cycle through mediation of zinc-finger transcription factors, *lin-29* could be such a transcription factor, possibly in response to a hormonal signal (Page and Winter, 2003).

1.14 The Nematode Astacins

The nematode astacins (NAS) are a large group of enzymes comprising 40 distinct members, (compared to the six of higher organisms such as mice and humans (Mohrlen *et al.,* 2003)) and all bar the pseudo gene NAS-40 can be shown to be expressed (Mohrlen *et al.,* 2003). In the *C. elegans* NAS enzymes there are three major discernable protein regions: a pre-pro portion, the central catalytic astacin domain and long C-terminal extension with its presumably regulatory functionality. Within this C-terminal extension: Epidermal Growth Factor like (EGF-like); Complement subcomponents C1r/C1s, the sea urcin protein Uegf and Bmp-1 (CUB); Six Cystine repeats (SXC or ShK); and Thrombospondin type-1 (TSP-1) domains can be distinguished (Mohrlen *et al.,* 2003). Mohrlen *et al* (2003) classed these 40 individuals into six distinct groups (I-VI) based upon the structural differences of their regulatory unit. The structural constituents of the astacin genes indicate processing of collagens as their likely function. This is supported by two subgroup V members which exhibit pro-collagen proteolytic activity (DPY-31/NAS-35) (Novelli *et al.,* 2004) and proteinaceous eggshell degradation (HCH-1/NAS-34) (Hishida *et al.,* 1996).

Astacin Domain

Astacin domains are present in all 40 of the *C. elegans* NAS family members. They lie N-terminally to various linked domains and are proteolytic in nature (Mohrlen *et al.,* 2003). As a zymogen the N-terminus of the pro-peptide must be cleaved to activate the astacin domain. As noted with NAS-37 this can be an auto-catalytic event (Davis *et al.,* 2004). However, other family members may lack this auto-regulatory capacity and may require accessory proteases in order to adopt their activated peptide conformation.

The astacin domain is found in many taxonomic kingdoms with; astacin, a digestive enzyme from Crayfish the first protein isolated containing this domain (Pfleider.G *et al.,* 1967); MEP1A, a human multiple domain membrane component that is constructed from a homologous alpha and beta chain; Bone Morphogenetic Protein 1 (BMP-1), which in

vertebrates induces cartilage formation, bone formation and expresses metalloendopeptidase activity (C-terminal pro-collagen processing); and tolloid from *D. melanogaster*, which is involved with dorso-ventral patterning within the developing embryo of *D. melanogaster* and which interacts with decapentaplegic (a TGF-β family member).

The nematode astacins are Zn^{2+} metalloproteases, with the Zn^{2+} coordinated by three amino acid ligands (Bond and Beynon, 1995). The known metal ligands are His, Glu, Asp or Lys with at least one other residue, which may play an electrophilic role, required for catalysis. Members of this family contain two conserved disulphide bonds, joined Cys1-Cys4 and Cys2-Cys3 (Bond and Beynon, 1995). A HExxH motif is present in the astacin domain and has been shown by crystallography to be, in part, associated with the co-ordination of the Zn^{2+} ligand (Bond and Beynon, 1995). HExxH is a common motif, but can be further refined for the metalloprotease class of enzymes to abxHEbbHbc, where 'a′ is most often valine or threonine, 'b' is an uncharged residue and 'c', a hydrophobic residue. 'c' is never a proline residue as this could break the helical structure adopted by this metalloprotease motif (Rawlings and Barrett, 1995). The astacin domain assumes a kidney shape with a deep grove (Gomisruth *et al.,* 1993), with the zinc ion at the bottom of this grove (Gomisruth *et al.,* 1993). Astacin protease domains also share common features with serralysins, matrix metalloendopeptidases, and snake venom proteases. They cleave peptide bonds in polypeptides such as insulin B chain badykinin and in proteins such as casein and gelatin; they also have arylamidase activity (Bond and Beynon, 1995).

Epidermal Growth Factor domain (EGF)

A homologous stretch of 30-40 residues in length, found in the protein epidermal growth factor (EGF), has been shown to be present in many animal proteins in a relatively well conserved form (Doolittle *et al.,* 1984; Appella *et al.,* 1988). The varied group of proteins found to contain the EGF like domain appear to be unrelated, thus the functional significance of the EGF like domain remains unclear. However, a common feature is that EGF like domains are found in the extracellular domain of membrane-bound proteins or in proteins known to be secreted (Appella *et al.,* 1988). Within the EGF domain are six cysteine residues, which have been shown to be involved with inter-domain disulphide bonding (Bond and Beynon, 1995), the distance between the conserved cysteines is varied. The EGF domain adopts a two-stranded beta sheet followed by a loop and a short C-terminal two-stranded sheet (Appella *et al.,* 1988).

CUB domain

The CUB domain, an extracellular approximately 110 residue long domain, is functionally diverse and predominantly found in developmentally regulated proteins (Bork, 1991; Bork and Beckmann, 1993), and in peptidases of the astacin and chymotrypsin families.

A large proportion of CUB domains contain four conserved cysteines that form two disulphide bonds, Cys1-Cys2 and Cys3-Cys4, and is predicted to occupy a beta-barrel conformation. Proteins that have been found to contain the CUB domain include mammalian complement subcomponents C1s/C1r (Bork, 1991), which form the calcium-dependent complex Cys1, the first component of the classical pathway of the complement system; hamster serine protease Casp, which degrades type I and IV collagen and fibronectin in the presence of calcium (Kinoshita *et al.,* 1989) and vertebrate BMP-1.

Six-Cysteine Domain (ShK)

The six-cysteine domain is comprised of a 30 amino acid sequence that has six conserved cysteines forming three disulphide bonds (Pennington *et al.,* 1999). This domain is found in a number of *C. elegans* proteins and also in metridin, a toxin from *Metridium senile* (brown sea anemone) (McElwee *et al.,* 2004). A number of proteins which contain this domain belong to the metalloproteinases families M10A, M12A and M14A. The majority belonging to the M12A astacin family of metalloproteinases (Pan *et al.,* 1998).

Thrombospondin domain (TSP-1)

An approximately 60 residue long domain characterised by a highly conserved motif of WSxW, and which also contains six conserved cysteine residues within its N- to C-terminal length. Structural studies have shown that the TSP-1 domain contains two amphipathic turn regions and a hydrophilic beta-strand (Smith *et al.,* 1991). The protein thrombospondin, in which the TSP-1 repeat was first determined, is a cell adhesion molecule that interacts *via* specific domains with a wide array of extracellular matrix components including collagens, fibrinogen, fibrin, fibronectin, and heparan sulfate proteoglycan (Smith *et al.,* 1991). The TSP-1 domains themselves have a number of functions, including effects on cell attachment, motility, proliferation, the activities of extracellular proteases, and inhibition of angiogenesis (Smith *et al.,* 1991). Proteins containing TSP-1 domains have been shown to mediate ecdysis and ECM (collagen) remodelling (Adams, 2001; Goicoechea *et al.,* 2002; Suzuki *et al.,* 2004); thus, NAS enzymes (subgroup V exclusively) which contain this domain were of interest with regard to their effects in ECM synthesis and degradation.

From the domain constituents of the NAS family of *C. elegans,* it is within reasonable probability to propose their role would be in the proteolytic cleavage of peptides. It was the aim of this thesis to determine which members of this expansive, other than DPY-31/NAS-35, were involved with processing of cuticle collagens and to what extent their involvement was in the generation/degredation of a functional ECM. Due to the expanded nature of the NAS family *C. elegans* is an ideal model organism in which to study NAS functionality.

1.15 Collagen N- and C-terminal proteases

Proteases are required for cleavage of the N- and C-termini of collagen precursors, this processing is an essential step for the proper folding of collagens (Prockop *et al.,* 1998; Page and Winter, 2003; Page *et al.,* 2006). Two such proteolytic enzymes in *C. elegans* are BLI-4 and DPY-31, which cleave the N- and C-terminal processing sites of the cuticular collagens respectively.

1.15.1 DPY-31/NAS-35 a C-terminal collagen proteases

Few gross morphological defects have been attributed to loss of NAS activity. Of those which do exhibit morphological defects the most severe is *dpy-31/nas-35*, which has been implicated in the C-terminal proteolytic cleavage of SQT-3 collagens (Novelli *et al.,* 2004).

Vertebrate collagens have been shown to be cleaved by a member of the astacin family of zinc-dependent M12 metalloproteases, bone morphogenic protease-1 (BMP-1), (Li *et al.,* 1996; Prockop *et al.,* 1998). BMP-1 and its larger splice variant, mammalian TOLLOID (mTld), both exhibit pro-collagen C-proteinase (PCP) activity (Takahara *et al.,* 1994), with the *Drosophila melanogaster* homologue of mTLD also having been shown to establish the dorsoventral axis of embryos (Hishida *et al.,* 1996; Li *et al.,* 1996). The vertebrate BMP-1/mTld astacin proteases have been shown to cleave a number of different substrates including ECM pro-collagens, and have also been shown to direct bone and cartilage formation, highlighting a wide range of roles for these enzymes in both developmental and mature systems (Hartigan *et al.,* 2003).

Novelli *et al.* (2004) demonstrated that the *dpy-31/nas-35* (subgroup V) loss-of-function mutants have severe cuticular defects (e.g., Dpy phenotype) as well as larval- and embryonic-lethality. These defects were attributed to the lack of C-terminal cleavage of

the SQT-3 substrate. The C-terminal protease recognition site of SQT-3 is the YCALD motif which all 49 members of the SQT-3 collagen family encode, making it likely that this subgroup of collagens are targets of C-terminal proteolysis by DPY-31/NAS-35 (Novelli *et al.,* 2004). Orthologues of DPY-31 have been identified in *B. malayi* and *H. contortus* and are currently being cloned and characterised (Dr G. Stepek University of Glasgow, personal communication).

1.15.2 BLI-4 an N-terminal collagen protease

BLI-4 is the *C. elegans* homologue of a family of calcium dependent subtilisin-like serine endoproteases (Thacker and Rose, 2000; Thacker *et al.,* 2000b). This family of proteases cleaves a wide range of proteins (such as pro-α-mating factor in yeast, prohormones, proneuropeptides, growth factors and adhesion molecules in humans, bacterial toxins and viral glycoproteins) in order to convert them from inactive pro-peptides to active mature peptides (Thacker and Rose, 2000).

C. elegans cuticle collagens are most similar to the vertebrate FACIT collagens, which are not subjected to N-terminal proteolytic cleavage (Mazzorana *et al.,* 2001). Despite this fact, all of the characterised *C. elegans* collagens contain the characteristic subtilisin-like RxxR cleavage recognition site at their N-terminus (Kramer, 1994), which may be targeted by the proteolytic activity of BLI-4 (Thacker *et al.,* 2000b). Four subtilisin-like genes exist in the *C. elegans* genome (*kpc-1*, *kpc-2*/*egl-3*, *kpc-3*/*aex-5* and *kpc-4*/*bli-4*) with only BLI-4 eliciting cuticle processing activities, demonstrated by the Bli phenotype associated with mutations in the *bli-4* coding region (Thacker *et al.,* 2000b). All bar one of the *kpc-4*/*bli-4* mutant alleles are embryonic or larval lethal (Thacker *et al.,* 2000b), the viable *e937* mutant allele exhibits adult specific cuticular blistering (Peters *et al.,* 1991). Embryonic lethality and adult blisters illustrate that BLI-4 is essential during embryogenesis and important in adult cuticle generation (Peters *et al.,* 1991). The early developmental role for BLI-4 could be in the maintenance of the larval cuticle or in the processing of other substrates not associated with the ECM (Peters *et al.,* 1991; Thacker *et al.,* 2000b). Since the viable *bli-4(e937)* worms appear wild type at larval stages, it seems that the larval and adult cuticle requirements are distinct, perhaps the different stages of development are dependant upon different splice isoforms, as the viable *e937* mutant allele only affects a subset of the nine possible *bli-4* isoforms (Peters *et al.,* 1991; Thacker *et al.,* 1995). Hypodermal and neuronal tissues have shown *bli-4* expression (Thacker *et al.,*

2000b), highlighting its cuticular association and possibly illustrating non-cuticular roles for BLI-4 also.

bli-4 is a complex gene which has multiple splice variants, as stated above. The first twelve of the 24 exons of the *bli-4* gene are alternatively spliced to specific downstream exons. This produces nine proteins (BLI-4 A-I) which, typically for the subtilisin-like family, are themselves synthesized as inactive precursors with common pro-, catalytic and P domains (P domains are only found in propeptide convertase subtilase enzymes (Lipkind *et al.,* 1998)) but different C-terminal domains (Thacker *et al.,* 2000b). The C-terminal domains are thought to contain motifs that determine different sub- and possibly extracellular localisations of the isoforms.

The blistered phenotypes associated with the viable *e937* mutant allele are only noted in adult worms, this is also the only stage of the worm where a clear medial layer and struts are evident. Blisters have been shown to be caused by incomplete or absent struts which leads to the separation of the cuticle at the medial layer (Page *et al.,* 2006). The struts, which are collagenous structures are absent in the *bli-1* and *bli-2* mutants, therefore implicating *bli-1* and *bli-2* encoded collagens as crucial components of the struts, reinforced by detection of BLI-1::GFP fusion protein in the adult struts (J. Crew and J. Kramer personal communication). It was also shown in the *e937* mutant that adult strut specific collagen BLI-1 was not secreted into the struts, suggesting that the target for BLI-4 was the BLI-1 and possibly BLI-2 collagens. The isoforms present in the mutant worms containing the *e937* allele must therefore modify all other collagens correctly during development but are not able to process the adult, strut specific collagens which leads to the Bli phenotype. This confers substrate specificity as well as stage specific activity for BLI-4.

A BLI-4 homologue, *blisterase*, has been isolated in the parasitic nematode *Onchocerca volvulus*, which contains a RRKR cleavage site. Seven subtilisin-like homologues have also been isolated from the human genome (Poole *et al.,* 2003).

1.15.3 BLI-5 a potential serine protease inhibitor of BLI-4

A kunitz-type serine protease inhibitor encoded by F45G2.5 has been proven to be the mutant locus *bli-5* (Simmer *et al.,* 2003; Page *et al.,* 2006). *bli-5* encodes an EB domain and a kunitz-type pancreatic protease inhibitor domain, similar kunitz-type inhibitor domains have also been described in a number of parasitic nematode species including

Ancylostoma caninum (Hawdon *et al.,* 2003) and *Ancylostoma ceylanicum* (Milstone *et al.,* 2000). The EB domain found in BLI-5 is a nematode specific moiety which contains eight conserved cysteine residues which are presumed to form disulphide bridges, and which are usually found in association with kunitz domains. From sequence analysis of a *bli-5* point mutant an essential serine residue was found within the EB domain. Changing this essential residue, such as in the *e518* mutant allele, to a hydrophobic leucine resulted in the pleiotropic mutations associated with the *bli-5* locus becoming evident (Page *et al.,* 2006). This serine residue was also found to be conserved in an *O. ostertagia* homologue of BLI-5 (Page *et al.,* 2006). Disruptions to *bli-5* result in moult and cuticle defects, the most notable being adult specific blisters. The adult specific Bli phenotype proposed an association of BLI-5 with the collagenous struts, as was illustrated by the incomplete, or lack of, struts noted in *bli-5(e518)* mutant worms viewed by TEM (Page *et al.,* 2006). How BLI-5 activity contributes to cuticle synthesis is as yet unknown. However, it is likely that its role is in the control of proteolysis through interaction with BLI-4, which is conceivable as the cuticle collagen disruption pattern of BLI-5, the shared phenotypes and the shared tissue expression patterns between BLI-5 and BLI-4 are all consistent with such an association (Page *et al.,* 2006). Further supporting this proposed association, kunitz-type inhibitors have been shown to control tissue remodelling enzymes in *D. melanogaster* (Kress *et al.,* 2004).

The RxxR motif of collagens targeted by BLI-4, is also shared by other, presumably proteolytically activated, enzymes. NAS-37, which is associated with moulting in *C. elegans*, (Davis *et al.,* 2004) and NAS-35/DPY-31 the C-terminal pro-collagen cleavage enzyme (Novelli *et al.,* 2004) (both of which belong to subgroup V) both contain an N-terminal RxxR site. Therefore the function of BLI-5 may be to direct control of BLI-4 and/or another subtilisin-like protease that is performing this critical proteolytic activation (Page *et al.,* 2006).

1.16 Basement membrane collagens

The basement membrane is the second type of ECM found in *C. elegans*. Basement membranes are thin sheets of specialised molecules that form an ECM underlying the hypodermis and surrounding tissues such as the pharynx, intestine and body wall muscles (Kramer, 1997). All animals have a basement membrane the primary function of which is to anchor down the epithelium to its loose connective tissue underneath. In *C. elegans* the basement membrane is comprised of just two essential collagens LET-2 and EMB-9 (Guo

et al., 1991; Gupta *et al.,* 1997; Norman and Moerman, 2000), homologues of the type IV vertebrate collagens. Mature basement membrane collagens also adopt the triple helical structure previously described for cuticular collagens. Mutation in either one of the basement membrane collagens results in temperature sensitive lethality at the 3-fold stage of embryogenesis for null mutants, and at the 2-fold stage for glycine substitutions (Guo *et al.,* 1991), such substitutions will disrupt the triple helix nature of the collagen trimers. Higher order structures are maintained by lysyl derived cross-links which require lysyl residue hydroxylation. The importance of such cross-linking is indicated by the embryonic lethality observed upon inhibiting LET-268, the only lysyl hydroxlylase found in the *C. elegans* genome and which is specific for basement membrane collagens (Norman and Moerman, 2000). Cuticular collagens of most developmental stages do not contain hydroxylysine (Cox *et al.,* 1981b).

1.17 Cuticle synthesis in parasites

1.17.1 Collagens of parasites

Collagens have been isolated in numerous parasitic nematode species: *Ascaris suum* (Kingston *et al.,* 1989), *Brugia malayi* (Selkirk *et al.,* 1989; Scott *et al.,* 1995), *Brugia pahangi* (Bisoffi and Betschart, 1996), *Globodera pallida* (Gray *et al.,* 2001), *Haemonchus contortus* (Shamansky *et al.,* 1989), *Meloidogyne incognita* (Vandereycken *et al.,* 1994), *Ostertagia circumcincta* (Johnstone *et al.,* 1996b) and *Trichinella spiralis* (Fu *et al.,* 2005). Estimates of collagen gene family size in parasites suggest that all are multi-gene families (Shamansky *et al.,* 1989; Gray *et al.,* 2001). Like the *C. elegans* collagens those isolated from parasitic nematodes are small (typically 3kb) and are highly conserved between species (Kingston *et al.,* 1989; Shamansky *et al.,* 1989; Gray *et al.,* 2001). Direct homologues have been demonstrated between the tandemly duplicated *C. elegans* collagen genes *col-12* and *col-13* and the similarly arranged *O. circumcincta* collagen genes *colost-1* and *colost-2* (Johnstone *et al.,* 1996b). It is proposed that the duplication event which gave rise to *col-12* and *col-13* in *C. elegans* is the same event which generated *colost-1* and *colost-2* in *O. circumcincta*. Such is the conservation between nematode species, that *C. elegans* collagens are more closely related to orthologues in other nematode species than they are to paralogous collagens, for example *col-1, col-2* and *dpy-13* are more closely related to the *H. contortus* 3A3, 8E and 2C collagen genes than they are to collagen genes in other *C. elegans* sub-families (Shamansky *et al.,* 1989).

Subtilisin-like cleavage sites can also be identified in parasitic nematode collagens such as *H. contortus* 3A3 cuticle collagen (Shamansky *et al.,* 1989), (at residues 76-79) *M. javanica Mjcol-3* product (Koltai *et al.,* 1997), (residues 88-91) and in the *colost-1* and *colost-2* encoded collagens from *O. ostertagia* (Johnstone *et al.,* 1996b).

1.17.2 Conservation of collagen biosynthetic enzymes in parasites

As a high degree of conservation of cuticular collagens is noted between nematode species, a logical assumption would be that the enzymes associated with the maturation of these conserved molecules would be similarly conserved. Two such key enzymes associated with collagen maturation have been isolated from parasitic species; PDI, isolated in *O. ostertagia* and *O. volvulus* (Wilson *et al.,* 1994; Geldhof *et al.,* 2003); and PHY, in *O. volvulus* and *B. malayi* (Merriweather *et al.,* 2001; Winter *et al.,* 2003). Of these orthologues the PHY-1 α-subunit of the *B. malayi* P4H, (P4H as described in section 1.9.1 is usually a tetrametic enzyme composed of two PHY α-subunits and two PDI β-subunits) was found to be soluble and active without PDI (Winter *et al.,* 2003). However, this isolated *B. malayi* PHY-1 homologue failed to rescue the complementary *C. elegans* mutant when introduced as a transgenic free-array. The only known example of heterologous rescue of *C. elegans* mutants using a *B. malayi* orthologue was achieved with *B. malayi* PDI-2 rescuing the *C. elegans pdi-2(tm0689)* mutant (Dr A. Winter University of Glasgow, personal communication). Enzyme conservation has been demonstrated between the trichostrongyles of clade V, where an unknown 44kDa Zn^{2+} metalloprotease, isolated in the exsheathment fluid of *H. contortus*, was able to cause exsheathment of *O. ostertagia, C.onchophorea* and *H. placei* isolated L3(2M) cuticles (Gamble *et al.,* 1989).

Work presented within this thesis highlights two Zn^{2+} metalloprotease enzymes of the NAS family which are responsible for ecdysis in *C. elegans* and which also elicit exsheathment responses in isolated cuticles of *H. contortus* (Davis *et al.,* 2004)*, O. ostertagia, C.onchophorea* and *H. placei*. Thus, such data supports that there is some degree of conservation of the enzymes associated with collagen maturation/degradation between the free-living and parasites nematodes of clade V. These enzymes could represent possible chemotherapeutic targets for anti-nematode drugs.

1.18 Trichostrongylid parasites

Trichostrongylid parasites have a general life cycle which has been adapted to suit the particular needs of each species; however, each life cycle retains certain key features, see Figure 1.5. The life cycle of trichostrongylids begins with adults, which may be attached to the villi of abomasum or small intestine (species-specific) of a host and which may feed on blood (e.g., *H. contortus)* producing smooth-walled eggs that are excreted in an unembryonated state in host faeces. Larvae then developed under favourable conditions inside the egg and the L1 hatches from the egg and feeds on detritus. After two moults the larvae have reached L3, the infective stage. The L3 larvae, retaining the previous stages L2 cuticle (sheath) and which may now be termed L3(2M) for larval stage three, second moult, can migrate to the tip of plants where the retained L2 cuticle allows the infective stage larvae to remain for a prolonged period without desiccating. If the host ingests the L3(2M) nematodes, exsheathment then occurs within the hosts' gastrointestinal tract, releasing the infective stage larvae. Some species may at this stage burrow into the mucosa while other species continue to moult and become L4s and adults while attached to the villi. In some species (e.g., *O. ostertagia)* the fourth-stage larvae may hibernate inside the mucosa for 3-5 months; this phenomenon is described as hypobiosis and is a common feature of nematode development. In spring these L4s complete their development and become mature after one further moult. Therefore a common feature of trichostrongylid parasites is their dependence upon a robust protective sheath and ability to shed that retained sheath. Conservation of the enzymes associated with the process of exsheathment has been shown between *C. elegans* and *H. contortus* (NAS-37 (Davis *et al.,* 2004)) and between *H. contortus* and other trichostrongylids (unknown Zn^{2+} metalloprotease (Gamble *et al.,* 1989)).

The whipworms *(Trichuris)* of clade I, which would be considered the most divergent from the trichostrongylids of clade IV (Gilleard, 2004), have a similar dependence upon removal of a retained protective structure, as they develop to L3 within a retained eggshell. Following ingestion, the eggshell is degraded and the infective parasite released. We have shown here, chapter 7, that NAS-37 (which is involved in ecdysis) also has an association with hatching along side HCH-1/NAS-34*,* a subgroup V nematode astacin gene in which mutants cause severe hatching delays (Hishida *et al.,* 1996), and which is a close homologue of *nas-37*. If orthologues to either of these genes are found in clade I parasites this would be a significant discovery as such genes could become specific common chemotherapeutic targets against diverse nematodes. If this was the case, and orthologues

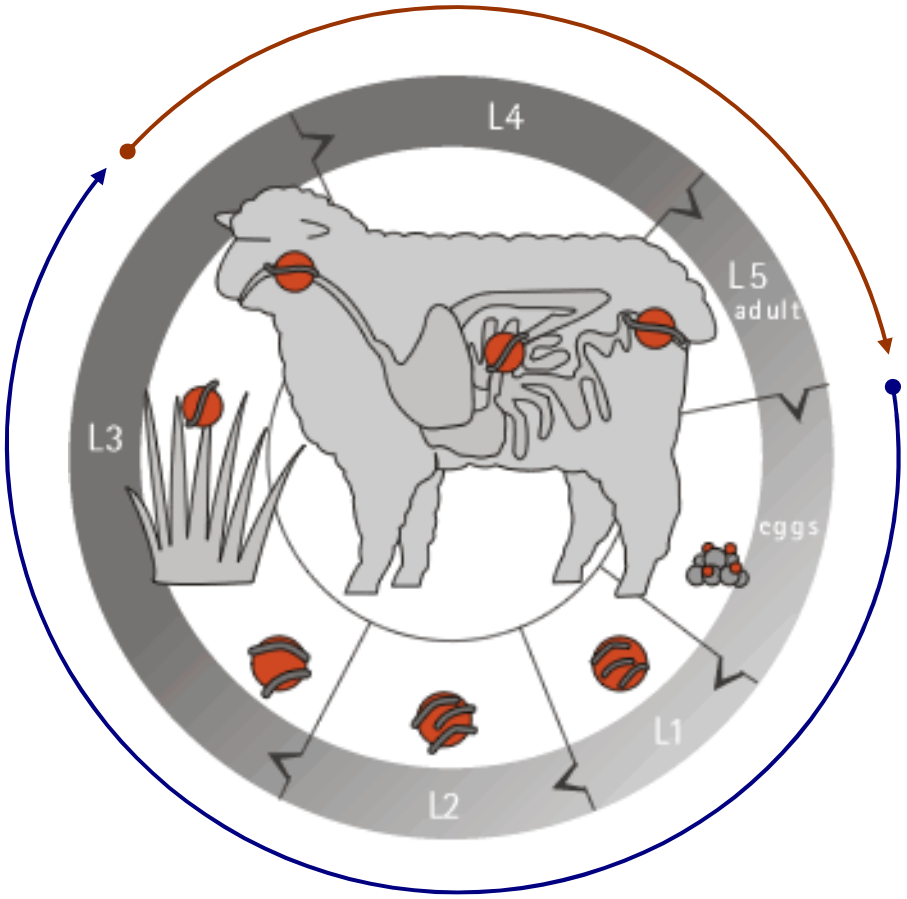

Figure 1.5: Generalised schematic representation of the trichostrongylid parasite life cycle. The blue arrow highlights the free-living stages, and the red arrow the parasitic stages of the life cycle. L3 trichostrongylids retain their L2 cuticle until they are within the host, whereupon it is shed releasing the infective L3 parasite. Taken from www.ovita.co.nz.

were found, it places an importance on the study of enzymes associated with cuticle degradation (moulting) and hatching.

1.19 Possible chemotherapeutic targets for parasite control

Current anti-nematode drugs, although effective, have notable limitations and resistance is becoming an issue (Dent *et al.,* 2000; Leathwick *et al.,* 2001). The commonly used anti-nematode drugs ivermectin and benzimidazol are both non-specific, targeting cellular processes shared by both host and parasite: glutamate-gated chloride channels (GluCls) and microtubule/actin cytoskeleton respectively. As such these drugs can target not only the parasite but the host too, which in some instances can prove fatal (Barkwell and Shields, 1997; Neff *et al.,* 2004). Therefore a need arises for specific drugs with specific parasitic targeting.

Given the ancestral roots of moulting, many of the components associated with this process are likely to be conserved among the nematodes, illustrated by Gamble *et al*, (1989) who demonstrated that *H. contortus* exsheathment fluid was conserved between trichostrongylid parasites. Consequently, an obvious target for a nematode-specific drug would be the moulting cycle, as there is likely to be little conservation between mammals and Ecdysozoans with respect to the enzymes associated with the moulting process. As previously stated, parasites such as the trichostrongylids, must shed a retained cuticle and moult at least once within the host before they become mature and can reproduce. Enzymes associated with this process could prove to be novel targets for anti-nematode drugs (Lustigman, 1993; Craig *et al.,* 2007). In *C. elegans* we have a suitable model to identify possible targets, and conservation has already been demonstrated between ecdysis in *C. elegans* and *H. contortus* exsheathment (Davis *et al.,* 2004).

1.20 Project aims

The aims of this study were as follows:

1) To screen the *qsox* and *nas* families by RNAi in various *C. elegans* backgrounds, principally TP12, a GFP collagen marker strain, to isolate possible cuticle associated candidates.

2) To generate deletion mutants in selected cuticular candidate genes of the *qsox* and *nas* gene families.

3) Characterisation of deletion mutants and functional determination of selected candidates with regard to their expression profiles and involvement in cuticle collagen biosynthesis and degradation.

4) Determination of enzymology and substrate conservation in the process of ecdysis between free-living *C. elegans* and veterinary important trichostrongylid parasites.

Chapter 2: Materials and Methods.

2.1 Standard Reagents

Ampicillin:	100 mg/ml ampicillin (Sigma) in sterile distilled H_2O Filter sterilised and stored at -20°C
BSA:	bovine serum albumin 10 mg/ml (NEB). Stored at –20°C.
Chloramphenicol:	12.5 mg/ml chloramphenicol (Sigma) in 100% ethanol. Stored at –20°C.
Coomassie blue solution:	0.25 g of Coomassie brilliant blue R-250, 45% methanol, 10% glacial acetic acid. The solution was filtered though a Whatman no. 1 filter to remove particles.
DEPC H_2O:	0.1% (v/v) diethylpyrocarbonate (Sigma) in sterile distilled H_2O mixed overnight and autoclaved. Stored at room temperature.
Destain solution:	45% methanol, 10 % glacial acetic acid.
DTT:	dithiothreitol (Sigma) in sterile distilled H_2O. 1M stock stored at -20°C.
EDTA:	ethylenediaminetetra-acetic acid in sterile distilled H_2O. Stock solution of O.5 M, pH 8.0. Autoclaved and stored at room temperature.
Ethidium bromide:	8 mg/ml in sterile distilled H_2O. Stored at 4°C.
IPTG:	isopropyl-β-D-thiogalactoside (Promega) in sterile distilled H_2O. Stock concentration of 1M filter sterilised and stored at –20°C
Kanamycin:	50 mg/ml stock in dH_2O. Stored at –20ºC
L-broth:	1% bacto tryptone (Difco), 0.5% yeast extract (Difco), 0.5% NaCl in sterile distilled H_2O, pH 7.0 NaOH. Autoclaved and stored at room temperature.
LB-agar:	L-broth + 15 g/L bacto-agar (Difco). Autoclaved and stored at room temperature.
M9 buffer	3% KH_2PO_4, 6% Na_2HPO_4, 5% NaCl, 10 mM $MgS0_4$. 10X stock autoclaved and stored at room temperature.
NGM-agar:	0.3% NaCl, 1.7% agar (Difco), 0.25% peptone (Difco), 0.0003% cholesterol (1 ml/L of 5 mg/ml stock in ethanol), in

	sterile distilled H_2O. Autoclaved and 1 ml/L 1M $CaCl_2$, 1ml/L 1M $MgSO_4$ and 25 ml/L KPO_4 (pH 6.0) added.
MOPS (20X):	1M MOPS, 1 M Tris base, 69.3 mM SDS (2% w/v), 20mM EDTA. Purchased from Invitrogen.
PBS:	phosphate buffered saline: 7.31 g NaCl, 2.36 g Na_2HPO_4, 1.31 g NaH_2PO_4 2H20 in 1 L, pH 7.2. Autoclaved and stored at room temperature.
PBST:	Same as the above with Tween® added to a final concentration of 0.2%. Stored at room temperature.
Proteinase K:	20mg/ml proteinase K (Roche) in sterile distilled H_2O. Stored at -20°C.
Recovery buffer:	2% glucose in 1X M9 (made fresh each time).
SDS:	sodium dodecyl sulphate (Sigma) in H_2O. Stock solution 10% stored at room temperature.
SOB medium:	20g bacto-tryptone, 5g bacto-yeast extract, 0.5g NaCl, 10ml of 250mM KCl in 1 L dH_2O (pH 7.0). Stored at room temperature.
SOC medium:	400µl of filter sterilised solution of 1M glucose added to 20ml SOB medium. Aliquots stored at –20ºC.
TAE:	50X stock, 2M Tris Base, 5.7% Acetic acid, 50mM EDTA. pH 8.0, in sterile ditilled H_2O. Stored at room temperature
TBE:	10X stock, 0.9M Tris-HCl, 0.9M Boric acid (Sigma), 25mM Na_2EDTA pH8.0, in sterile distilled H_2O. Stored at room temperature.
TE buffer:	10 mM Tris, 1mM EDTA, pH 8.0).
Tetracycline:	12.5mg/ml tetracycline hydrochloride (Sigma) dissolved in 50% ethanol. Stored at -20°C
Tris-HCl:	2-amino-2-(hydroxymethyl)-1,3-propanediol-hydrochloride.
Tween-20:	Polyoxyethylenesorbitan monolaurate (Sigma).
Tetracycline (1000X):	12.5 mg/ml stock dissolved in 50% ethanol. Stored at -20ºC
X-gal:	5-bromo-4-chloro-3-indoyl-β-D-galactoside (Promega) dissolved in N,N'-dimethyl-formamide and stored at –20°C out of light. Stock concentration of 2% (w/v) X-gal.

For all other solutions see (Sambrook *et al.,* 1989).

2.2 *E. coli* strains

Name	Genotype	Notes	Use
OP50	Tet^R	Variant of the uracil-requiring OP50 strain Tet^r marker. A gift from CGC.	Food source of *C. elegans*
HT115 (DE3)	F-, mcrA, mcrB, In(rrD-rrE)1, rnc14::Tn10(DE3 lysogen: lacUV5 promoter-T7 polymerase)	Tetracycline resistant, IPTG inducible promoter, T7 polymerase, RNAse III minus (Timmons *et al.,* 2001).A gift from CGC.	RNAi feeding
XL10-gold™	Tet^RΔ(mcrA)183Δ(mcrCB-hsdSMR-mmr)173 endA1 supE44 thi-1 recA1 gyrA96 relA1 lac Hte [F' proAB $lacI^qZ\Delta M15$ Tn10 (Tet^R) Amy Cam^R]	Ultra competent cells, blue white selection, recA and endA1 mutations that cleave cloned methylated DNA have been deleted. (Stratagene)	General cloning
OneShot® TOP10 cells	F^- mcrA Δ (mrr-hsdRMS-mcrBC) Φ 80lacZΔM15 ΔlacX74 recA1 araΔ139 Δ (ara-leu)7697 galU galK rpsL (Str^R) endA1 nupG	Competent cells that are derived from DH10B™ cells, blue white selection, recA and endA1 minus (as above), mutations in mcrA, mcrB and mrr genes (as above), do not require IPTG during cloning. (Invitrogen).	General cloning
M15(pREP4)	NaI^S, Str^S, Rif^S, Thi^-, Lac^-, Ara^+, Gal^+, Mtl^-, F^-, $RecA^+$, Uvr^+, Lon^+	Contains a repressor plasmid (pREP4) that produces high levels of *lacI* to prevent leaky expression prior to induction. Kanamycin resistance. (Qiagen).	Expression of recombinant proteins
BL21 (DE3)	*E. coli* B F– *dcm ompT hsdS*(rB – mB –) *gal* λ(DE3)	Used in conjunction with PQE series of plasmids for (Invitrogen).	Expression of recombinant protein
BL21(DE3) pLysS	*E. coli* B F– *dcm ompT hsdS*(rB– mB–) *gal* λ(DE3) [pLysS Camr]	Provide tighter control of protein expression than BL21 (DE3): resistant to chloramphenicolc (Invitrogen).	Expression of recombinant protein
BL21 Star™ (DE3)	F^- *ompT hsdS*$_B$ (r_B^- m_B^-) *gal dcm rnel31* (DE3)	BL21 Star™ cells significantly improve the stability of mRNA transcripts and increase protein expression yield from T7 promoter-based vectors (Invitrogen).	Expression of recombinant protein

Table 2-1: *E. coli* strains used in cloning and protein expression.

2.3 Vectors and Plasmids

Name of vector/plasmid	Notes and use
PCR-Script	A PCR fragment cloning system used for cloning blunt end PCR fragments (Stratagene).
PCR® 2.1 TOPO TA	A PCR fragment cloning system used for cloning A-tail PCR fragments (Invitrogen).
pGEM-T	A PCR fragment cloning vector used for cloning A-tail PCR fragments (Promega).
pQE-30	An IPTG inducible vector for high-level expression of N-terminally His-tagged recombinant proteins (Invitrogen).
pPD129.36 (L4440)	Vector with two T7 promoter regions flanking the multiple cloning site. Functions as a template during *in vitro* RNA synthesis for RNAi microinjection and soaking. Can also be transformed into HT115(DE3) an *E. coli* strain for RNAi by feeding (Timmons *et al.,* 2001). A gift from A. Fire (Carnigie Institution of Washington, Baltimore, USA).
pPD95.03	Used to fuse the promoter of a heterologus gene in-frame to a *lacZ* reporter. A gift from A.Fire
pPD95.75	Used to fuse the promoter of a heterologous gene in-frame to a GFP marker. A gift from A. Fire.
pAB-1	PCR-Script backbone fused with an *unc-54* 3′ UTR, with the restriction sites *Sph*1/*Nco*1 added to 5′ of the UTR as a MCS. Used for *in vivo* expression of *C.elegens* genes, see section 2.29.3.2.2 and Figure 2.1.

Table 2-2: List of vectors and plasmids used.

2.4 Nematode strains

2.4.1 Maintaining nematode strains

Most strains and transgenic lines were maintained at 20ºC (unless otherwise stated) on NGM agar plates (9 cm, 5.5 cm or 3.5 cm diameter plates (Greiner)) seeded with OP50 as a food source, according to standard procedures (Sulston and Hodgkin, 1988). Starved plates (i.e. those devoid of bacteria and containing dauer larvae) were stored at 15ºC. Worms were picked onto fresh plates when necessary.

C.elegans strains

Strain	Genotype	Source
N2	Wild Type	CGC
TP12	*kaIs12* (COL19::GFP)	Page laboratory
TP73	*qsox-1(ka2);TP12(kaIs12)*	Page laboratory
F35G2.1a	*qsox-2(tm1977)*	NBP-Japan
TP87	*nas-36(tm1636)*	Page laboratory
VC1209	*qsox-2(ok1669)*	CGC
TP101	*qsox-1(ka2);qsox-2(tm1977)*	Page laboratory
TP55	*nas-37(ox199);*TP12*(kaIs12)*	Page laboratory
TP99	*nas-37(tm410)*	NBP-Japan
JC201	*nas-34/hch-1(ut110)*	CGC
TP93	*nas-36(tm1636);nas-37(tm410)*	Page laboratory
TP97	*nas-34(ut110)/nas-37(tm410)*	Page laboratory
TP67	*pdi-1(ka3)*	Page laboratory
TP68	*pdi-2(tm689)*	NBP-Japan
TP66	*pdi-3(ka1)*	Page laboratory
TP88	*TP70 (ka2);TP66 (ka1)*	Page laboratory
TP64	*nas-28(ka5)*	Page laboratory
TP111	*(ka6)*	Page laboratory
TP20	*sqt-3(e2117)*	CGC
*dpy-31**	*nas-35(e2770)*	J.Hodgkin laboratory
ero-1	*ero-1(ok1287)*	CGC
Trichostrongylid parasites		
Species	**Allele**	**Source**
Haemonchus contortus	Wild Type	Moredun Research Institute
Teladorsagia circumcincta	Wild Type	Moredun Research Institute
Trichostrongylus colubriformis	Wild Type	Moredun Research Institute
Trichostrongylus vitrius	Wild Type	Moredun Research Institute
Cooperia oncophora	Wild Type	Moredun Research Institute

Table 2-3: Nematode strain list. * Grown at 15°C

2.4.2 Prolonged storage of C. elegans

Large populations of *C. elegans* strains were washed from NGM agar plates into 15 ml tubes using 1X M9 buffer. Worms were allowed to settle and form a pellet and washed thoroughly in the same buffer (3 x 15 ml washes). Worms were transferred to 1.5ml screw top microfuge tubes in 500 µl 1X M9 and then a similar volume of freezing solution (5.85g NaCl, 6.8g KH_2PO_4, 300g glycerol, 5.6ml of 1 M NaOH in 1L dH_2O. Autoclaved and 3ml of 0.1M $MgSO_4$ added.) was added. After mixing well, tubes were slowly frozen at –80ºC using an insulated container. Worms were stored at –80ºC or in liquid nitrogen. Worm cultures could be recovered by thawing tubes and pipetting worms onto an OP50 NGM agar plate and incubating at 20ºC.

2.5 Bacterial cultures

2.5.1 Antibiotic concentrations for bacterial culture

Antibiotics in bacterial cultures were used at the following final concentrations:

Ampicilin: 100 µg/ml

Tetracycline: 12.5 µg/ml

Kanamycin: 25 µg/ml

Streptomycin: 12.5 µg/ml

Chloroamphenicol 37.5 µg/ml

2.5.2 Bacterial culture on solid media

All *E. coli* strains were grown by incubation at 37ºC for 16 hours on L-agar plates (9 cm diameter plates, Greiner Ltd) supplemented with the appropriate antibiotic and 1 mM IPTG for colour selection if appropriate.

2.5.3 Liquid cultures of bacteria

Using sterile techniques, single colonies were transferred to L-broth supplemented with an appropriate antibiotic. Cultures were grown for 16 hours at 37ºC in an orbital shaker.

2.5.4 Making competent M15 cells

25 µl of a 10 ml L-broth cultures of M15 (non-competent) cells that had been grown overnight were used to inoculate 25 mls of L-broth and cultures were grown in an orbital shaker until an OD600 of 0.4 was reached. Cultures were then centrifuged (10 minutes, 3000 rpm, 4ºC) to form a cell pellet, which was subsequently resuspended in 0.5 x volumes (of the original culture volume) of cold 10 mM $CaCl_2$. This cell suspension was kept on ice for 30 minutes, centrifuged and resuspended in 0.1 volumes of 75 mM$CaCl_2$. Glycerol (sterile) was added to 10 %, the cell suspension was aliquoted and fast frozen on dry ice.

2.6 Purification and synthesis of DNA and RNA

2.6.1 Phenol:chloroform extraction and ethanol precipitation

High purity DNA or RNA was obtained using phenol:chloroform extraction. This involved the addition of 1X volume of phenol:chloroform:isoamyl alcohol (24:25:1) (Sigma-Aldrich) to a DNA/RNA solution. It was important that for DNA, phenol at pH 8.0 was utilised while phenol at pH 4.5 was used for RNA purification. The mixture was vortexed for 1 minute and then spun at full speed in a bench top centrifuge for 2 minutes. The top layer was removed to a fresh tube and an equal volume of chloroform:isoamyl alcohol (24:1) added to it. This was vortexed, spun and separated as the previous step. DNA/RNA was precipitated using 100% ice-cold ethanol (2 volumes) and either $1/25^{th}$ volume of 5 M NaCl or $1/10^{th}$ volume of 3 M Sodium acetate ($C_2H_4O_2Na$) (pH 6.0). This mixture was stored for 15 minutes at –80ºC and then pelleted in a bench top centrifuge at full speed for 30 minutes. The pellet was washed using 1 ml of 75% ice-cold ethanol (spun immediately for 10 minutes and then discarded). The DNA/RNA pellet was air dried and resuspended in an appropriate volume of TE buffer.

2.6.2 N2 genomic DNA isolation

Mixed stage populations of the N2 strain of *C. elegans* were washed off NGM agarose OP50 plates using 1X M9 buffer. After multiple washes with the same buffer, the worms were pelleted by centrifugation, 6 volumes of 1X worm lysis buffer was added. Worm suspensions were disrupted in a glass hand-held homogeniser and subsequently incubated at 65ºC for 4 hours. Debris was removed by centrifugation and multiple phenol:chloroform (pH 8.0) and chloroform extractions, followed by an ethanol precipitation. Purified DNA, resuspended in 500 µl of TE buffer was treated with RNace-It ™ Ribonclease Cocktail (Stratagene) (a cocktail of RNase A and RNase T at a final concentration of 80 µg/ml (RnaseA) and 4 Units/ml (RNase T)) for 1 hour at 37ºC. Finally, DNA was purified by phenol:chloroform extraction and ethanol precipitation and the resulting pellet of genomic DNA was resuspended in 150 µl of TE buffer. Throughout the process of genomic DNA extraction, extreme care was taken to avoid the shearing of DNA. Thus, vortexing or vigorous pipetting was avoided. 100-500 ng of genomic DNA was used in 50 µl PCR reactions.

5X worm lysis buffer:	0.25 M Tris-HCl (pH 8.0), 0.5 M NaCl, 0.25 M EDTA pH to 8.0, autoclave and store at 4ºC.
1X worm lysis buffer:	The above 5X stock solution was used to make 1X solution freshly, resulting in final concentrations of: 50 mM Tris-HCl (pH 8.0), 100 mM NaCl, 50 mM EDTA, 1% SDS, 30 mM β-mercaptoethanol, 100 µg/ml Proteinase K (Roche).

2.6.3 Production of mixed stage N2 cDNA

Production of cDNA required that mRNA be isolated from cultures, purified, and then used as a template for synthesis of first strand cDNA.

2.6.3.1 Total RNA isolation

100-1000 µl of mixed populations of *C. elegans* were pelleted and then lysed in a 4 x volume of Trizol reagent (Invitrogen) using vigorous intermittent vortexing over a 20 minute period (in a fume hood). Insoluble material was removed by centrifugation (at 14 k on a bench top centrifuge (Avanti™ 30- Beckman) for 10 minutes at 4ºC) and the resulting supernatant was subjected to purification using 2 x volumes of chloroform isoamyl alcohol (vortex 15 seconds, incubate at room temperature for 2 minutes and then centrifuge 14 K for 15 minutes at 4ºC). Isopropanol was used to precipitate the RNA from the aqueous phase by mixing, incubating at room temperature for 10 minutes and centrifugation at top speed for 10 minutes to form a pellet. The RNA pellet was subsequently washed in 75% ethanol (which had been made up in DEPC-treated H_2O), pelleted by centrifugation at 7,500 k for 10 minutes (4ºC), and resuspended in 200 µl of DEPC-treated H_2O.

2.6.3.2 Purification of mRNA

A Poly (A) Quik® mRNA isolation kit (Stratagene) column kit was used to purify the total mRNA from the total RNA isolated above. Supplied oligo (dT) columns accommodate up to 500 µg of total RNA in volumes ranging from 200 µl to 1 ml and therefore the concentration of the purified total RNA was calculated and the sample diluted and aliquoted accordingly. Procedures, as detailed in the manufacturer's instructions, were followed with the final pellet being resuspended in 15 µl of DEPC-treated H_2O. mRNA was quantified using a spectrophotometer.

2.6.3.3 Synthesis of first strand cDNA

A heterogeneous population of cDNA molecules was generated *via* first-strand synthesis. In this study, the Stratagene RT-PCR Kit was utilised and the manufacturer's instructions followed. In order to use the amounts of mRNA required in each reaction (50-100 ng), the samples from above were aliquoted into an appropriate number of reactions. The primers utilised were the oligo(dT)primers.

2.7 Polymerase chain reaction (PCR) based amplification and cloning

2.7.1 PCR conditions and polymerases

All PCR reactions were carried out using a Robocycler Gradient 96 PCR machine (Stratagene) in 25 µl volumes, unless otherwise stated. Conditions of the program were altered according to the requirements of the PCR product and were altered in single reactions in order to optimise the purity and efficiency. In terms of the program cycle, an initial denaturing step was generally carried out for 5 minutes at 95ºC, with the cycling program typically consisting of 35 cycles with: a denaturation step of 92-95ºC for 1 minute and an annealing step of 52-56ºC (primer dependant) for 1 minute and elongation step at 72ºC. The length of the elongation step was adjusted according to the length (in bp) of the amplified region and the identity of the DNA polymerase used: *Taq* polymerase (Applied Biosystems, Promega) has an activity of approximately 1 kb/minute while *Pfu* (Stratagene) and *Vent* (New England Biolabs) polymerases have extension times of roughly 0.5 kb/minute.

Each of these polymerases were used with suitable buffers at a final concentration of 1X in the 25 µl reaction: Pfu (used at 2.5-5 unit of enzyme per reaction) was used with the supplied Pfu buffer (10X) while Vent (used at 2-4 units per reaction) was used with the supplied Thermopol buffer (10X). Reactions in which Taq was the polymerase, used a mix containing separate 25 mM $MgCl_2$ (final 2.5 mM) and buffer (either 5X or 10X Applied Biosystems, Promega respectively). 1 unit of Taq was typically used per reaction. 25 µl Reactions also contained: 15 pmols of each oligonucleotide primer (forward and reverse) (purchased from Invitrogen), 100-500 ng of DNA and 90-250 µM of each dNTP (Promega). The exact PCR conditions and primers used are detailed specifically where appropriate. Pfu and Vent were utilised when the highest accuracy of amplification was required since these enzymes can proof-read for nucleotide miss-incorporations using their 3′ to 5′-exonuclease activity.

Buffers:

10X Cloned *Pfu* buffer:	200 mM Tris-HCl (pH 8.8), 20 mM $MgSO_4$, 100 mM KCl, 100 mM $(NH_4)_2SO_4$, 1% Triton X-100, 1 mg/ml nuclease-free BSA.

10X Thermopol buffer: 100 mM KCl, 200 mM Tris-HCl (pH 8.8 at 25°C), 100 mM $(NH4)_2SO_4$, 20 mM $MgSO_4$, 1% Triton X-100.

2.8 Purification of PCR products

2.8.1 Agarose gel electrophoresis

Linear fragments of nucleic acids were separated according to size using agarose gel electrophoresis. Agarose (Invitrogen) was dissolved in 1X TAE buffer to form gels with w/v ratios ranging from 0.6% to 2%. Samples were loaded into gel wells with DNA sample buffer at a final 1X concentration alongside a suitable DNA size standard (1kb ladder or 50kb ladder (both from GibcoBRL) and gels were run in 1X TAE-filled electrophoresis tanks from GibcoBRL with typical voltages of 100-150V.

DNA was visualised by soaking gels in a bath of 0.2 µg/ml of ethidium bromide in H_2O for 20 minutes (ethidium bromide, which is visible under UV light, chelates to the major groove of nucleic acids). A UV tranilluminator (Biorad) was then used to visualise images which were then captured using a QualityOne program (Biorad). Alternatively, ethidium bromide could be added to the molten agarose (2 µl/100 ml, 0.002%).

2.8.2 Gel purification

The PCR products resulting from the above reactions were run on agarose gels and, to separate any unwanted amplification products and primers, the band of the required size was excised. A QIAquick (Qiagen) Gel extraction kit was used, following the instructions as directed for using a mini-spin column and microcentrifuge. Two consecutive elutions were carried out, in which 15 µl of dH_2O, that had been incubated at 50ºC, was loaded onto the mini-spin column and allowed to stand for 1 minute before being centrifuged. The two elution fractions, containing the purified DNA were pooled. This protocol was also used to separate out DNA fragments from restriction digests (section 2.13).

2.9 Transfer vectors

All gel purified PCR products were first cloned into a transfer vector before being inserted into the vector of specific function. This method was used because the efficiency of restriction digestion is reduced when sequences flanking the recognition sites are shorter in

length. Thus, in some cases, the efficiency of restriction digestion of pure PCR products would be low. The use of transfer vectors is also useful because they provide a means of ligating a DNA insert into a vector that is generally much more efficient than many other vectors in terms of ligation. Thus, instead of repeating the PCR reaction as a means of producing more product, the original PCR product can be efficiently ligated into these vectors and can be replicated via transformation into bacteria.

The two predominant transfer vectors utilised were pCRScript (Stratagene) and TOPO T-A (Invitrogen). These differ because the former requires inserted DNA to have blunt ends (for insertion into an *Srf* I site) while the latter requires A-overhangs. Taq and other low fidelity polymerases generate T-overhangs and so were cloned into TOPO vectors immediately. However, polishing the ends was required in order to prepare them for insertion in to pCRScript. Conversely, fragments generated by Pfu and Vent are blunt ended and therefore, it was necessary for A-overhangs to be generated for their insertion into TOPO. Protocols for both the polishing of PCR product or the addition of 3′ A-overhangs are detailed in the pCRScript and TOPO TA cloning instruction manuals respectively. Similarly, the methods by which PCR products were ligated into each of these vectors is detailed in the manufacturer's instructions.

2.10 Transformation of *E. coli* bacteria

2.10.1 E. coli strain transformation

pCRScript ligations were transformed into 40 µl of XL10-Gold ultracompetent cells (Stratagene) while TOPO-TA ligations were transformed into 50 µl of the supplied TOP10 One Shot® cells (chemically competent). All transformations carried out in this thesis were carried out in the same way, i.e. a heat shock method, unless otherwise stated. Approximately 5-10 ng of plasmid DNA was added to competent cells (on ice). These were left on ice for 30 minutes and then incubated in a water bath at 42ºC for exactly 30 seconds. Cells were allowed to recover for 2 minutes on ice before 400 µl of pre-warmed SOC medium was added. Cells were placed in an orbital shaker at 37ºC for 1 hour (in which time the antibiotic resistance gene product could be synthesised). Cell suspensions were spread on LB + antibiotic plates, dried and grown overnight at 37ºC. For blue/white colour selection of transformants, plates were supplemented with 100 µl of 0.1M IPTG and 100 µl of 2% X-Gal.

The same method as described above was used to transform plasmid DNA into HT115(DE3) cells (which are tetracyclin resistant), the strain used in the RNAi feeding method. However, the heat shock step was carried out at 37ºC for 1 minute.

A similar method to that above was used to transform both BL21(DE3) and BL21(DE3) pLysS cells with the exception that 1-50 ng of DNA was used per reaction and the heat pulse was carried out at 42ºC for 20 seconds. BL21(DE3) pLysS strains are chloroamphenicol resistant < 40 µg/ml.

Similarly to BL21(DE3) and BL21(DE3) pLysS cells M15 cells are transformed with 1-50 ng of DNA per reaction with the heat pulse adjusted to 90 seconds at 37ºC all other stages of the transformation procedureare as outlined above.

2.11 Selection of positively transformed colonies

In order to determine positively transformed bacterial colonies colour selection (blue/white selection), colony PCR screening or restriction digestion was utilised.

2.11.1 Blue/white colour selection

When vector permitted, blue/white screening of colonies was performed. Vectors that can be used for colour screening contain the regulatory sequences and N-terminal sequences for *E. coli* protein β-galactosidase, coded for by *lacZ* gene. Embedded within the *lacZ* coding sequence is a multiple cloning site that does not affect the reading frame of the peptide but results in the addition of a few amino acids. Plasmids encoding the N-terminal of β-galactosidase are used in conjunction with host *E. coli* cells that code for the C-terminal portion of protein. Neither peptide alone is active but when both are present they can associate and form an active protein. Cells expressing both peptides turn blue when grown on the artificial substrate analogue X-gal. Consequently, colonies that have failed to take up any insert are blue while successfully ligated plasmids appear white. It must be taken into account that a white colour is not a guarantee that there is an insertion or that, if there is an insertion, that it is the sequence of interest. Thus, this screening method should be used in conjunction with the following colony PCR screening or with a restriction digestion analysis using appropriate enzymes, sections 2.11.2 and 2.13.

2.11.2 Colony PCR screening

Transformants resulting from ligation into PCRScript, TOPO or other functionally specific vectors were identified as to whether they contained the desired insert using a PCR method with gene specific- or vector specific- primer sets. Alternatively a combination of one of each could be used which allowed for directional screening of insertions. For each construct, typically 30 (often many more) colonies were screened. A toothpick was used to pick a colony and streak some of the cells onto a gridded LB + antibiotic agar master plate which was then incubated overnight at 37ºC. The cells remaining on the toothpick were transferred to separate 50 µl aliquots of dH_2O and lysed by boiling for 5 minutes. 5 µl of the resulting cell lysate was then added to a 25 µl PCR reaction mixture containing 1 unit of Taq polymerase and 15 p/mols of a forward and reverse primer. A simple PCR program was used: 92°C 1 minute, 56°C 1 minute, 72°C 1 minute (35 cycles) and the products run on an agarose gel but, as stated previously, longer extension times were used if the fragment was particularly long. The maximum fragment length attainable by colony PCR was 3kb. Colonies amplifying fragments of the expected size were presumed to be positive transformants, and DNA preparations were made from them by returning to the gridded master plate to start L-broth cultures.

Vector	**Primer combinations (sequences in Table** 2-7**)**
pCRScript	1224 and M13 reverse
pGEM (Promega)	pGEM forward and pGEM reverse
pTAg (Invitrogen)	M13 Reverse and 1224.
PCR 2.1TOPO (Invitrogen)	M13 reverse and pGEM forward
pPD95.03*	M13 reverse and NLS reverse
pPD95.75*	M13 reverse and 96.04 or NLS reverse
pPD129.36* (L4440) (Timmons *et al.,* 2001)	L4440 F and L4440 R
PQE-30 (Qiagen)	PQE-30 forward and PQE-30 reverse

Table 2-4: Primer combinations for colony PCR screening of relevant vectors
*pPD series of vectors were a gift from A. Fire (Carnegie Institution of Washington, Baltimore).

2.12 Plasmid DNA preparations

The QIAGEN mini-spin columns and midi purification techniques are based on the alkaline lysis of cells in L-broth (+ antibiotic) cultures (5 ml for mini preps and 100 ml for Midi preps). The protocols supplied by the manufacture were used apart from an adjustment to the midi prep protocol that introduced an additional DNA precipitation step subsequent to isopropanol precipitation. Instead of proceeding immediately with the 70% ethanol wash, the isopropanol-derived pellet was resuspended in 200 µl TE buffer, ethanol precipitated (as detailed in section 2.6.1) and washed in 70% ethanol. The dried pellet was resuspended in 200 µl of TE buffer. Mini preps were eluted in 100 µl elution buffer. Midi preparation of DNA was used when higher purity of DNA was required. Such preparation also results in higher yields of DNA.

2.13 Restriction endonuclease digestion

Restriction enzyme digestion was used to verify the inclusion of an insert within a plasmid. However, the methods described here are relevant for all the restriction digestion reactions carried out in this thesis, apart from where otherwise stated. For analyses, 200-500 ng of plasmid DNA and approximately 2-5 units of restriction enzyme were used in 50 µl reaction volumes of 1X buffer supplied with the enzyme. Many enzymes are compatible with each other and could be used simultaneously in the same reaction mixture, even if it entailed using one of the enzymes at sub-optimal conditions (e.g. 50-75% efficiency). However, when this was not possible, it was necessary to digest using the two enzymes in succession, using one enzyme (2 hours 37ºC followed by heat inactivation) and ethanol precipitating the linear DNA before setting up the restriction digest with the second enzyme in its appropriate buffer. Incubations were typically carried out at 37 ºC for 2 hours unless another temperature was specified for the enzyme as recommended by the supplier.

These reactions were scaled up if the production of large amounts of linear fragments were required, for example, for ligation reactions (described below). In such cases 5 µg of DNA were used in similar 50 µl reactions. Even larger quantities of DNA could be digested by scaling up the volume of the reaction and using Midi prep DNA. For purification of specific products of restriction digestion, the reaction mixture was run on an agarose gel (of an appropriate percentage), the correct sized fragment was excised, and the DNA was extracted and purified as described in section 2.8.

2.14 Calf alkaline phosphotase (CIP) treatment of linearised vectors

In cases where restriction digestion of a vector had left blunt ends or two similar ends, prior to ligation, it was necessary to prevent recircularisation of the plasmid (without an insert) by dephosphorylation of the 5′ end. 10-20 units of CIP (New England Biolabs) were used in a 50 µl reaction volume that also contained 5 µg of linearised (and gel purified) DNA and any of the New England Biolab standard buffers (buffers 1-4) at a 1X concentration. Reactions were incubated at 37ºC for 1 hour, after which the dephosphorylated DNA was purified using the standard phenol:chloroform extraction method (including the choloroform purification and ethanol precipitation steps).

2.15 Ligations into other vectors

Ligation of insert and vector DNA was performed in a 20 µl reaction with 100 ng vector DNA and a 3:1 molar ratio of insert to vector in 1X T4 DNA ligase buffer. Ligations were left at 16°C overnight, or, 25ºC for 2hrs. 5-10 ng of DNA was then used to transform XL10-Gold ultracompetent cells. All subsequent manipulations including bacterial transformation, screening of bacterial colonies, plasmid preparations and restriction digests were performed as described earlier in Sections 2.10, 2.11 and 2.13.

2.16 Sequence analysis

The integrity of inserted DNA was verified by sequence analysis. Ethanol precipitated DNA samples (2 µg) were sent to MWG sequencing along with appropriate oligonucleotide primers. In some cases, primers were required that ensured the sequencing of the entire cloned sequence. However, in other circumstances, the cloning junctions (ligation sites) were the only segments that were required to be sequenced. Returned sequences were analysed using Vector NTi (Invitrogen) and its associated program, Contig Express, and compared against published gene sequences from WormBase[1].

[1] http://www.wormbase.org

2.17 Semi quantitative reverse transcriptase PCR (SQ RT-PCR)

A semi-quantitative reverse transcriptase PCR (sq RT-PCR) approach was used in order to examine the temporal expression patterns of members of the QSOX and NAS family. *sqt-3* collagen was also analysed. This method exploits the principal that *ama-1*, which encodes for a subunit of RNA polymerase II, is constitutively expressed throughout the larval and adult stages and that the expression level of a gene of interest can therefore be expressed in relative terms to the constant level of expression of *ama-1*. A set of staged cDNA samples representative of the mRNA population at two hours intervals throughout development (a gift from Iain Johnstone, WCMP, University of Glasgow, UK) (Johnstone and Barry, 1996) was used to amplify *ama-1* and the gene of interest using the sets of primers listed in Table 2-7. It was only necessary that short fragments of each be amplified. However, it was important that the region between the primers fell on either side of an intron that would not be present in the cDNA. This would enable the products amplified from any contaminating genomic DNA in the cDNA fraction, whose levels would not alter temporally, to be separated from products amplified from cDNA.

The conditions of the PCR reaction are based on the protocol described by the authors in (Johnstone and Barry, 1996) where the importance of not exhausting the reagents was emphasised. For each stage represented by a cDNA sample, a reaction was set up containing each of the four primers (a forward and reverse for both *ama-1* and the target gene) in excess (100 pmoles per reaction), appropriate amounts of the PCR buffer, 1-3 µl of the mixed stage cDNA sample and 1 µl of Taq polymerase. Refer to Table 2-7 for details of primers. 30 PCR cycles of 92 ºC 1 minute, 56ºC 1 minute and 72ºC 1 minute were used. 25 µl of each reaction mixture was run on a 200 ml 1% agarose gel containing 0.002% ethidium bromide and the DNA fragments visualised on a UV transilluminator. The images from the transilluminator were saved as a TIFF file which was analysed using ImageQuant software (Amersham Bioscience).

2.18 Splice leader PCR

To determine splice leader (SL) *trans*-splicing for *C. elegans qsox* and *nas* genes, RT-PCR was performed on *C. elegans* N2 mixed stage cDNA with Taq for 35 cycles. The primer sets used in SL-PCR were the forward primers; SL1, consensus nematode splice leader sequence 1; SL2, consensus nematode splice leader sequence 2, which were used singly in

conjunction with the reverse RT-PCR primers for *nas-36, nas-37*, T10H10.2, F35G2.1 and F47B7.2, see Table 2-7. Products from these reactions determined if primary transcripts were *trans*-spliced by either the SL1 or SL2 *trans*-spliced leader RNA sequences.

2.19 Promoter analysis

In order to asses the special expression of target genes, fusion constructs were generated between a designated promoter element from a target gene fused in-frame to a promoterless GFP or *lacZ* containing reporter vector.

pPD95.03 a vector containing the *lacZ* gene, that encodes the β-galactosidase enzyme, and a 5′ MCS in which to insert the *cis*-acting promoter element, was predominately used. In order to visualise the expression patterning of the target promoter element X-Gal staining was employed. X-Gal, being a substrate for the β-galactosidase enzyme, could be visualised in regions of β-galactosidase activity as a blue dot. The activity could be localised specifically to structures throughout *C. elegans* due to the presence of an SV40 nuclear localisation signal (NLS) inserted between the MCS and the *lacZ* element. A variety of similar pUC19-derived reporters are available from the laboratory of A. Fire.

Putative promoters for *qsox-1, qsox-2* and *qsox-3* were all PCR amplified from mixed stage N2 genomic DNA and T-A cloned into a suitable transfer vector before being excised and cloned into pPD95.03. *nas-36* was similarly amplified and cloned. The putative promoter elements included the ATG start codon and continued 5′ for distances of 2 and 4kbp. pPD95.75, a promoterless GFP vector which lacks a NLS was also used to assay the expression profile for *nas-37*. 3806bp of upstream genomic DNA was PCR amplified TA-cloned then excised as a *Pst*I/*Bam*HI fragment and cloned in frame to pPD95.75. This work carried out by M.Wayne Davis (University of Utah).

Transformation of *C. elegans* was performed by microinjection into the syncytial gonad of N2, as described in section 2.21. N2s were injected with constructs at 20 µg/ml and plasmid marker *dpy-7*::GFP at 10 µg/ml. At least three independent lines were examined for expression of β -galactosidase for each reporter construct.

Target gene	**Promoter fragment**	**Transfer vector**	**Restriction enzymes**	**Reporter vector**
qsox-1	3001bps	2.1 TOPO TA	*Sph* I/*Sma* I	pPD95.03

Target gene	Promoter fragment	Transfer vector	Restriction enzymes	Reporter vector
qsox-2	4001bps	TOPO 4 TA	*Pst* I/*Bam*H I	pPD95.03
qsox-3	2101bps	2.1 TOPO TA	*Pst* I/*Sma* I	pPD95.03
nas-36	2001bps	2.1 TOPO TA	*Pst* I/*Sma* I	pPD95.03
*nas-37**	3806bps	2.1 TOPO TA	*Pst* I/*Bam*H I	pPD95.75

Table 2-5: Promoter/reporter fusing constructs analysed. * Work carried out by M.Wayne Davis (University of Utah).

2.20 Staining for β-galactosidase activity

The method used is a variation on the procedure described in (Fire, 1992). Transgenic *C. elegans* containing reporter constructs were washed from mixed population NGM plates in 1X M9, concentrated by centrifugation and washed twice. The volume was reduced to 100 µl and an equal volume of 2.5% gluteraldehyde (Sigma) added. Suspensions were incubated for 20 minutes at room temperature with occasional gentle mixing, followed by two washes with 1X M9. The volume was reduced to 100 µl, worms pipetted onto microscope slides, vacuum dried, immersed in acetone at –20°C for 5 minutes and air-dried. 50-100 µl of staining mixture was added per slide, a microscope coverslip (BDH) added and sealed with nail varnish. Worms were checked every hour for staining or left overnight.

Staining mix (1 ml): 500 µl 0.4 M $NaPO_4$ (pH7.5), 1 µl $MgCl_2$, 100 µl Redox buffer (50 mM potassium ferricyanide, 50 mM potassium ferrocyanide), 4 µl 1% SDS, 400 µl H_2O. For the standard staining procedure 12 µl of 2% (w/v) X-gal was used in the mix; for sensitive staining, the mixture was pre-heated to 65°C then 12 µl freshly made 20% (w/v) X-gal added.

2.21 Transformation of *C. elegans*

2.21.1 Microinjection procedure

C. elegans was transformed by microinjection (Mello *et al.,* 1991), detailed methods for which can be found in (Mello and Fire, 1995). DNA for microinjection was prepared using the standard QIAGEN method. Plasmid constructs were co-injected with a selectable

marker to identify transformed progeny. Mixes for injection were made up to a final concentration of 120-200 µg/ml plasmid DNA in sterile distilled H_2O typically by the addition of pBluescript SKM, and centrifuged for 25 minutes at 13,000g before use (to pellet debris). Pads for mounting worms for injection were made from a small volume of molten 2% agarose (dissolved in distilled H_2O) solution added to a large coverslip, which was covered with another coverslip to spread solution into a thin layer. The top coverslip was removed and the agarose pad air-dried, or baked at 80ºC for 30 minutes. Needles were pulled on a computer controlled electrode puller model 773 (Campden Instruments) using 1.2 mm O.D X 0.69 mm I.D. borosillicate glass capillaries with standard wall and inner filament (Clark Electromedical Instruments). Nematodes were added to agarose pads under mineral oil (Sigma) and injected using an Axiovert-100 inverted microscope (Zeiss) equipped with a flat, free-sliding glide stage with centred rotation with DIC/Normaski optics. DNA was injected in to the hermaphrodite gonad using a micromanipulator guided needle and pressurised nitrogen. Recovery buffer (2% glucose, 1X M9) was added to injected worms on pads, after which they were transferred to fresh NGM OP50 plates in a pool of recovery buffer. Transformed progeny from injected hermaphrodites (F1 generation) were identified by the phenotype conferred by the co-injected marker plasmid. These are selected either clonally or in small groups of 4-10, and the next generation (F2) surveyed for transformants.

2.21.2 Behaviour of injected DNA

Oocyte nuclei in the adult gonad share a common core of cytoplasm. As they mature, individual nuclei are incorporated into plasma membranes along with a portion of the core cytoplasm. DNA injected in to this syncitium can also become incorporated into the oocyte. In a fraction of the F1 progeny (1-10%), recombination reactions occur between injected sequences that result in the formation of large tandem arrays. Recombination between co-injected plasmids occurs due to regions of homology within their vector backbones e.g. antibiotic resistance genes. Arrays that attain a large size can become heritable as extrachromosomal elements. Once assembled these elements are no longer targets for further intra-array recombination. The arrays are then transmitted at a frequency of between 5-95% and lines can be maintained indefinitely by selection of the phenotype conferred by the marker DNA. Both marker and construct DNA should be contained within these arrays thus nematodes expressing the marker phenotype should contain the construct. It is possible for arrays to form that do not contain any copies of the construct, especially if this is injected at a low concentration. To ensure construct DNA was

examined and that a result found in one line is not due to the particular rearrangement of DNA within a particular array, multiple lines (generally three or more) were normally examined for each set of injections. Only one F2 line was selected from any positive F1 plate of transformants, thus ensuring different lines were the product of separate rearrangement events.

2.21.3 Selectable markers of transformation

Plasmid pRF-4 (Mello *et al.,* 1991) (a gift from A. Fire, Carnegie Institution of Washington, Baltimore) was used as a marker for transformation by co-injecting it at 100 µg/ml. Plasmid pRF-4 contains a semi-dominant allele of the collagen gene *rol-6(su1006)* which is expressed from L3 onwards and in dauers. Transformants were identified by the right-hand roller phenotype conferred by this gene. Expression of GFP (Chalfie *et al.,* 1994); (Heim *et al.,* 1995), from the construct *dpy-7*::GFP (a gift from I. Johnstone, WCMP, Glasgow), which contains the DPY-7 cuticle collagen promoter fused to GFP, was also used as a selectable marker. This construct gives non-nuclear localised GFP expression in the hypodermal cells of transformed worms, with strong GFP expression detectable from embryo to L4, in dauers, and less strongly in adults. *dpy-7*::GFP was co-injected at a concentration of 5-10 µg/ml and transformants were selected by detection of GFP expression under UV light using a Stemi SV-6 dissecting microscope (Zeiss).

2.22 Cosmid rescue of *qsox* mutants

To specifically assign the effect absence of *qsox-1* in *C. elegans* a rescue cosmid T10H10 was injected into TP70*(ka2)* worms. T10H10 contains the entire coding region and 3′ UTR of *qsox-1*. Cosmid DNA was prepared by the same procedure used for plasmid DNA preparations (section 2.12). The cosmid was checked for the presence of *qsox-1* sequences by PCR using primers T10 PRO Fwd and T10 Prot Rev and microinjected into the strain TP70 at a concentration of 1 µg/ml or 5 µg/ml, with 10 µg/ml *dpy-7*-GFP marker and 150 µg/ml pTAG. Similarly *qsox-2(tm1977)* worms were injected with the cosmid F35G2, which contains the promoter, entire coding region and 3′ UTR for *qsox-2,* the presence of the transgene was determined by SWPCR, see section 2.26, using the F35 BX primer set, Table 2-7.

2.23 Microscopy of live nematodes

Nematodes were transferred to microscope slides (with 2% agarose/0.065% sodium azide pads). A small volume of 1X M9 was kept on the pad to prevent drying of samples and the coverslip added and sealed with white soft paraffin BP and viewed immediately. Nematodes were viewed as live specimens using an Axioskop 2 plus microscope with a AxioCam Mrm camera. Images were processed using Axiovision software.

2.24 Preparation of freeze-cracked specimens for immunolocalisation

Specimens for immunolocalisation assays were prepared using a freeze cracking method. Slides were prepared by the application of poly-L-lysine (0.1% w/v in H_2O) (Sigma diagnostics, MO, USA) and incubated at 80ºC until dry. Poly-L-lysine is an adhesive solution for adhering tissue sections to glass slides. Large populations of worms, prepared by washing either mixed stage or synchronous populations from NGM OP50 plates, were washed three times with 1X M9 buffer and allowed to settle and form a loose pellet. Sufficient buffer was left around the pellet to enable the worms to be pipetted using a glass pasteur. Approximately 20 µl of worm pellet was spread/spotted onto the dried poly-L-lysine slides. A glass coverslip was placed on top and slides were immediately placed at -80ºC for 20 minutes on a metal block. The cracking of the worms was carried out by using a scalpel blade to quickly remove the coverslip. Slides were then transferred to 100% methanol (20 minutes) at -20ºC, and then to 100% acetone (20 minutes) again at –20ºC, after which they were left to air dry at room temperature. Slides could be stored at -20ºC overnight or used immediately for immunolocalisation experimentation.

2.25 Immunolocalisation procedure for whole worm staining

Slides that had freeze cracked nematodes adhered to their surface were blocked with PBS 0.1% v/v Tween-20 and 1% w/v dried milk in PBST. This primary block could be incubated at RT for 2hrs or could be done at 4ºC overnight in the dark. Non-adherent worms were washed off the slides with PBST into 1.5 ml eppindorfs and retained. The slides were washed 3 times with PBST. The nematodes in the eppindorfs were spun gently, 200 rpm for 1 min, to remove the supernatant and washed, process repeated three times.

Primary antibodies were added at concentrations outlined in Table 2-6 and incubated for 2hrs at RT or overnight at 4ºC, in the dark. Sufficient primary mix was made to cover fully the adherent worm on the slides and also to add 200 µl to each of the eppindorfs containing the non-adherent nematodes, which were mixed gently. Slides and eppindorfs were washed extensively with PBST (in the dark) as above. The secondary antibody was added to the washed slides and eppindorfs at the concentrations outlines in Table 2-6 and incubated in the dark for a further 2hrs at RT. The slides again were washed in PBST similarly the eppindorfs. Following the final wash of the non-adherent worms the tube contents were taken up in 20 µl volumes of mount solution (50% glycerol, 0.5X PBS, 2.5% DABCO (Sigma)) and added back to the original slides, coverslips added and the slides sealed with nail varnish: slides were either viewed immediately or stored at 4ºC in the dark and viewed within 24hrs.

Antibody	Block	Primary	Secondary
DPY-7 monoclonal	1% milk (PBST)	1:50	1:100 Alexa flour 488 goat anti-mouse IgG (molecular probes)
MH27 monoclonal	1% milk (PBST)	1:100	1:100 Alexa flour 488 goat anti-mouse IgG (molecular probes)
SQT-3 polyclonal	1% milk (PBST)	1:100	1:100 Alexa flour 488 chicken anti-rabbit IgG (molecular probes)

Table 2-6: Probes and concentrations for antibody staining.

2.26 Single Worm PCR

Single worms were picked into 5µl of single worm lysis buffer, placed on dry ice for 15 minutes and then immediately incubated at 65ºC for 90 minutes. Finally, they were incubated at 90ºC for 20 minutes and allowed to cool. 20µl of PCR mix (section 2.7.1) was added to each lysis reaction and used in the following PCR programme: 30 cycles at 92ºC 1min, 56ºC 1 minute and 72ºC 1 minute per kbp (as non-proof reading low fidelity Taq was used): 3kbps is the maximum fragment length that can be easily amplified employing this method. Primers used for genotyping strains and for detection of microinjected constructs are outlined in Table 2-7.

Lysis buffer: 100 µg/ml proteinaseK, 10 mM Tris (pH 8), 50 mM KCl, 2.5 mM $MgCl_2$, 0.45% Tween® 20 (Sigma-Aldrich), 0.05% gelatin.

2.27 RNA interference (RNAi)

2.27.1 Construction of plasmids and transformation

Constructs that were not included in the RNAi library supplied by Julie Ahringer (Kamath *et al.,* 2003) had to be synthesised. Target genes were amplified by PCR, using the primers designated RNAi in Table 2-7, and were cloned into either TOPO or pCRScript transfer vectors. Fragments were excised from their transfer vectors by restriction digest and ligated into the similarly restriction digested MCS of the L4440 vector at a locale between L4440s two T7 promoters. During these standard cloning procedures, transformation of *E. coli* strains was into XL10-gold cells.

2.27.2 Growth of library RNAi clones

The library supplied by Julie Ahringer which has facilitated various genome wide screens (Kamath *et al.,* 2003; Simmer *et al.,* 2003; Frand *et al.,* 2005) contains 16, 757 bacterial clones that represent the RNAi feeding constructs of 86% of the *C. elegans* genome. Clones could be retrieved from the library by streaking LB Agar plates (Amp + Tet) with glycerol stock supplied in the feeding library. Plates were thereafter incubated at 37ºC overnight.

2.27.3 RNAi by feeding

Purified plasmid DNA of the clones that were not found within the RNAi library and which had been generated in accordance with section 2.27.1 were transformed into *E. coli* HT115 (DE3) cells (Timmons *et al.,* 2001) by the method described in section 2.9. Single colonies from Tet and Amp plates were used to inoculate 10 ml liquid LB cultures (Amp) and incubated at 37ºC overnight with shaking. Approximately 200 µl of culture was pipetted onto 4.5 cm diameter NGM Agar plates that had been supplemented with 1mM IPTG and 100 µg/ml of ampicillin. These were incubated at room temperature overnight in order to induce T7 RNA polymerase. Typically five L4 animals were picked onto each plate. Plates were incubated at 20ºC and/or 25ºC. However, *sqt-3* and *dpy-31* targeted RNAi experiments were carried out at 15ºC. After 24 hours the P0 worms should have egg laid and were scored for any phenotypes, then picked off and viewed (section 2.23). The plates containing the F1 larvae were monitored for phenotypes and allowed to develop for a further 24hrs. This method is based on the protocol described in (Kamath *et al.,* 2000).

2.27.4 In vitro transcription of RNA

In vitro synthesis of dsRNA was required in order to administer RNAi by microinjection and soaking. A construct containing a target fragment within an L4440 vector was used as a template for RNA synthesis by T7 RNA polymerase. As described above, the L4440 construct had been designed in order that the two T7 promoter regions encoded by the vector flanked the inserted gene. 10 µg of plasmid DNA was restriction digested in two separate reactions to create two populations of linearised DNA. Each had been digested appropriately in order that T7 polymerase would transcribe the inserted gene from opposing directions. It was important that complete digestion occurred. DNA was precipitated and extracted as described in section 2.6.1, and was diluted in 40 µl of DEPC-treated dH_2O. RNA was synthesised using a RiboMAX™ Large Scale RNA production system from Promega. The T7 reaction was set up and the subsequent removal of the DNA template steps were carried out as describe in the manufacturer's instructions. RNA was quantified with a spectrophotometer.

dsRNA was obtained by annealing the two complenentary RNA products together by incubating a mixture, containing 1 mg/ml of each RNA strand (in a 50 µl reaction (DEPC-treated H_2O)), at 37ºC for 30 minutes.

2.27.5 dsRNA microinjections

Double-stranded RNAi was administered by microinjection at a concentration of 0.4 mg/ml. Prior to injection, as described previously, samples were centrifuged to remove debris. A microinjection technique identical to that described in section 2.21.1 was performed. However, unlike DNA, it was not essential that the gonads were injected with the RNA solution as the RNAi effect spreads through the tissues of *C. elegans*.

2.28 Preparation of samples for electron microscopy

2.28.1 Scanning electron microscopy (SEM) preparation

An osmium tetroxide (O_2O_4) method of preparing SEM samples is required for *C. elegans,* due to the cuticle of the animal slowing the diffusion of the reagents used in other preparations. This work was carried out at the University of Glasgow's internal electron microscopy centre. 10 X 9-cm plates were used to produce a large mixed population of the

particular strain of nematodes being analysed. Nematodes were washed off plates using 1X M9 buffer, rinsed three times in the same buffer and transferred to a microfuge tube. 2.5% gluteraldehyde in PBS (pH 7.4) was added, the tube incubated for 90 minutes on ice, with occasional disruption of the pellet. The gluteraldehyde supernatant solution was discarded and the worms were washed three times in PBS + 2% sucrose. After the final wash, the volume was reduced to 50µl and an equal volume of 2% O_2O_4 was added. The tube was left at room temperature (in a fume hood) for 1 hour. Subsequently, the O_2O_4 was discarded and the pellet was thoroughly rinsed with 3 x 10 minute washes of PBS and 3 x 10 minute washes with dH_2O. Supplementary fixation to increase the stability of the tissues and increase the conductivity of the sample, was carried out using 0.5% uranyl acetate (aq) (1 hour in foil in fume hood) after which worms were washed 3 x 5 minutes in dH_2O. Worms were then dehydrated in a stepwise manner using increasing concentrations of acetone: 30% acetone, 50% acetone, 70% acetone, 90% acetone, absolute acetone and finally dried absolute acetone. For each step the incubation was 10 minutes at room temperature with the exception of absolute acetone which had 2x10 minute incubation. At this stage, animals were transferred to a critical point dryer (CPD) filter chamber containing 1µm polycarbonate filters. Samples were then processed in the critical point dryer (CPD) for 1hr 20 minutes. Worms were mounted onto copper double-sided tape by picking individual worms using a toothpick with an eyelash attached to the end, and were viewed using a Phillips 500 scanning electron microscope.

2.28.2 Transmission electron microscopy (TEM) preparation

The preparation of TEM samples is initially similar to that of SEM (section 2.28.1) with regard to each stage up to dehydration in acetone. For TEM, alcohol is used to dehydrate the samples rather than the acetone used in SEM and the nematodes are chopped on a glass slide using a razor blade rather then processed whole.

Following dehydration in alcohol the nematodes are added to propylene oxide (100%) for 5 minutes, and transferred to fresh propolyene oxide two further times, and incubated for 5 minutes each time. After the final propylene oxide stage the nematodes are transferred v/v to there embedding resin, either LR White™ (London Resin Company) or EPON™ epoxy resin can be used at this stage and left overnight (at least 5hrs). The following day the cap of the eppindorf was removed to allow the propylene oxide to evaporate leaving pure resin. Two changes of resin are then performed. Suitable moulds were then selected in which the resin and samples were to be polymerised. Polymerisation is carried out at 60ºC for 48hrs (can be altered depending on the resin type used).

The polymerised stubs were sectioned in a Reichert-Jang Ultracut E using a diamond knife and stained with 10% uranyl acetate and 5% Reynolds lead citrate solution then mounted on copper grids (100 or 200 mesh) and viewed on a Carl Zeiss 902 transmission electron microscope.

2.29 Protein techniques

2.29.1 Sodium dodecyl sulfate polyacrylamide gel electrophoresis (SDS PAGE)

A NuPage XCell Sure Lock system (Invitrogen), was set up as described in the manufacturer's instructions and was used with 4-12% gradient Bis-Tris high performance pre-cast gels to separate proteins. In preparation for loading onto the gels, 4X LDS sample buffer (Invitrogen) was added to samples for a final 1X concentration. For reducing conditions, the 4X LDS sample buffer was made to 20% final concentration of β-ME. Broad range molecular weight markers (not-prestained) (New England Biolabs) were run alongside the samples. Gels were run at 200 V in 1X MOPS buffer (Invitrogen) until the dye front reached the bottom of the gel. Gels were removed from the gel cases and were rinsed in H_2O and were then transferred to a Coomassie blue solution (0.25 g of Coomassie brilliant blue R-250, 45% methanol, 10% glacial acetic acid) in order to visualise proteins. Gels were stained for 1 hour on a rocker, then transferred to destain solution (45% methanol, 10% glacial acetic acid) and left on a rocker overnight at room temperature.

2.29.2 Western blotting

A NuPAGE XCell II system (Invitrogen) was used for the transfer of proteins to a Hybond-P PVDF membrane (Amersham Pharmacia Biotech). The membrane was briefly soaked in methanol and dH_2O and then the apparatus was set up as per the manufacturer's instructions. The transfer was run for 1 hour at 30 volts in 1X Transfer Buffer. Subsequently the membrane was transferred to a blocking solution (1% BSA in TBS-X) and blocking performed overnight at 4ºC. Primary antibody was then added. TBS-X, 3% BSA + 1/4000 dilution of the anti-SQT-3 antibody for SQT-3 detection, or, PBST, 2.5% milk, 0.02% sodium azide +1/5000 Anti-His(C-term) Antibody (Invitrogen) for His tagged protein detection. The primary incubation was for 1½ - 2hrs at RT and followed by 3X 10min washes with TBS-X, no BSA. The secondary for anti-SQT-3 antibody, anti Rabbit Alkaline Phosphotase (Sigma), was made up at a 1/15,000 dilution in TBS-X and 3% BSA.

The secondary for anti-His detection was anti Mouse Alkaline Phosphotase (Sigma) similarly used at 1/15,000. The secondary was incubated for 1½ - 2hrs at RT, followed by 3X 10 minute washes in TBS-X no BSA.

To develop the blots Sigma FAST™ BCIP/NBT made up dH_2O in was exposed to the blots for 5-10 minutes at RT. To stop the reaction the blot was washed in dH_2O.

Buffer:

TBS X20:	1 M Tris, 3 M NaCl, (pH7.9)
TBS-X:	20 mls TBS X20, 1 ml Triton X-100 (0.1% final) made up to 1 litre with dH_2O
Blocking Solution:	1% BSA in TBS-X

2.29.3 Construct preparation for protein expression

2.29.3.1 QSOX protein expression constructs

QSOX protein expression constructs were made by fusing a cDNA PCR amplified region which covered from the ATG start, to the stop codon of the target. These fragments were then T-A cloned into a suitable transfer vector and subsequently digested *via* the specific restriction enzyme sites designed into the primers used in the initial amplification of the fragment, then ligated into the similarly digested pQE-30 or pQE-80L protein expression vector for expression in *E. coli*. All fragments made in this manner were sequenced to check the frame and integrity of the sequence.

2.29.3.2 NAS expression constructs

2.29.3.2.1 E. coli expression constructs

A cDNA PCR amplified fragment of the target gene *nas-36* was cloned into a transfer vector (TOPO 2.1) before being sub cloned into a suitable protein expression vector (pQE-30) under control of the lactose operon. The final plasmids being transformed into both BL21(DE3) and BL21(DE3) pLysS and single positive colonies used to inoculate liquid cultures.

Two fragments were cloned to this end. A full length fragment (1885bp) including the pre/pro domains to the stop codon of *nas-36.* The second fragment (1552bp), which did not contain the pre-pro domain, begun at the 5′ end of the astacin domain of *nas-36* and continuing through to the stop codon similarly to the full length fragment. Fragments were sequenced and checked for integrity and frame with the vector.

nas-37 was cloned by PCR amplification of a full length cDNA clone which included from the ATG up to, and including, the stop codon. This fragment was then cloned in frame into pET42a (Novagen) under control of the lactose operon. The construct was designed to express a GST::6HIS::NAS-37::6HIS fusion protein.

The NAS-37 expression construct, which was termed pWD100.4, was transformed into BL21 (DE3) and the protein extracted (section 2.30.2) and purified (Davis *et al.,* 2004).

2.29.3.2.2 C. elegans in vivo expression/rescue constructs

NAS-36 and NAS-37 were also expressed as a HIS tagged rescue construct in *C. elegans*, see Figure 2.1.

The expression fragments were designed such that a 9XHIS tag was inserted 5′ to the stop codon of the gene achieved by having a reverse primer which contained a 20bp target fragment, the 9XHIS fragment, the stop codon and the restriction digest site used in cloning.

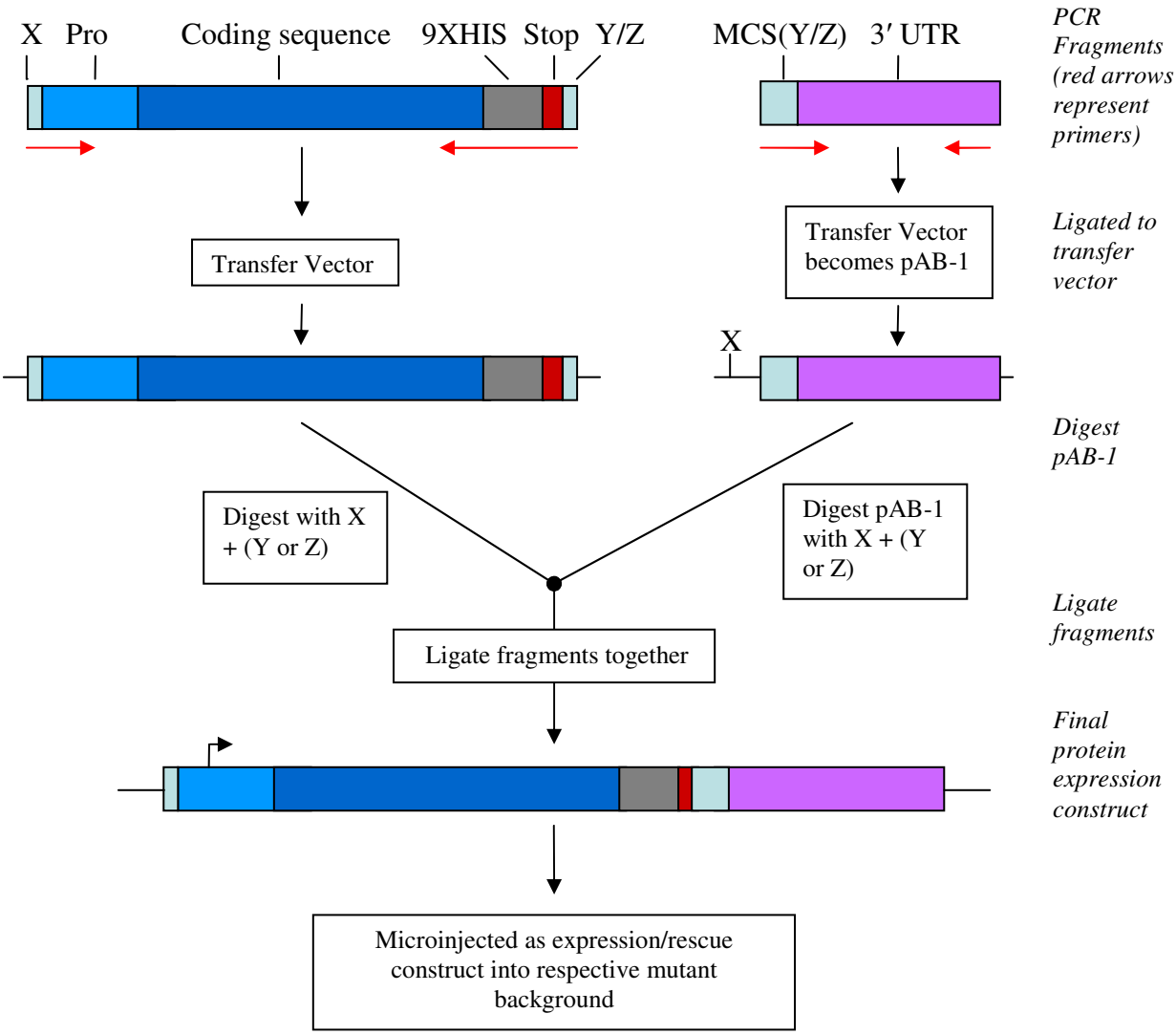

Figure 2.1: NAS expression/rescue construct generation in pAB-1. X, Y and Z represent restriction enzyme sites (not to scale). Red arrows represent the fragment coded by primer sequence. Not to scale.

To amplify these fragments by PCR cosmid DNA was used as a template under the following conditions.

X1		95ºC - 5 mins
X35	⎡	95ºC - 1min
	⎢	56ºC - 1min 30 sec
	⎣	72ºC - 8 mins
X1		72ºC - 15 mins

Each 50 µl reaction contained 100-500 ng of cosmid DNA and 15 pmols of forward and reverse primer. Taq and Pfu Turbo (in a 6:1 unit ratio) were used to amplify the fragments leaving a 3′ A tail overhang and also providing proof reading exonuclease activity. Taq buffer was used in the reactions as per section 2.7.

The products of the PCR reactions were cloned into TOPO2.1 transfer vector and then subcloned into pAB-1. pAB-1 constitutes a pCRScript backbone with the *C. elegans unc-54* 3′ UTR (734bp) blunt end ligated into it. *unc-54* 3′ UTR was cloned by PCR amplification from the vector pPD95.81, and had a short MCS added to it's 5′ end. The MCS restriction fragments were cloned as part of the forward primer used to amplify the UTR.

2.30 Protein purification

2.30.1 E. coli expressed protein from pQE30 vector fusion constructs, by beads and columns (native)

The colonies derived from the transformation of BL21 (DE3) or BL21 (DE3) p*LYS*s cells with recombinant protein constructs were used the same day to inoculate 20 ml liquid L-broth cultures plus antibiotics (ampicillin at 100 µg /ml and kanamycin at 25 µg/ml). Cultures were incubated in a rotary shaker overnight at 37ºC. The following day all 25 ml of culture was used to inoculate a 500 ml liquid culture (Amp 100 µg/ml and Kan 25 µg/ml) and this was incubated at 37ºC in a rotary shaker until an OD600 of 0.6 had been reached. At this stage, a 1 ml aliquot was removed and centrifuged for 1 minute to form a cell pellet and the rest of the culture was inoculated with IPTG to a final 1mM concentration. Cultures were grown for a further 2/4 hours before cells were pelleted in 250 ml Nalgene flasks (1 ml of post-induction culture was kept separate and pelleted in a microfuge tube to be run on an SDS PAGE gel at a later stage). Pellets were frozen at –80ºC overnight.

Native protein extracts were made following the QIAexpress® Ni-NTA Fast Start system (Qiagen).

The cell pellet was thawed on ice for 15 minutes and resuspended in the kits native Lysis Buffer and incubated on ice for a further 30 minutes with occasional gentle mixing. The lysate was then centrifuged (14,000g for 30 minutes at 4ºC) to pellet cellular debris and the somatic retained. At this stage a 5 µl aliquot was taken as the induced sample and retained at -20ºC to be resolved later by SDS-PAGE analysis. The resin in the pre-prepared columns was resuspended and drained off. The somatic solution containing the soluble protein was then added to the column and the flow through collected and prepared for SDS-PAGE analysis. The columns were washed twice and again fractions (5 µl) taken and prepared for SDS-PAGE analysis. To elute the bound protein Elution buffer (2 X 1 ml) was added and the elution collected for SDS-PAGE analysis. All were then run on SDS-PAGE gels and visualised either by coomassie staining or Western blotting.

Buffers:

Lysis Buffer: 50 mM NaH_2PO_4, 300 mM NaCl, 10 mM imidizol pH8.0

Wash Buffer: 50 mM NaH_2PO_4, 300 mM NaCl, 20 mM imidizol pH8.0

Elution Buffer: 50 mM NaH_2PO_4, 300 mM NaCl, 250 mM imidizol pH8.0

* 600 µl of ProBond™ Resin (Invitrogen) could be added to 5 ml disposable plastic columns (Pierce) as opposed to using the kit columns.

2.30.2 E. coli expressed NAS-37 from pWD100.4 construct, by Ni-NTA spin columns.

pWD100.4 was transformed into BL21(DE3) cells, grown to log phase and induced with 1 mM IPTG overnight (16 hours) at 25°C. Sonicates were prepared using standard methods (section 2.30) and cleared subsequent lysates purified on Qiagen Ni-NTA spin columns as per the kits instruction.

Cells were thawed on ice for 15 minutes prior to being resuspended in 1ml lysis buffer with the addition of 1 mg/ml lysozyme. This mix was then further incubated on ice for a further 30 minutes. The cell slurry was sonicated (10 x 10 second pulses with 10 second

pauses) using a wide tip probe. The cellular debris was pelleted by centrifugation (30 minutes at 10,000g at 4ºC). The columns were equilibrated with 600 µl lysis buffer and spun at 700g for 2 minutes. The cleared lysate was added (≤600 µl) to the equilibrated columns and spun for 2 minutes at 700 g, the flow through being collected and prepared for SDS-PAGE analysis. The columns were then washed twice with 600 µl wash buffer, samples of which were collected and prepared for SDS-PAGE analysis. The protein was eluted off with 100 µl of elution buffer twice, 2 minutes at 700 g, fractions of which were collected and prepared for SDS-PAGE analysis.

2.30.3 Purification of E. coli expressed protein from pQE30 vector fusion constructs using beads and columns (denaturing)

The colonies derived from the transformation of BL21 (DE3) or BL21 (DE3) cells with recombinant protein constructs were used the same day to inoculate 20 ml liquid L-broth cultures plus antibiotics (ampicillin at 100 µg /ml and kanamycin at 25 µg/ml), as described in section 2.30.1.

The buffers utilised in the next steps were those described in the manual for the pQE vectors. The frozen pellet was allowed to thaw slowly and then was resuspended in 20 ml of 'buffer B'. This was placed at –80ºC for 30 minutes before again, being slowly thawed in H_2O. The cell slurry was sonicated (10 x 10 second pulses with 10 second pauses) using a wide tip probe. Great care was taken during the sonication step to ensure that the slurry was on ice at all times and that during sonication, foam did not form. The cellular debris was pelleted by centrifugation (30 minutes at 10,000g at 4ºC) and afterwards the supernatant (containing soluble protein) was removed to a fresh tube while the pellet (containing insoluble proteins) was resuspended in 5 ml of 'buffer B'. 4 ml of ProBond resin (Invitrogen) that comes as a 50% slurry in 20% ethanol (to give a column with a volume of 2 ml) was loaded into a disposable polypropylene 5 ml column (Pierce) as per manufacturers instructions. The resin used was a nickel-charged affinity resin that uses the chelating ligand iminodiacetic acid (IDA) coupled to a highly cross-linked 6% agarose resin. The column was equilibrated with 20 ml of buffer B before the soluble protein-fraction from the centrifugation step was loaded onto it (20 µl of the soluble protein-fraction was kept to be run on a SDS PAGE gel at a later stage). Proteins not binding to the column were washed out using 25 ml of 'buffer C' and finally, any proteins bound to the column were eluted into a fresh tube with 5 ml of 'buffer E'.

To prepare samples for the SDS PAGE gel, pre-induction and post-induction pellets were diluted in 50 µl and 100 µl of 1X β-ME sample buffer respectively. 5 µl of 2X SDS β-ME sample buffer was also added to a 5 µl aliquote of these crude extracts. 5 µl of 4X β-ME SDS buffer was added to 20µl of each of the flow through, wash, and elution fractions. Samples were boiled for 5 minutes and centrifuged for 1 minute. 10 µl of the cell pellet fractions and the crude sample fractions and 15 µl of fraction samples were loaded onto a gel alongside 15 µl of pre-boiled Broad Range marker or Precision Plus protein standard (BIORAD). The proteins on gel were visualised using coomassie blue and destained as described previously (section 2.29.1).

Buffers:

Buffer B: 100 mM NaH2PO4, 10 mM TrisCl, 8 M urea (pH 8.0)

Buffer C: 100 mM NaH2PO4, 10 mM TrisCl, 8 M urea (pH 6.3)

Buffer E: 100 mM NaH2PO4, 10 mM TrisCl, 8 M urea (pH 4.0)

2.30.4 C. elegans in vivo expressed NAS-36 and NAS-37

With the constructs made as per Figure 2.1/section 2.29.3.2.2, these constructs were injected into their respective mutant background i.e. NAS-37 expression/rescue construct was injected into TP99*(nas-37(tm410))* and stable lines established. The resultant transformed lines were scored for the presence of both the marker, and, the rescue of the corresponding phenotype, indicating the expression of a functional rescue protein.

2.30.4.1 Extraction of NAS protein under native conditions

Rescued lines were cultured to harvest the HIS tagged protein (NAS-36 or NAS-37). 20-30 9cm OP50 plates, each containing 15-20 GFP +ve worms were set up and incubated for 4 days at 20ºC. The nematodes were then washed off the plates with 1XM9 and allowed to clear on ice and washed again. The worms were washed three times with 1XM9 and the clear supernatant removed to leave packed worms. These were then resuspended in 2.4 ml Native Binding Buffer and homogenised in a 3 ml glass homogeniser on ice. The homogenate was then spun for 15 minutes at 3,000g at 4ºC and the somatic added to nickel purification columns as per the instructions in the ProBond™ Purification System hand book. 15µl of the soluble protein-fraction was retained to be run on a SDS PAGE gel at a

later stage. The protein was allowed to bind for 30-60 minutes with gentle agitation to keep the resin suspended in the somatic. The resin was then settled by gravity and the supernatant carefully aspirated off. 15 µl of the soluble protein-fraction was kept to be run on a SDS PAGE gel at a later stage. The columns were washed three times with 2.4 mls Native Wash Buffer and the resin allowed to settle by gravity and the supernatant aspirated off. 15 µl of the soluble protein-fraction was kept to be run on a SDS PAGE gel at a later stage. The column was then clamped in a vertical position and the protein eluted with 2.4/3.6 mls Native Elution Buffer. The elutions were collected in 10 equal volume fractions, and 15 µl of the soluble protein-fraction was kept to be run on a SDS PAGE gel at a later stage.

Following SDS-PAGE/Western analysis of all the collected samples, those most enriched with target protein were then further purified and concentrated using Ultracell YM-30 columns (Microcon). By concentrating any protein equal to or over 30kDa and removing any of a lesser weight.

Buffers:

5X Native Purification Buffer:	250 mM $NaPO_4$, 2.5 M NaCl
Native Wash Buffer (50mls):	50 ml of 1X Native Purification Buffer, 335 µl of 3 M Imidizol (20 mM final) adjust to pH 8
Native Elution Buffer (15mls):	13.75 mls 1X Native Purification Buffer, 1.25 ml 3 M Imidizol (250 mM final) adjust to pH8.0

2.30.4.2 Preparation of ProBond™ Columns

ProBond™ columns were used in the purification process of the NAS proteins and were prepared for use as follows.

600 µl of resin was pipetted into 5 ml Pierce disposable columns and allowed to settle by gravity for 10 minutes. 1.8 ml of distilled H_2O was added and the resin resuspended by gently tapping the column. The resin was then allowed to resettle and the supernatant aspirated off. For purification under native conditions 1.8 mls of Native Binding Buffer was added, for denaturing conditions 1.8 mls of Denaturing Binding Buffer was added. Resin was resuspended by gently tapping the column. The column was then allowed to

settle by gravity and the supernatant aspirated. The binding buffer step was then repeated. Such prepared columns were then used to bind HIS tagged NAS proteins.

Buffers:

Native Binding Buffer: 1X Native Purification Buffer (section 2.30.4.1)

Denaturing Binding Buffer: 20 mM $NaPO_4$, 500 mM NaCl, 8 M urea, pH 7.8

2.30.4.3 Extraction of NAS protein under denaturing conditions

Rescued lines were cultured to harvest the HIS tagged protein (NAS-36 or NAS-37). 20-30 9cm OP50 plates, each containing 15-20 marker +ve worms were set up and incubated for 4 days at 20ºC. The nematodes were then washed off the plates with 1XM9 and allowed to clear on ice and washed again. The worms were washed 3 times with 1XM9 and the clear supernatant removed to leave packed worms. Which were then resuspended in 2.4 ml Guanidinum lysis Buffer and homogenised in a 3 ml glass homogeniser on ice. The homogenate was then spun for 15 minutes at 3,000g at 4ºC and the somatic added to nickel purification columns as per the instructions in the ProBond™ Purification System hand book. 15 µl of the soluble protein-fraction was retained to be run on a SDS PAGE gel at a later stage. The protein was allowed to bind for 15-30 minutes with gentle agitation to keep the resin suspended in the somatic. The resin was then settled by gravity and the supernatant carefully aspirated off. 15 µl of the soluble protein-fraction was kept to be run on a SDS PAGE gel at a later stage. Denaturing Binding Buffer (1.2 mls) was used to wash the column by rocking for 2 minutes and repeated. 15 µl of both soluble protein-fractions was retained to be run on a SDS PAGE gel at a later stage. The columns were then washed twice with 1.2 mls of Denaturing Wash Buffer (pH 6.0), 15 µl of both soluble protein-fractions was retained to be run on a SDS PAGE gel at a later stage. The columns were washed two further times with 1.2 mls Denaturing Wash Buffer (pH 5.3), 15 µl of both soluble protein-fractions was retained to be run on a SDS PAGE gel at a later stage. The elution was in 1.5 mls of Denaturing Elution Buffer which was collected in 10 equal volume samples 15 µl of the soluble protein-fractions was retained to be run on a SDS PAGE gel at a later stage.

The collected sample were then visualised on SDS-PAGE and Western blots with anti-His antibody (Invitrogen).

Buffers:

5X Denaturing Purification Buffer:	250 mM $NaPO_4$, 2.5 M NaCl
Guanidinium Lysis Buffer, 6 M:	6 M Guanidinium HCL, 20 mM $NaPO_4$ (pH 7.8),
Denaturing Binding Buffer:	8 M Urea, 20 mM $NaPO_4$ (pH 7.8), 500 mM NaCL
Denaturing Wash Buffer:	8 M Urea, 20 mM $NaPO_4$ (pH 6.0), 500 mM NaCL
Denaturing Elution Buffer:	8 M Urea, 20 mM $NaPO_4$ (pH 4.0), 500 mM NaCL
Imidazole, 3 M	Imidazole (pH 6.0)

2.31 Determination of protein concentration by Bradford assay

It was important to determine the concentration of the recombinant protein purified by the above methods before they could be used in assays. To do this Bradford Assays were performed, plotting the BSA standard curve ranging form 0-0.1 mg/ml and plotting dilutions, ranging between 1 to 50 and 1 to 1, of sample to determine their concentration.

Reagents**:**

Dye stock:	0.5 mg/mL Coomassie Blue G, 25% methanol, and 42.5% phosphoric acid. The solution is stable indefinitely in a dark bottle at 4°C (pH 0).
Assay reagent:	1 volume of the dye stock with 4 volumes of distilled H_2O (pH 1.1). Stable for 2/3 weeks in a dark bottle at 4°C.
Protein Standards:	Bovine serum albumin (BSA) with concentrations of 0, 250, 500, 1000, 1500, 2000 µg/mL.
Sample preparation**:**	Prepare a range of dilutions, 1 to 1 and 1 to 50. A wide range of concentration samples may be used.

Assay**:** The spectrophotometer was warmed before use. Samples were diluted to obtain between 5 and 100 µg of protein in at least one assay tube containing 100 µl sample. If desired, add an equal volume of 1 M NaOH to each sample and vortex (the addition of 1 M NaOH was suggested by (Stoscheck, 1990) to reduce the protein-to-protein variation in colour yield). Standards containing a range of 5 to 100 µg of protein in 100 µl volume were prepaired. Add 5 ml dye reagent and incubate for 5 minutes. Measure the absorbance at 595 nm.

Analysis: A standard curve of absorbance versus micrograms protein was plotted, and a line of best fit determined. Using the spectrophotometer readings of the unknown(s), determine the concentration for the unknown sample(s) from the standard curve, then multiply that by the dilution factor to give the final concentration in µg/ml.

2.32 Deletion screen

To generate strains carrying mutants within specific genes of interest a deletion screen was enacted. The screen required the generation of a large population (~600,000 individual nematodes) of randomly mutagenised *C. elegans* which were screened *via* the poison primer PCR method (see chapter 4 section 4.2.1 for an explanation of the poison primer method of deletion detection by PCR and primer design) to isolate a specific deletion carrying nematode. The mutagenised worms were maintained in a deletion library at 15°C throughout the screening process. The initial mutagenisis, generation of the library and pooling of the mutants was a whole lab effort.

2.32.1 Mutagenesis and Library generation

A large population of worms was grown on 10 15cm RNGM plates. The worms were then washed off the plates with 1XM9 and bleached with hypochlorite (0.25M KOH, 1-1.5% hypochlorite) to harvest the eggs. Eggs were then distributed over 10-20 15cm plates made with RNGM and seeded with OP50. After 52hrs at 20°C the worms were collected in 1XM9, washed and mutagenised by addition of 140 µl of 3 mg/ml stock of 4,5′-8-trimethylpsoralen in DMSO (Sigma) and left on a shaker at 20°C for exactly 15 minutes. The worms were then transferred to a 15cm glass petri dish and exposed to an 850-900 $\mu W/cm^2$ dose of UV irradiation for 20-25 seconds. The mutagenised worms were then washed to remove excess psoralen before being transferred back to OP50 seeded 15cm plates and incubated for 24hrs at 25°C. The F1 eggs were then collected by hypochlorite

treatment, as described above, and allowed to hatch on unseeded 15cm plates. The resulting F1/paused L1s were then collected in 1XM9 and distributed in groups of 500 onto 1152 6cm OP50 seeded RNGM plates using a repeating pipettor. Plates were then stored in groups of 96 (labelled A-L) and allowed to grow for five days at 20°C.

2.32.2 Library harvesting

To harvest the library 750 ml of sterile distilled H_2O with streptomycin (100 mg/ml) and myostatin (12.5 mg/ml) was added to each plate and then placed on a rocker for 3 minutes. Plates were harvested in batches of six. 150 ml of worm suspension was taken up and aliquoted into deep 96 well plates and the tip ejected into the well to aid co-ordination. Each well represented a sample of ~500 mutagenised *C. elegans* genomes. The 96 well plate were labled A-L accordingly.

2.32.3 DNA preparation

DNA was prepared by addition of proteinase K to each of the wells of the 96 well plates harvested in section 2.32.2, sealing the block thoroughly to ensure no well-to-well contamination. The plates were frozen at –80°C for 20-30 minutes and then incubated for six hours or overnight at 65°C.

2.32.4 Sample pooling

Prior to PCR screening it was essential to make pooled samples of the DNA preps. The samples were diluted with an equal volume of sterile dH_2O. The pools were a two dimensional array with pools representing the entirety of the columns in one 96 well block, and a separate pool representing the entirety of the rows in another 96 well block, thus reducing twelve 96 well blocks into a more manageable two (see Figure 2.3). To make the pools 50 µls of the given sample from each block (in sets of eight for columns, and 12 for rows) was transferred to the appropriate wells in a single deep 96 well plate. The pools then had proteinase K activity removed by heating to 95°C for twenty minutes, ensuring that the blocks are properly sealed to prevent well-to-well transfer of sample.

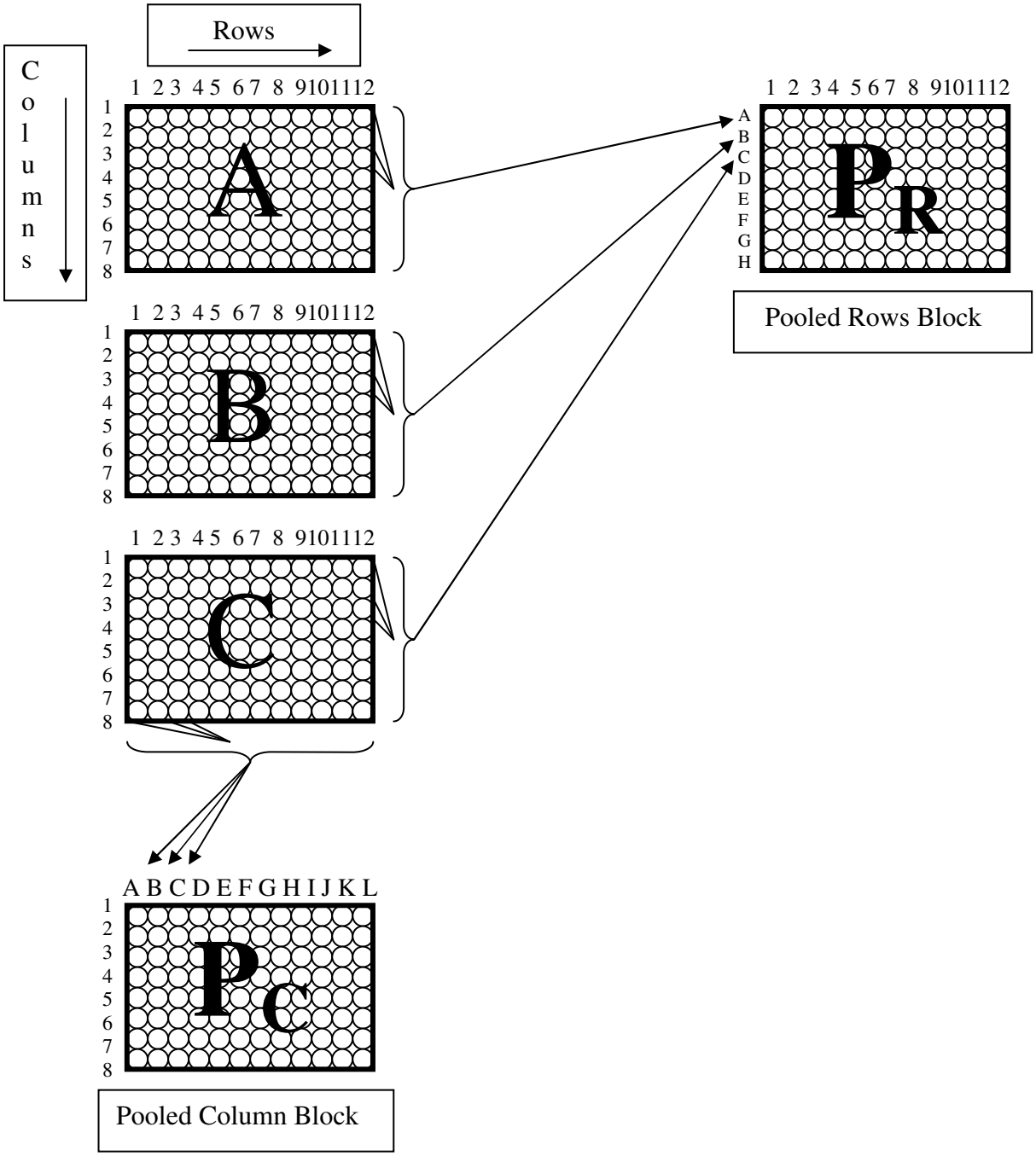

Figure 2.2: Schematic representation of the pooling of the library blocks A-L (only showing A-C for clarity) in both dimensions, rows and columns. The pooling procedure results in all 96 wells of any given library block (A-L) being represented by 12 horizontal sample wells and 8 vertical sample wells, pooled rows and columns respectively.

2.32.5 Identification of mutants by PCR amplification of pooled samples

Primary screening of the pools was performed on the 1st dimension by selecting either the pooled column samples or the pooled row samples and performing PCR on all 96 samples using the external primers 1+2 as well as poison primers 5+6. Then transferring a sample of the first round of PCRs products by means of a Bokel Replicator, and PCR amplifying the second fragments from this first round template using the nested primers 3+4. This would allow visualisation of deletion containing DNA samples on a standard ethidium gel by band shift. Positive 1st dimension samples would mean that the 2nd dimension PCRs were more targeted, only requiring analysis of either 8 or 12 samples depending up on which 1st dimension, rows or columns respectively, was chosen. Employing this pooled system allowed for more economical use of resources and time.

Co-ordinating the results from positive 1st and 2nd dimension PCRs enabled the identification of the specific plate that contained a population of mutagenised worms, of which a percentage should be carrying a deletion in the target gene.

2.32.6 Sib selection

First round

Sib selection, was used to enamble the incremental isolation of the target mutation and the nematode containing it. Worms were washed off the positive plate identified above, and their concentration determined e.g. 100 worms/ml. The solution was then scaled to dispence 50 worms in a given volume and that volume was applied to 192 6cm RNGM OP50 seeded plated and left to grow at 20ºC for five days. A sample of the positive plates worms was also frozen down (section 2.4.2) and retained. Samples of these 192 plates were then washed off with 5ml sterile distilled H_2O with streptomycin (100 mg/ml) and myostatin (12.5 mg/ml) and 500 µl collected in 96 well plates and pools generated as described above. An equal volume of Proteinase K solution was then added to the well and they were frozen at –80°C for 20-30 minutes then incubated at 65°C for 4 hours followed by heat killing of the proteinase K at 95°C for 15 minutes. These samples were then PCR amplified as described in section 2.32.5 and plates containing the mutant were isolated, with positive plates being used to set up the second round of sib selection.

Second round

Technically similar to first round, but with a smaller pool of worms being plated out. 10 worms per plate over 48 6cm OP50 seeded RNGM plates. Samples were not pooled at this stage as the numbers were now manageable. A sample of the positive plates worms were also frozen down (section 2.4.2) and retained. Samples again were subject to PCR to identify positive mutation containing plates. Positive plates were used to set up the third round of sib-selection.

Third round

Single worms are plated out across 192 plates from second round sib selection positive plates and allowed to egg lay for one to two days at 20°C. The original adult was then removed and screened by SWPCR (section 2.26) with positive isolates being maintained as mutation carrying strains. Prior to freezing down and backcrossing of the mutation strain, homozygous mutants were obtained. To achieve this 10-100 single worms were plated out, allowed to egg lay, and genotyped with respect to the mutation by SWPCR using the respective backcross primers found in Table 2-7. These homozygous deletion carrying strains could now be genetically purified by backcrossing to N2s (no fewer than four times).

2.33 Oxidation assays

2.33.1 Oxidative capacity determined by DCF method

The DCF method of native oxidative capacity determination relied upon the use of 2',7'-dichlorodihydrofluorescein diacetate (H_2DCFDA) (Molecular Probes), a fluorogenic probe commonly used to detect cellular production of reactive oxygen species such as H_2O_2 (which is produced by the QSOX family members following their actions in oxidising reduced thiols) in a dose dependent manner. This method depends on the de-acetylation of H_2DCFDA by cellular esterases, to form the oxidant-sensitive compound, 2',7'-dichlorodihydrofluorescein (H_2DCF) (Brubacher and Bols, 2001). H_2DCF fluoresces when exposed to UV irradiation and as such can be viewed using a UV equipped microscope. By this rationale H_2DCFD could be used as a marker to detect the native *in vivo* oxidative capacity of cells/whole organisms.

Worms were treated with 500 µl tunicamycin (5 µg/ml) in M9 on 9cm OP50 seeded plates and left overnight, the worms were then washed (with 1XM9 three times) spun at 3,000g for 1 minute, and resuspended in 500 µl of H_2DCFDA (2 mM in M9) and incubated for 1hr

on a rocker in the dark. Following incubation the worms were washed as before with 1XM9 three times. The following steps were performed as quickly as possible to reduce osmotic shock, induced by toxicity, to the worms. To remove aggregated H_2DCF, bacteria and dead worms (which cause high background) the worms were rapidly resuspended in 1ml ice cold 30% sucrose which was over layered with 250 µl ice cold 0.1M NaCl and centrifuged at 5,000g for 5 minutes at 4ºC. The worms which were on the interphase were then collected and added to 1 ml M9, pelleted and washed again (2-4 times). The worms were then immobilized by embedding them on agarose pads ready for microscopy. Because H_2DCF is reactive to UV light it was important while viewing the worms not to search the stage with the UV on. To view the worms it was better to use visible light, locate a worm, photograph it, activate the fluorescent light and capture a florescent image. The light could then be changed back to visible and the slide moved past the area that had been exposed to the UV light and the next worm photographed in the same sequential manner. It was important never to go over the same area twice, as the background would be considerably higher in previously viewed areas.

2.33.2 Swimming assay

Swimming assays were performed with both oxidising and reducing environments, H_2O_2 and dithiothreitol (DTT) respectively as described previously (Larsen, 1993).

Synchronous populations of *C. elegans* were generated by hypochlorite treatment of gravid adults and allowing the eggs to hatch on unseeded plates. The paused L1s were washed off and plated onto OP50 seeded plates and incubated at 25ºC. Once the nematodes had developed to the desired stage they were washed off in 1XM9 and their concentration determined (worms/ml). The worms were then aliquoted out into one row (12 wells) of a 96 well plate at 35 worms per well. At time zero serial diluted H_2O_2/DTT was added to the 12 wells to cover the range of 0 mM to 50 mM, with a final volume of 50 µl, and the worms incubated for 2hrs at 25ºC. Following incubation the worms in each well were scored for survival. Survival was classified under the following criteria: movement, movement when prodded, or, in immobile worms, pharyngeal pumping. Worms which showed no pharyngeal pumping were classified as dead. No difference was noted in mortality when longer incubation periods were tested (up to 24hrs) (Larsen, 1993). The LD_{50} concentration, with respect to H_2O_2 and DTT, was defined after the experiment had been repeated in triplicate.

2.34 Isolation and digest of *C. elegans* cuticles

Isolation of cuticles was performed as outlined in (Cox *et al.,* 1981) with some modification. 20 individual nematodes (20 individuals used per reaction) where selected and picked into 1 ml of ST buffer (1% SDS, 0.125 M Tris-HCL, pH6.8) with or without 2% β-mercaptoethanol, and boiled for 2 minutes at 100ºC. The worms were then rotated for up to 4hrs at room temperature and washed with 1XM9. These cleared cuticles could now be used in cuticle digestion assays.

To digest the cuticle preps *Clostridium histolytica* type VII collagenase (Sigma) was used at 2 mg/ml in 100 mM Tris-HCl pH7.4, 1 mM $CaCl_2$. Incubations were carried out at 37ºC for 4hrs in 96 well plates, and the resultant cuticles viewed by DIC microscopy.

2.35 Refractile ring assay

Cuticles from a range of trichostrongylid parasites, *H. contortus, T.circumcincta T.colubriformus, T.vitrius* and *C. oncophora* were exposed to *C. elegans* NAS proteins in order to determine heterologous activity in enzymes involved in moulting and refractile ring formation (Gamble *et al.,* 1989; Davis *et al.,* 2004).

To isolate the L3(2M) cuticle heads the parasites were heat killed by immersion in 100ºC dH_2O for 10 seconds before being rapidly cooled on ice and transferred to a glass slide, were they were extensively chopped using a razor blade. The chopped worms were then washed off the slide with PBS, and either stored at 4ºC for a short period, or used immediately in a refractile ring assay. The refractile ring assays were performed in 96 well plates containing 100 µl of 100 mM Tris buffer (pH 8.0) and either; 10 or 20 µg/ml of *C. elegans* purified NAS protein; 10 or 20 µg/ml of BSA or no protein (BSA/no protein as controls) and approximately 50 sheath heads. The plate was then placed at 37ºC for 1hr and refractile ring formation was assessed visually by DIC. All assays were performed in triplicate. As an inhibitors of astacin activity 10 mM (final) 1,10 phenanthroline or EDTA were used.

2.36 Oligonucleotide primer sequences

Table 2-7: Primer sequences are given in 5′ to 3′ orientation with engineered sequences given in lower case and restriction sites in lower case and underlined. * denotes primers used in conjunction with consensus splice leader oligonucleotides to determine splice leader processing of particular transcripts. ** denotes deletion screen primers which were also used in backcrossing/genotyping of the respective mutants.

Oligonucleotide primer	Sequence (5′ to 3′)
Genotyping, cloning and screening, RNAi, rescue construct and vector primers	
1224	CGCCAGGGTTTTCCCAGTCACGAC
96.04 reverse	TCTGAGCTCGGTACCCTCCAAGGG
B. malayi ContigA (SL)* Rev-1	CTTTATCTGTAGCAAATTGTAAATTC
B. malayi ContigA (SL)* Rev-1 (2)	GAATTTACAATTTGCTACAGATAAAG
B. malayi ContigA Fwd-1	CGATTGAGACACGCGATCGTCGG
B. malayi ContigA Fwd-1 (2)	CCGACGATCGCGTGTCTCAATCG
B. malayi ContigB Rev-2	GTTGTTATAGATGTAGTAGTAG
B. malayi ContigB Rev-2 (2)	CTACTACTACATCTATAACAAC
cut-4 RNAi Fwd (*Hind* III)	gcgcaagcttATGTTCCATTTTACTCGAATCC
cut-4 RNAi Rev (*Hind* III)	gcgcaagcttTTATGGCTTGAAAAAAGCGGTTTG
F35G2.1 RNAi Fwd	ATGCGGAGTCCGCACGGGACAGTG
F35G2.1 RNAi Rev	TCAGAAGGCGAGACGTTGATCTGCC
F56C11.3 Fwd	ATGGAAATCGGTCCAGATGGAAAG
F56C11.3 Rev	TTAATAATCACACGATCCATCTTTC
hch-1 TC1 FLANK Fwd	GCCACATTCTCCCGATACTCTCC
hch-1 TC1 FLANK Rev	CAGAATCGTGCTCCAACTCTGCTG
hch-1 TC1 Rev	CTGATCGGAGGATGTTGCGATC
L4440 F	GAGTGAGCTGATACCGC
L4440 R	GTGCTGCAAGGCGATTAAG
M13 reverse	AACAGCTATGACCATGATTA
NLS	CACCCACCGGTACCTTACGC
pGEM forward	GTTTCCCAGTCACGACGTTG
pGEM reverse	CAGGAAACAGCTATGACCA
SL1	GGTTTAATTACCCAAGTTTGAG
SL2	GGTTTTAACCCAGTTACTCAAG
T10 rescue Fwd2 (*Sal* I)	gcgcgtcgacCGCACTTCTTCAGTACTCATG
T10 Rescue Fwd2 Colony-PCR	CACTTTACGAGTTTACTACAC
T10 rescue Rev2 (*Bam* HI)	gcgcggatccTTCGATTTGATAAGAGTGGAATTGG
T3	AATTAACCCTCACTAAAGGG

Oligonucleotide primer	Sequence (5′ to 3′)
T7	GTAATACGACTCACTATAGGGC
Promoter analysis	
T10 Pro2 Fwd (*Sph* I)	gcgcgcatgcGCTTTAGATTTCTCCAGAAATTG
T10 Pro2 Rev (*Sma* I)	gcgccccgggACATCTGGAAATATCATGAGTGAG
F35 Pro Fwd (*Pst* I)	gcgcctgcagGAACAGTGTTCAAACAGTTTGAC
F35 Pro Rev (*Bam* HI)	gcgcggatacCGCATTCTGAAAGAAAC
nas-36 Pro Fwd (*Pst* I)	gcgcctgcagCAGACACAACTAACATTCAATTTG
nas-36 Pro Rev (*Sma* I)	gcgccccgggACATGTGTCGATTTACGGACAAGAG
RT-PCR Primers	
ama-1 FWD	TTCCAAGCGCCGCTGCGCATTGTCTC
ama-1 REV	CAGAATTTCCAGCACTCGAGGAGCG
T10 RTPCR Fwd	TGTCGTCACATATGGAGAACTTTG
T10 RTPCR Rev*	CAAGAAATGATCCCTACAGTG
F35 RTPCR Fwd	TACTTCGCAAGGACGGCCAC
F35 RTPCR Rev*	CACAGACGTTGTTCTCTTCG
F47B7.2 RT-PCR Fwd	ATCACGGGAACAATGGTGTCAAAG
F47B7.2 RT-PCR Rev*	GTGAGCCAGAAAGGCGCTTGTTG
nas-28 RTPCR Fwd	TTTGGTACTGCAACCCACGAG
nas-28 RTPCR Rev	ATCATTCCAAATAAGTCAAAC
nas-34(hch-1) RTPCR Fwd	GGCCGGTGCTGATCGTTCTGTG
nas-34(hch-1) RTPCR Rev	GCAAAGTTAATTCTCTTGACATC
nas-36 RTPCR Fwd	ATGCTACTCTATGATCGGACG
nas-36 RTPCR Rev*	CTGAATCCAGTATTTCTCAAG
nas-37 RTPCR Fwd	ATGAAGTCTCAAGCTTGTCTAAAAG
nas-37 RTPCR Rev*	CTCTACAGTTTCACAATATGTTCC
nas-38 RTPCR Fwd	GTTAGCACTCCATTGCCGCCAAC
nas-38 RTPCR Rev	TTAGTGTTCTCCTCGCATCATTC
nas-9 RTPCR Fwd	CCATTTGTATATGCACAGCTTTTG
nas-9 RTPCR Rev	CTAATGAATCATCCAAAGTATAC
sqt-3 RTPCR Fwd	ATGGAAACTGACGGTAGGCTC
sqt-3 RTPCR Rev	GGACAGATTCCCTTCTCTCCTGG
Protein expression	
F47B7.2 Prot/Exp Fwd (*Kpn* I)	cgcgggtaccATGAACGAAAAAGAGCCAGGAGTG
F47B7.2(A) Prot/Exp Rev (*Kpn* I)	gcgcggatccTCAGAACCAGAACCTAGTCTTACC
F47B7.2(B) Prot/Exp Rev (*Kpn* I)	cgcgggtaccTTAGACGATATTCTGCTTTACCG
F47B7.2(C) Prot/Exp Rev (*Kpn* I)	gcgcggatccTTACCGGTGAGGAACTCCAAG
T10 Prot/Exp (*Bam* HI) Fwd	cgcgcggatccATGTTCCTGTTAATCCTCTTAATAAC
T10 Prot/Exp Int Rev	AATCATCCATTACTGCCTTTGTAAG
T10 Prot/Exp (*Bam* HI) Rev	cgcgcggatccTCAGTTCGATTTGATAAGAGTG

Oligonucleotide primer	Sequence (5′ to 3′)
F35 Prot/Exp (*Bam* HI) Fwd	gcgcgcggatccATGCGGAGTCCGCACGGGACAG
F35 Prot/Exp Int Rev	CAGAATGTGGCGTCTCAAACAG
F35 Prot/Exp (*Bam* HI) Rev	gcgcgcggatccTCAGAAGGCGAGACGTTGATCTGC
NAS-36 Fwd Full length PROT (*Sph* I)	gcgcgcatgcGATGATCCTGCACTTTTGGTTGC
NAS-36 Fwd Partial PROT(*Sph* I)	gcgcgcatgcGCCACGTGGAAAACCATGCCAATC
NAS-36 Rev PROT (*Pst* I)	gcgcctgcagTTAAATAGAAAGCCATAATTCATC
NAS-36 I.V.P.E Fwd (*Kpn* I)	gcgcggtaccTTGATATTTTAATATTTTAGAAGC
NAS-36 I.V.P.E Rev 9XHIS (*Sph* I)	gcgcgcatgcTTAcaccaccaccaccaccaccaccaccacCATAG AAAGCCATAATTCATC
NAS-37 I.V.P.E Fwd (*Kpn* I) III	gcgcggtaccGTCCCAGCATGCAACGAAAG
NAS-37 I.V.P.E Rev 9XHIS (*Nco* I)	gcgcccatggTCAcatcatcatcatcatcatcatcatGTTTT TGTAGCAAACTCCTC
unc-54 UTR Fwd (*Sph* I/*Nco* I)	gcgcgcatgcccatggCATCTCGCGCCCGTGCCTCTG
unc-54 UTR Rev	AAACAGTTATGTTTGGTATATTGG
pQE-30 Fwd	TTTGCTTTGTGAGCGGATAAC
pQE-30 Rev	AGCTAGCTTGGATTCTCACC
Deletion screen primers	
T10 ONE	TGTCGTCACATATGGAGAACTTTG
T10 TWO	CCGGTTACCATTAGTCTTATTTTGCC
T10 THREE	ACGAGTCATCATCTTCTGCCAATC
T10 FOUR*	CTTGAATGCAGAAACTGTGAGAG
T10 FIVE	CACGAAATAATTAGGTTTGCATC
T10 SIX	GAAGTAGATATGCTGAAAGCCATG
F35 ONE	ACCAACACCCTGGCTTTGGATG
F35 TWO	CGAATGATAGGAAGTATCAGGTG
F35 THREE	GCACTTCCCGGTTCTTTCCTTC
F35 FOUR	CTTGTTATAAATTGGGGGAGCAAC
F35 FIVE	CTTCACCCATCCCTGAATTGTG
F35 SIX	GCTATTTCGGATGTGAACACTG
F35 ONE (2nd SET)	GCAATTGTGCTGCGCGTTTGTTC
F35 TWO (2nd SET)	CTCGATCTTGTCTAAATCTGTC
F35 THREE (2nd SET)	GGAGATACAAGGCGAGCAATGG
F35 FOUR (2nd SET)	GTCATAAACTCGTGCAAATTGG
F35 FIVE (2nd SET)	GAAGAGTATGATGGAGTTGGTGC
F35 SIX (2nd SET)	CGGGAGATAAGATCCATAACG
nas-28 ONE	ATGCTGAATGAGAAACAAGCC
nas-28 TWO	CAGTCTACAGTCCGTCTACAG
nas-28 THREE*	CATTGCAACTGCAATTGAAAATGG
nas-28 FOUR	CCCTACAGTACCCCATCAAAG
nas-28 FIVE	TCGTGGGTTGCAGTACCAAAC
nas-28 SIX	CATGCATGCCATTGGCTTCTG

Oligonucleotide primer	Sequence (5′ to 3′)
nas-36 ONE	TTAGACGCTGAATGTGGTGG
nas-36 TWO	GAGATTGAATCTCCAAATTATCCGG
nas-36 THREE	CACTTTTCCATTGCAAAGCC
nas-36 FOUR	CCATATCAACTCACTTGGTAC
nas-36 FIVE	CTTGGTTCGGCATCGGCTG
nas-36 SIX	GACAACAATTGCTCCAACAATTATC
nas-38 ONE	AAGTGCAATGCTCCTATGGCAG
nas-38 TWO	CACATTGAGCGTTTGACGGGTAC
nas-38 THREE*	CATACATGCCTCCGATTTGAAG
nas-38 FOUR*	CACAATATCTTCCTGATAAACC
nas-38 FIVE	ACCATAATGCATGACGCTTCC
nas-38 SIX	GTACGGGTTTGCGTCTGATCC
Backcross primers	
T10/F1	TCGTAGCGCGAAGATGCTTG
T10/F2	TCCAGACAGTACTCCATCTC
F35 BX Fwd	CACCAATTTGCACGAGTTTATG
F35 BX Int	GATATTCATCAGATGAGACAGAAC
F35 BX Rev	CCATAATAGCGGAGTAGGAAG
nas-28 BX Rev1	CCCAAGAGGATGTAGCCTGAAAG
nas-28 BX Rev2	CCAACATCCTCCTGCAGATG
nas-36 BX Fwd	CGAGTTTTTCAGTGGACAAG
nas-36 BX Rev1	CCAATTTCATGTTCAATGACGCC
nas-36 BX Rev2	CAATCTCTTTCCATTCTTCAG
nas-36 BXII Fwd	GGATAAAACTGCCACGTGGAAAAC
nas-36 BXII Int	ATATACGAAGGAAGAATAAAATCTC
nas-36 BXII Rev	TTGGTACACACTTTTCCATTG
nas-37 DEL Fwd	GTCAGAGAAGTCTTCCATGTTTAAATG
nas-37 DEL Rev1	CTGTCGATGTCTTCTGGCTGAG
nas-37 DEL Rev2	GAGATAGTTGCGATAGATCATG
nas-38 BXII Rev	CCTGTAAAATTCGACAACTTC

Chapter 3: *qsox* and *nas* family screen by RNAi.

3 Introduction

In order to determine the enzymes of importance to the distinct steps of collagen maturation a targeted RNA interference (RNAi) screen was carried out which centred around two groups of enzymes namely: the quiescin-sulfhydryl oxidase (QSOX) and the nematode astacins (NAS). The QSOX family comprises four individual members; T10H10.2 (*qsox-1*), F35G2.1 (*qsox-2*), F47B7.2 (*qsox-3*) and F56C11.3.

The QSOX family of enzymes are characterised by an N-terminal thioredoxin domain and a downstream ERV1/ALR domain and are a fusion of two distinct disulphide bond generating moieties (Raje and Thorpe, 2003). As such the QSOX enzymes were expected to be important in the maturation and generation of the nematode cuticle, a structure largely dependent on disulphide bonding (Cox *et al.,* 1981; Winter and Page, 2000).

The second class of enzymes investigated were the Nematode Astacin (NAS) metalloproteases. The NAS group of enzymes belong to the subgroup, bone morphogenic proteins (BMPs) of the transforming growth factor-β (TGF-β) superfamily. In comparison to higher order organisms the NAS family of *C. elegans* is unusually large. In humans and mice for example, only six astacin genes have been found in each and only 12 in *Drosophila melanogaster,* but, *C. elegans* has 40 distinct members (Mohrlen *et al.,* 2003), thirty-nine of which are expressed and presumed to be functional, with one pseudogene (Mohrlen *et al.,* 2003).

To visualise the effects of *qsox* and *nas* targeted RNAi upon the cuticle, a strain expressing a GFP tagged adult specific collagen marker was employed. This allowed for the visualisation of the collagen network of the cuticle in live nematodes, and gave a degree of characterisation previously only achievable by antibody staining of fixed worms. This greatly aided the characterisation and detection of target genes which had no gross morphological effect, but had collagen distortions that may have gone undetected by DIC microscopy alone.

3.1 The GFP tagged collagen marker strain TP12

The marker strain TP12 was constructed by Melanie Thein (University of Glasgow) (Thein *et al.,* 2003). TP12 allows for quick and easy characterisation of the collagen matrix following either targeted mutagenisis, RNAi, or by crossing of TP12s with a mutant strain.

By using TP12 strain mutations which do not exhibit gross morphological defects, either as nulls or by gene silencing, can be screened and their cuticle visualised. Previously to visualise the collagen matrix, antibody staining was employed. This method however has limitations in comparison to a marked translational fusion strain. Primarily, the worms being studied must be fixed in gluteraldehyde prior to exposure to the antibodies. Also, due to the conserved nature of the collagens, designing antibodies to specific collagens is difficult. The similar basic primary and quaternary structure can also preclude the access of antibodies to their specific epitopes. Due to these limitations only three specific, effective, antibodies have yet been raised; SQT-1 (Yang and Kramer, 1994), SQT-3 (Novelli *et al.,* 2006) and DPY-7 (McMahon *et al.,* 2003).

3.1.1 COL-19::GFP wild type patterning and localisation in TP12.

A specific banding pattern is discernable in adult stage (GFP positive) TP12 worms, Figure 3.1, GFP is detectable in circumferential rings around the long axis of the nematode and the tri-laminate lateral alae, thus localising COL-19 to the dorso-ventral hypodermis and the lateral syncytial seam cell. The hypodermis and seam cells are areas inherently associated with cuticle synthesis, thus COL-19 localises to regions of collagen production. COL-19 also localises to the hermaphrodite vulva and the male tail (Thein *et al.,* 2003). To determine the specific region of cuticle in which COL-19 was incorporated, antibody staining using a DPY-7 antibody was performed (Thein *et al.,* 2003). DPY-7 localises to the annular furrows of the cuticle (McMahon *et al.,* 2003). When TP12s were analysed using the DPY-7 antibody and the FITC/UV images overlaid, it would appear that the two markers were mutually exclusive (Thein *et al.,* 2003). DPY-7 highlighting the annular furrows (McMahon *et al.,* 2003) and COL-19::GFP marking the intervening 1.2 µm wide annulae, see Figure 3.1.

The wild type cuticle of the TP12 strain alters as the worm ages. Time courses were set up to allow TP12 to age for 2, 4, 6 and 8 days following the L4-adult moult at 25ºC. From this it could be seen that as the worm aged the clear annuli and lateral alae staining associated with young adult TP12s distorted, in particular over the seam cell derived cuticle. By day six COL-19 had fragmented in seam cell derived cuticle, but structures such as the annular rings and alae were still distinguishable. The annular staining became amorphic by eight days with structures of the cuticle hard to differentiate.

These changes were probably due to the dynamic nature of the cuticle and the inevitable changes imposed upon the cuticle as the nematode aged. No significant distortions were

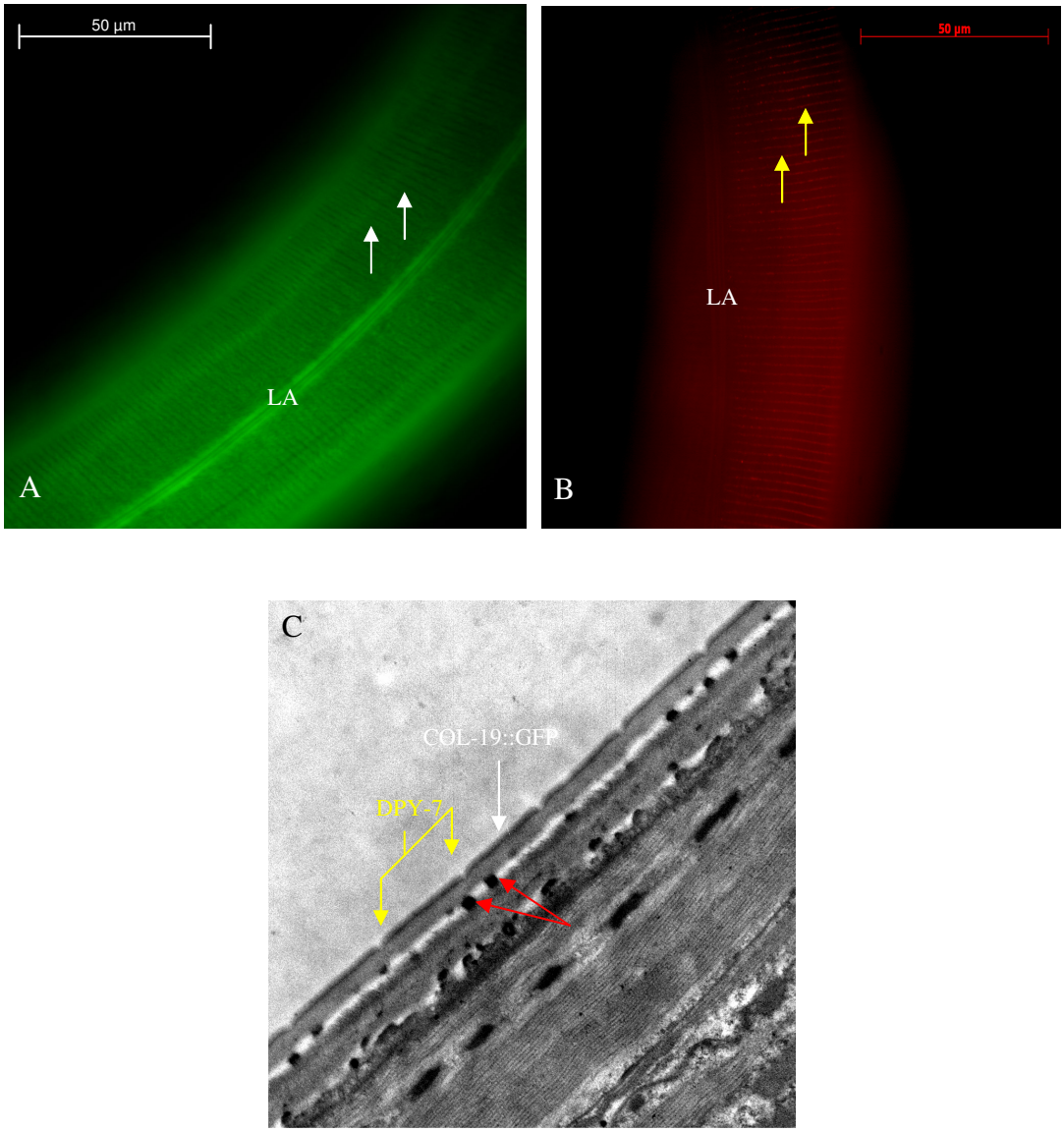

Figure 3.1: Patterning and localisation of COL-19::GFP in the strain TP12. (A) Shows the circumferential banding pattern exhibited by the TP12 strain. COL-19 is localising to the annulae (white arrows). (B) DPY-7 antibody stained N2 highlighting the narrow annular furrow staining characteristic of DPY-7 (yellow arrows). (C) Transmission electron microscope image of N2 *C. elegans* showing the regional localisation of the COL-19 and DPY-7 collagens, highlighting their mutual exclusivity. White arrow denotes an annulus and COL-19 localisation. Yellow arrows denote the annular furrow and DPY-7 localisation. The struts that underlie the annular furrows of a wild type adult cuticle are shown by the red arrows. The lateral alae are denoted LA.

visible in the cuticle before four days post L4-adult moult. Thus wild type patterning of TP12s endured until at least four days post L4-adult moult, by which time any worms undergoing targeted RNAi, for example, would have been screened.

3.2 Results

3.2.1 The quiescin-sulfhydryl oxidase in C. elegans

The QSOX enzymes were postulated to be involved with cuticle generation by insertion of disulphide bonds based upon; similarities to the PDI class of enzymes, which have been shown to be associated with the process of disulphide bonding and from the literature (Gerber *et al.,* 2001; Thorpe *et al.,* 2002; Winter *et al.,* 2002; Eschenlauer and Page, 2003; Coppock and Thorpe, 2006). *qsox-1, qsox-2* and all splice variants of *qsox-3* contain an N-terminal thioredoxin CxxC motif. This motif can be more stringently classified in QSOX proteins as wCgxC. An identical motif can be found in PDI a/a′ thioredoxin domains (Thorpe *et al.,* 2002).

The mechanism for disulphide bond generation by QSOX can be seen in Figure 3.2. Based upon domain similarities to the QSOX group, F56C11.3 was also proposed as a QSOX family member. This was shown however not to be the case with F56C11.3 being more closely related to *S. ceravisaie* Erv1p than to any QSOX family member, see Appendix A.

3.2.2 Molecular analysis of the QSOX family

QSOX-1, QSOX-2 and QSOX-3 all contain signal peptides as defined using Signal P (Zhang and Henzel, 2004). The QSOX-1 signal peptide lies within the first 20 N-terminal residues and is cleaved between residues 19-20 (97% probability reported by Signal P). QSOX-2 has a signal peptide that lies within the first 30 residues, cleaved between residues 29-30 (87% probability reported by Signal P). EST data shows there to be three different splice variants of QSOX-3; QSOX-3 (a) produces a peptide 623 residues in length; QSOX-3 (b), a 678 residue peptide and QSOX-3 (c), a peptide 624 residues in length. Variant (b) includes an exon 12, which contains a transmembrane domain not found in the other two isoforms. By mixed stage cDNA RT-PCR, isoform (b) was shown to be the predominant splice variant. The three isoforms of QSOX-3 however do have identical N-terminal regions. QSOX-3 is weakly predicted to have a signal peptide within

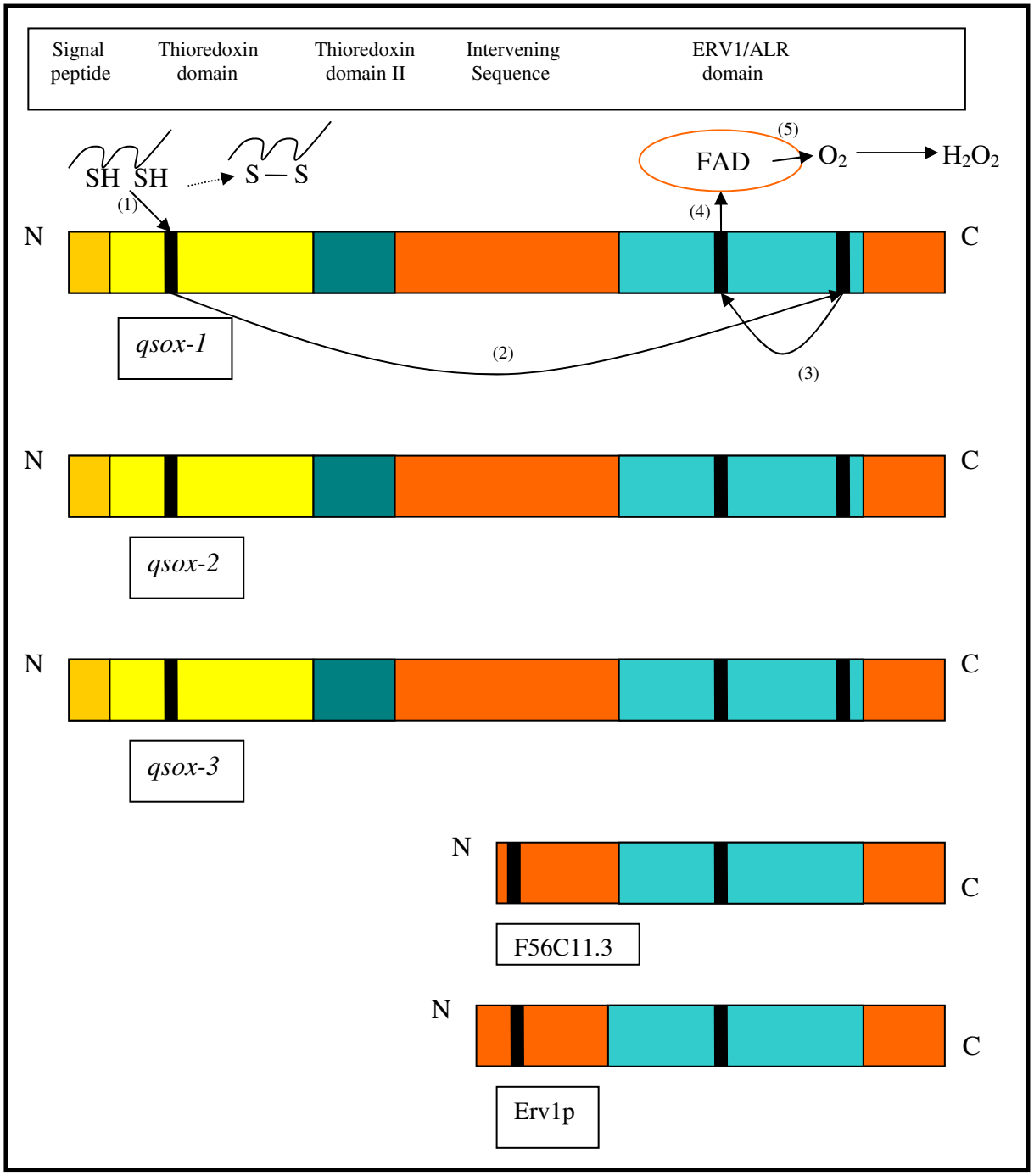

Figure 3.2: Schematic representation of the QSOX family members, and F56C11.3 with its close homologue Erv1p. Thick vertical lines denote approximate location of CxxC motifs. Arrows show the flow of reducing equivalents between the domains of the QSOX family members. QSOX have a signal peptide, an N-terminal thioredoxin domain containing a wCgxC motif that accepts the dithiols electrons and begins the shuttling of reducing equivalents (1). The second N-terminal thioredoxin domain does not contain a CxxC domain and is thought to play little role in electron transfer. (2 /3) Shows the interdomain communication of the ERV1/ALR domain within itself, and in receiving reducing equivalents from the thioredoxin domain. (4) At this stage a strong charge transfer takes place between the proximal disulphide of the ERV1/ALR domain and the oxidised electron deficient flavin prosthetic group (FAD). This results in the reduction of the FAD group and reformation of the disulphide bond between the ERV1/ALR cysteines. Catalysis is concluded with oxidised FAD reacting with molecular oxygen and generating H_2O_2 (5) (Coppock and Thorpe, 2006). F56C11.3 does not contain the N-terminal thioredoxin domin but posseses an N-terminal CxxC, homologous to yeast Erv1p, that is used to facilitate the flow of reducing equivalents in a similar manner to QSOX enzymes. (Hofhaus *et al.,* 2003)(not to scale).

its first 41 residues, cleaved between residues 40-41 (20% probability reported by Signal P analysis).No QSOX to date, *C. elegans*, human, mouse or avian have been found to contain a KDEL endoplasmic reticulum retention sequence (Coppock and Thorpe, 2006), but, similar to avian QSOX, *C. elegans* QSOX-1 and QSOX-2 contain RxR motifs at their C-terminus, consistent with retention/retrieval to the ER (Standley *et al.,* 2000). QSOX-3 does not possess either an RxR motif or a KDEL sequence. Localisation of QSOX-3 to specific cell types could be achieved by the presence of the transmembrane domain which is located C-terminal to the ERV1/ALR domain, and is found in the predominant splice variant *qsox-3* (b). This splice variant includes a 12^{th} exon which encodes a 17 residue transmembrane domain (residues 627-644). This domain could anchor QSOX-3 to the cell surface, where upon it could process peptides that were not fully processed internally. Both human QSOX, one of the four *Drosophila melanogaster* QSOX and the single *Trypanasoma brucei* QSOX all contain a homologous transmembrane region downstream of their ERV1/ALR domain (Coppock and Thorpe, 2006).

SL-PCR of qsox-1, qsox-2 and qsox-3

The SL-PCR reactions were carried out using gene specific antisense primers, see Table 2-7, in conjunction with the SL1 and SL2 consensus primers and mixed stage N2 cDNA. Standard PCR conditions were used as per section 2.18. From Figure 3.3 it can be seen that: *qsox-1* is SL1 *trans*-spliced (lane 1); *qsox-2* is both SL1, and SL2 *trans*-spliced (lane 3 and 4) with SL1 the principal splicing form, and *qsox-3* is SL2 *trans*-spliced (lane 6).

3.3 Initial screen of the QSOX family of enzymes by RNAi feedings and injections

In order to assess the importance of the QSOX family of enzymes to *C. elegans,* with regards to the generation of a functional cuticle, an initial RNAi screen was performed. This involved the feeding and injection of dsRNA targeted towards specific QSOX genes (*qsox-1, qsox-2* and *qsox-3*) into N2s and TP12s and visualising the effect on the cuticle of the worm by DIC and UV microscopy.

3.3.1 RNAi of qsox-1 qsox-2 and qsox-3

To determine the specificity of the RNAi constructs BLAST searches were performed with full length coding fragments of *qsox-1, 2* and *3*. The RNAi fragments were also aligned

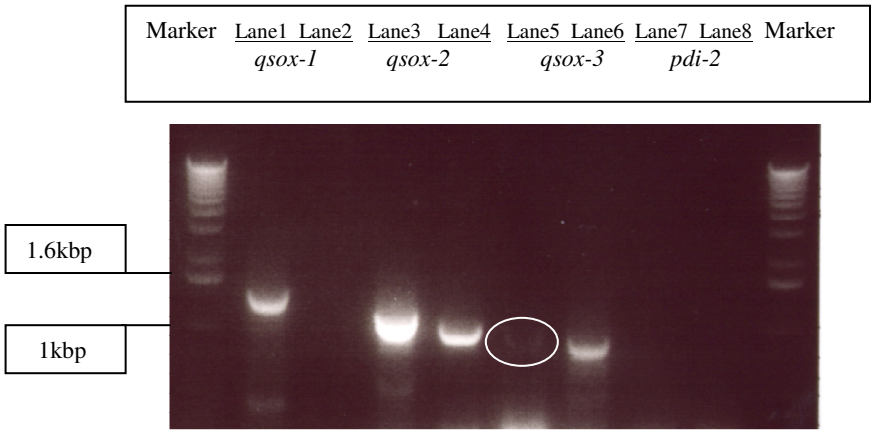

Figure 3.3: Splice Leader PCR of *qsox-1, qsox-2* and *qsox-3* amplified from mixed stage N2 cDNA. (Lane 1 and 2) show the product of SL1 and SL2 (respectively) amplification in conjunction with an antisense primer for *qsox-1*. (Lane 3 and 4) show the product of SL1 and SL2 (respectively) amplification in conjunction with an antisense primer for *qsox-2*. *qsox-2* is both SL1 and SL2 *trans*-spliced, with SL1 trans-splicing being the prevailing form. Size discrepancy due to concentration of DNA. (Lane 5 and 6) show the product of SL1 and SL2 (respectively) amplification in conjunction with an antisense primer for *qsox-3*. (Lane 6) shows that *qsox-3* is *trans*-spliced by SL2. (Lane 5) contains a faint band (white circle) of the correct size; SL2 is the prevailing form of splicing with regard to *qsox-3*. (Lane 7 and 8) *pdi-2* is neither SL1 nor SL2 *trans*-spliced and was included as a negative control. Marker is a 1kb DNA marker from Invitrogen.

using Vector NTI Align X (Invitrogen), to determine the degree of similarity between the specific RNAi fragments and the full length coding sequences for the entire *qsox* family.

The BLAST results showed that there would be sufficient confidence to ascribe specificity to the respective genes when subjecting *C. elegans* to targeted RNAi. Table 3-1 shows the percentage similarities between each of the QSOX family members over their full-length coding sequence. The highest nucleotide similarity between the *qsox* RNAi fragments and coding sequences is 27.2% identity, less than that proposed to cause cross interference (Tabara *et al.,* 1998). Thus RNAi effects could be ascribed to the specific target and not cross reactivity within the family or other gene classes. Included in Table 3-1 are the full-length coding sequences for *pdi-1, 2* and *3,* as association had previously been shown between these two classes of enzymes in an avian model (Hoober *et al.,* 1999), and both QSOX and PDI enzymes also contain thioredoxin domains it was important to rule out possible cross reactivity between these two groups. No significant regions of homology were noted between the *qsox* RNAi fragments and the *pdi* coding sequences, and no region of any RNAi fragment shared 100% identity to any other cDNA included in the table below for longer then 10bp, except for the corresponding cDNA fragments which showed 100% identity over the RNAi fragments length.

RNAi fragment	**Full-length cDNA**					
	qsox-1 *(1725bps)*	*qsox-2* *(1806bps)*	*qsox-3* *(2037bps)*	*pdi-1* *(1458bps)*	*pdi-2* *(1482bps)*	*pdi-3* *(1467bps)*
qsox-1 *(1052bps)*	60.9%	23.6%	19.8%	15%	14%	13%
qsox-2 *(1806bps)*	-	100%	27.2%	20.1%	19.9%	20.6%
qsox-3 *(1679bps)*	-	-	82.4%	25.1%	26.4%	29.6%

Table 3-1: Percentage nucleotide identity between the *qsox* RNAi constructs and whole *qsox* coding sequence. Also shown are the *pdi* coding sequences and the relative sequence identity shared between the *qsox* RNAi fragments and the *pdi* coding sequences.

qsox-1 RNAi by feeding

The *qsox-1* RNAi construct was derived from the RNAi feeding library (Kamath *et al.,* 2003). RNAi of *qsox-1* at 25ºC (RNAi was performed at 20ºC with similar results) in TP12 backgrounds produced a disrupted COL-19 banding pattern, in particular at the head region and over the lateral seam cell derived cuticle, Figure 3.4.A and B respectively. The seam cell derived lateral alae appeared to maintain a wild type tri-laminar confirmation, Figure 3.4.A and B. Distortions to the gross morphology of the worm were also noted.

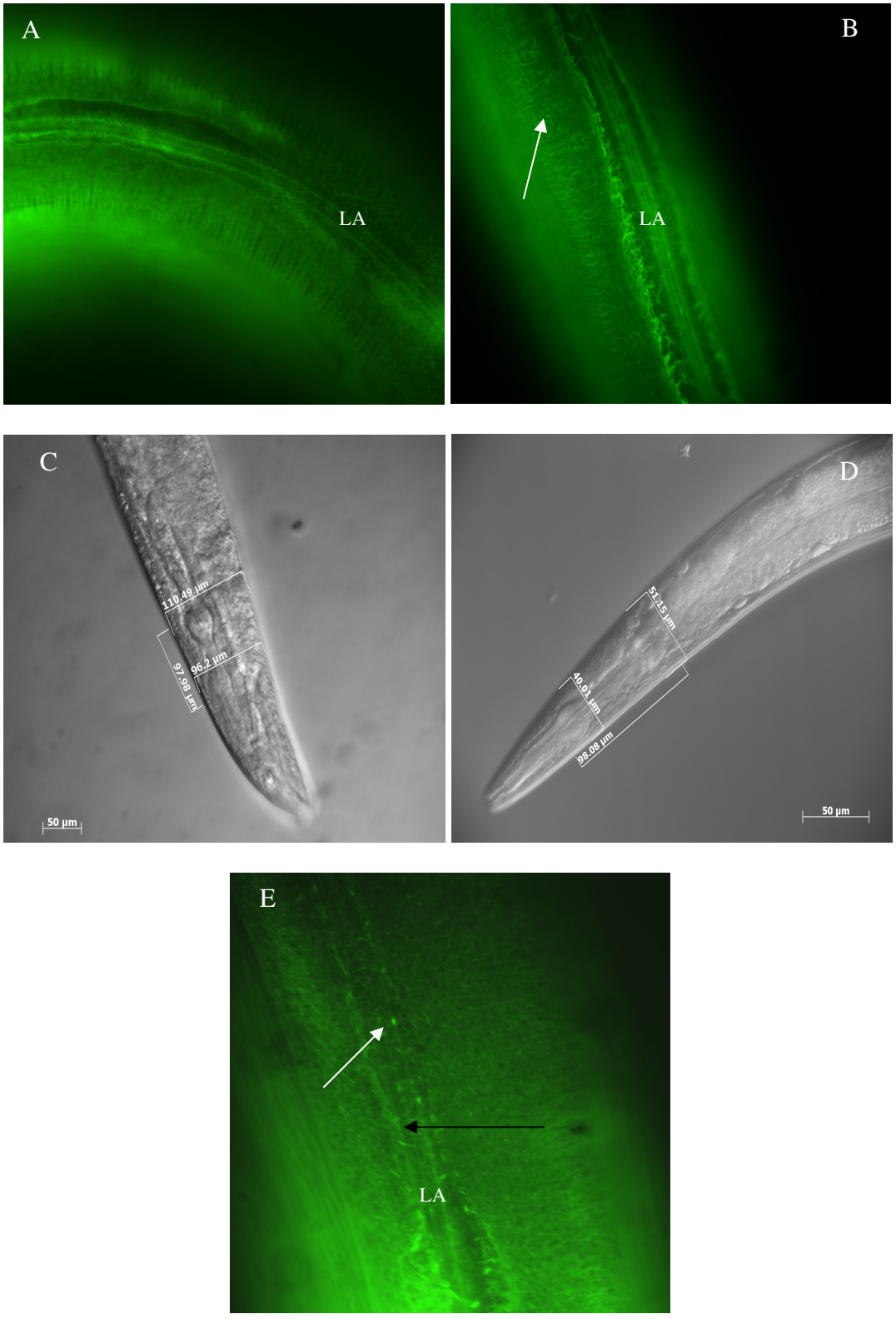

Figure 3.4: Targeted RNAi of *qsox-1* by feeding and injection. (A,B,C) RNAi by feeding (25C). (E) RNAi by injection (25C). (A) Illustrates the COL-19::GFP disruption associated with RNAi of *qsox -1*. The tri-laminar lateral alae (denoted LA) appeared to be of a wild type conformation. The cuticle above the seam cells and around the lateral alae was severely fragmented and whispy, also the circumferential banding pattern appeared to be distorted (B, white arrow). (C) A DIC image of a targeted worm illustrating a greater diameter than (D) a wild type worm (E) TP12 following injection of *qsox-1* dsRNA at 0.4 mg/ml and incubation at 25ºC. The lateral alae is still discernable (black arrow) however most other structure had been lost leading to an amorphous COL-19::GFP patterning. Aggregates of collagen could also be seen (white arrow).

qsox-1 RNAi feeding at 25ºC carried out upon N2 worms gave similar gross morphological defects, Figure 3.4.C. The worm had an expanded appearance (approximately twice the diameter of a similarly aged N2) having failed to contract circumferentially over the lateral alae: most noticeable at the head of the worm. The pharynx remained wild type in structure below the distorted cuticle. This cuticular loosening did not appear to be blister like, and when viewed in the TP12 strain the expanded appearance worms gave a COL-19 patterning similar to that seen in Figure 3.4.B with "whispy" fragmented cuticle around the seam cells and the lateral alae region of the cuticle.

qsox-1 RNAi by injection

Injected dsRNA was identical in sequence to the feeding construct. In both TP12 and N2s the effects noted with feeding RNAi were more severe following injection RNAi. The TP12 cuticles were more severely disrupted, Figure 3.4.E, with the gross morphological distortions associated with feeding of *qsox-1* dsRNA also evident by injection RNAi.

It is appealing to postulate that *qsox-1* may perform a role in the disulphide bond generation of collagens secreted form the lateral seam cells, the hypodermal cells, but not those involved with lateral alae generation.

qsox-2 RNAi by feeding

Full-length coding sequence for *qsox-2* was amplified by PCR from mixed stage cDNA, the primers used are listed in Table 2-7, and cloned into the vector L444O, which was subsequently transformed into HT115 (DE3) *E. coli* and served as the RNAi template for these experiments.

Disruption could be seen in the seam cell derived cuticle following RNAi of *qsox-2* at both 20ºC and 25ºC. The cuticle surrounding the lateral alae was fragmented and "whispy", Figure 3.5.A, illustrating failure in processing of the collagens in this area of the worm. The lateral alae did not appear to be disrupted however, and maintained its tri-laminar form, Figure 3.5.C. The cuticle also maintained a discernable annular furrow pattern, Figure 3.5.B, over the dorso-ventral hypodermal expressed cuticular regions, but lost the wild type banding pattern in the seam cell derived cuticular regions. The gross morphology of the nematode was unaffected.

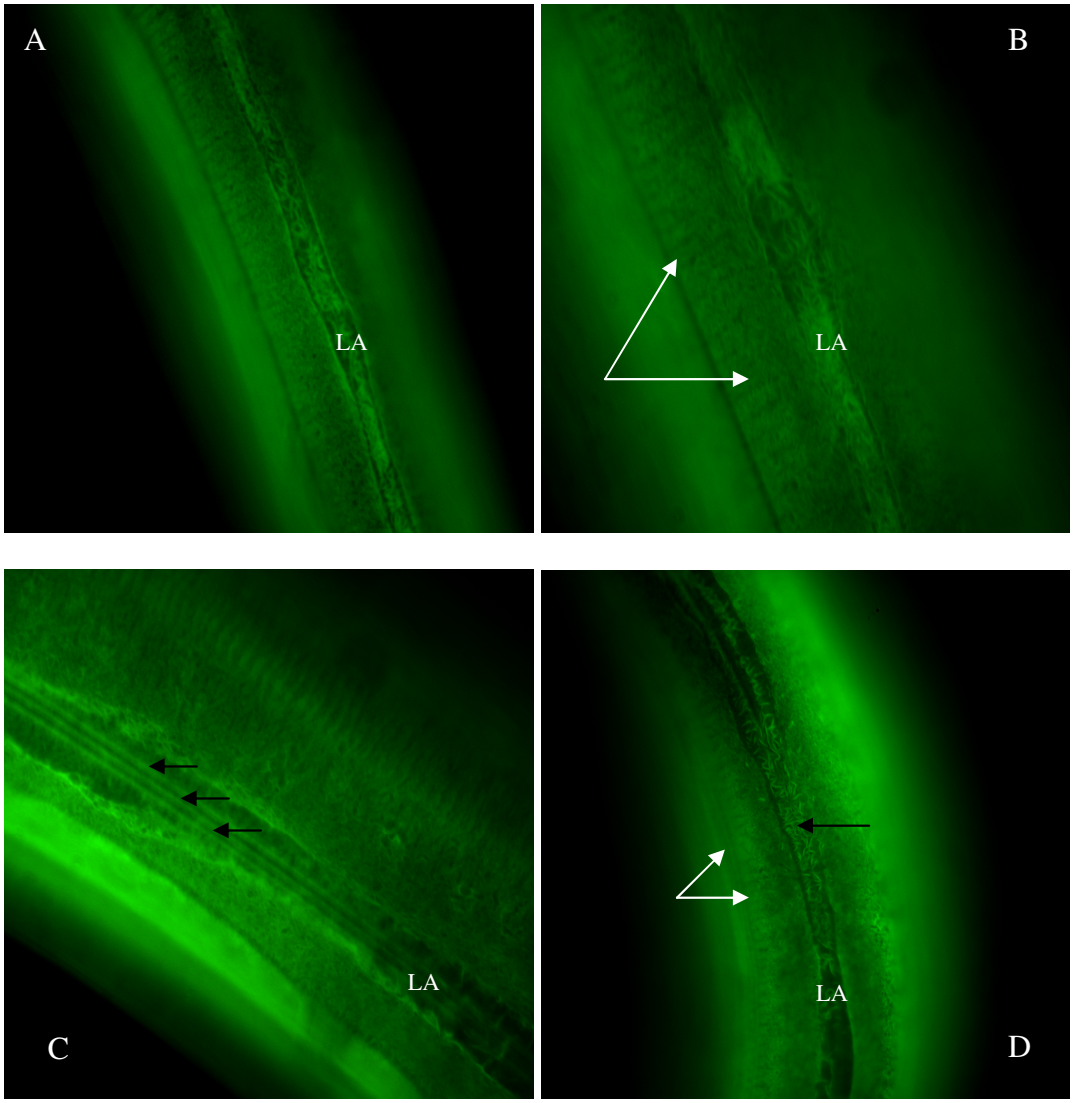

Figure 3.5: Targeted RNAi of *qsox-2* by feeding and injection in TP12s. (A, B, C) RNAi by feeding. (D) RNAi by injection. The disruption associated with a knockdown of *qsox-2* was in seam cell derived cuticle around the lateral alae, illustrated in (A). The annular banding pattern endures, denoted by the white arrows (B). (C) An intact tri-laminar lateral alae overlying the distorted seam cell derived cuticle (black arrows). (D) TP12 following injection of *qsox-2* dsRNA at 0.4 mg/ml and incubation at 25ºC. The seam cell derived cuticle shows distortion (black arrow). The cuticle still maintains some structural characteristics notably the hypodermaly generated annular rings (white arrows). The lateral alae remain intact (not shown). Lateral alae are denoted LA.

qsox-2 RNAi by injection

The fragment used to generate the dsRNA was identical to the feeding fragment. TP12s being injected with *qsox-2* dsRNA at 0.4 mg/ml and incubated at 25ºC, with the resultant F1 progeny being scored. Distortions similar to the feeding RNAi were noted following injection of *qsox-2* dsRNA, Figure 3.5.D. Annular furrows and annulae were visible, with amorphic seam cell generated cuticle, except for the lateral alae, which maintained a wild type conformation (data not shown). There was no noticeable gross morphological defect associated with the injection of *qsox-2* dsRNA and the worms, when viewed under DIC, appeared wild type.

qsox-3 RNAi by feeding

RNAi feeding of *qsox-3* led to distortion in the seam cell derived cuticle of TP12 and N2 at both 20°C and 25°C. Distortion of the cuticle around the lateral alae in the TP12 strain can be seen in, Figure 3.6.A and B. Also of note was the aggregation of COL-19 collagens which appeared as high intensity fluorescent granules, consistent with improperly folded proteins, Figure 3.6.A. The seam cell derived cuticle is the most severely disrupted, however a wild type lateral alae endures. The dorso-ventral hypodermally expressed cuticle is wild type, Figure 3.6. Gross morphological examination of *qsox-3* RNAi treated worms revealed an uncoordinated (Unc) and slow growth phenotype (Gro). Confirmed by genome wide screens carried out by (Kamath *et al.,* 2003; Simmer *et al.,* 2003).

From the initial RNAi screening of the QSOX family of enzymes it was evident that the enzymes were involved in cuticle collagen processing, most likely in the seam cells. *qsox-1* illustrated the most severe mutations, with greatly distorted cuticle and distinct gross morphological mutations. RNAi is however limited by being a knockdown of gene expression, not a knockout, to discern the true effects of QSOX depletion in *C. elegans bona fide* knockouts had to be generated.

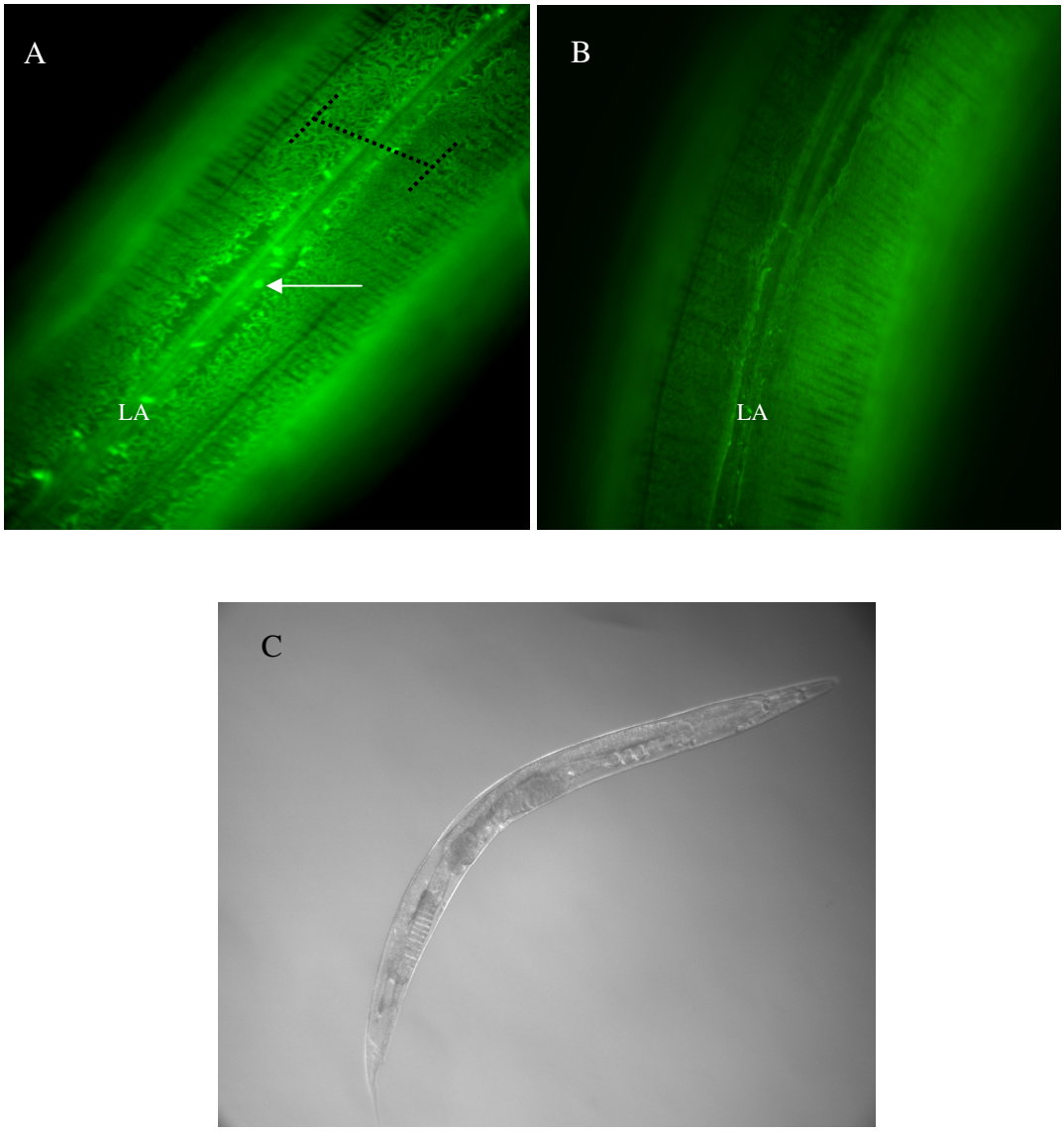

Figure 3.6: Targeted RNAi of *qsox-3*. (A) Disruption could be seen in the cuticle derived from the seam cells (highlighted by the black dotted bar). Also visible are COL-19 inclusion bodies (white arrows). The cuticle which was non-seam cell derived appeared to show some minor disruption in the banding pattern (B). (C) Shows a DIC image of a targeted worm. This worm appears morphologically wild type but had a slow growth and un-coordinated phenotype associated with the knockdown of *qsox-3*, which agreed with data published from genome wide RNAi screens (Kamath *et al.,* 2003; Simmer *et al.,* 2003). The lateral alae are denoted LA.

3.4 Initial screen of the NAS family of enzymes by RNAi feeding and injection

The *C. elegans* astacins have three major domains; a pre-pro portion, the central catalytic astacin domain and long C-terminal extensions that presumably have regulatory functions. Within the regulatory moiety, epidermal growth factor like (EGF-like), CUB domain (CUB), six cystine repeats (SXC/ShK), and thrombospondin type-1 (TSP-1) domains can be distinguished (Mohrlen *et al.,* 2003). Mohrlen *et al* (2003) classified these 40 individuals into six distinct groups (I-VI) based upon the structural differences of their regulatory unit. Given the structural domains of the astacin genes; previous knowledge regarding metalloproteinases and work highlighting the potential for the astacin NAS-35 to C-terminally cleave SQT-3 (Novelli *et al.,* 2004), proteolytic cleavage of collagens was proposed as the most likely involvement of NAS genes with regard to collagen maturation.

A number of phenotypes arose following RNAi of the *C. elegans* astacins, and are listed in Table 3-2. Worms were scored for COL-19 disruption, with additional morphological/behavioural defects also noted.

3.4.1 RNAi results

RNAi of the NAS family members was performed at 20ºC and 25ºC, as per section 2.27. Unless stated, the results shown were gathered from the 25ºC set of RNAi experiments. *C. elegans* strains; N2, TP12 and TP55 were used in these experiments. All RNAi feeding/injection constructs were derived from the RNAi feeding library (Kamath *et al.,* 2003).

3.4.1.1 Strain TP55

EG199*(ox199)* was obtained from the CGC (Caenorhabditis Genetics Centre) and contains a point mutation at base 1798 of the cDNA sequence for *nas-37*. The C →T point mutation constitutes a non-sense mutation that generates an opal stop codon (TGA) from an arganine codon (CGA) resulting in a truncated NAS-37, that is presumably ubiquinated and thus considered a null (Davis *et al.,* 2004). The strain that carried this non-sense mutation was then backcrossed, and subsequently crossed to TP12, and is referred to as, TP55. TP55 allowed for disruption of two genes by feeding of only one RNAi construct. Of particular interest are those genes that have similar domain structures to *nas-37*, notably

the other subgroup V astacins. TP55 exhibited a moult defect and showed limited disruption to the COL-19 patterning.

The results of the initial screen of the NAS family with TP12 and TP55 can be seen in Table 3-2.

Gene	Subgroup	Domains present	RNAi approach	Phenotype scored in strains TP12 and TP55, bracketed.
nas-5	I	Pre-pro, A.	Feeding	Seam cell derived ECM shows disruption. (no added effect)
nas-6	II	Pre-pro, A, SXC.	Feeding	Wild type COL-19 patterning. (No added effect).
nas-7	II	Pre-pro, A, SXC.	Feeding	Wild type COL-19 patterning. (No added effect)
nas-8	II	Pre-pro, A, SXC.	Feeding	Wild type COL-19 patterning. (No added effect)
nas-9	II	Pre-pro, A, SXC.	Feeding	Wild type COL-19 patterning. (No added effect)
nas-10	II	Pre-pro, A, SXC.	Feeding	Wild type, slight disruption to COL-19 patterning (No added effect)
nas-11	II	Pre-pro, A, SXC.	Feeding	Wild type, slight disruption to COL-19 patterning (No added effect)
nas-12	II	Pre-pro, A, SXC(x2).	Feeding	Seam cell derived COL-19 shows disruption. (No added effect)
nas-13	II	Pre-pro, A, SXC(x2).	Feeding	Seam cell derived COL-19 shows severe disruption. (No added effect)
nas-14	II	Pre-pro, A, SXC(x2).	Feeding	Wild type COL-19 patterning. (No added effect)
nas-15	II	Pre-pro, A, SXC(x2).	Feeding	Wild type COL-19 patterning. (No added effect)
nas-28	III	Pre-pro, A, EGF, CUB	Feeding & injection	Seam cell distortions and gross morphological defects by feeding and injection. (No added effect)
nas-31	IV	Pre-pro, A, EGF, CUB, SXC	Feeding	Wild type COL-19 patterning. (No added effect)
nas-32	IV	Pre-pro, A, EGF, CUB, SXC	Feeding	Wild type COL-19 patterning (No added effect)
nas-34(hch-1)	V	Pre-pro, A, EGF, CUB, TSP-1	Feeding	Wild type COL-19 patterning but showed delayed hatching. (No added effect)
nas-35(dpy-31)	V	Pre-pro, A, EGF, CUB, TSP-1	Feeding	Wild type. (No added effect)
nas-36	V	Pre-pro, A, EGF, CUB, TSP-1	Feeding	Moult defective. Slight disruption to COL-19 patterning. Also evident was a quad alae. (No added effect)
nas-37	V	Pre-pro, A, EGF, CUB, TSP-1	Feeding	Moult defective. Seam cell distortions to COL-19 patterning. Also evident was a quad alae. (No added effect)

Gene	Subgroup	Domains present	RNAi approach	Phenotype scored in strains TP12 and TP55, bracketed.
nas-38	V	Pre-pro, A, EGF, CUB, TSP-1	Feeding & Injection	Distortion to COL-19 banding pattern. (No added effect)
nas-39(BMP-1like)	VI	Pre-pro, A, EGF(x2), CUB(x5),TSP-1	Feeding	Wild type COL-19 patterning. (No added effect)

Table 3-2: Effects on *C. elegans* following RNAi of the astacin family members. Pre-pro, pre-pro domains; A, astacin domain; EGF, epidermal growth factor like domain; CUB, CUB domain; TSP-1, thrombospondin type-1 domain; SXC, six cysteine domain (ShK domain). Colour coding denotes severity of mutation. Wild type = white, minimal disruption = yellow, intermediate disruption = orange and severe disruption = red.

Initial observations illustrated phenotypically diverse results. The TP55 background did not amplify any of the RNAi phenotypes, other than conferring the characteristic TP55 mutations of Mlt, four alae and minor COL-19 disruption upon the targeted worms.

3.4.1.2 *nas* RNAi result analysis by subgroup classification

Basic Astacin containing genes (subgroup I)

Limited scope was placed upon the screening of those *nas* genes which were comprised primarily of an astacin domain, with limited C-terminal ancillary domains. *nas-5* was screened against TP12s and N2s with particular importance placed on characterisation of males, Figure 3.7. Males were screened due to reports of *nas-5* transcripts being more abundent in males over hermaphrodites, in a logarithmic ratio of [(0.197) male/female] (Jiang *et al.,* 2001). Jaing *et al* (2001) performed microarray experiments which compared fluctuations between gene expression profiles of the two *C. elegans* sexes. Thus *nas-5* is a *bona fide* transcript and was presumably expressing a functional protein. From genome wide screens, a wild type phenotype was reported following RNAi of *nas-5* (Kamath *et al.,* 2003; Simmer *et al.,* 2003). Neither of these genome wide screens could view in detail the collagenous structure. Using the TP12 strain a discernable collagenous phenotype associated with the knockdown of *nas-5* was discovered.

To view males under targeted RNAi, crosses were set up between males (x4 or x5) and a single hermaphrodite *C. elegans* on RNAi plates that had been seeded with the target expressing bacteria. The resultant progeny of successful crosses, plates that contained ~50% males, were scored. The crosses and RNAi were carried out at 25ºC.

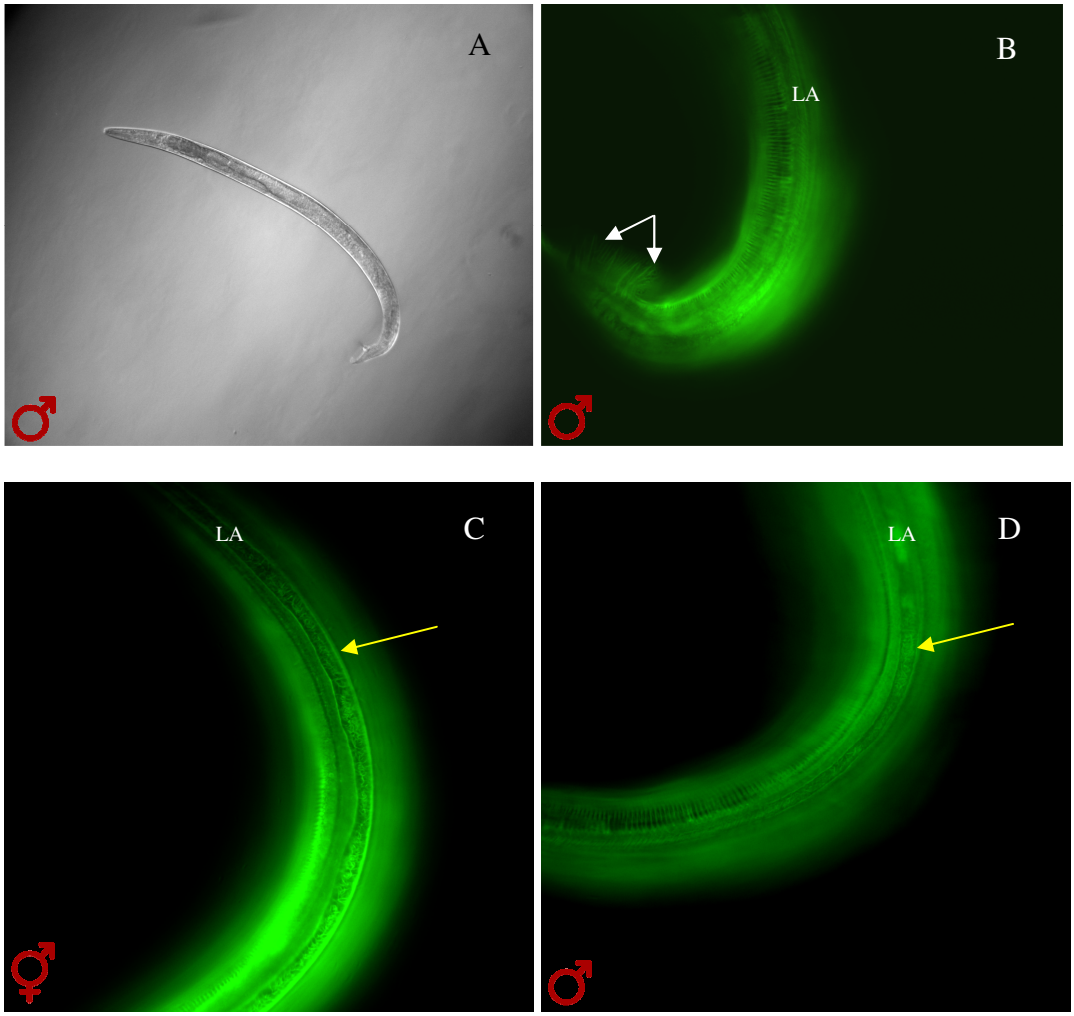

Figure 3.7: RNAi mediated interference of TP12 with *nas-5* dsRNA by feeding. NAS-5 belongs to subgroup I. (A) N2 *C. elegans* exhibit no gross morphological defects associated with the RNAi of *nas-5*. (B) TP12 male tail adopts wild type morphology with no distortion of the COL-19 containing rays (white arrows). (C) TP12 hermaphrodite exhibits seam cell disruption, as does the male (D) , (yellow arrows). LA denotes lateral alae**.**

Particular importance was placed on scoring the development of the male tail. The male tail is composed of nine pairs of rays, digitations which protrude from the lateral side of the worm, and have a webbed appearance. This webbing is termed the fan. Ray 1 is derived from seam cell V5, rays 2–6 are derived from seam cell V6 with rays 7–9 derived from seam cell T (Zhang and Emmons, 2002). Both the ray and fan structures express COL-19 (Thein *et al.,* 2003) and can be visualised by UV microscopy. Following feeding RNAi of *nas-5,* no gross morphological defects associated with N2 males or hermaphrodites was noted, Figure 3.7.A. The male tail was viewed and appeared wild type in conformation in TP12 backgrounds, Figure 3.7.B. Disruption was noted however in both hermaphrodite and male seam cell derived cuticular areas, Figure 3.7.B, C and D, which illustrated a fragmented and "whispy" COL-19 patterning.

Astacin domain and Six cysteine domains (subgroup II)

All members of this subgroup were screened by RNAi feeding in the TP12 and TP55 background. 60% of the subgroup members (*nas-6, 7, 8, 9, 14* and *15*) returned a wild type collagen phenotype. 20% exhibited slight disruption (*nas-10* and *nas-11*) and 20% had intermediate and severe disruptions, *nas-12* and *nas-13*, respectively.

A wild type COL-19 banding pattern remained following targeted RNAi for *nas-9*. However, 6% lethality had been reported with the knockdown of this gene (Maeda *et al.,* 2001) and as such it was considered for further investigation. No gross morphological defects were noted with RNAi of *nas-9*. *nas-12* and *nas-13* appeared wild type at the gross morphological level in agreement with the genome wide RNAi screens (Kamath *et al.,* 2003; Simmer *et al.,* 2003). When TP12 was challenged with the RNAi feeding construct and the COL-19 arrangement visualised, a phenotype associated with the knockdown of each gene was evident, Figure 3.8. *nas-12* feeding RNAi, performed at 25ºC, caused seam cell derived COL-19 disruption, with the lateral alae endured in a wild type tri-laminar form, Figure 3.8.A and B. *nas-13* feeding RNAi, performed at 25ºC, also generated a disrupted cuticle, but to a greater extent than *nas-12*. The cuticle generated in *nas-13* RNAi targeted TP12s, showed an extensively disrupted COL-19 pattern in the seam cell regions, Figure 3.8.C and D.

A TP55 background for the *nas-12* and *13* RNAi experiments did not lead to any further mutations, other than TP55s own characteristic defects, being scored.

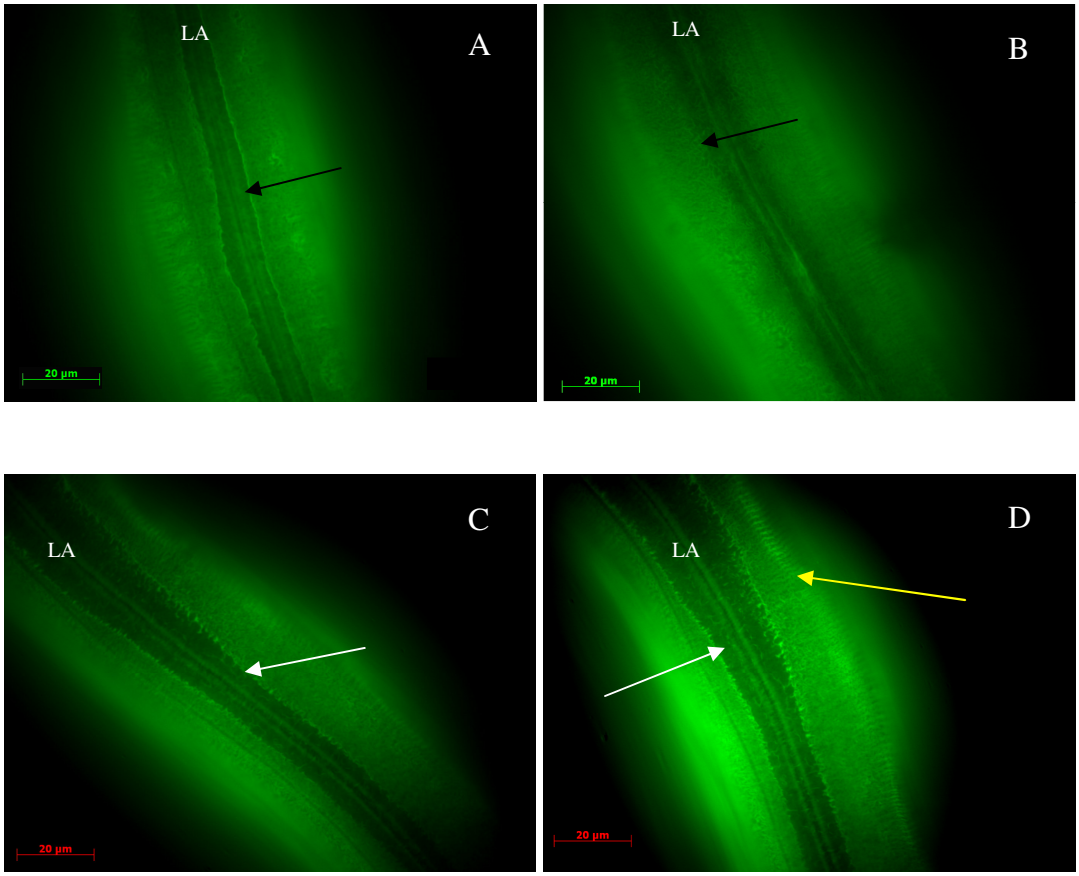

Figure 3.8: RNAi mediated interference of TP12 with *nas-12* and *nas-13* dsRNA by feeding. NAS-12 and 13 belong to subgroup II. (A and B) RNAi of *nas-12* in TP12 background. (A) A heavily distorted COL-19 pattern can be seen under *nas-12* RNAi but the tri-laminar alae endures (black arrow). (B) Further examples of the distortion of TP12s COL-19 deposition following RNAi of *nas-12*. (C and D) RNAi of *nas-13* in TP12 background. (C) Severe disruption of the seam cell derived cuticle can be seen (white arrows). (D) COL-19 deposition is severely distorted and "whispy". Some annular banding can be seen (yellow arrow). LA denotes the lateral alae.

Astacin domain, Epidermal Growth Factor domain and CUB domain (subgroup III)

Only one of the 14 members of subgroup III was screened. The rationale for the selection of this particular family member was based upon previous work that associated a marked phenotype with the RNAi of *nas-28* (Melanie Thein University of Glasgow, personal communication). These included branching of the lateral alae and an amorphous collagen network in the associated overlying seam cell derived cuticle. Figure 3.9.A and B shows the results obtained from feeding RNAi of *nas-28,* and Figure 3.9.C shows an injected TP12 worm, both at 25ºC. Following the knockdown of *nas-28,* in N2 and TP12, noticeable gross morphological mutations were visible Figure 3.9.A and B. The anterior head region of the worm remained unaffected by the knockdown of *nas-28,* but the body and tail regions of the worm appeared mutant, resulting in an overall dumpy (Dpy) phenotype. Also noted was an egg laying defective (Egl) phenotype, Figure 3.9.B, which could have been caused by vulval defects, either in presence or structure, as the vulva has a seam cell derived component required for functionality (Hanna-Rose and Han, 1999).

Following injection of dsRNA for *nas-28,* Figure 3.9.C, the cuticle generated from the seam cells became distorted, and aggregates of protein were apparent, a characteristic of incorrectly processed proteins, results which prompted further investigation.

Astacin domain, Epidermal Growth Factor domain CUB domain and Six cysteine domains (subgroup IV)

Subgroup IV comprises two members, *nas-31* and *nas-32*. Both of which were screened by feeding RNAi in TP12 and N2 backgrounds. Both returning wild type COL-19 patterning and wild type gross morphology. It appeared that this subgroup is not involved with the generation of the cuticle. Genome wide RNAi screens (Kamath *et al.,* 2003; Simmer *et al.,* 2003) reported similar wild type phenotypes associated with knockdown of these two subgroup members.

Astacin domain, Epidermal Growth Factor domain, CUB domain and Thrombospondin domain (subgroup V)

RNAi of subgroup V members in N2, TP12 and TP55 strains exhibited various distinct phenotypes namely; hatching defects (*nas-34*), moulting defects (*nas-36* and *nas-37*) and disrupted COL-19 arrangements (*nas-38*). *nas-38* RNAi by feeding and injection in N2 and TP12 worms gave no gross morphological defects, but some disruption of the COL-19

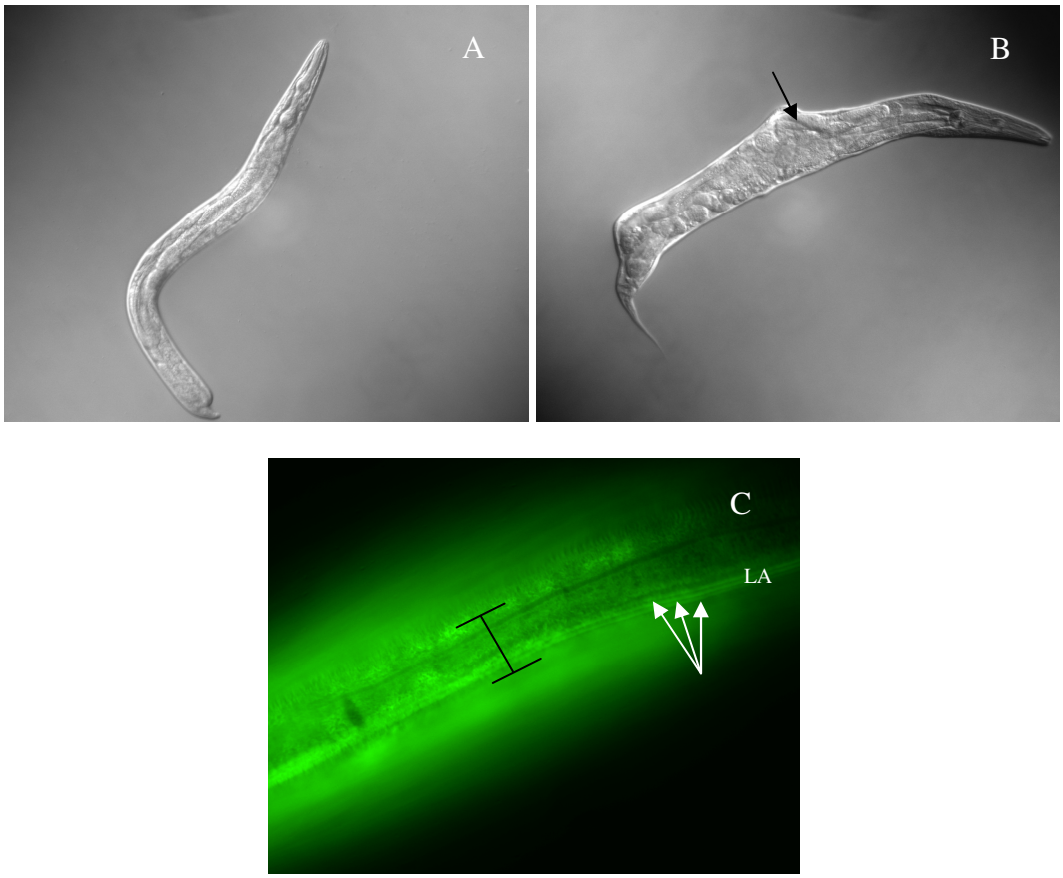

Figure 3.9: RNAi mediated interference of TP12 and N2s with *nas-28* dsRNA by feeding and injection. NAS-28 belongs to subgroup III. (A) TP12 (L4) showing aberrent body plan morphology; distorted/missing tail region. (B) N2 *C. elegans* adult exhibiting an Egl phenotype (black arrow) and an overall dumpy apperance. The head region remains wild type in appreance in both (A) and (B). (C) TP12 injected with dsRNA identical to the feeding construct. Distortion can be seen in the seam cell derived cuticle, which appears amorphous. The lateral alae (denoted LA) still maintains a tri-laminar structure (white arrows).

banding pattern was noted. Feeding of TP12 at 25ºC led to seam cell derived COL-19 disruption, with annular pattering enduring, see Figure 3.10.A. A similar phenotype was noted upon injection, but the distortion was more severe, a characteristic of the injection mediated RNAi procedure. The lateral alae in both instances remain wild type in morphology. The injected fragment of dsRNA was identical in sequence to that which the animals were fed.

nas-34/hch-1 was a previously characterised *nas* gene (Hishida *et al.,* 1996), disruption of which results in delays in hatching of up to 11hrs at 25ºC. This was also noted with RNAi of *nas-34* on both the N2 and TP12 strains of *C. elegans.* No detectable mutant phenotype was evident at the COL-19 level in adults, possibly due to the embryo specific expression profile of *nas-34/hch-1* (Hishida *et al.,* 1996).

nas-36 RNAi in TP55, TP12 and N2 backgrounds resulted in moult defects which could also be described as "wasp waist" in appearance due to the constriction, commonly found around the vulva, of the worm, see Figure 3.11.A and B. This constriction can be seen clearly in Figure 3.11.B as a fibrous circumferential band around the worm. The COL-19 banding pattern of TP12 worms subject to *nas-36* RNAi feeding is mildly disrupted in the seam cell derived cuticle, Figure 3.11.C, also TP12 and N2 worms were noted as often having lateral alae with a quad-laminar structure, as opposed to the tri-laminar wild type structure, see Figure 3.11.D.

TP55 worms, when subjected to *nas-36* RNAi, showed no greater/less incidence of Mlt than the untreated strain. 24.8% (n=145) showed Mlt phenotype, the untreated strain (TP55 fed on OP50 and stored at 25ºC) showed 24% Mlt (n=301). Thus the evidence suggests that *nas-36* is involved with the process of ecdysis in *C. elegans,* and was therefore considered for further investigation.

nas-37 RNAi, in TP12 and N2 backgrounds, produced worms that were incapable of proper ecdysis from the previous stage cuticle. The constriction, which is consistent with the moult defect in the TP55 strain, could be seen following RNAi of *nas-37,* thus proving the efficacy of RNAi for *nas-37*, in TP12 and N2 strains of *C. elegans*, Figure 3.11.E and F. The constriction itself could be seen to fluoresce, and must contain, at least in part, a COL-19 collagenous component. Similar to *nas-36*, a quad-laminar lateral alae was also noted in *nas-37* RNAi worms. This was a variable phenotype which was not exhibited in all worms.

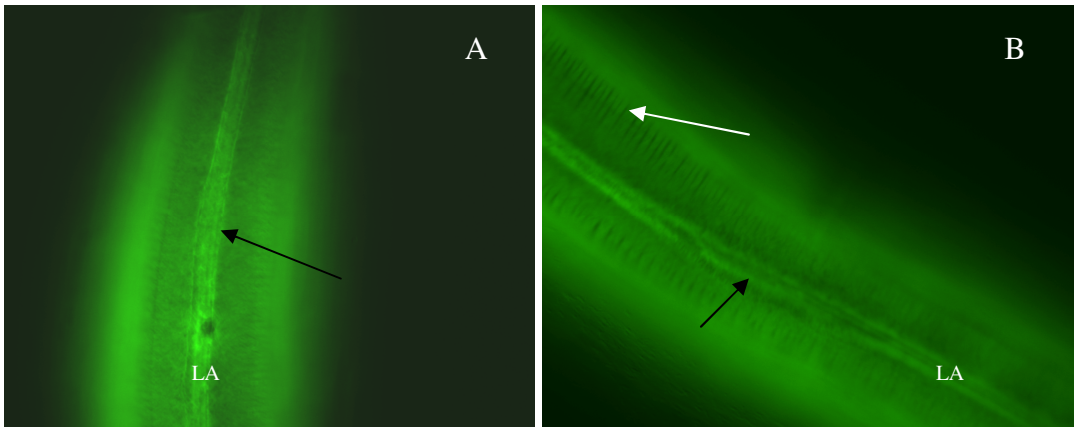

Figure 3.10: RNAi mediated interference of TP12 with *nas-38* dsRNA by feeding and injection. NAS-38 belongs to subgroup V. (A) Feeding RNAi causes seam cell derived COL-19 disruption (black arrow), with the annular pattern enduring. (B) RNAi by injection generates a similar disruption. The annular patterning is more disrupted with RNAi by injection and the seam cell derived COL-19 also appears more fragmented (black arrow). The lateral alae (both by feeding and injection) remains wild type in conformation. LA denotes the lateral alae.

Figure 3.11: RNAi mediated interference of TP12 with *nas-36* and *nas-37* dsRNA by feeding. NAS-36 and 37 belong to subgroup V. (A to D) Characteristic effects of *nas-36* RNAi upon *C. elegans* strains TP12 and N2. (A) A constriction around the mid section of the worm just posterior to the vulva (black arrows) (B) X100 magnification of a constriction around *C. elegans*. (B) Fibrous constrictive band around the worm (black arrow). (C) COL-19 disruption associated with *nas-36* RNAi, which is mild. Of note is the lateral alae which appears to be wild type but can be seen in image (D) to be quad-laminar (black arrows), (D) is the corresponding UV image of (C).

(E to H) *nas-37* RNAi in *C. elegans* strains TP12 and N2. (E) TP12 worm subjected to RNAi of *nas-37*. Low level seam cell disruption can be seen (yellow arrow). Mlt can be seen under RNAi of *nas-37*. The constriction can be seen to fluoresce (white arrow). Corresponding DIC image of the same worm can be seen to retain a previously unshed cuticle (F) (black arrow). (G) A quad-laminar lateral alae (black arrows). (H) *nas-37* RNAi in N2 *C. elegans,* adult showing a network of fibres (black arrow) that underlie the lateral alae. These fibres are not present in wild type worms. Similar networks of fibres have been noted in other collagen mutants (Thein *et al.,* 2003). LA denotes the lateral alae.

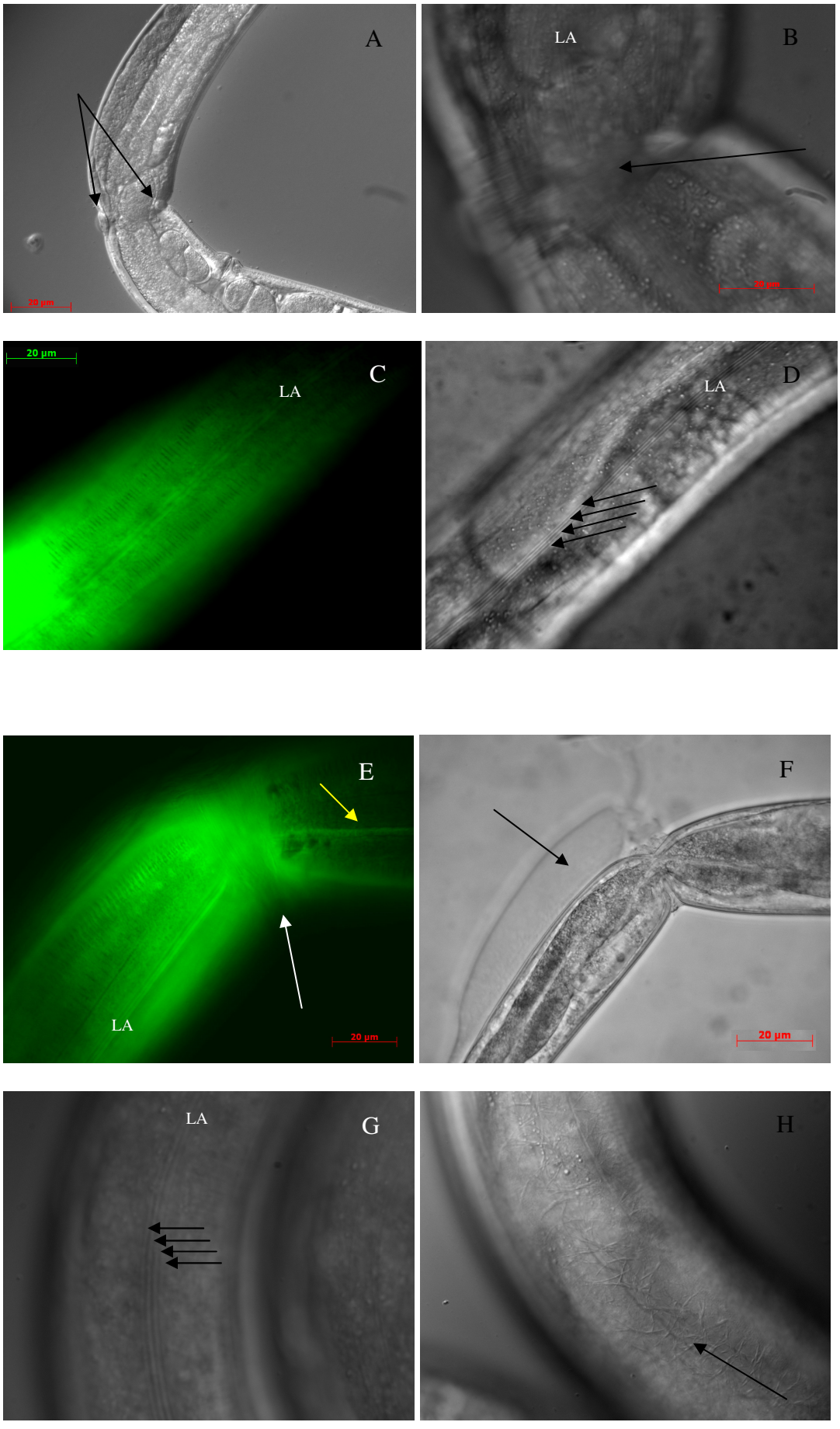
A
LA
B
20 µm
C
LA
D
LA
E
LA
20 µm
F
20 µm
LA
G
H

TP55 and worms subject to RNAi of *nas-37,* showed a network of fibres that underlie the lateral alae that are not present in wild type worms, Figure 3.11.H. Similar networks of fibres have been noted in collagen processing mutants (Thein *et al.,* 2003). The COL-19 pattern was also mildly disrupted. Thus, similarly to *nas-36*, the evidence would suggest that *nas-37* is involved in the process of ecdysis in *C. elegans,* both of these enzymes were selected for further characterisation.

Subgroup V RNAi fragments were analysed to establish their specificity within the subgroup, Table 3-3. No fragments of 100% identity exceeded 10bps in length, except for corresponding RNAi/cDNA fragments which shared 100% identity for the full length of the RNAi fragment.

RNAi fragment	**Full length cDNA**				
	nas-34 *(1818bps)*	*nas-35* *(1779bps)*	*nas-36* *(1956bps)*	*nas-37* *(2298bps)*	*nas-38* *(2238bps)*
nas-34 *(1651bps)*	90%	44%	27.9%	22.4%	21.6%
nas-35 *(1093bps)*	-	61%	19%	18%	17%
nas-36 *(1699bps)*	-	-	86.8%	28.2%	22.8%
nas-37 *(1193bps)*	-	-	-	51.9%	21.8%
nas-38 *(1640bps)*	-	-	-	-	73.3%

Table 3-3: Percentage nucleotide identity of RNAi fragments to whole cDNA coding sequences of subgroup V family members

Astacin domain, 2x Epidermal Growth Factor domains, 5x CUB domains and Thrombospondin domain (subgroup VI, BMP-1 like)

RNAi of subgroup VIs only member, *nas-39,* resulted in a wild type worm with regard to gross morphology and COL-19 patterning. This was the case for all the tested strains (TP12, N2 and TP55). The TP55 strain, in concert with *nas-39* RNAi, exhibited no further mutant phenotypes other than those characteristic of the TP55 strain alone.

3.5 Discussion

The initial screen of the QSOX and NAS family of enzymes, by RNAi in the TP12 background, uncovered candidates involved in *C. elegans* cuticle ECM biosynthesis and degradation.

3.5.1 Splice leader processing of the QSOX family members

Splice leader PCR was carried out using N2 mixed stage cDNA and the consensus primers, SL1 and SL2 in conjunction with gene specific antisense primers for *qsox-1, 2* and *3*. *qsox-1* was *trans*-spliced with the SL1 sequence. *qsox-3* was *trans*-spliced with the SL2 sequence, this would tend to denote *qsox-3* as a downstream gene found within an operon (Page, 1997). However, the positioning of the genes flanking *qsox-3* (F47B7.6 upstream and F47B7.7 downstream) is not consistent with *qsox-3* being downstream in an operon. Thus *qsox-3* is among the small proportion, 4%, (Blumenthal *et al.,* 2002) of *C. elegans* genes that are SL2 *trans*-spliced and are not downstream genes in operons. *qsox-2* however, was both SL1 and SL2 *trans*-spliced.

3.5.2 Knockdown of QSOX family members causes improper formation of collagens

Following RNAi, feeding and injections, it was concluded that *qsox-1, 2* and *3* were functionally associated with the generation of the *C. elegans* cuticle, to varying degrees. *qsox-1* exhibited gross morphological disruption in RNAi treated worms, with the expansion of the entire cuticle resulting in an increased diameter in the targeted worm. The expanded nature of the *qsox-1* knockdowns could be due to a failure of the worms to circumferentially contract, as per the model proposed by Sapio *et al* (2005) for wild type alae formation. At the developmental stages in which alae are present, biochemical modifications and cross linking reactions compact the non-covalently assembled network of components of the lateral cuticle, which in turn generates force and pulls on the dorso-ventral cuticle, reducing the width of the lateral cuticle and generating the lateral alae (Sapio *et al.,* 2005). If this mechanism had failed in *qsox-1* RNAi worms, this could account for the expanded seam cell regions, Figure 3.4, and the overall expanded nature of the worm. Also particular importance would be placed upon the anchorage of the larval cuticle to the basal layer which would be required for the force transmission and thus wild types alae and cuticle formation. However, the lateral alae of worms which had the expanded phenotype did appear to be wild type. Another hypothesis could be that the expanded appearance was solely a consequence of the collagens being disorganised following *qsox-1* RNAi, and thus not conforming to their usually highly ordered nature.

qsox-2 RNAi, by feeding and injection, resulted in no gross morphological distortions, but distortions of the cuticle collagens, particularly those generated by the seam cell

hypodermis were noted. This did not however affect the lateral alae, which appeared wild type and may demonstrate that although the QSOX enzymes are affecting wild type collagen production in the seam cell hypodermis, they may not be involved with the generation of the lateral alae in these tissues.

qsox-3 showed a seam cell specific disruption of the cuticle collagens. The lateral alae and dorso-ventral hypodermally secreted collagens remained wild type. An Unc/Gro phenotype was also noted confirming genome wide screening results (Kamath *et al.,* 2003; Simmer *et al.,* 2003), proposing a distinct functional element to *qsox-3* activity. Homologous QSOX enzymes have been shown to localise to neuronal tissues, both rat QSOX and guinea pig QSOX having been spatially determined to their respective central nervous system (Amiot *et al.,* 2004; Mairet-Coello *et al.,* 2005; Radom *et al.,* 2006). The occurrence of rQSOX (rat QSOX) in foetal brain neurons suggests a role in brain development, possibly by intervening in the correct folding of secreted proteins, or of components of the ECM necessary for neuronal migration. As an Unc phenotype was noted by means of RNA interference, a likely explanation of this effect is that *qsox-3* is in some regard involved with neuronal migration

From the initial screening of the QSOX family members it could be seen that all QSOX were associating with regions of the ECM involved with the generation of cuticle collagens, most noticeably in the seam cell hypodermis. The association of QSOX enzymes with regions of high secretory load has been noted in human sulfhydryl oxidases (HS-QSOX) where localisation has been shown in: skin apocrine glands, at the luminal surface and in a perinuclear manner; the parotid gland, in the secretory ductile epithelial cells; islets of Langerhans; and in the small intestine, where QSOX is detectable in the columnar absorptive cells and the neuroendicrine cells (Thorpe *et al.,* 2002). Localisation of *C. elegans* QSOX to the hypodermal cells would be consistent with the pattern of QSOX orthologs localising to regions of high secretory load.

In order to characterise and determine the functionality of the QSOX family it would prove necessary to generate knockouts, as RNAi alone is not sufficient to silence target genes in some instances (Fire *et al.,* 1998). Knockouts would also afford combinatorial studies of *qsox* with other gene classes, which would prove difficult by RNAi. *qsox-1* and *qsox-2* were to be the targets of a deletion screen, as these appeared to have the greatest association with cuticle generation. To determine the localisation of the QSOX family of enzymes *lacZ* translational fusions were generated, see chapter 5.

3.5.3 Domain structure of QSOX family members is important in functionality

Avain QSOX cleaved by chymotrypsin will produce two fragments. The N-terminal fragment contains the thioredoxin domains and the larger C-terminal fragment contains the ERV1/ALR domain. The N-terminal fragment does not retain any sulfhydryl activity against reduced DTT, whereas the larger C-terminal portion does. A capacity to bind FAD is also retained by the C-terminal portion. (Raje and Thorpe, 2003; Coppock and Thorpe, 2006). Of note is that the reduced N-terminal fragment is a substrate for the ERV1/ALR containing C-terminal fragment. Re-enforcing the advantage QSOX has by unifying both of these domains in a single protein.

An intervening region is found between the thioredoxin and ERV1/ALR domains of the *C. elegans* QSOX family members. This region has been shown to have homology (35% identity) to an extracellular portion of a high affinity peptide transporter protein (Coppock and Thorpe, 2006). This could prove to be an association site for the dithiol substrates or other peptides.

In F56C11.3, see Appendix A, a conserved CxxC, found N-terminally to the ERV1/ALR domain, is structurally similar to the *S. cerevisiae* yeast protein Erv1p, which also has a homologus N-terminal CxxC. Hofhaus *et al* (2003) showed this domain (by complementarity) to be key in the flow of reducing equivalents from the dithiol substrate to the proximal disulphide of the ERV1/ALR. This demonstrates the need for maintenance of the N-terminal CxxC motif, (thioredoxin domain) and their importance to the functional protein, even if distinctly they can not generate disulphide bonds (Coppock and Thorpe, 2006). Based upon reported findings regarding the ERV1/ALR domains the ability to bind FAD and generate disulphide bonds while cleaved from the N-terminal thioredoxin domain (Coppock and Thorpe, 2006), and the possible importance of the spacer region in binding the dithiol substrate, it can be seen that maintenance of the domain structure and the motifs that lie within these domains is important to their functionality. Thus disruption to either the domain structure of the protein or to the conserved CxxC residues, for example by inducing a deletion mutation within the coding sequence, is likely to have a deleterious effect upon the proteins function.

3.5.4 RNAi of nas genes provide a wide range of phenotypes associated with improper digestion of proteins

The NAS family provided phenotypically distinct mutants when targeted by RNAi. The range of phenotypes may reflect radiative adaptation of members of this family towards specific functions within *C. elegans* which are perhaps not present in some of the higher order animals, hence their reduced number of astacin genes in comparison to *C. elegans.* The mutants revealed by RNAi were hypothesised to be failures in cleavage of structural proteins.

Relation of C-terminal domains to phenotypes exhibited

It would appear that subgroup V which contained; astacin, EGF, CUB, and TSP-1 domains were involved with cuticle generation and proteinaceous degradation of cuticular collagen components. Lacking these domains did not preclude other NAS family members from also exhibiting similar collagen processing phenotypes. *nas-12* and *nas-13* (subgroup II) showed disruption to the COL-19 arrangement, but shared only the astacin domain in common with the subgroup V astacins. *nas-12* and *nas-13* also contained, C-terminally to the astacin domain, two ShK domains not found in the subgroup V members. Subgroup IV contained astacin, CUB, EGF and ShK domains but lacked the TSP-1 domain found in subgroup V, and showed no detectable effect on collagens following RNAi. Thus inclusion of the TSP-1 domain would seem to dictate a stronger probability of collagen processing than when lacking the TSP-1 domain.

Of the *nas* genes that were postulated to provide collagenous defects, *nas-39* (BMP-1 like) was hypothesised to be the most likely to have an effect, based upon domain structure and similarities with bone morphogenetic protein-1 (BMP-1). BMP-1 is a pro-collagen C-peptidase (PCP) that has key roles in regulating formation of the vertebrate extracellular matrix. BMP-1 cleaves the C-propeptides of the major fibrillar procollagens I-III and processes precursors to produce the mature forms of the cross-linking enzyme: prolysyl oxidase (Hartigan *et al.,* 2003); the proteoglycan biglycan, a small leucine-rich proteoglycan enriched in extracellular matrices of skeletal tissues (Chen *et al.,* 2004) and the basement membrane protein laminin 5 (Unsold *et al.,* 2002). Hartigan *et al* (2003) demonstrated that the first CUB domain, CUB1 of BMP-1 was required for proper secretion. The location of this domain was also shown to be essential since its movement to any other position within BMP-1, other than immediately C-terminally to the

metalloprotease domain, resulted in retention of BMP-1. CUB2, the second CUB domain, was shown to be essential for PCP activity. As such both of these CUB domains could be considered as essential for the activity of the protein. The RNAi fragment used in the silencing experiments outlined in this chapter covered the second of the CUB domains and an EGF domain of *C. elegans nas-39* (BMP-1 like) and should, based upon similarities to orthologous BMP-1s, be sufficient to remove functionality of the protein. Subsequently a deletion strain VC775(*gk343*) has been generated by UV/TMP mutagenesis, with homozygotes reported as being superficially wild type, thus supporting the wild type appearance noted here by RNAi. PCP activity has been inferred upon *nas-35* (Novelli *et al.,* 2004) (subgroup V), which contains a TSP-1 domain, lacking in *nas-39*, further supporting the hypothesis that the presence of a TSP-1 domain dictates a stronger probability of that particular NAS protein as being involved with collagen processing.

Gross morphological defects associated with RNAi of NAS family members in C. elegans

Notable gross morphological defects were evident following RNAi by feeding and injection of the NAS family of enzymes. These included hatching, moulting and body morphology defects. These defects were hypothesised to be due largely to a failure in degradation of protein constituents of the cuticular ECM.

RNAi of *nas-34,* and in strain JC201 (*hch-1(ut110))*, which carried a Tc1 transposon insertion within the *nas-34* coding sequence (Hishida *et al.,* 1996), exhibited a failure to degrade proteinaceous components of its eggshell, resulting in a delayed (~11hrs at 25ºC) hatching phenotype. The embryos develop in a normal manner, at a normal rate but remained trapped as L1s inside the eggshell. The delay was proposed to be a failure to degrade proteinaceous components of the eggshell, perhaps the collagenous components (Hishida *et al.,* 1996). The eggshell of *C. elegans* consists of three structural layers: the inner vitelline membrane, which is a barrier to most solutes; a chitinous layer and an outer layer, composed of lipids and collagens (Johnston *et al.,* 2006). The eggshell is normally a firm structure, but characteristic *hch-1(ut110)* mutants have a softer malleable eggshell lacking chitin. Trypsin digest of the soft *hch-1(ut110)* mutant eggshells facilitates normal hatching (Hedgecock et al 1987), thus the soft eggshell is presumed to be the proteinaceous component which has not been digested due to the lack of the HCH-1 protease. Thus, HCH-1 either digests the proteinaceous component of the eggshell, or facilitates its

digestion by some other means, perhaps by processing of some other proteinaceous zymogen(s) to allow the activated partner to facilitate eggshell digest.

nas-36 and *nas-37* (subgroup V) when targeted by RNAi, or deletion *(nas-37(tm410))* caused similar moult defective and a quad-laminar lateral alae phenotypes. The moult defect is proposed as failure to degrade a collagen rich circumferential fibrous band found at the anterior of the worm. The available evidence thus implies that *nas-36* and *nas-37* are functionally involved with the process of ecdysis, and specifically with the degradation of the collagen containing anterior circumferential fibrous band responsible for the moult defect. Similar anterior bands have been seen in *trichostrongylids,* such as *H. contortus* (Gamble *et al.,* 1989), prior to moulting and are termed refractile rings. The refractile ring of *H. contortus* is a collagen rich band that forms 20 µm from the tip of the worm, and is degraded by an as yet undetermined Zn^{2+} metalloprotease component of the worms exsheatment fluid. By degrading this circumferential ring the anterior portion of the cuticle is removed allowing the worm to wriggle free of the previous stage cuticle (Gamble *et al.,* 1989; Gamble *et al.,* 1989b), in a manner that is mechanistically similar to moulting in *C. elegans*, see chapter 7 for more detail.

nas-12, 13, 28 and *38* would appear to be associated with the generation of a wild type cuticle. Figure 3.7-10 illustrate the affect on collagen processing exhibited in a knockdown environment for these particular *nas* genes. *nas-28* provided the most severe phenotype of these *nas* genes and as such became the target for further investigation. *nas-38* was also selected for further investigation

As mentioned earlier *nas-35* has PCP activity (Novelli *et al.,* 2004). Mutant strains lacking the PCP activity of *nas-35* are temperature sensitive (ts) lethal at 20ºC and 25ºC and are barely viable at the permissive temperature (15ºC). Novelli *et al.,* (2004) showed that *nas-35* was C-terminally cleaving the essential collagen SQT-3. At 25ºC the embryos would develop normally until the 3-fold stage and following completion of elongation the embryos retracted and failed to hatch. Also of note was the poor phenocopy exhibited by RNAi of *nas-35* (with only 5% of the F1 progeny in N2, n=5 and 24.5% of the F1 progeny in *rrf-3* mutants, which are RNAi hypersensitive, n=4 exhibiting the lethal phenotype by RNAi at non-permisive temperatures (Novelli *et al.,* 2004)). This relative insensitivity to RNAi had been noted previously with the astacins (Mohrlen *et al.,* 2003), and as such no firm conclusions could be drawn regarding the functionality of members of this group based upon RNAi alone. Null mutants would need to be generated in order that the true functionality/redundancy of particular members could be discerned. Spatial and temporal

localisation for the selected candidates (*nas-9, 28, 34, 36, 37* and *38)* would also need to be determined, as it would for the *qsox* genes.

In this chapter several candidates for cuticular biosynthesis were identified. These will be further characterised in the remainder of this thesis with particular focus upon disulphide bond generation and the process of moulting.

Chapter 4: Deletion screen for selected *qsox* and *nas* genes.

4.1 Introduction

Following the findings of the initial RNAi screen, selected genes of interest were screened in an attempt to isolate deletion carrying strains. The screen was directed towards isolating specific mutants in *qsox-1, qsox-2, nas-28, nas-36* and *nas-38* due to their importance in cuticle formation. This involved the generation of a randomly mutagenised library comprised of ~600,000 4,5′-8-trimethylpsoralen /UV mutagenised *C. elegans.* The mutagen used predominantley produces small deletions and was therefore subsequently screened by PCR to isolate specific deletion carrying nematodes. The poison primer method for PCR detection of deletions was used due to its increased sensitivity at detecting smaller (<600bp) deletions. By nested PCR alone such deletions would prove harder to detect.

4.2 Results

4.2.1 Poison primers design, considerations and theory

The poison primer method of deletion screening required that six distinct primers be designed and used in a two step reaction. The outermost primers, termed 1 and 2, were as close as possible to 1kb (genomic) apart with nested primers, termed 3 and 4, sitting down inside of 1 and 2. The poison primers, termed 5 and 6, which were not overlapping, were located midway between the outer primers, Figure 4.1. The primer set was to be designed towards the 5′ end of the target gene, and enclose an exon rich region. If introns were to be included, they were advised not to exceed 200bps. These considerations increase the possibility of isolating a loss-of-function mutation. The rationale behind the poison primer method of deletion screening is dependent on the fact that smaller PCR products amplify more favourably over larger fragments. In the first of the two rounds of PCR amplification, the poison primers limit amplification of the full-length wild type fragment (1 and 2 product), see Figure 4.1. The second round of PCR is performed on diluted first round products, using primers 3 and 4 which flank the deleted fragment. The poison primer fragments at this stage can no longer be amplified as a reverse/forward primer to complement primers 3 and 4 would not be present. As such, the deletion fragment amplifies in excess over the longer wild type fragment in the second round, and after 70 cycles becomes the predominant fragment which could be easily visualised on an ethidium stained polyacrylamide gel Figure 4.2.

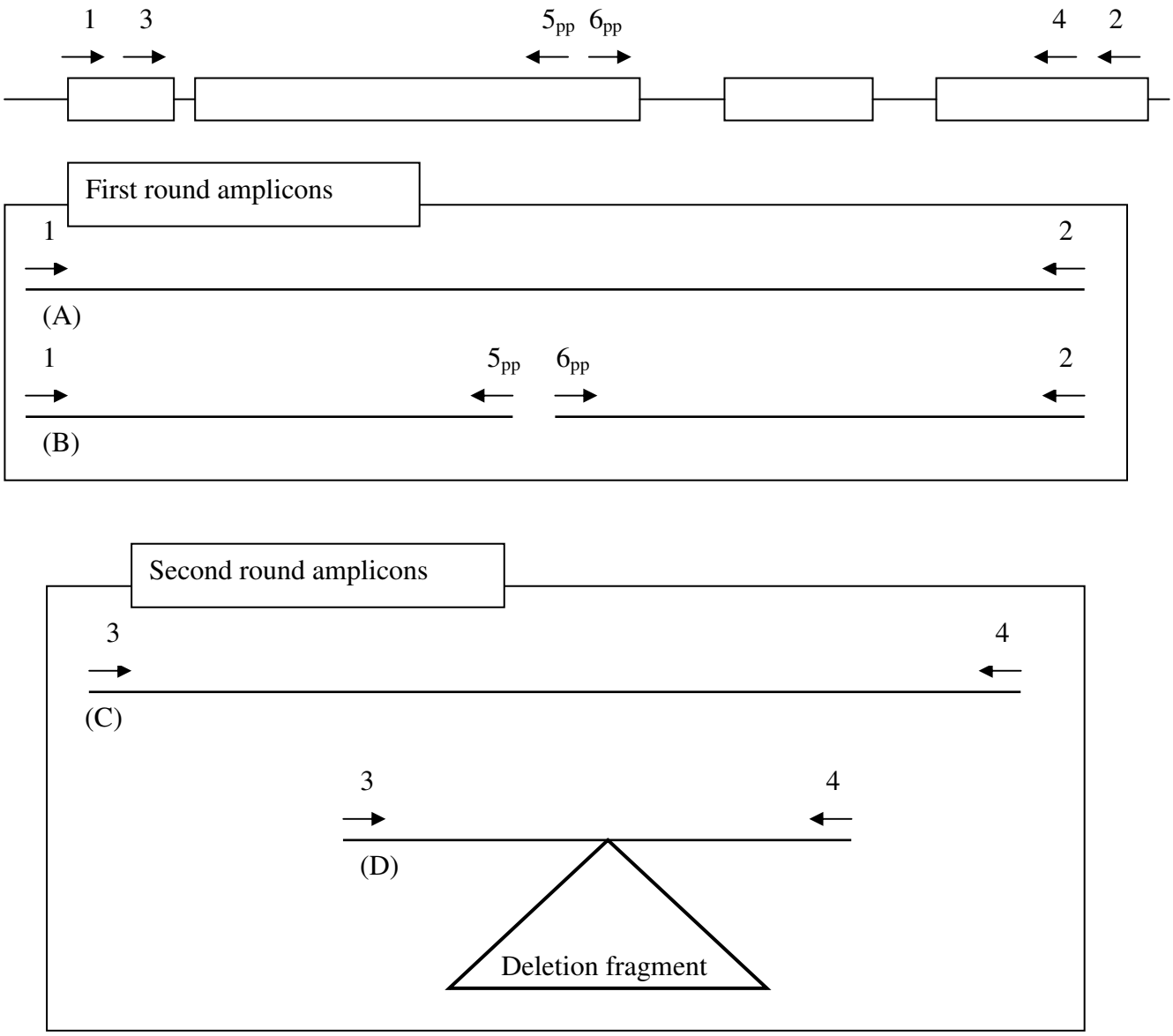

Figure 4.1: Schematic representation of PCR amplification of a deletion using the poison primer method (A) First round amplicons from the two outer primers. Not shown is the amplicon produced from 1+2 that includes the deleted fragment, these will be too low abundance to be visualised. (B) First round poison product concurrent with (A). (C) Second round amplicon, amplified off (A) of the first round. (D) Amplicon off first round, deletion containing fragment which would have been too low abundance to visualise on a gel. Due to its length there is a selective advantage for its amplification over (C) in the second round, and this product could now be visualised easily on a gel (arrows represent primers, $_{pp}$ denotes poison primers). For an actual representation of these products and the appearance of deletions within a PCR screen, see **Figure 4.2**

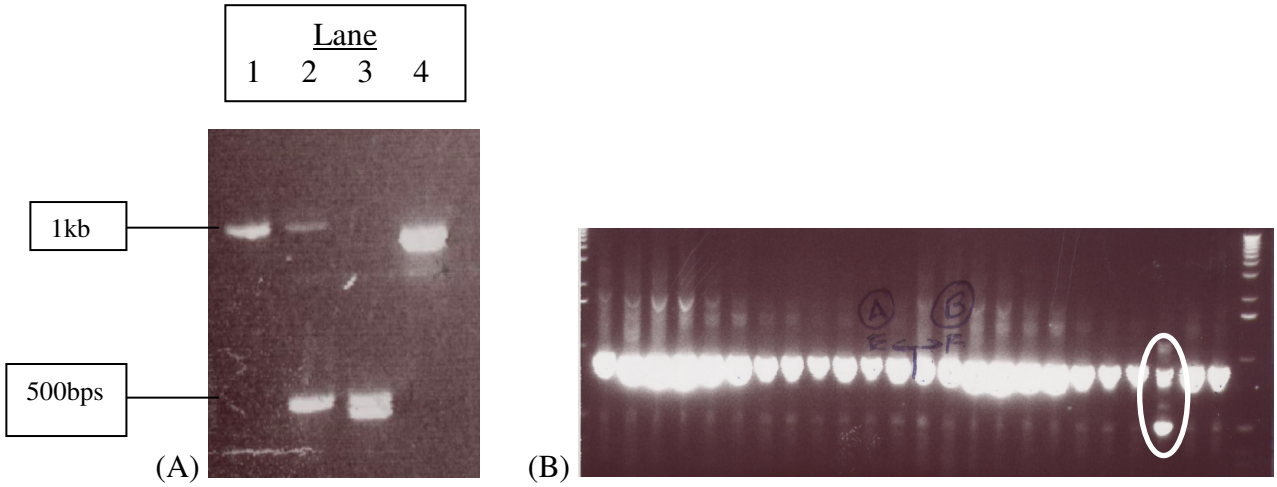

Figure 4.2: Representation of poison primer PCR and its use in deletion detection. (A) *qsox-1* deletion primer set used to demonstrate how the inclusion of the poison primer(s) discriminates against the larger fragment in favour of the shorter poison primer amplified fragment(s) (lanes 2 and 3). (Lane 1) shows amplification with primers 1+ 2. (Lane 2) shows amplification with primers 1+ 2 + 5_{pp}. (Lane 3) shows amplification with primers 1 + 2 + 5_{pp} + 6_{pp}. (Lane 4) shows amplification with primers 3 + 4. (B) Shows a preliminary screening round of deletion isolation for *nas-28*. Circled is the characteristic banding representative of a deletion amplified by the poison primer method. Of note is the depleted expression level of the upper wild type band. Marker used was Invitrogens 1kb ladder, $_{pp}$ denotes poison primer.

4.2.2 QSOX deletion screens

qsox-1 deletion screen

Deletion primers were designed for an exon rich region of *qsox-1*. This meant that the deletion fragment could not be designed towards the most 5′ end of the gene, but started after the first thioredoxin domain, position 1433bps to 2465bps on *qsox-1* genomic DNA. This allowed for a large, 782bp, intron to be avoided. The fragment enclosed by the outermost set of primers, 1 and 2, was sufficient however to cover the thioredoxin like domain, the intervening sequence and the 5′ end of the ERV1/ALR domain, in total 1032bps (genomic).

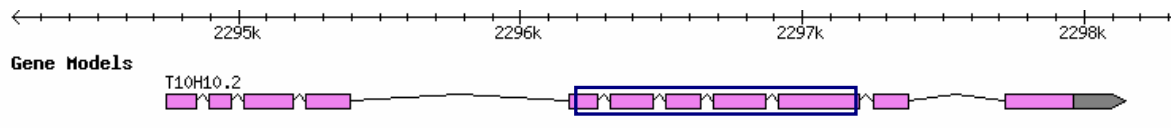

Figure 4.3: Schematic representation of *qsox-1* and the regions targeted by deletion primers. The blue box represents the targeted fragment. Image taken from wormbase.org.

The screening for *qsox-1* was performed by Gillian McCormack (University of Glasgow) who managed to isolate a *qsox-1* mutant worm from the deletion library and through three rounds of sib selection, produced a non-backcrossed homozygous *qsox-1* mutant line.

The mutation was then amplified, using *qsox-1* primers 3 and 4, with Pfu polymerase, cloned into pGEM T Easy Vector (Promega) and sequenced. Backcross primers were designed from the sequence information, Figure 4.4. These allowed genotyping of single worms by PCR, using two flanking primers and one primer within the deletion itself, Figure 4.5.

The generation of this 390bp deletion within the coding sequence of *qsox-1* removed part of the thioredoxin like domain and part of the intervening sequence. The deletion causes a one bp frame shift to the left, and the generation of an *amber* (TAG) premature stop codon at 932bps (genomic), less than a 1/3 of the way through the coding sequence of *qsox-1,* and was thus presumed to be a null.

```
                    501                                                  ↓
qsox-1 gDNA     TTTCTTGAAG GATGTCGTCA CATATGGAGA ACTTTGGAAC GAGTCATCAT

                    551
qsox-1 gDNA     CTTCTGCCAA TCATATTGCC ATTATTTTTG AAACCAACCA AGCGAGTTTA

                    601
qsox-1 gDNA     ACTGGAGCTC AGgtaaagtt tctttcaaaa taatttctaa aacccactaa

                    651
qsox-1 gDNA     cattttagCTT CTTCTCGACC TCAGCGGAAA CCGTGATCGT CTCGTAGCGC

                    701
qsox-1 gDNA     GAAGATGCTT GAAGAGCCAC CCACTCGCTG AAGCGTTGAA GATCACCGAT

                    751
qsox-1 gDNA     TTCCCATCAT TAGCCATTTT TAAGCGCGGC GAGCGTAAAC CAGTTTTGAT

                    801
qsox-1 gDNA     TGCTGAgtaa gtagtttgaa aaaagtttta ttcaacgtct tgaatatcca

                    851
qsox-1 gDNA     gACTTCGTCG GCTCTTACTC CGTGAGATTG ATCAATTCCT TGGAAAGCCC

                    901
qsox-1 gDNA     ACCGACAACC ACCTGCAAAC AATTCATTTC AGTAGCCGAA AGAATAAAAC

                    951
qsox-1 gDNA     AATTGATTGC AACAAAAATC CTGAACTATG CAAACCTAAT TATTTCGTGT
```

Figure 4.4: *qsox-1* deletion map. The highlighted sequence above shows the region deleted in the *qsox-1* mutant, which resulted in a frame shift and generation of an amber stop codon (highlighted pink). The original frame is shown by the arrow pointing to position one of a wild type codon. Lower case nucleotides represent intronic sequences; number values are for the corresponding genomic bases.

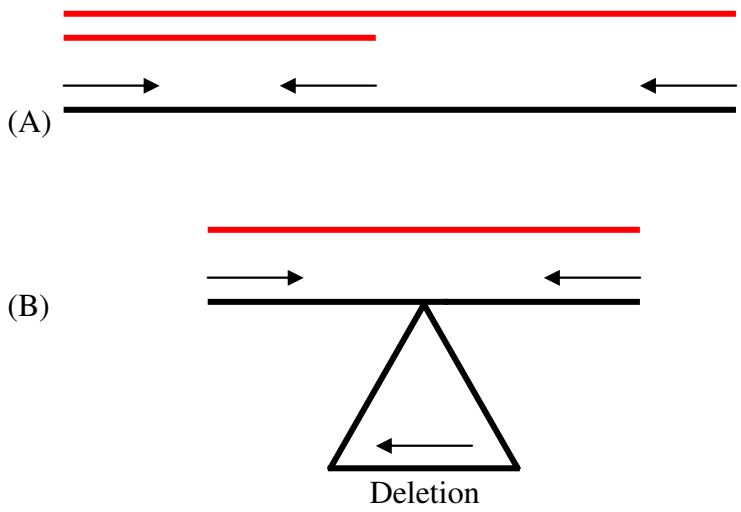

Figure 4.5: Schematic representing backcross primers. Primers are designed to flank the deletion and one primer is designed to sit down inside the deletion fragment. Red lines denote the products of PCR amplification and arrows denote primers. (A) A large fragment and a short fragment (preferentially the short fragment) will be produced in wild type backgrounds. (B) The mutant will produce an intermediate length fragment. In heterozygotes there will be a mix of all three products produced (preferentially the intermediate and shorter fragments).

Phenotypically the non-backcrossed worms which carried the *qsox-1* deletion were highly distorted with regard to overall body morphology. A variety of phenotypes were noted, some of which are particularly uncommon. The affects of this mutation are characterised in more detail in chapter 6.

qsox-2 deletion screen

The first attempt to isolate a *qsox-2* mutant from the library failed. The primers were redesigned for another portion of the gene and the library rescreened. Both sets of primers had to be designed towards the 3′ end of the gene. This was due to the structure of *qsox-2*, which contains some large intronic sequences, Figure 4.6. This limited the possible regions that could be screened and thus the chance of finding a deletion. Any deletion that fell within a large intron would have proved useless.

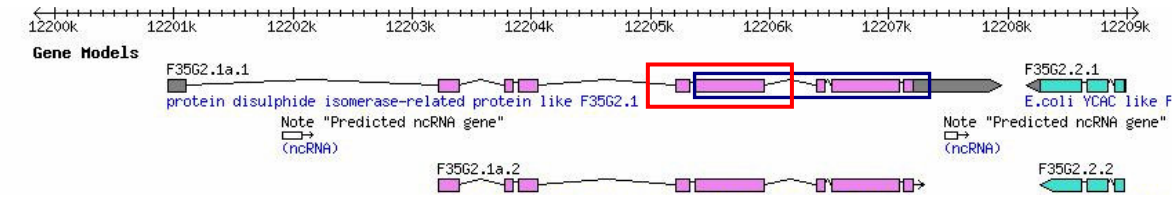

Figure 4.6: Schematic representation of *qsox-2* and the regions targeted by both sets of deletion primers. The blue box shows the region covered by primer set 1. The red box shows the region covered by primer set 2. Image taken from wormbase.org.

The region enclosed by the first set of primers, blue box in the figure above, covered the entire ERV1/ALR functional domain. So although the deletion would have been towards the 3′ end of the gene a deletion within this region would have been presumed to ablate the proteins functionality. The second set of primers, red box in the figure above also covered part of the ERV1/ALR domain. There was the potential for both sets of primers to remove the conserved CxxC motifs found within the ERV1/ALR domain.

The second primer set also returned a wild type banding pattern, as such it was believed that *qsox-2* had been unaltered by the psorlean/UV mutation process, in the region screened, or had been mutated at a level undetectable by the methods used in this screen.

4.2.3 NAS deletion screen

nas-28 deletion screen

Deletion primers were designed for *nas-28* at the 5′ end of the gene. The region enclosed by the outermost set of primers, 1 and 2, covered 994bps (genomic). This region contained within it most of the astacin domain and the zinc binding domain. Five small introns were also found within this region, the largest intron being 98bps, Figure 4.7.

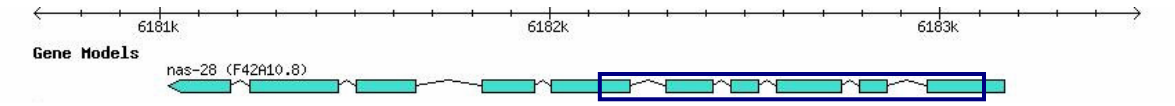

Figure 4.7: Schematic representation of *nas-28* and the regions targeted by deletion primers. The blue box represents the targeted fragment. Image taken from wormbase.org.

A population of worms within the deletion library which contained a mutant *nas-28* gene were isolated, and through three rounds of sib selection a non-backcrossed homozygous line was produced.

The mutation was then amplified, using *nas-28* primers 3 and 4, with Pfu polymerase, cloned into pGEM T Easy Vector (Promega) and sequenced, Figure 4.8, shows the mapped deletion. Backcross primers were designed similarly to those of *qsox-1*, Figure 4.5.

The deletion generated within the coding sequence of *nas-28* was 487bps long, covering 619bps to 1106bps of the *nas-28* genomic sequence and thus the deletion lay within the astacin domain. The deletion resulted in a frame shift, one base to the left, and the generation of an *ochre* (TGA) premature stop codon at position 1166bps. The deletion removed the zinc binding domain and the entire consensus metalloprotease sequence, and as such, was considered to be a null. Three intronic regions were covered by this deletion fragment totalling 185bps, the longest intron being 91bps.

In contrast to previous RNAi findings, described in chapter 3, the non-backcrossed strain of worms carrying the *nas-28* deletion appeared phenotypically wild type.

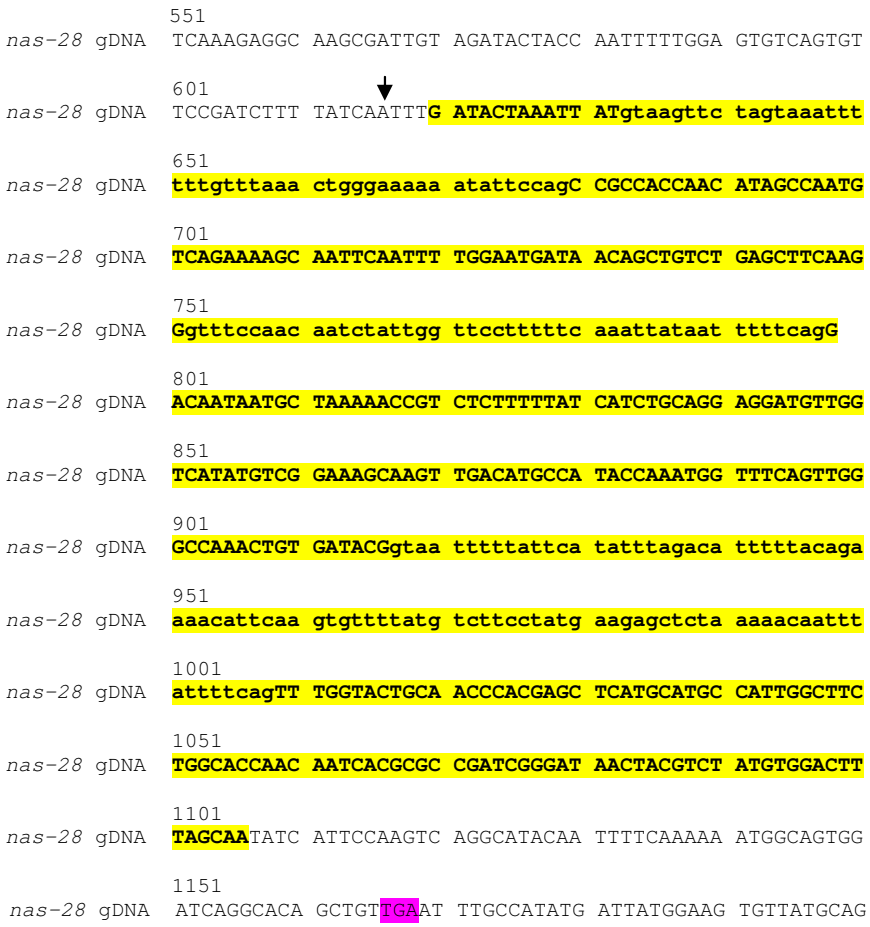

Figure 4.8: *nas-28* deletion map. The highlighted sequence above shows the region deleted in the *nas-28* mutant. There is a resulting frame shift and generation of an ochre stop codon (highlighted pink) caused by this deletion. The original frame is shown by the arrow pointing to position one of a wild type codon. Lower case nucleotides represent intronic sequences; number values are for the corresponding genomic bases.

nas-36 deletion screen

nas-36 was screened and a population of worms were found to be carrying a deletion within the range of *nas-36* primers 3 and 4. *nas-36* had a deletion primer set which was designed towards the 3′ end of the gene. This was the case as a set of primers designed towards the 5′ end, and which covered the most exon rich portion, would have covered only a 500bp region of the gene. This was considered too small a fragment for the poison primer mechanism to have an effect, and therefore a larger 1kb fragment located towards the 3′ end of the gene was targeted, Figure 4.9.

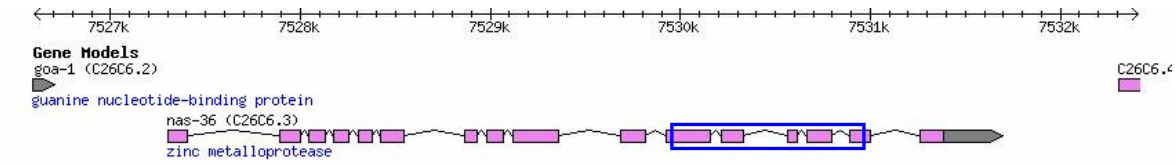

Figure 4.9: Schematic representation of the *nas-36* fragment targeted by deletion screen. The blue box represents the targeted fragment. Image taken from wormbase.org.

The chosen region contained five exons and four introns, two of which were large at 111bps and 237bps and two smaller, 48bps and 56bps in length. The exons of this region coded for the CUB domain of *nas-36*.

From the initial screen of the library it was noted that there was a population of worms within the library which contained a deletion bounded by this primer set. These worms were located on one of the 1152 plates which constituted the library. This plate was used to establish the sib selection process; the excess worms from this stage were frozen at -80ºC.

The first round of the sib selection process produced three plates out of 100 which contained a population of worms with a mutated *nas-36*. One of these plates was used to establish the second round of sib selection and the others, along with the excess of the plate used to establish the second round, were frozen down. The sib selection process continued in this vein of isolation and decreasing population sizes until single worms were being plated out, where upon the deletion became unrecoverable and was lost from the population. 340 single worms were plated out from the previous rounds positive plate; the previous round contained a population of 10 worms per plate over 200 plates.

Various back tracking steps were taken in an attempt to recover the deletion containing population, all ultimately proved ineffectual and did not result in isolation of a deletion containing strain.

nas-38 deletion screen

nas-38, similarly to *nas-36*, could not be isolated from the deletion library despite its presence being detected and confirmed by sequencing. The region screened in *nas-38* was located towards the 5′ end of the gene and covered a portion of genomic sequence that comprised five exons interspersed by four introns. The largest intron was 213bps with the average size of the three smaller introns 52bps. The region coded by this cluster of exons encoded the astacin metalloprotease domain.

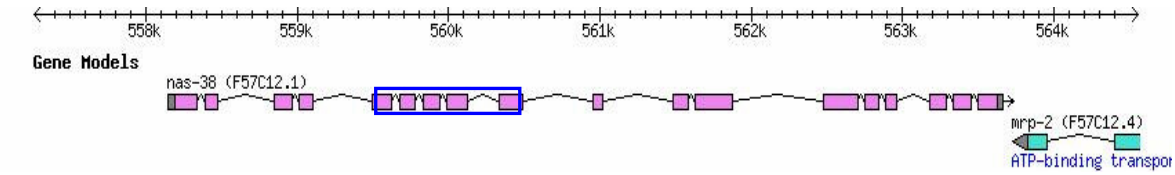

Figure 4.10: Schematic representation of the *nas-38* fragment targeted by deletion screen. Image taken from wormbase.org.

From the initial screening of the library plates a deletion was detected within the population of mutated worms. Through two rounds of sib selection the deletion containing worms were traced, and the population size reduced down to 100 worms per plate spread over 100 plates, a proportion of which would contain the *nas-38* deletion. Unfortunately at this point, during the transition from the second round of sib selection to the third round of sib selection (10 worms per plate), the deletion was lost and failed to amplify in the third round PCR screens. In an attempt to recover the deletion the previously positive second round, first round and initial positive library plates were re tested. All ultimately failed to produce any deletion carrying worms. Frozen stocks of the excess worms not plated at each sib selection also failed to produce worms containing a deletion in *nas-38*.

It was believed that due to the random mutagenesis used to generate the deletion library other genes, within the genomes of worms containing the desired deletion, may also have been mutated. If these other unknown genes were essential and became homozygous, through continued self replication, this could have caused a lethal phenotype to emerge which would make it impossible to recover these genomes and the target gene mutation would become unrecoverable. This was a likely explanation for the disappearance of the

nas-36 and *nas-38* (in which a deletion was confirmed by sequencing) deletion containing worms. Figure 4.11 shows the deletion generated within *nas-38*.

To produce the deletion fragment used for sequencing, the second round of PCR was repeated upon a sample known to carry the deletion. The subsequent fragment produced by *nas-38* primers 3 and 4 was then cloned and sequenced.

The deletion generated within the *nas-38* sequence removed a section of the active astacin domain and key features found therein. The consensus astacin sequence, highlighted green in Figure 4.11, was unaffected by the deletion but the Met-turn, which provides a hydrophobic environment for the Zn^{2+} ion and histidine residues at the catalytic centres of the enzyme (Bode *et al.,* 1993) were removed. This would have likely diminished or completely ablated the functionality of the enzyme. Also removing an 80 residue section from the active domain would have affected the tertiary structure of the final protein, perhaps removing functionality, or severely impinging upon it. The frame of the transcript was unaltered.

4.3 Discussion

Following the deletion screen for the selected genes, *qsox-1, qsox-2, nas-28, nas-36* and *nas-38* mutant strains were produced that contained deletions in *qsox-1* and *nas-28*. The remaining genes of interest were either not mutated, the mutation was undetectable by the poison primer method or mutant strains were unable to be recovered/isolated from the deletion library. The latter being the situation with *nas-36* and *nas-38*.

The *qsox-1* mutant proved of great interest as it illustrated the first gross morphological defects associated with loss of QSOX activity. This deletion would become the focus for characterisation of the *C. elegans* QSOX family, as described in chapter 6. Requests to isolate mutants in both *qsox-2* and *nas-36* were sent to NBP Japan[2]. The two deletion carrying strains returned were used as resources in further characterisation experiments.

[2] http://shigen.lab.nig.ac.jp/c.elegans/ChangeLocale.do?url=home&lang=en

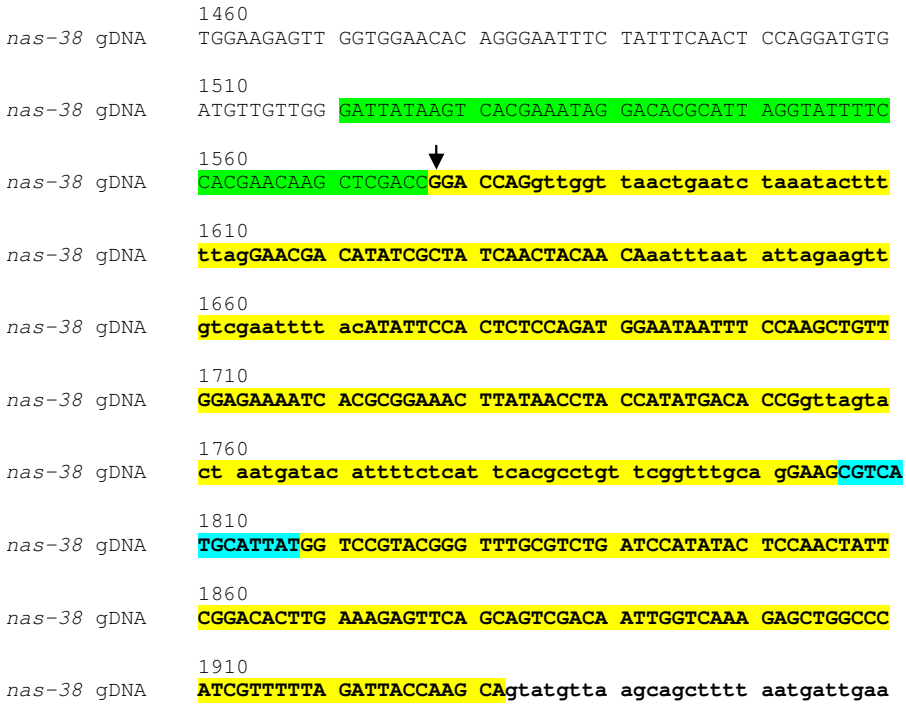

Figure 4.11: Sequence of *nas-38* deletion. This deletion was unrecoverable. Green shows the astacin consensus sequence; the arrow shows position one of a wild type codon; yellow shows the deleted region of DNA and the blue highlights the Met turn removed by this deletion. Lower case nucleotides represent intronic sequences; number values are for the corresponding genomic bases.

Chapter 5: Expression profiling of selected *qsox* and *nas* genes.

5.1 Introduction

Following the findings of the initial RNAi/deletion screen, selected genes of interest were further characterised. This chapter deals with their spatial and temporal expression profiles.

5.1.1 Temporal and spatial expression patterning

To determine the temporal expression profile of the entire QSOX family and selected *nas* genes; *nas-9, nas-28, nas-34, nas-36, nas-37* and *nas-38* sq RT-PCR was carried out using staged cDNA samples (Johnstone and Barry, 1996). These 20 samples represented from the L1 arrest until 10 hours subsequent to the L4-adult moult, with each of the samples representing two hour stepwise increments of development.

The semi-quantitative aspect of these PCR reactions was conferred by inclusion of a second set of primers (ancillary to the target gene primers) that were directed towards the RNA POL-II large subunit *ama-1* (Bullerjahn and Riddle, 1988; Rogalski and Riddle, 1988), which is expressed at a constant level throughout the life cycle. This would allow for the target gene to be compared to a constitutively expressed gene, and allow for an expression profile to be determined relative to this amplification standard at any given point in the life cycle. To determine an expression ratio of the target gene relative to *ama-1* ImageQuant software (Amersham Bioscience) was used to analyse ethidium stained polyacrylamide gels, as per section 2.17. All sq RT-PCR experiments were performed in triplicate.

To determine the spatial expression profile of selected genes, N2 transgenic lines (≥ three lines for each construct) carrying promoter elements fused in frame to either a multi-intron containing *lacZ* reporter element (pPD95.03) or a GFP reporter element (pPD95.75) were generated. The resultant *lacZ* lines were then fixed and treated with either 2% (normal) or 20% (sensitive) β-galactosidase stain, as per section 2.20, and visualised by DIC microscopy. GFP lines could be visualised without fixation by UV microscopy.

From the temporal and spatial expression profiles, functionality of genes could be proposed.

5.2 Results

5.2.1 Temporal expression profile of qsox-1, qsox-2 and qsox-3

Collagen expression follows a multiphasic pattern of oscillating cuticular collagen gene expression which repeats at each moult. The collagen genes can thus be described as either: early, ~4hrs pre moult; intermediate, ~2hrs pre moult; or late, which are coincidental with the moulting cycle (Johnstone and Barry, 1996). Early collagens include DPY-7, intermediate collagens include SQT-1, SQT-3 and DPY-13 and late collagens include COL-12 and COL-14 (Johnstone and Barry, 1996). The primers used in these RT-PCR experiments are listed in Table 2-7.

qsox-1 temporal expression profile

Figure 5.1.A, and the corresponding graph, Figure 5.1.B, clearly show peaks of *qsox-1* expression that coincide with intermediate collagen mRNA production.

qsox-2 temporal expression profile

Figure 5.2.A, and the relevant graph, Figure 5.2.B, show that *qsox-2* is expressed in all samples at a high level, comparable to the standard *ama-1*. There does not appear to be any clearly discernable fluctuations in *qsox-2* mRNA abundance with early, intermediate or late collagen synthesis.

qsox-3 temporal expression profile

Figure 5.3.A, and the graph, Figure 5.3.B, show peaks of expression for *qsox-3* that coincides with collagens that belong to the intermediate group. The expression profile of *qsox-3* is in this regard similar to that of *qsox-1*, with peaks in expression at 10, 16, 20 and 28 hrs post L1 arrest. The main difference being that *qsox-3* had a higher basal level of expression than *qsox-1* and is expressed over a wider time period.

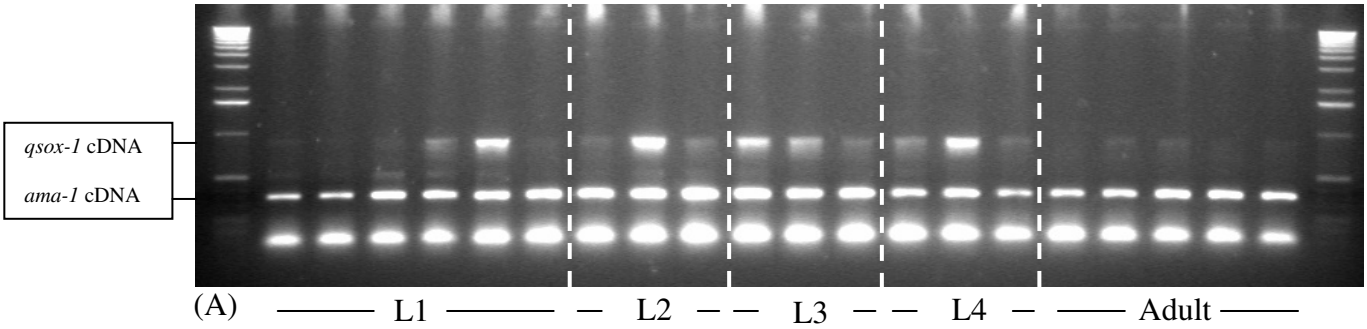

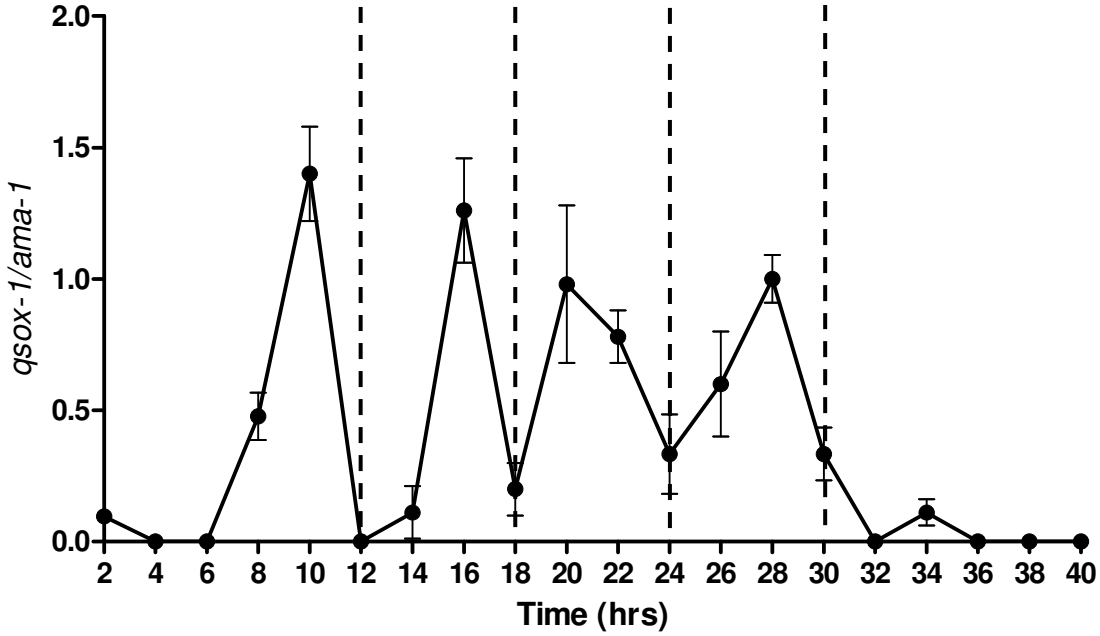

(B)

Figure 5.1: sq RT-PCR of *qsox-1*. (A) Picture of ethidium stained agarose gel showing *qsox-1* sq RT-PCR. Marker used was Invitrogens 1kb ladder. (B) Graphical representation of sq RT-PCR of *qsox-1*. Vertical lines denote the time of each moult. Error bars indicate the standard deviation.

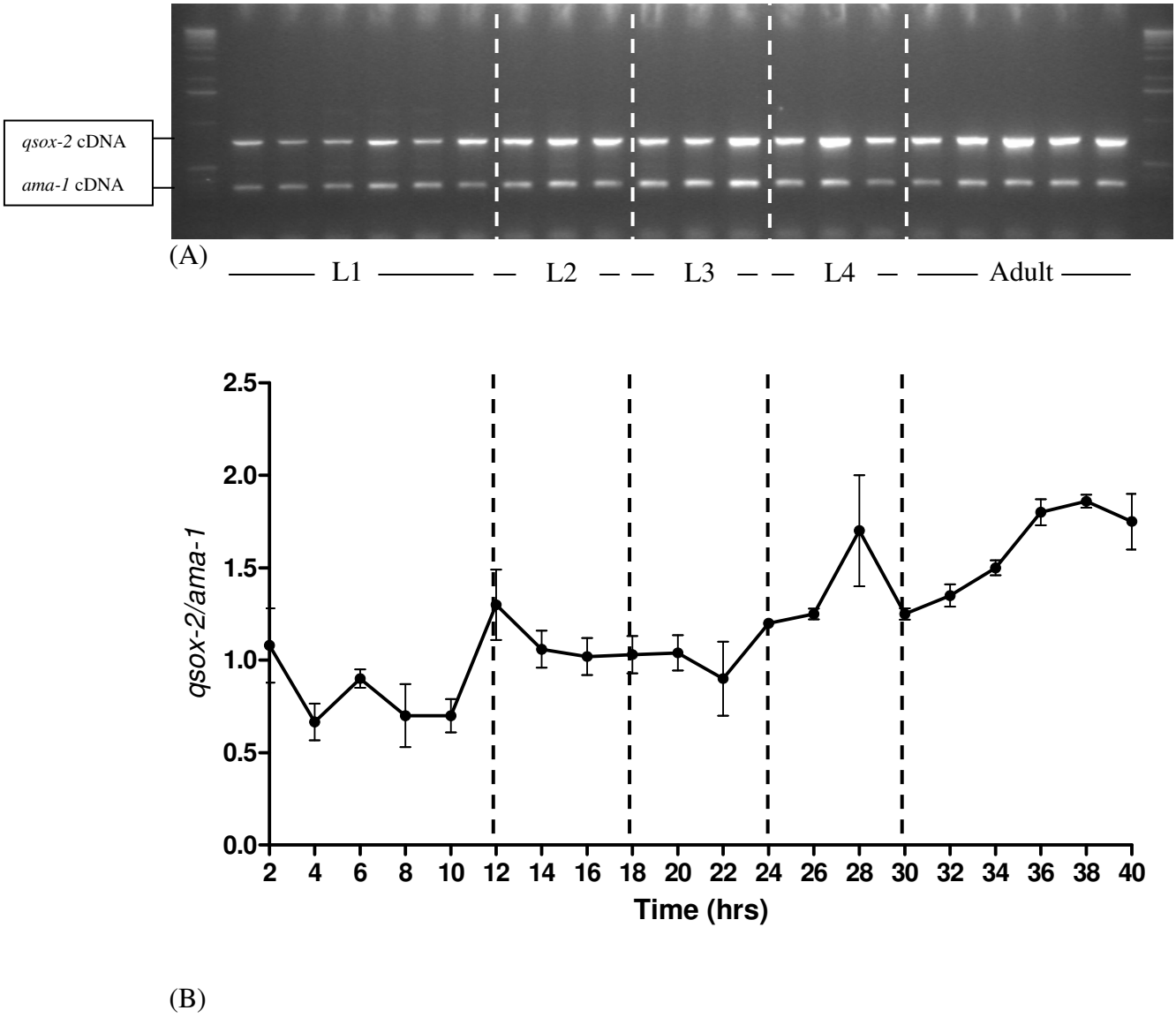

Figure 5.2: sq RT-PCR of *qsox-2*. (A) Picture of ethidium stained agarose gel showing *qsox-2* sq RT-PCR. Marker used was Invitrogens 1kb ladder. (B) Graphical representation of sq RT-PCR of *qsox-2*. Vertical lines denote the time of each moult. Error bars indicate the standard deviation.

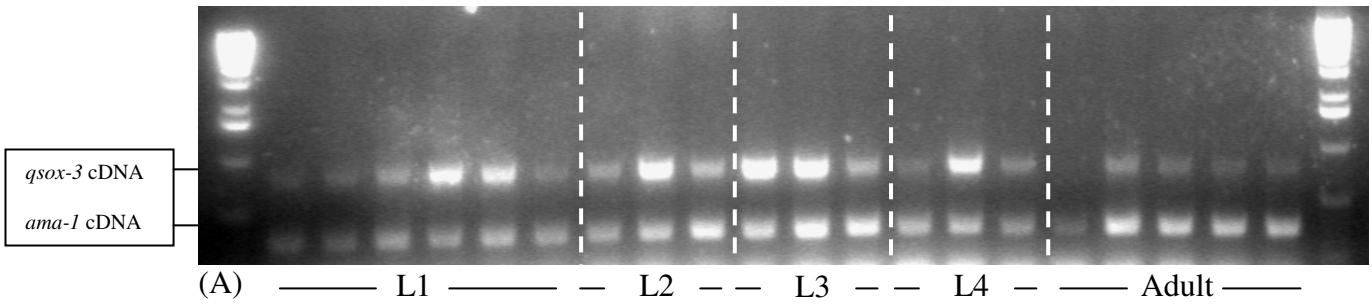

(A) ——— L1 ——— — L2 — — L3 — — L4 — —— Adult ——

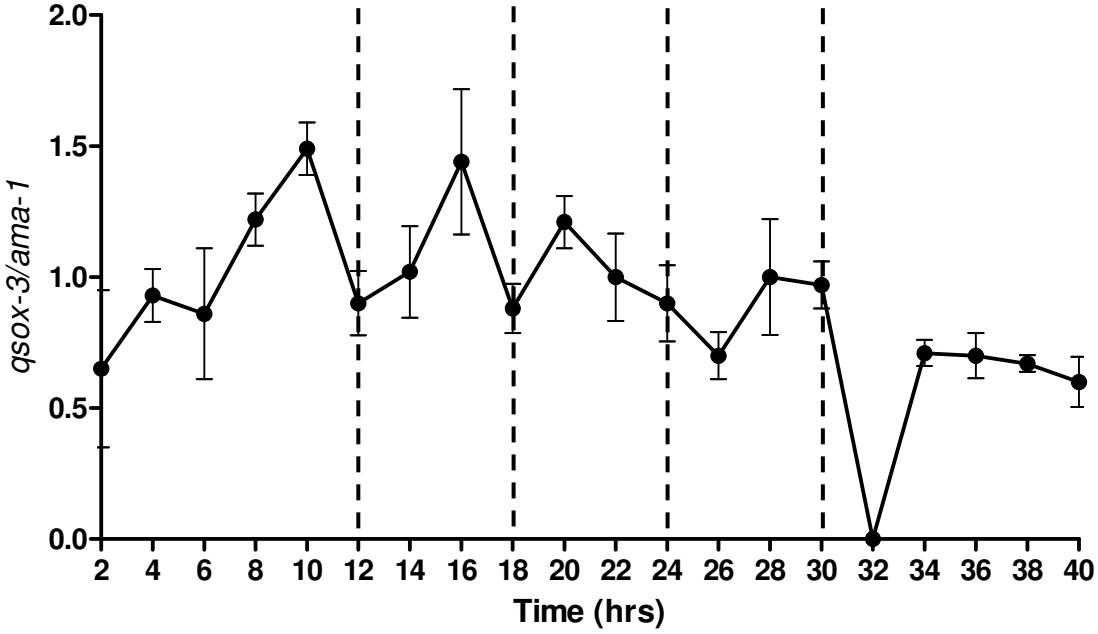

(B)

Figure 5.3: sq RT-PCR of *qsox-3*. (A) Picture of ethidium stained agarose gel showing *qsox-3* sq RT-PCR. Marker used was Invitrogens 1kb ladder. (B) Graphical representation of sq RT-PCR of *qsox-3*. Vertical lines denote the time of each moult. Error bars indicate the standard deviation.

sqt-3 temporal expression profile

To determine whether the temporal association of the *qsox* genes (in particular *qsox-1*) with the intermediate collagens was genuine, a comparison of the expression profiles for *sqt-3* and *qsox-1* expression was made. From the gel picture, Figure 5.4.A, and the reciprocal graph, Figure 5.4.B, overlapping expression patterns for *qsox-1* and *sqt-3* can be seen. This temporally associates enzyme and potential substrate together.

sqt-3 was chosen as a representative of the intermediate group as there is a polyclonal SQT-3 specific serum (Novelli *et al.,* 2006) which was used in subsequent characterisation experiments, see chapter 6. SQT-3 has also been shown to be an essential collagen for *C. elegans* development (Novelli *et al.,* 2006) and as such enzymes which may associate with its processing were of interest to this study.

5.2.2 Spatial expression profile of qsox-1, qsox-2 and qsox-3

5.2.2.1 Reporter gene fusions

Transgenic reporter lines were generated to determine the tissue specific localisation of *qsox-1, qsox-2* and *qsox-3.* Other techniques, such as immuno-cytochemistry and *in situ* hybridisation, are also valid techniques used in the spatial determination of target genes. Immuno-cytochemical localisation would determine the localisation of the target protein, but relies upon having a specific antibody raised against a specific target protein. However, no such antibodies are available for any of the *C. elegans* QSOX or NAS family of enzymes. *In situ* hybridisation, a technique which determines the localisation of the target by highlighting its RNA distribution, has proved difficult in *C. elegans* and is technically more involved when compared with the translational fusions favoured in this study. *Cis*-acting promoter driven expression of the *E. coli lacZ* gene, which encodes β-galactosidase, was chosen as the means of spatial determination of target genes. β-galactosidase has been shown to be a reliable reporter molecule in various organisms and various tissues. *C. elegans,* due to its transparency, makes this a favourable method for tissue specific determination of target gene expression.

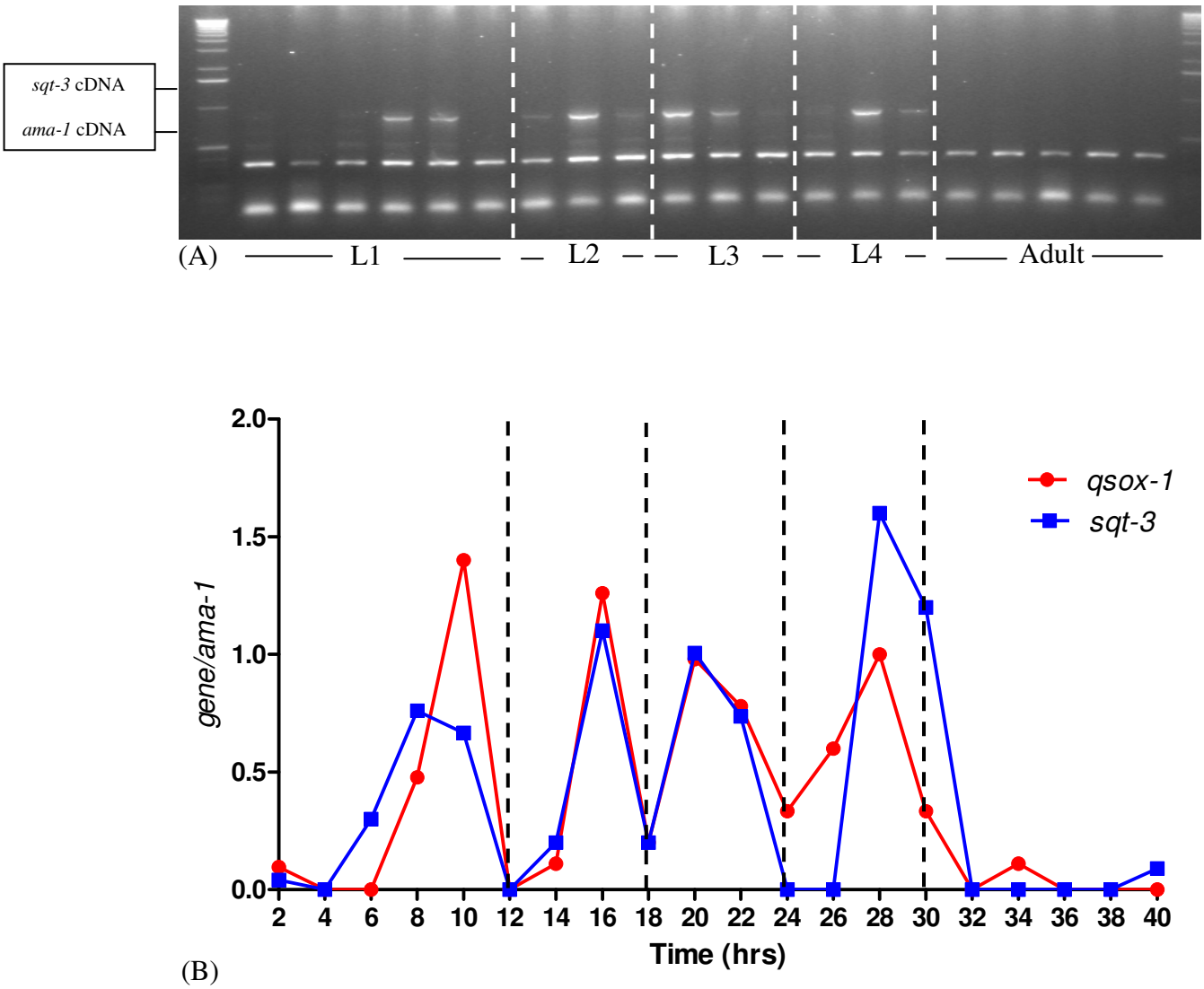

Figure 5.4: sq RT-PCR of *sqt-3* and comparison to *qsox-1* (A) sq RT-PCR of *sqt-3*, see Figure 5.1 for comparison with *qsox-1*. Marker used was Invitrogens 1kb ladder. (B) Graph comparing *sqt-3* and *qsox-1* temporal expression. Notable is the overlapping expression exhibited by these genes. Vertical lines denote the time of each moult.

A myriad of vectors have been generated with *lacZ* and GFP reporter elements in the Laboratory of A.Fire, specifically for spatial determination of target gene expression (Fire *et al.,* 1990). Figure 5.5 shows a schematic representation of the vectors: pPD95.03, a *lacZ* reporter vector and pPD95.75, a GFP reporter vector, both of which were used in the spatial determination of specific genes in this series of experiments. These vectors all share a pUC19 backbone and the 5′ multiple cloning site (MCS) is the same as that found in pUC19. The *lacZα* region of pUC19 was deleted so as to avoid duplication that would result from the insertion of a complete *lacZ* gene. The β-lactamase gene however remains intact, and as such all vectors in the series retain resistance to ampicillin. The last 51bp of the *lacZ* gene were replaced by a synthetic oligonucleotide to facilitate the incorporation of a 3′ MCS following the *lacZ* translational terminator. This oligonucleotide modification contains silent mutations which eliminates uncommon codons, with respect to *C. elegans* codon usage, but retain the exact C-terminal sequence of *LacZ.* Into this 3′ MCS, 3′ flanking sequences could be inserted. In the instances of pPD95.03 and pPD95.75 *C. elegans unc-54* (which encodes for the major myosin heavy chain) 3′ UTR was inserted. The 3′ element of specific target genes, if required for expression or if the 3′ is the target of investigation, can replace the existing 3′ element of the vector.

Located 5′ to the *lacZ* gene of pPD95.03 is an ATG and nuclear localisation signal (NLS) containing cassette. This cassette, 45bp in length, localises the expression of the reporter element to the nucleus of the cell in which expression has been initiated. The NLS is an eight residue element (APKKKRKV) derived from the SV40 T antigen which directs the T antigen to the nucleus, and is stringent enough to direct heterologous proteins, such as β-galactosidase, a normally cytoplasmic protein, towards the nucleus when placed either N or C terminally. The confinement of the reporter gene to the nucleus aids specific tissue determination. For transcriptional fusions the ATG found within this cassette is the point of initiation, thus the NLS lies N-terminally to the β-galactosidase gene. For translational fusion constructs the ATG of the target gene, and the first few nucleotides, are included thus initiation is directed from the target genes ATG. This positions the NLS at the junction of the resulting fusion peptide. A 42bp synthetic intron is incorporated between the 5′ MCS and the NLS as expression has been shown to be more efficient from spliced than unspliced transcripts. In addition to this 5′ synthetic intron, *lacZ* has also been modified to contain 11 synthetic introns. GFP, in pPD95.75, contains 5 synthetic introns and one within its 3′ UTR. To reduce background expression levels a decoy intron has been inserted 5′ to the MCS which has an open reading frame which terminates prior to the MCS thus reducing background expression, this decoy intron is present in both vectors.

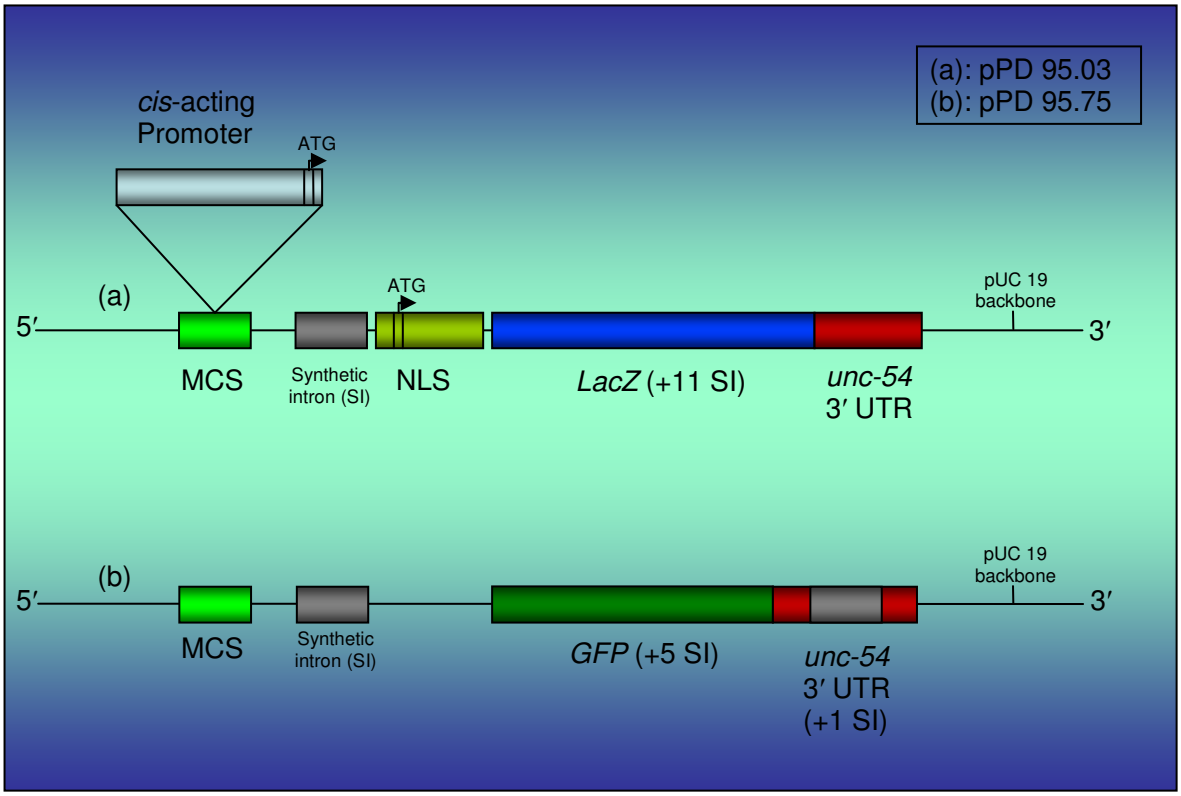

Figure 5.5: Schematic representation of reporter vectors used to determine the spatial expression profile of *cis*-acting promoter elements. Promoter elements were inserted into the 5′ MCS located upstream of the multiple synthetic intron (SI) containing *lacZ* and GFP reporter elements. The 3′ UTR of *C. elegans unc-54* is a component of both vectors pPD95.03 and pPD95.75, whereas the SV40 nuclear localisation signal (NLS) is only present in the pPD95.03. Not drawn to scale.

pPD95.03 contains a decoy sequence, 12 synthetic introns in total (one between the MCS and NLS and 11 in the *lacZ* coding sequence) an NLS and the 3′ UTR of *unc-54*. This was the predominant vector used to assess the expression of the *qsox* family. pPD95.75 was used to assess the expression profile of *nas-37,* the results of which will be discussed later in this chapter.

To decipher the expression profiles of lines carrying reporter constructs an atlas of the hypodermal cells in *C. elegans* body tissue and head was constructed, see Figure 5.6.

qsox-1 spatial expression determination by *lacZ* reporter

The spatial expression of *qsox-1* was examined using a *lacZ* reporter construct that contained 3001bps of upstream promoter sequence, the ATG start codon plus one other base to maintain the frame of the transcript. This promoter element was ligated into the multi-intron containing *lacZ* reporter vector pPD95.03 and sequenced to ensure that the frame was maintained. Three separate lines carrying the transgene were established as per section 2.21. All lines were checked to ensure a similar expression profile.

lacZ expression was detectable from early in development, Figure 5.7.A and B show expression in undetermined cells at 2-fold and elongated stages of development respectively. Expression was noted in approximately bean stage embryos and appeared evident in all stages there after. Expression was also noted in embryos within adult hermaphrodites which had not yet been laid. It would thus appear that *qsox-1* is expressed early in embryogenesis. *lacZ* expression was also observed during all stages of post embryonic development in the main body hypodermis hyp7, and very strongly in all seam cells, Figure 5.7, with expression visible in head hypodermal cells hyp3, 4, 5, 6 and 7 as well as the muscle cells and seam cells H0 and H1. Expression was evident in tail hypodermal cell types hyp8, 9, 10, 11 and the most posterior seam cell, T. Weak adult pharyngeal expression was also noted.

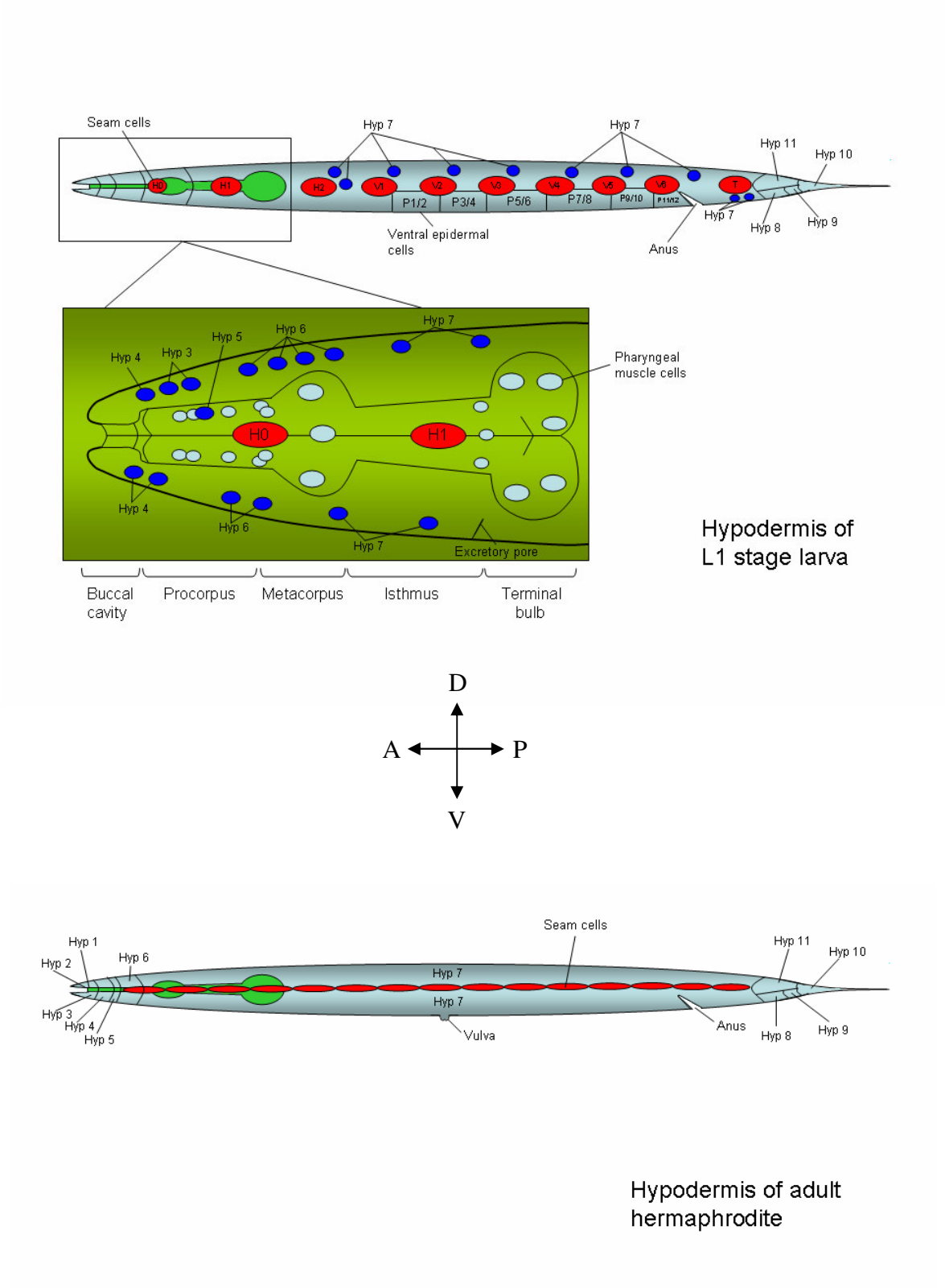

Figure 5.6: Schematic representation of hypodermal distribution in L1 and adult *C. elegans*. L1 hypodermal cell nuclei are represented by blue dots. A close up of the pharyngeal region of the worm highlights the array of hypodermal cells present, also represented are the pharyngeal muscle cells and the seam cells H0 and H1. The ventral epidermal cells, P1 to P12; seam cells, (as yet unfused) and the tail hypodermal regions hyp8 to 11 are also represented in the L1 schematic. In the adult worm the seam cells have fused to make a syncytial lateral track and the majority of the ventral epidermal cells have fused and become hyp7 cell types.

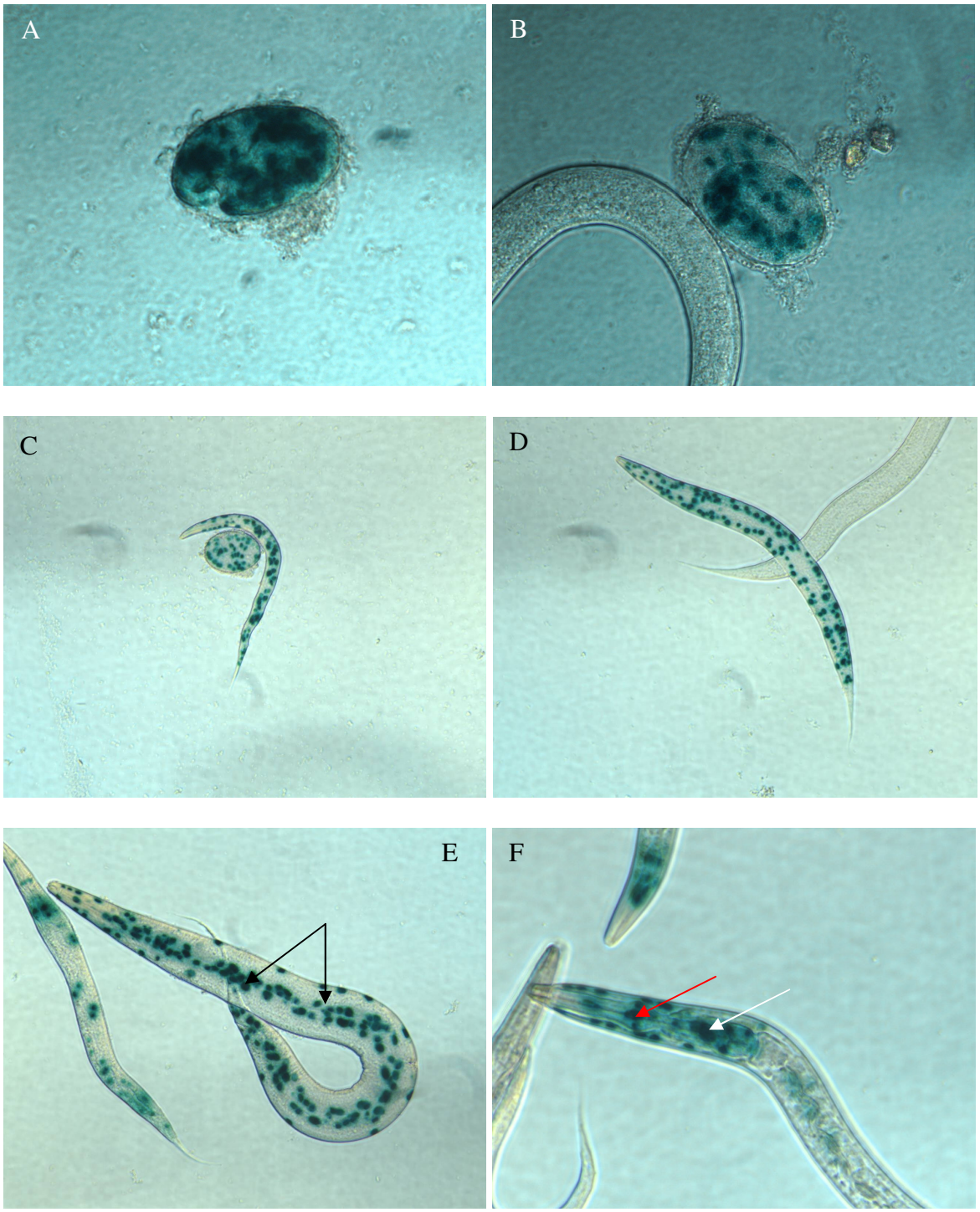

Figure 5.7: *qsox-1* promoter driven *lacZ* expression. (A) 2-fold embryo showing expression in undetermined cells. Magnification x60. (B) Elongated embryo similarly showing expression of *qsox-1* in undetermined cells. Expression has been noted at earlier stages (pre 2-fold) but is not shown here. Magnification x60. (C) L1 larvae and early stage embryo, the larva showing hypodermal expression of *qsox-1*. Magnification x20. (D) L2 showing body hypodermal expression, seam cell expression was noted but is out of plane in this image. Magnification x20. (E) L3 showing intense seam cell staining (black arrows) running along the midline of the worm. The tail hypodermal cells V5, V6 and T are also stained; pharyngeal staining is also seen. Magnification x20. (F) Head staining can be seen in hyp3, 4, 5, 6 and 7, muscle cells and the seam cells H0 and H1 (arrowed red and white respectively). Magnification x60.

qsox-2 spatial expression determination by *lacZ* reporter

The spatial expression of *qsox-2* was determined using a *lacZ* reporter construct which contained 4001bps of upstream promoter sequence and the ATG start codon, with two other bases to ensure the frame of the transcript. The promoter element was then fused to the multi-intron containing vector pPD95.03 which was sequenced to ensure that frame was maintained. Three separate lines carrying the transgene were established as per section 2.21. All lines were checked to ensure a similar expression profile.

lacZ expression driven by the *qsox-2* promoter was noticed constitutively in the pharyngeal muscle cells, Figure 5.8.A, which have been shown to be associated with cuticle secretion (Avery, 1997; Hao *et al.,* 2006). Expression was also detected within hyp7, lateral seam cells of hermaphrodite larval stage *C. elegans* and within the tail hypodermis (syncytium generated by fusion of tail hyp8, 9, 10 and hyp11) of males, Figure 5.8.B and D. This syncytium has been shown to be associated with L4/adult male tail remodelling (Nguyen *et al.,* 1999).

qsox-3 spatial expression determination by *lacZ* reporter

A 2001bp promoter fragment, which included the ATG and two other bases to ensure the frame of the transcript was maintained, was fused to the multi-intron containing *lacZ* reporter vector pPD95.03 and sequenced to ensure that the frame was maintained. Three separate lines carrying the transgene were established as per section 2.21. All lines were checked to ensure a similar expression profile.

lacZ expression driven by the *qsox-3* promoter was noted during embryogenesis in pre 1-fold, 2-fold and 3-fold embryos, Figure 5.9.A to C. The cell types stained at these stages is undetermined. Throughout larval development *lacZ* expression was detectable in head hypodermal cells hyp3, 4, 6 and 7, Figure 5.9.D to F, and was also noted in body hyp7 and seam cells. Expression was also evident in tail hypodermal cell types hyp8, 9, 10, 11 and the most posterior seam cell, T.

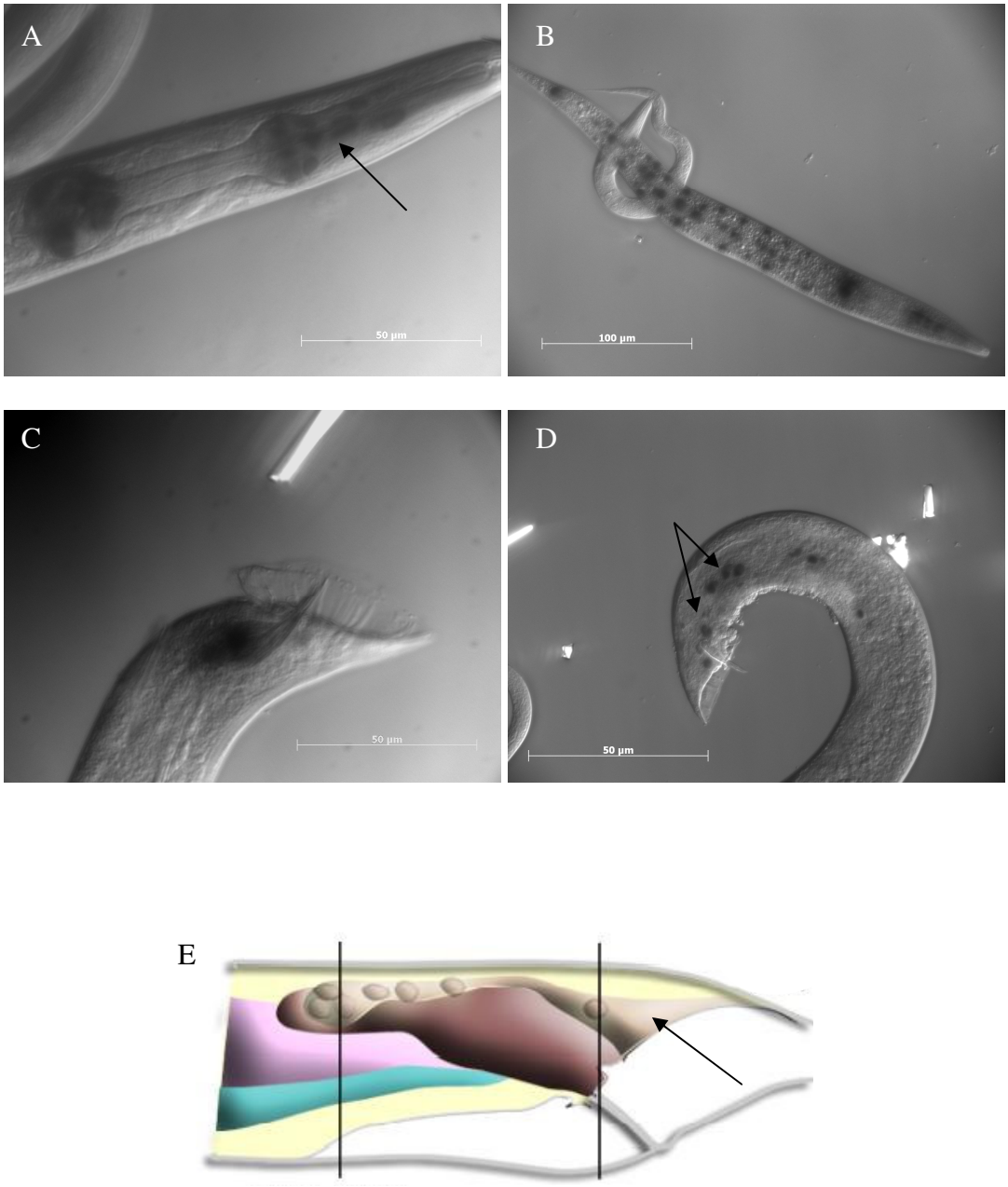

Figure 5.8: *qsox-2* promoter driven *lacZ* expression. (A) Shows staining of the pharyngeal muscle cells and the H0 seam cell (arrowed). (B) Expression was noted in hyp7 cells in L2 larvae. (C/D) staining was evident in adult male tail (D) shows staining localised to the male tail hypodermis. (E) Shows a schematic representation of the male tail (adapted from the wormbook) with an arrow showing the tail hypodermis. The pink colouring highlights the intestine, brown the proctodeum and green the vas deferens.

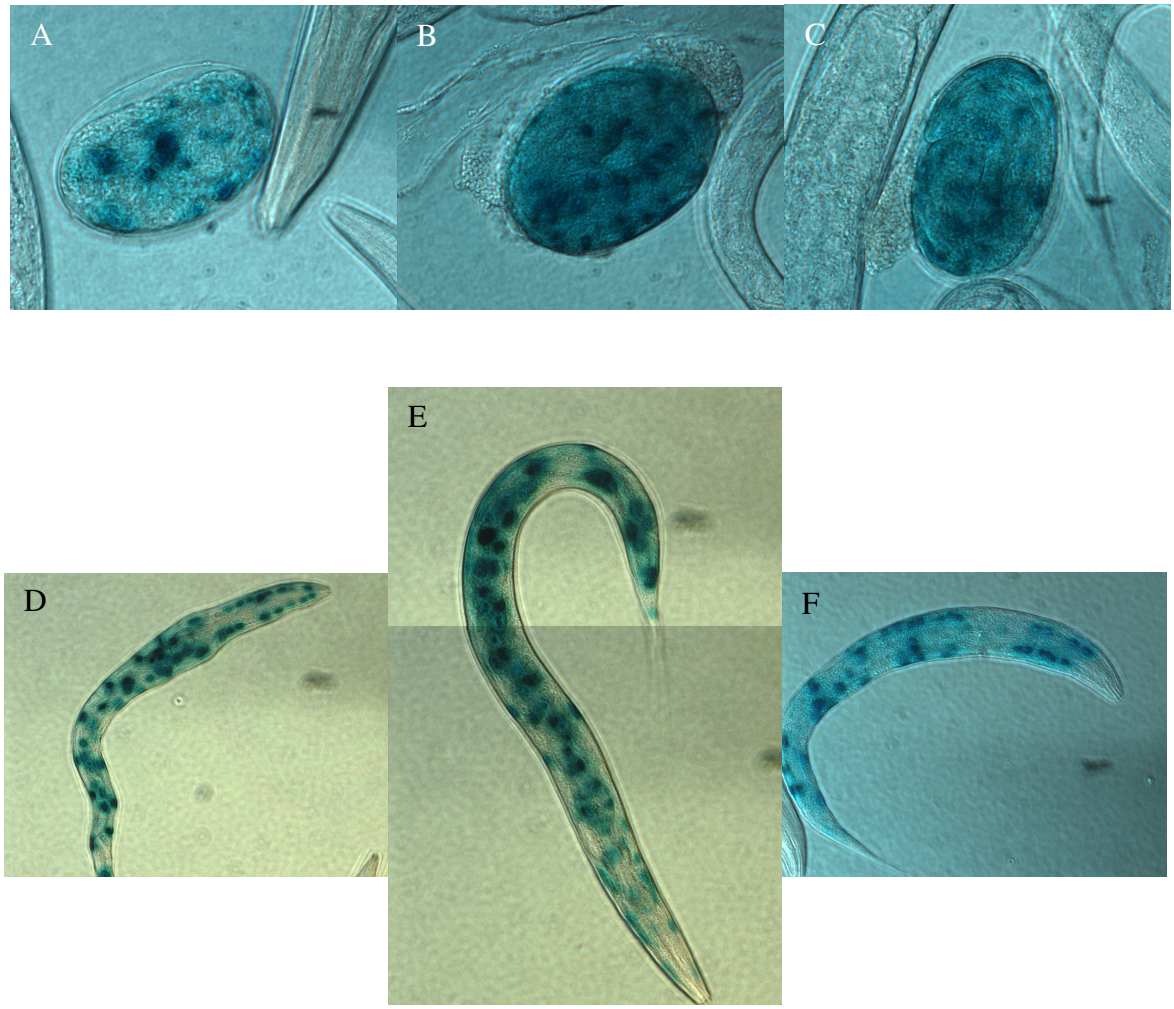

Figure 5.9: *qsox-3* promoter driven *lacZ* expression. (A, B, and C) Shows expression of *qsox-3* in developing embryos, cell types undetermined. Magnification x100. (A) Shows a pre 1-fold (B) a 3-fold and (C) an elongated worm. (D, E and F) Expression can be seen in head hyp3, 4, 6 and 7, body hyp7 and seam cells of these L2 (D and F) and L3 (E) worms. Magnification x60.

5.2.3 Temporal expression profile of nas genes

The temporal expression profile of the selected *nas* genes *nas-9, 28, 34, 36, 37* and *38* was determined using the same approach used to determine temporal expression of the *qsox* genes, see section 5.2.1.

nas-9 temporal expression profile

sq RT-PCR of *nas-9* showed an expression profile which cycled with moulting, Figure 5.10.A and B. *nas-9* expression was thus cycling with those collagens which have a late expression profile, namely *col-12* and *col-14*. When the temporal expression profiles for *col-14* and *nas-9* were examined a similar profile was noted, Figure 5.10.C

nas-28 temporal expression profile

No detectable expression was evident following sq RT-PCR of *nas-28,* Figure 5.11.A. Products have however been returned following standard RT-PCR with mixed stage template. These products have been sequenced and verified as transcripts of *nas-28.* Mohrlen *et al* (2003) also reported a genuine *nas-28* expression that was similarly confirmed by sequence analysis of an RT-PCR product.

nas-34 temporal expression profile

No expression was detected for *nas-34* in any of the larval or adult stage of development, Figure 5.11.B, confirming the previously reported embryo specific expression profile (Hishida *et al.,* 1996).

nas-38 temporal expression profile

No detectable expression was evident following sq RT-PCR of *nas-38,* Figure 5.11.C. However expression of *nas-38* can be validated as EST data is available on wormbase[3].

[3] http://wormbase.org/

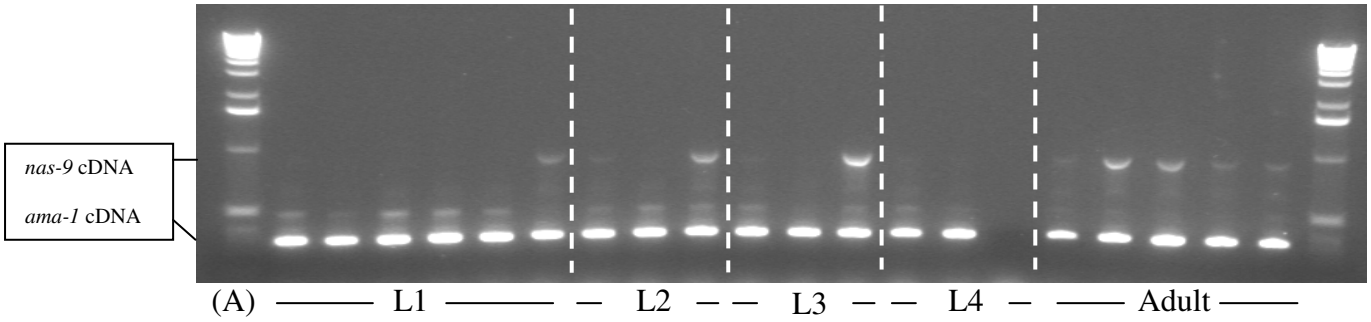

(A)

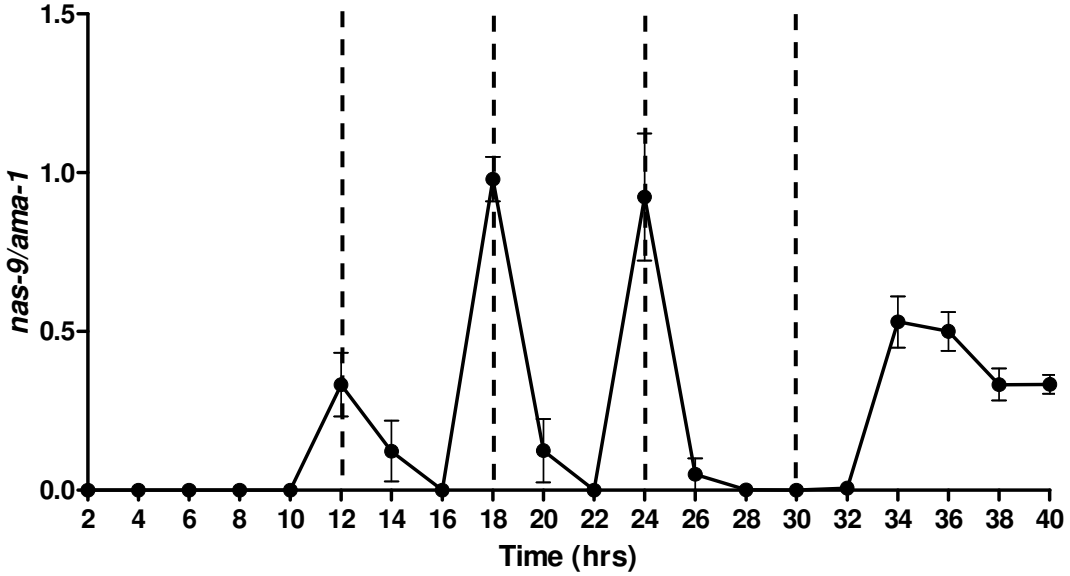

(B)

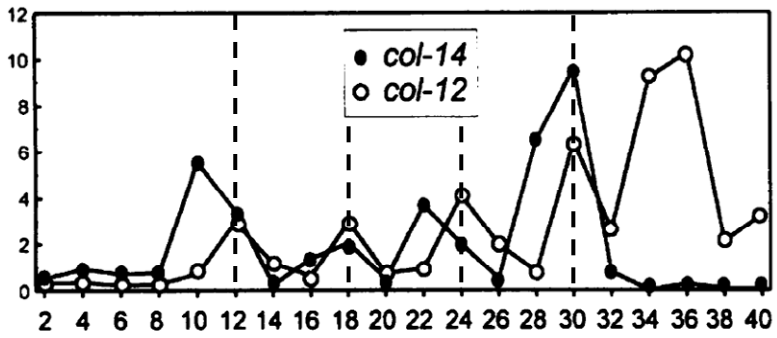

(C)

Figure 5.10: sq RT-PCR for *nas-9* (A) Picture of ethidium stained agarose gel showing *nas-9* sq RT-PCR. Marker used was Invitrogens 1kb ladder. (B) Graphical representation of sq RT-PCR of *nas-9*. (C) Graphical representation of late expressed collagens which show a similar temporal expression profile as *nas-9.* Taken from (Johnstone and Barry, 1996). Vertical lines denote the time of each moult. Error bars indicate the standard deviation.

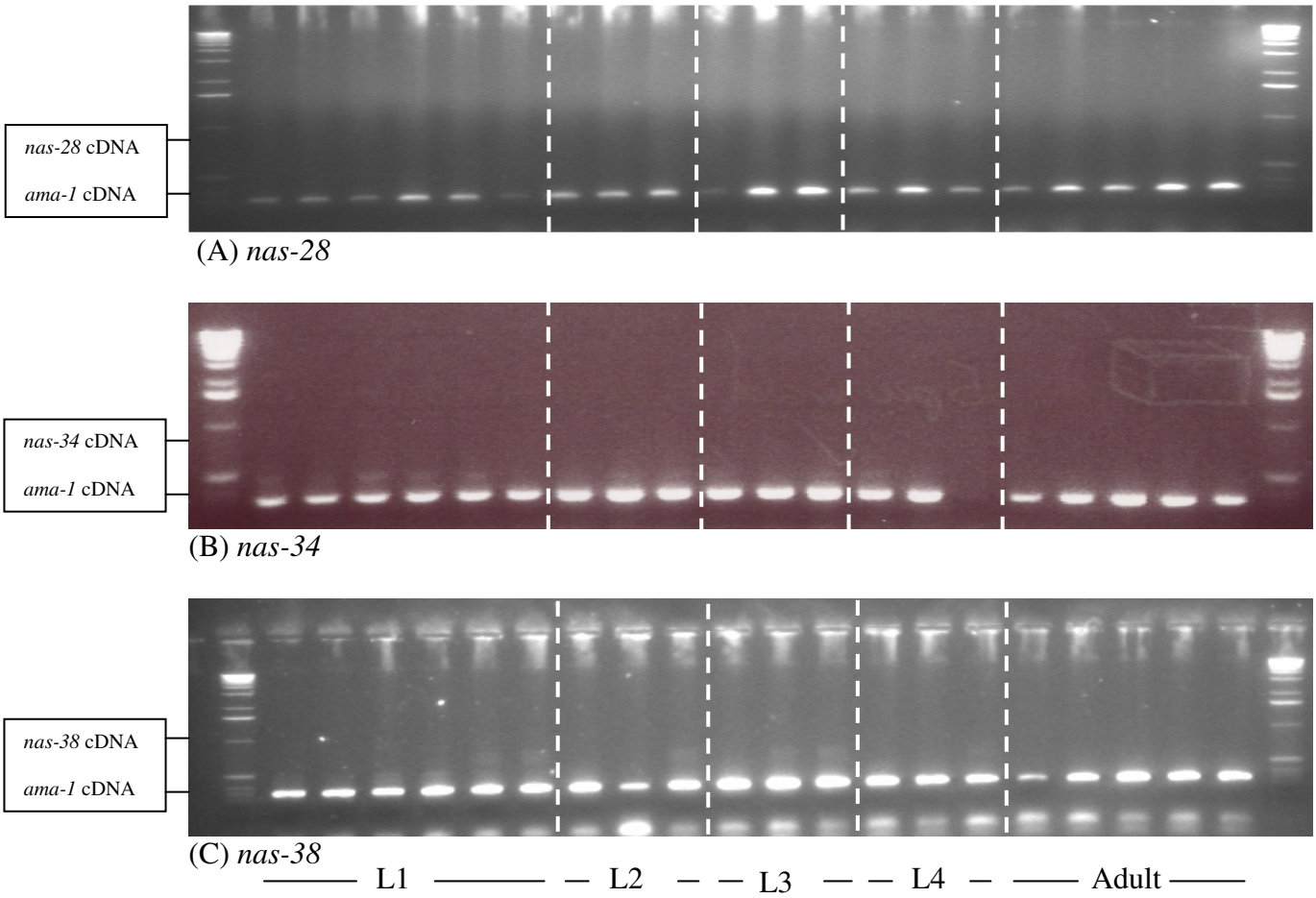

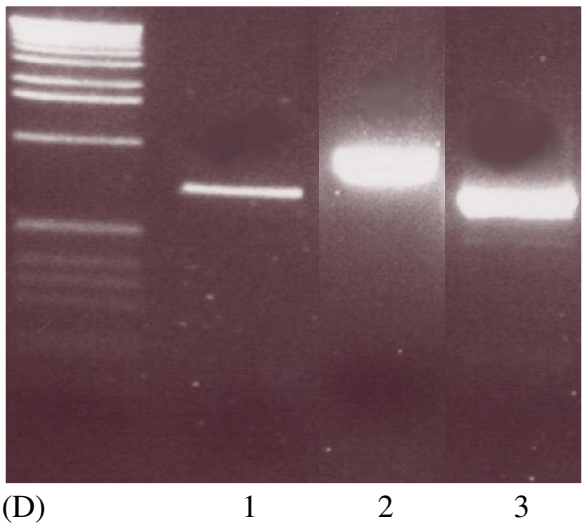

Figure 5.11: sq RT-PCR for *nas-28, nas-34* and *nas-38* (A,B and C) respectively. (D) Primer test for genes *nas-28, 34* and *38*. (A, B and C) Show no detectable expression following sq RT-PCR. (D) The primers used in (A, B and C) were tested on mixed stage N2 cDNA, Lane 1 shows *nas-28*, lane 2 shows *nas-34* and lane 3 shows *nas-38* RT-PCR primer amplified cDNA products of the predicted size. The image has been spliced to remove intervening unimportant lanes of the gel, all lanes were part of the same gel. Marker used was Invitrogens 1kb ladder. Vertical lines denote the time of each moult.

Expression data can also be found for *nas-38* at the Genome BC *C. elegans* Gene Expression Consortium[4] web page.

nas-36 temporal expression profile

Figure 5.12.A, and the respective graph, Figure 5.12.B, illustrate that *nas-36* expression was detectable two hours prior to each moult, a pattern that is concurrent with the expression profile of the intermediate collagens. *nas-36* has a relatively low level of expression that peaks at approximately 65% of the *ama-1* expression level. Average peak expression was 20 to 25% the level of *ama-1,* Figure 5.12.B.

nas-37 temporal expression profile

Figure 5.13.A, and the associated graph, Figure 5.13.B, illustrate that *nas-37* peaked in expression four hours prior to each moult and once in the adult (34hrs). Such a profile is coincidental with the expression of the early collagens. The expression profile illustrated that *nas-37* is not a highly expressed gene, peaking at approximately 55% the level of *ama-1.* Average peak expression level was 35% the level of *ama-1,* Figure 5.13.B.

5.2.4 Spatial expression profile of nas-9, nas-36 and nas-37

nas-9 spatial expression determination by translational fusion to a GFP reporter

The spatial expression pattern of *nas-9* was determined by the Genome BC *C. elegans* Gene Expression Consortium[5] as localising to the hypodermis of larval and adult worms. Expression was also noted in undetermined cell types within developing embryos.

nas-36 spatial expression determination by a *lacZ* reporter

The spatial expression of *nas-36* was examined using a *lacZ* reporter construct that contained 2001bps of the upstream promoter sequence of *nas-36* and included the ATG start codon with one other base to ensure the frame of the transcript.

[4] http://gfpweb.aecom.yu.edu/index
[5] http://elegans.bcgsc.ca/perl/eprofile/strain?name=BC13411

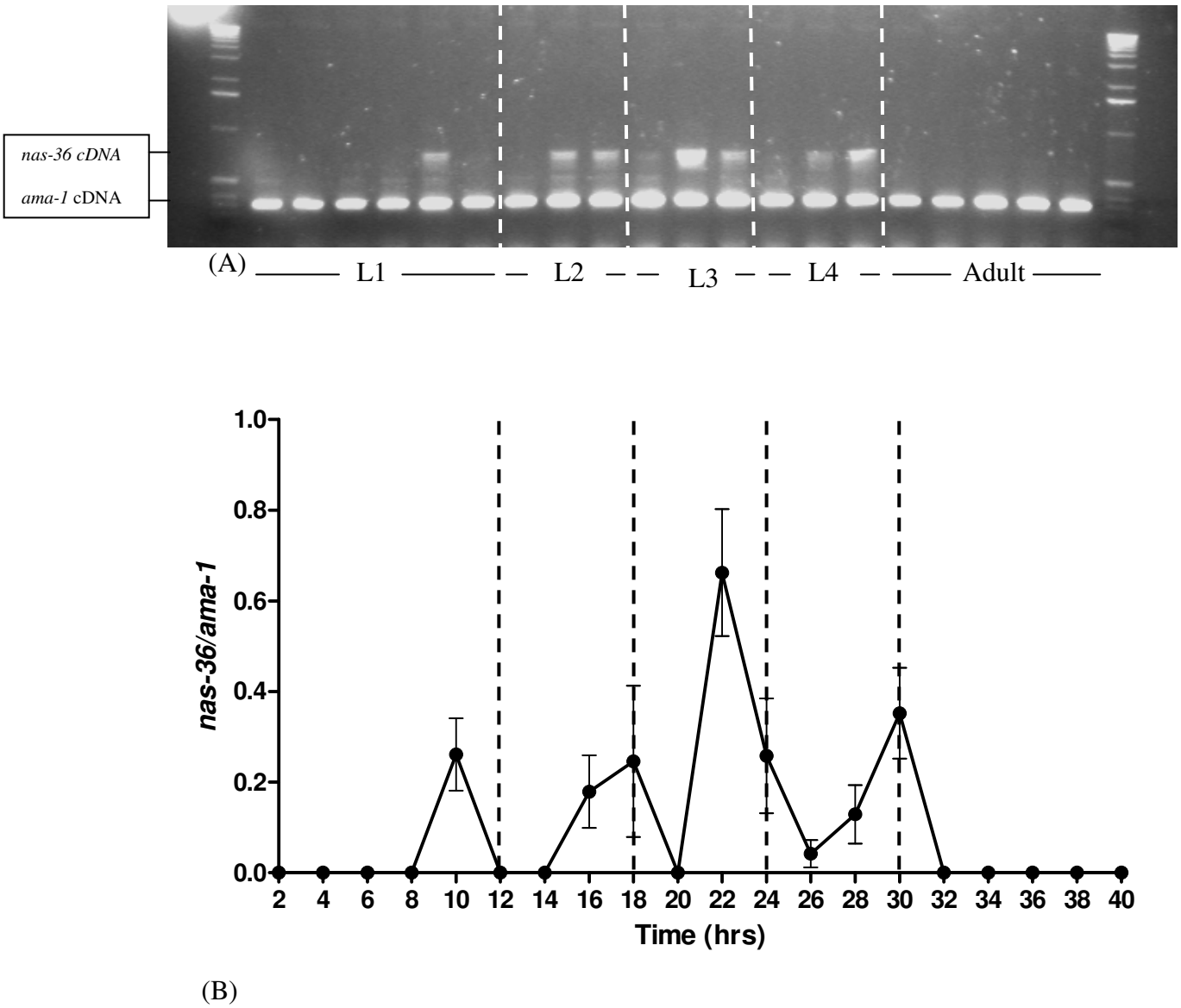

Figure 5.12: sq RT-PCR *nas-36* (A) Picture of ethidium stained agarose gel showing *nas-36* sq RT-PCR. Marker used was Invitrogens 1kb ladder. (B) Graphical representation of sq RT-PCR of *nas-36*. Expression is noted as 2hrs pre-moult. Vertical lines denote the time of each moult. Error bars indicate the standard deviation.

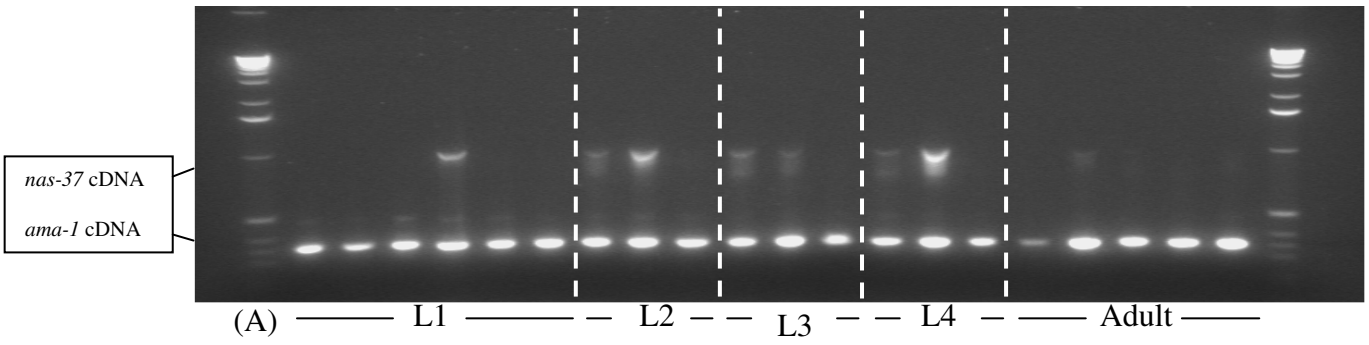

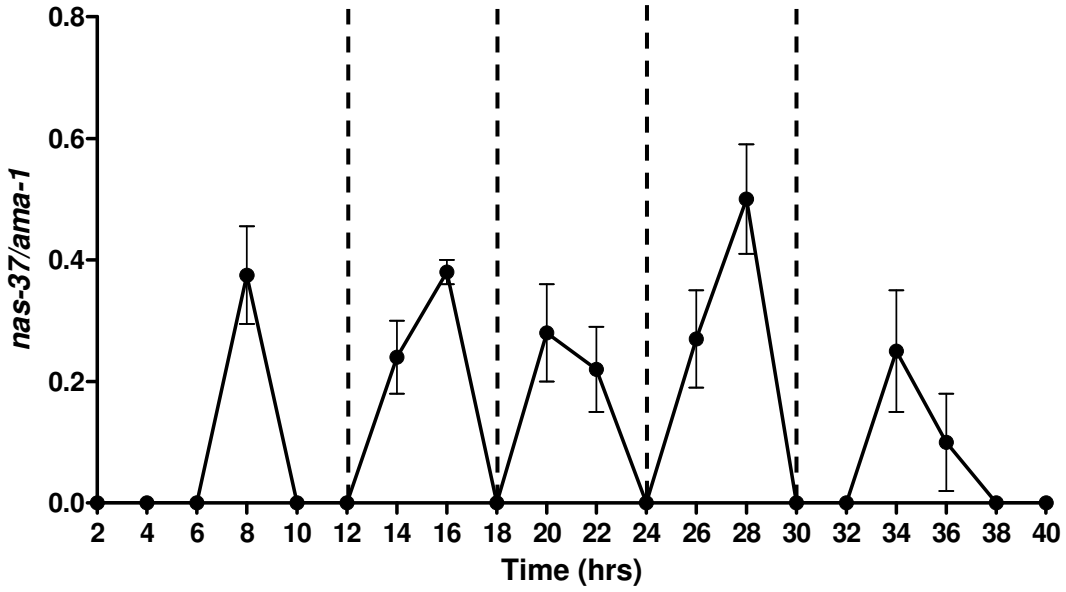

(B)

Figure 5.13: sq RT-PCR of *nas-37* (A) Picture of ethidium stained agarose gel showing *nas-37* sq RT-PCR. Marker used was Invitrogens 1kb ladder. (B) Graphical representation of sq RT-PCR of *nas-37*. Expression peaks 4hrs pre-moult. Vertical lines denote the time of each moult. Error bars indicate the standard deviation.

This promoter element was ligated into the multi-intron containing *lacZ* reporter vector pPD95.03 and sequenced to ensure that frame was maintained. Three separate lines carrying the transgene were established as per section 2.21.

Expression of *lacZ* was not easily detectable when driven by the *nas-36* promoter fragment, Figure 5.14. Sensitive staining (20% β-galactosidase) was used to improve the situation. Expression was detectable in the vulva of adults and also during embryogenesis in undetermined cell types, Figure 5.14.A and B. Weak expression was also determined in the body hypodermis at levels considerably lower than *nas-37*. Similar expression profiles for *nas-36* have been reported by Suzuki *et al.,* (2004), who fused a promoter element (-1453 to +8bps) of *nas-36* to the GFP reporter vector pPD95.67. A similar GFP reporter construct would need to be generated in order to fully confirm the expression profile for *nas-36.*

nas-37 spatial expression determination by translational fusion to a *GFP* reporter

The spatial expression of *nas-37,* determined by Davis *et al.,* (2004), was examined using a translational *GFP* reporter construct which contained all genomic material between the upstream gene C17G1.7 and C17G1.6 (*nas-37*) and the ATG start codon of *nas-37*. This 3806bps promoter element was ligated into the multi-intron containing GFP reporter vector pPD95.75 (Davis *et al.,* 2004).

A translational fusion construct which contained the *nas-37* promoter and full genomic coding sequence fused to pWD103T (an altered version of pWD103 which contains the GFP (S65T) of pPD113.35) was also generated (Davis *et al.,* 2004). Figure 5.15 and Figure 5.16 show that *nas-37* is a hypodermally expressed transcript and a secreted protein. Figure 5.15 shows that at the L2 stage *nas-37* expression was not detectable in the lateral seam cells but was detectable in tail hyp8, rectal epithelial (REP) cells and in hyp7.

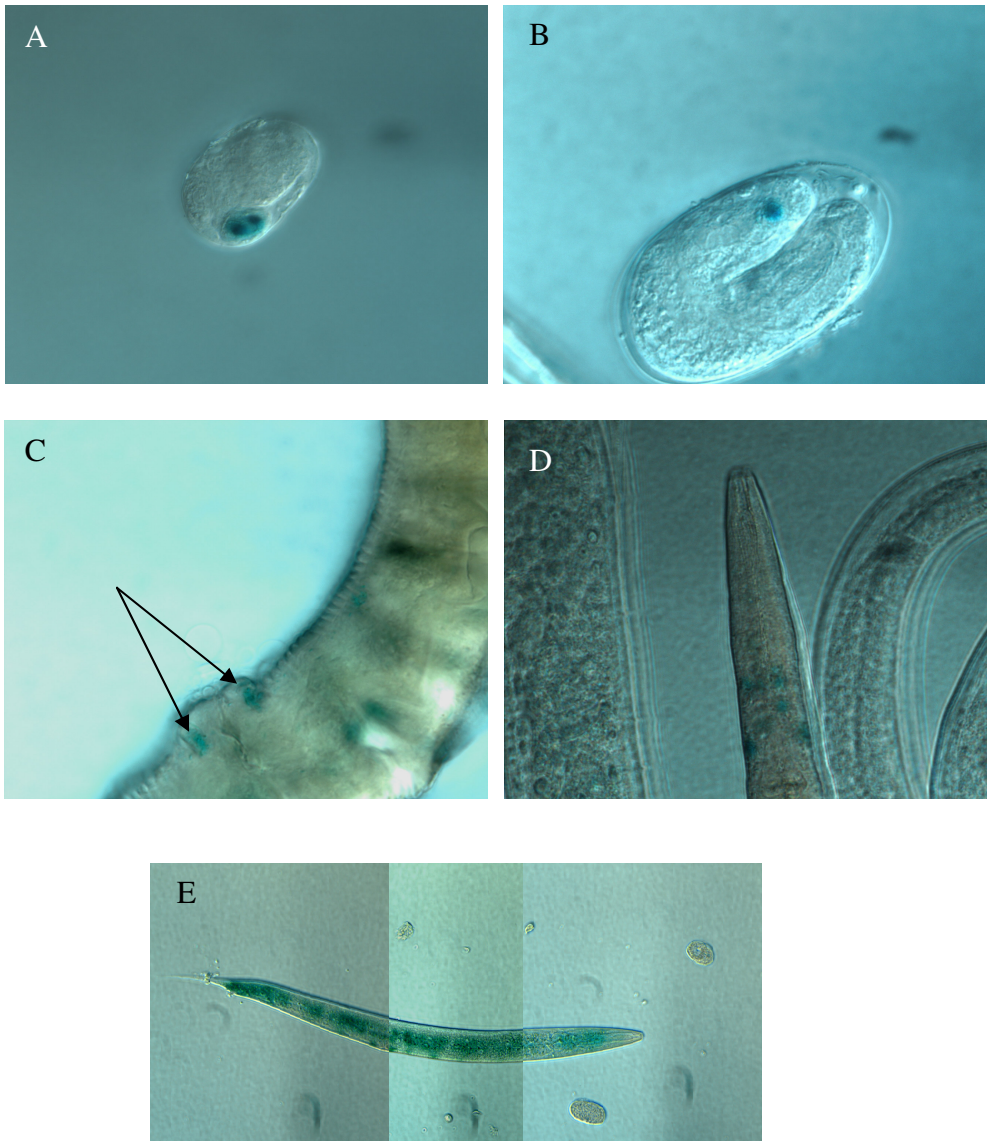

Figure 5.14: *nas-36* promoter driven *lacZ* expression. (A/B) Show expression in undetermined cells in 3-fold embryos, magnification x60 and x100 respectivley. (C) Shows expression in the vulval epithelial cells (arrows). Magnification x100. (D) Expression was noted at the anterior of the worm. Magnification x60. (E) A late L3 expressing *nas-36* across the body. Sensitive (20% β-galactosidase staining approach was used to highlight *nas-36* expression). Magnification x20.

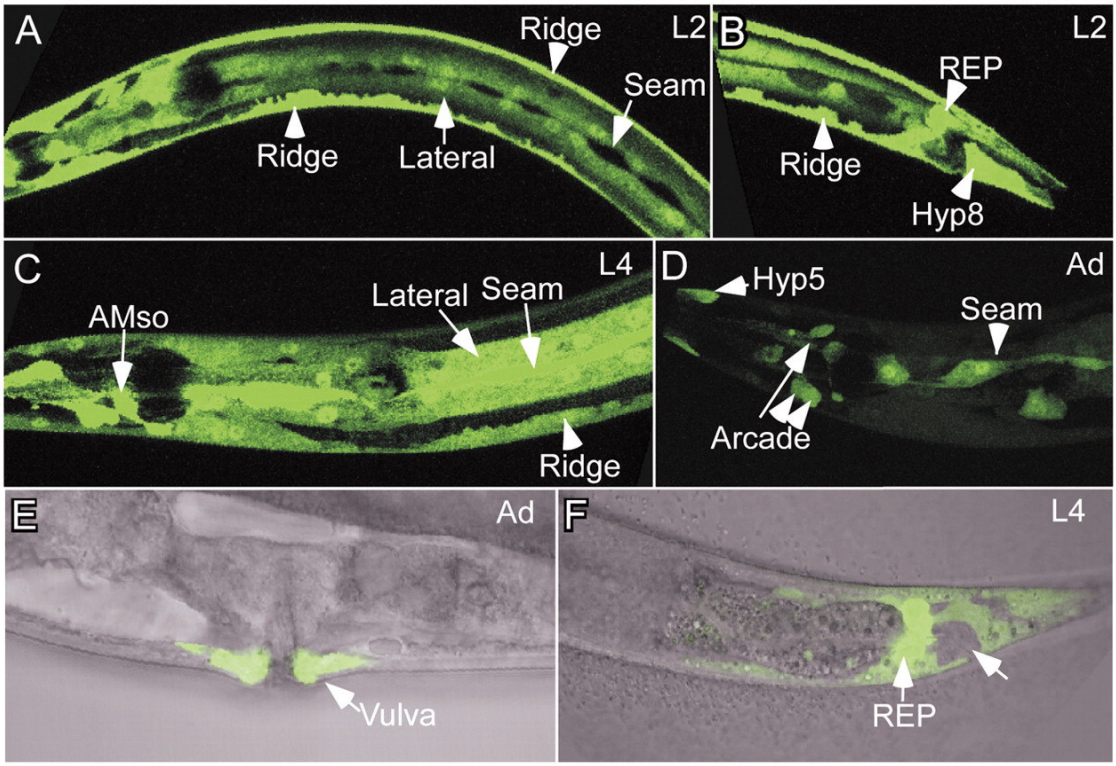

Figure 5.15: *nas-37* is transcribed in the hypodermis. (A) Expression of *nas-37* is noted on the hypodermal ridges. Expression is not found in the seam cells or nervous system of L2 stage larva. (B) A posterior view of the same worms as (A) showing expression in hyp8 and the Rectal Epithelial (REP) cells. (C) L4 larva showing seam cell and hypodermal expression. (D) Adults show weak expression in the arcade, seam and hyp5 cells. (E) Adults also show expression in the vulval epithelium (F) REP cells show expression but not in the adjacent hypodermal cells (arrow). Taken form (Davis *et al.,* 2004).

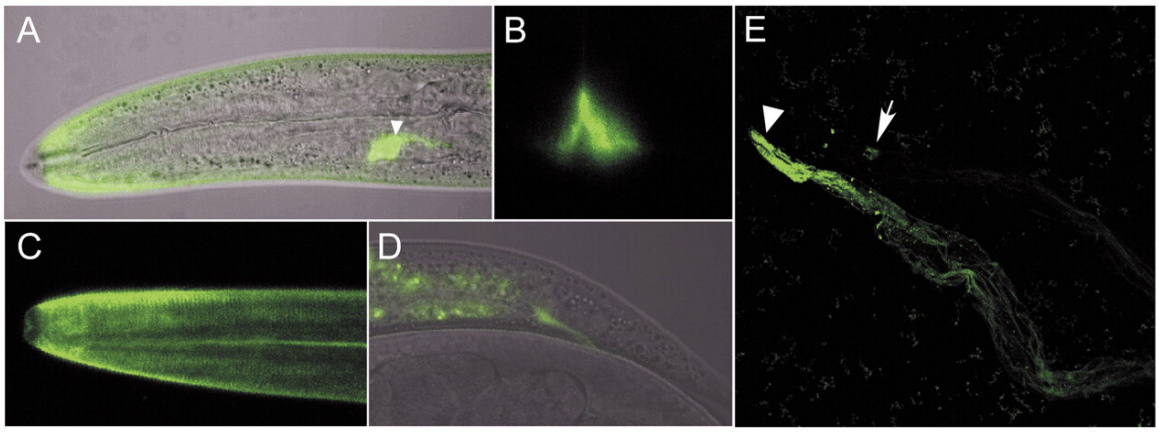

Figure 5.16: NAS-37::GFP protein is secreted. (A) Shows an overlay of a confocal/DIC image illustrating that NAS-37 is found in the anterior end of the worm and strongly in the excretory duct (arrowhead). (B) NAS-37 is also detected in the vulva. (C) NAS-37 localises to the annular rings and lateral cuticle in L4s. (D) Shows that NAS-37 accumulates in the cuticle of the rectum. Gut auto-fluorescence can also be seen. A confocal micrograph of a shed cuticle (E) shows that the NAS-37 protein accumulates in the anterior (arrowhead) and posterior (arrow) ends of the shed cuticle. Taken from (Davis *et al.,* 2004).

By L4 the seam cells were expressing *nas-37* strongly. Adults showed expression in the REP cells; the vulval epithelial cells; the arcade cells, which firmly hold the outer body wall and the lips to the inner cylinder of the pharynx; hyp5; and the seam cells.

Figure 5.16 shows that NAS-37 is a secreted protein which localises to the anterior and posterior of the worm. Anterior accumulation of NAS-37 is noted in the excretory pore and in the annular rings of the cuticle. NAS-37 is also detectable in the adult vulva and rectum, both of which are points of cuticle attachment. Thus NAS-37 is localised to regions of cuticle attachment and points of cuticle degradation.

5.3 Discussion

In this chapter QSOX enzymes were shown to associate with hypodermal tissues at times associated with collagen synthesis. NAS-37, which had previously been shown to be involved with moulting, localised to regions of cuticle attachment and degradation.

5.3.1 QSOX enzymes localise to hypodermal tissues at times of collagen production.

qsox-1 expression

The temporal expression of *qsox-1* was analysed by means of a sq RT-PCR approach, which showed that synthesis of the gene product was cyclical, peaking coincidentally with intermediate collagen synthesis. This is a typical expression profile for modifying enzymes of the cuticle (Page, 1997; Winter and Page, 2000; Eschenlauer and Page, 2003).

The spatial expression profile of *qsox-1,* determined with a *lacZ* transcriptional fusion construct, confirmed it as a hypodermally expressed gene. Expression was detectable early in embryogenesis, and at each subsequent larval stage in the seam and main body hypodermal cells. Expression was also noted in the pharyngeal hypodermal cells. This localises *qsox-1* expression spatially to regions of collagen synthesis and secretion. Together with the temporal expression data it is appealing to propose *qsox-1* as an enzyme involved with cuticle collagen modification.

qsox-2 expression

The temporal expression of *qsox-2* was shown by sq RT-PCR to be constitutive, being expressed at every larval stage of development covered by the staged cDNA samples.

Spatial expression was determined by transcriptional fusion of a *qsox-2* promoter element to a multi-intron containing *lacZ* expression vector. The resulting expression profile showed *qsox-2* as predominantly pharyngeal (detectable in all larval and adult stage), with expression also noted in hypodermal cells and male tail hypodermis.

Localisation to the pharyngeal muscles may associate *qsox-2* with type IV (basement membrane) collagen modification in this tissue. Localisation to the male tail hypodermis may propose a further functionality for *qsox-2,* perhaps in male tail remodelling.

Hypodermal male tail remodelling takes place at the L4-adult transition, and results in the generation of a male tail and a tail hypodermal syncytium. The process can be divided into five stages with breaking of cell boundaries and fusion events processing in an anterior to posterior manner (Nguyen *et al.,* 1999). The fusions of the tail hypodermal cell types leads to the generation of this syncytium, which then migrates into the body at the midline leading to the generation of a strip of central hypodermis that extends from the tail to the anterior edge of the proctodeum.

This remodelling process requires enzymes associated with cuticle modification, the α subunit of prolyl 4-hydroxylase (DPY-18) and thioredoxin-like protein (DPY-11) being two such enzymes. These enzymes are likely to be responsible for post-translational modifications of collagens and other matrix molecules synthesized in the hypodermis (Hill *et al.,* 2000; Winter and Page, 2000; Ko and Chow, 2002). *qsox-2* may also be required, a hypothesis that remains to be proven.

qsox-3 expression

Temporal expression of *qsox-3* was determined by sq RT-PCR and showed a gene with peaks in expression concurrent with the peak expression of collagens belonging to the intermediate group (Johnstone and Barry, 1996).

Spatially *qsox-3* was detectable in developing embryos which were pre 1-fold in development. Embryonic expression was also detectable in 2- and 3-fold embryos enduring

throughout all larval development stages into adult worms. Tissues expressing *qsox-3* included the head hypodermal cells, the main body hypodermis and seam cells. This, along with the distorted COL-19 patterning shown following *qsox-3* RNAi, data highlights a role of collagen post-translation modification for QSOX-3.

The QSOX family of enzymes associate with collagen production spatially and temporally.

The major pattern observed following *qsox-1, 2* and *3* spatial and temporal determination was that of QSOX family members being expressed at times of collagen production, and localised spatially with regions of collagen secretion, namely the hypodermal cells. This is consistent with the expression profiles of many QSOX orthologues which localise to regions of high secretory load and disulphide bond requirement (Thorpe *et al.,* 2002; Amiot *et al.,* 2004; Mairet-Coello *et al.,* 2005; Radom *et al.,* 2006).

A trend of overlapping peak expression for *qsox-1* and *3* with the intermediate collagens, particularly SQT-3, was noted, and was indicative of enzyme and substrate association. Further characterisation would be required to determine any association between these QSOX and possible substrates. The polyclonal SQT-3 specific serum (Novelli *et al.,* 2006) would aid in the characterisation of *qsox* mutants, allowing for Western blot analysis and immuno localisation to be performed.

The cyclical expression profile of *qsox-1* is also similar to *pdi-1* and *pdi-2* which are involved with cuticle post translation modification, (Winter and Page, 2000; Eschenlauer and Page, 2003). Of relevance to this, avian PDI has been shown to be a substrate for avian QSOX (Hoober *et al.,* 1999). It is unclear whether any such association is present between the QSOX and PDI families of *C. elegans*, this association was however further investigated, see chapter 6.

5.3.2 Spatial and temporal localisation of nas genes

nas-9 expression

Temporal expression of *nas-9* was determined by sq RT-PCR, which illustrated a pattern of expression which increased in level and cycled coincidentally with the moults. Such an expression pattern overlapped temporally with the late expressed collagens that also had increased levels of expression with age, an effect noted with other collagen processing

enzymes (Page, 1997; Winter and Page, 2000). *nas-9* has been shown to be hypodermally expressed by the Genome BC *C. elegans* Gene Expression Consortium, however no phenotypes were evident following targeted RNAi of *nas-9* in either N2, TP12, TP55 or in the RNAi hypersensitive strain *rrf-3* (Simmer *et al.,* 2003). TP55 exhibited no significant change in Mlt phenotype penetrance under *nas-9* RNAi. Thus due to a failure to produce any noticeable phenotype, or to reproduce the previous 6% lethality phenotype (Maeda *et al.,* 2001) with any of the strains mentioned above, *nas-9* was omitted from any further characterisation.

nas-28 and *nas-38* expression

Temporal expression data could not be gathered for *nas-28* or *nas-38* using a sq RT-PCR approach; however expression has been confirmed through RT-PCR with mixed stage cDNA for both. In addition EST data is available for *nas-38*. This discrepancy may have been due to the conditions in which the cDNA samples were collected, or, that the reverse transcriptase phase of cDNA generation was inefficient and did not produce transcripts of either gene. Two different staged samples were tested, neither produced any definite bands after 35 cycles of PCR and products when resolved on a 1% agarose, 0.08 µg/ml ethidium stained gel. *nas-38* was at this point omitted from further characterisation within this thesis.

Spatial expression data has since become available for *nas-38*[6] which has demonstrated expression in the hypodermal tissues, consistent with the RNAi effects reported in chapter 3.

nas-34 expression

sq RT-PCR confirmed that *nas-34* had no larval or adult expression phase in accord with Hishida *et al*, (1996). This also showed that *nas-34* was unlikely to be co-operative in the analogous process of moulting.

nas-36 and *nas-37*, two group V astacins associated with the process of moulting

Both *nas-36* and *37* had been shown by RNAi to produce moult defective *C. elegans*. In this chapter it is highlighted that both localise to regions associated with cuticle attachment

[6] http://gfpweb.aecom.yu.edu/index

and degradation (Davis *et al.,* 2004; Suzuki *et al.,* 2004). Temporally they are produced two and four hours before each moult, *nas-36* and *nas-37* respectively, perhaps being required to process collagens that are being expressed at these periods, as both exhibit a limited COL-19 disruption by RNAi in TP12. Alternatively they may be being processed by some other yet unknown enzyme, changing them from zymogens to active proteins; or, they are active and functional for the entire period between their expression and the moult. These and other aspects of *nas-36* and *nas-37* functionality will be addressed in chapter 7.

Chapter 6: Characterisation of QSOX family members.

6.1 Introduction

Following the generation of the *qsox-1* deletion strain and obtaining a deletion mutant for *qsox-2* from NBP Japan[7], characterisation of these mutants and functional determination experiments were carried out, the results of which are discussed within this chapter.

The native oxidative capacity of the QSOX enzymes was revealed using 2',7'-dichlorodihydrofluorescein diacetate (H_2DCFDA) (Molecular Probes): a fluorogenic probe commonly used to detect cellular production of the reactive oxygen species (ROS) H_2O_2, a by-product of disulphide bonding mediated by QSOX enzymes. This method depends on the de-acetylation of H_2DCFDA by cellular esterases, to form the oxidant-sensitive compound, 2',7'-dichlorodihydrofluorescein (H_2DCF) (Brubacher and Bols, 2001). H_2DCF fluoresces when exposed to UV irradiation and as such could be used as a marker to detect the *in vivo* oxidative capacity of cells/whole organisms. A reduction of oxidative capacity within the cell or organism would be mirrored by a reduction in H_2DCF fluorescence, with the opposite also being true.

As had previously been shown avian PDI enzymes are substrates of avian QSOX enzymes (Hoober *et al.,* 1999). An aim of this part of the project was to determine if such an association occured between the *C. elegans* QSOX and PDI enzymes. *C. elegans* has three PDI enzymes and three QSOX enzymes. *pdi-1* which when mutated produces no noticeable defects; *pdi-2*, in which mutations result in very distorted cuticles and which is also a component of the prolyl 4-hydroxylase enzyme; and *pdi-3*, in which mutations result in a minor Dpy phenotype but has been shown to be essential in ECM cuticular formation in specific mutant backgrounds (Eschenlauer and Page, 2003; Winter *et al.,* 2007). Figure 6.1 shows a simplistic model for PDI disulphide bond formation, adapted from (Chakravarthi *et al.,* 2006).

[7] http://shigen.lab.nig.ac.jp/c.elegans/index.jsp

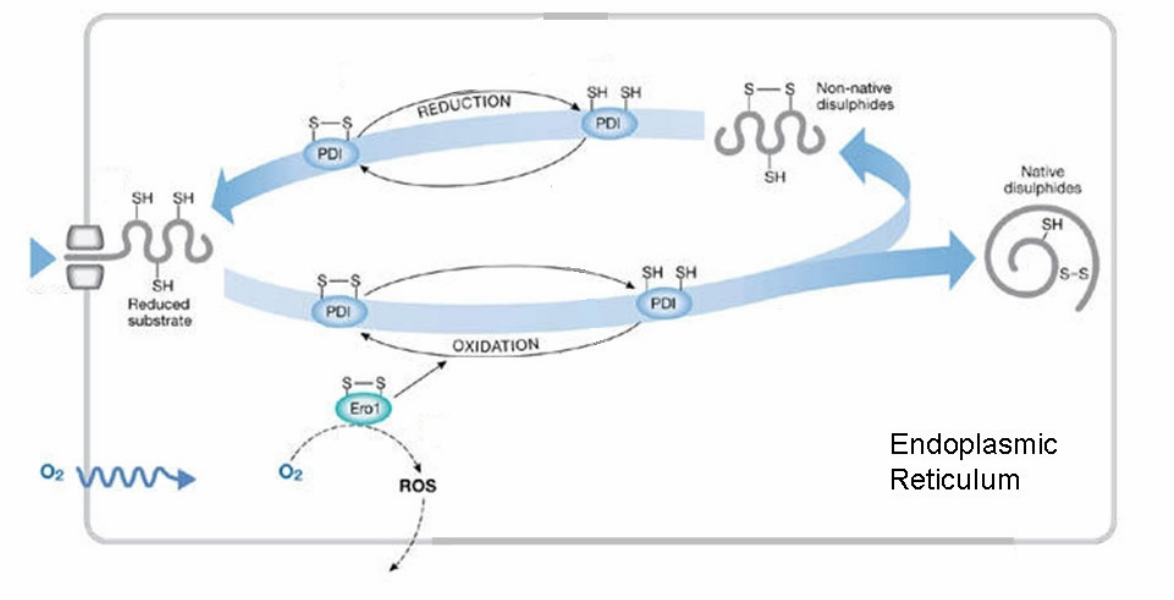

Figure 6.1: Proposed mode of action for PDI enzymes with regard to disulphide bond formation and their re-oxidation by Ero-1. PDIs insert disulphide bonds by themselves acting as a transient between Ero-1 and the reduced thiol (Frand *et al.,* 2000). PDIs however are dissimilar to QSOX enzymes in that reduced QSOX pass their reducing equivalents to molecular O_2 in turn producing H_2O_2 and resetting the QSOX to an oxidised state (Thorpe *et al.,* 2002). PDIs require the attention of other oxidising components, such as Ero-1, to readopt their oxidised state. For a recent characterisation of *C. elegans* PDIs see (Winter *et al.,* 2007). Adapted from (Chakravarthi *et al.,* 2006).

It was later discovered that the *qsox-1(ka2)* carrying mutant strains TP70, and TP73, contained another deletion mutation within their genome. This was uncovered following crosses between TP70 and the mutant strain TP66 (*pdi-3(ka1)*), which resulted in the segregation of the *qsox-1(ka2)* allele from what had been regarded as its mutant phenotypes. This also led to the production of another deletion mutant line, which was given allele designation *ka6*, in which the mutant phenotypes were still evident, but are genetically wild type for *qsox-1*. Therefore, reference to the strain TP70 is to a mutant strain which carries both *qsox-1(ka2)* and the as yet unknown *ka6* allele. Reference to TP110 (*qsox-1(ka2)*) is to the segregated strain which has a homozygous *qsox-1* locus and none of the previous cuticle mutations. TP110 (*qsox-1(ka2)*) is a pure deletion mutant in the *qsox-1* gene.

Following are a list of the mutants used in this chapter, their strain name and allele designation.

Strain name	Genotype
TP70	*qsox-1(ka2), ka6*
TP73	*qsox-1(ka2), ka6, kaIs12*
TP110	*qsox-1(ka2)*
TP88	*qsox-1(ka2);pdi-3(ka1)*
TP102	*qsox-2(tm1977)*
TP101	*qsox-1(ka2)*(TP110 derived)*;qsox-2(tm1977)*
TP111	*ka6*
TP66	*pdi-3(ka1)*
TP68	*pdi-2(tm0689)*
TP67	*pdi-1(ka3)*

Table 6-1: Mutants used, their strain name and genotype.

6.2 Results

6.2.1 Backcrossing of the qsox-1 and qsox-2 deletion containing strains

As the mutant library screened in chapter 4 was a randomly mutagenised pool of living worms, this meant that worms which were isolated as carrying a mutation in a specific target gene may also have been carrying other unknown mutations in their genome. The backgrounds of isolated worms were reverted to wild type by no less than four consecutive crosses with N2 worms. The mutant alleles were tracked and the worm's genotype determined at the target locus by SWPCR using gene specific backcross primers. The animals which carried the *qsox-1(ka2)* deletion underwent four rounds of backcrossing and a homozygous strain, denoted TP70, was established. The strain showed cuticle disruptions at each stage of the backcross procedure. Selection of worms to establish the next round of crosses, or to establish the eventual TP70 strain, was made randomly with no selection bias for phenotype. TP70 was then crossed with the COL-19 GFP marker strain TP12 to establish the line TP73. TP73 worms when viewed by UV microscopy had cuticle structures which appeared amorphous and severely disrupted. The cuticle overlying the seam cells showed the greatest disruption, Figure 6.2.F-H.

Animals carrying the *qsox-2(tm1977)* deletion were backcrossed in a similar manner as that described above and denoted TP102; however, TP102 did not exhibit any noticeable gross morphological defects during, or following the backcross procedure.

6.2.2 Characterisation of the qsox-1 and qsox-2 mutants

6.2.2.1 Structural predictions for QSOX enzymes

Appendix B shows structural predictions for the QSOX enzymes modelled using 3Djigsaw[8] and visualised with RASMOL v2.6. Of note is the positional conservation of the CxxC motifs within the N-terminal thioredoxin fold.

[8] www.bmm.icnet.uk/servers/3djigsaw/

Figure 6.2: TP70 and TP73 viewed by DIC and UV microscopy. Head and pharynx distortions can be seen under high power (A and B) respectively. Egg laying (Egl) defects are also noted in TP70 and 73 (C). (D and E) Larval TP70 animals showing head distortions. TP73 worms were viewed under UV; the COL-19 pattern was amorphous in nature (F – G). (F) Clearly shows the lack of structure in the seam cell produced cuticle, white arrow. (I) Larval TP70 exhibit the most severe disruptions; in this instance the worm has both Dpy and Bmd phenotypes. (J) A "missing sections" phenotype is also associated with the TP70 and 73 strains. This often occurs over the vulva in hermaphrodites. The arrow highlights an improperly shed cuticle. All phenotypes noted are seen in both TP70 and TP73 worms.

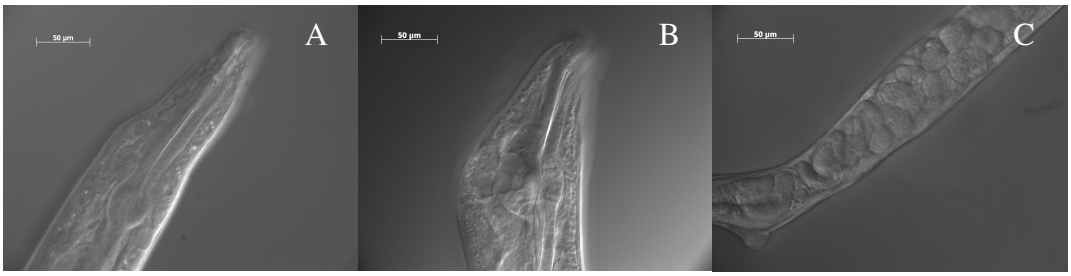
A
B
C
50 µm

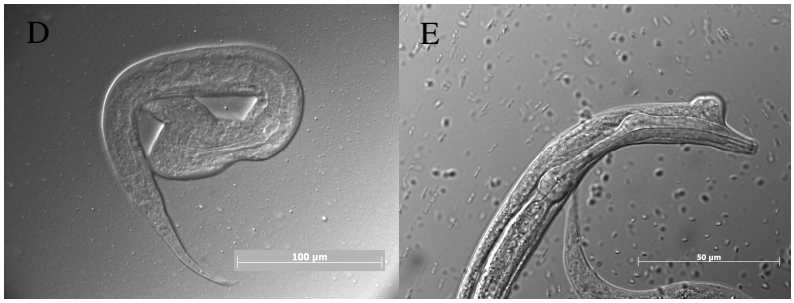
D
E
100 µm
50 µm

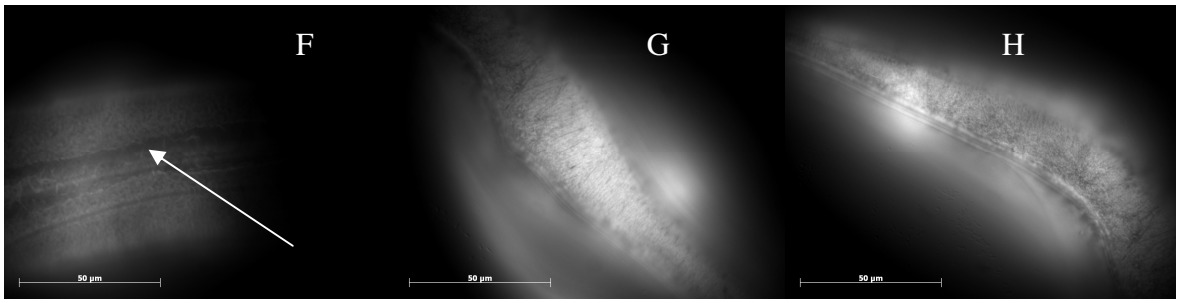
F
G
H
50 µm


I
J
100 µm

6.2.2.2 Phenotypes exhibited in the TP70 and TP73 strains

The strains TP70 and TP73 were scored for the pleiotropic mutations they displayed, see Table 6-2 and Figure 6.2.

Phenotype	Description
Dpy	Common mutant phenotype in which the body is short and somewhat fat. Dumpy animals differ from small (Sma) mutants, which produce "miniature" animals that are very short and not fattened (Savage *et al.,* 1996; Zimmerman and Padgett, 2000).
Mlt	Failure to shed the previous life cycles cuticle.
Gro	Delays in development, slow growth.
Egl	Congestion of the adult hermaphrodite uterus with excess fertilized eggs due to a decrease in the rate of egg-laying.
Bleb	Protuberance of the cuticle in a localized spot, often near the lips or tail tip.
Emb	Embryonic lethality, death occurs during embryogenesis.
Pointer	Distorted head morphology which resembles a pointing hand.
Alae defects	Alae do not adopt there regular stage specific conformation.
Missing sections	Sections of the worms body plan missing, often the vulval region (seam cell derived organ) of hermaphrodites.

Table 6-2: Phenotypes scored in strains TP70 and TP73.

6.2.2.3 Time course for strains containing the *qsox-1(ka2)* allele

A series of five single plates each containing one TP73 worm homozygous for the *ka2* allele, determined by SWPCR, were used to establish a time course, see Table 6-3 and Table 6-4. The worms were grown at 15°C, 20°C and 25°C and allowed to egg-lay for 12hrs before being transferred to fresh OP50 plates and returned to their respective growth temperatures. The eggs laid during each 12hr incubation were counted to determine an average brood size, and the resulting progeny were recounted after 24hrs to determine a "hatched" percentage. N2 eggs hatch ~20hrs post lay at 15°C, 18hrs at 20ºC and 10hrs at 25°C, (Krause, 1995). The hatched larvae were scored for the presence of the *qsox-1*

associated mutations, see Table 6-2, and were allowed to develop until adulthood, whereupon the worms were checked again for persistence of the scored larval phenotypes. N2 worms were included as a control. The initial adults used to establish these populations were transferred seven times over the three day duration of the timecourse.

Incubation Temperatures (°C)	**Average Brood Size per worm** (n=total scored)	**% Hatched**	**Larval Penetrance** (Average percentage of hatched exhibiting a phenotype)	**Adult Penetrance** (Average percentage of adults exhibiting a phenotype)
15	53 (n=1855)	97%	-	-
20	56 (n=1958)	97%	-	-
25	40 (n=1407)	96%	-	-

Table 6-3: N2 timecourse. Average brood size and % of eggs hatched from N2 control *C. elegans* at 15°C, 20°C, and 25°C, n=5 for each temperature.

Incubation Temperatures (°C)	**Average Brood Size per worm** (n=total scored)	**% Hatched**	**Larval Penetrance*** (Average percentage of hatched exhibiting a phenotype)	**Adult Penetrance*** (Average percentage of adults exhibiting a phenotype)
15	35 (n=1214)	60.9%	80%	45%
20	48 (n=1697)	47%	55%	30%
25	34 (n=1190)	39%	58%	41%

Table 6-4: **TP73 time course.** Average brood size, % of eggs hatched, % of hatched larvae showing phenotype and % of adults that exhibited the phenotypes associated with the TP73 strain. n=5 for each temperature. *Penetrance calculated as; presence of any of the noted mutant types associated with the *qsox-1(ka2)* deletion (see**Table 6-2**) over total number of worms.

Comparison of Table 6-3 with Table 6-4 illustrates that TP73 worms showed a reduction in brood sizes and an increase in embryonic lethality (61% lethality at 25°C) when compared with N2 worms. Percentage embryonic lethality was directly proportional to temperature, a common feature of cuticle defect mutations (Wood, 1988; Novelli *et al.,* 2006; Winter *et al.,* 2007). Of note was that larval animals were more disrupted than adults, with 80% of larvae exhibiting a phenotype compared with only 45% of adults in the TP73 strain at 15ºC.

6.2.2.4 Time course for strains containing the *qsox-2 (tm1977)* allele

The strain containing the backcrossed *qsox-2(tm1977)* allele, strain TP102, was tested in the same manner as that described above, except that the 20ºC temperature was omitted from the assay. See Table 6-3 for wild type control.

Incubation Temperatures (°C)	**Average Brood Size per worm** (n=total scored)	**Eggs Hatched**	**Larval Penetrance*** (Average percentage of hatched exhibiting a phenotype)	**Adult Penetrance*** (Average percentage of adults exhibiting a phenotype)
15	19 (n=651)	99%	-	-
25	4 (n=141)	100%	-	-

Table 6-5: TP102 (*qsox-2(tm1977)*) time course. n=5 for each temperature.

From this experiment it could be concluded that TP102 produced no body morphology defects, but had severe fecundity defects at higher temperatures. Even at lower temperatures the production of progeny was significantly lower than N2.

6.2.2.5 Immunolocalisation of *qsox-1* and *2* mutants with SQT-3, MH27 and DPY-7 antibodies

TP70 stained with R584 anti-SQT-3

The specific anti-SQT-3 rabbit polyclonal serum (R584) was used to determine the distribution of SQT-3 in *qsox-1(ka2)* containing mutants. In N2 worms peri-nuclear staining became evident at the comma stage of embryogenesis. At 3-fold the signal diffuses from peri-nuclear to extra cellular, consistent with cuticle collagen secretion. By the 4-fold stage of development, immediately prior to hatching, SQT-3 is localised within the annulae of the embryonic cuticle, Figure 6.3, (Novelli *et al.,* 2006). Similar patterns of expression are noted with other cuticle collagens, such as DPY-7 (McMahon *et al.,* 2003). SQT-3 is expressed in a ubiquitous manner (Kramer *et al.,* 1985), being detectable with antibody in all developmental stages. For the characterisation of the *qsox* mutants, focus was upon the embryonic stages of development.

Staining of TP70 revealed that SQT-3 was not being secreted into the cuticle of the developing embryo, instead it was retained in its early developmental peri-nuclear form,

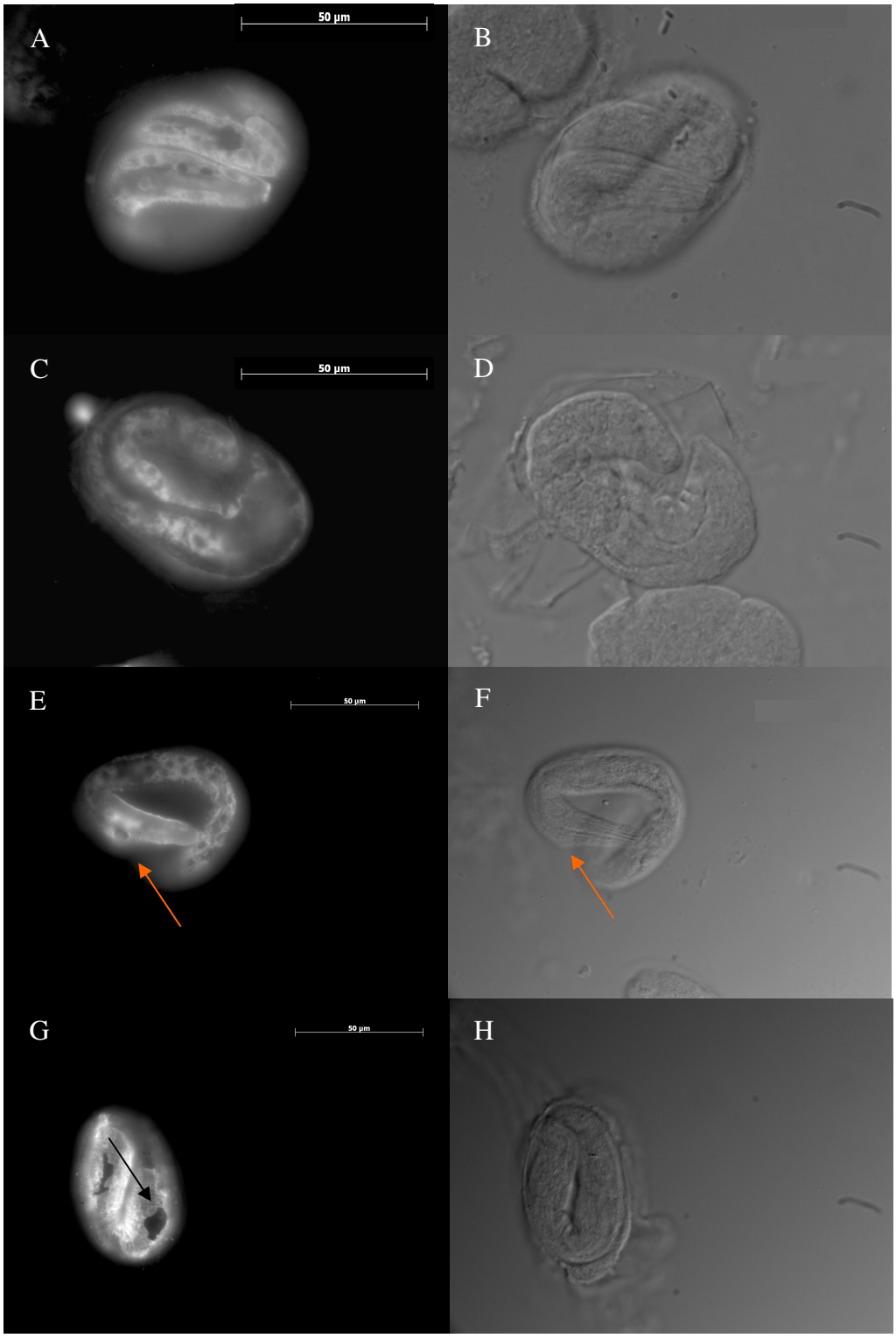

Figure 6.3: SQT-3 antibody staining of *C. elegans* strain TP70 *qsox-1(ka2)*. (A) FITC image of an elongated embryo, SQT-3 can be seen to be retained and not been secreted into the cuticle. (B) DIC image of (A). (C) An unhatched L1; SQT-3 is still retained and not correctly secreted, the corresponding image (D) shows the morphological distortion of this unhatched larvae. (E and F) L1 larva showing retained SQT-3 (red arrow showing Bleb structure on cuticle). (G) Elongated N2 showing wild type SQT-3 collagen patterning. Comparatively, in similarly staged N2s, SQT-3 can be seen to be deposited in a wild type circumferential banding pattern (arrow). (H) Corresponding DIC image to (G).

Figure 6.3. This effect was noted in elongated worms and endured in L1 larvae, by which time SQT-3 should have been deposited within the L1 cuticle. The SQT-3 collagen did not appear to be degraded, despite its retention in this peri-nuclear fashion. The retained SQT-3 phenotype found in TP70 worms is also common in *sqt-3* mutants. *sqt-3(e2117)*, a temperature sensitive lethal glycine substitution, shows a similar phenotype when stained with this antibody (Novelli *et al.,* 2006). Thus equating the *qsox-1(ka2)* mutant to the loss-of-function *sqt-3* alleles reported in Novelli *et al* (2006), with regard to SQT-3 deposition.

TP70 stained with DPY-7

DPY-7 monoclonal antibody (McMahon *et al.,* 2003) localises the DPY-7 protein to the circumferential annular furrows at all stages of development in N2 *C. elegans*. The specific antibody is raised against a distinct C-terminal region of the DPY-7 protein shared by no other members of this family (Johnstone and Barry, 1996). TP70 displayed a mild disruption of the DPY-7 patterning, Figure 6.4, with the cuticular ECM showing disruption in regions secreted by the hypodermal seam cells only. A lack of DPY-7 disruption in the dorso-ventral hypodermal tissue hyp7, could be attributed to the early expression profile of *dpy-7* (Johnstone and Barry, 1996), which is not concurrent with the intermediate expression profile of *qsox-1*.

TP70 stained with MH27

To determine if the seam cell derived cuticle defects associated with the TP70 strain was reflected in the lateral hypodermal seam cells beneath, MH27 immuno-fluorescence was performed. MH27 is a monoclonal antibody raised against the JAM-1 (also-known-as AJM-1) protein of the adherin junctions that surround the seam cells (Mohler *et al.,* 1998). MH27 staining of N2 worms highlights cell boundary formation; fusion; and death in the lateral seam cells, pharynx, male tail, vulva and intestine, Figure 6.5. TP70 worms stained with MH27 demonstrate irregular shaped seam cells which are scattered across the lateral surface of the worm. Often the cells are not in contact with their neighbour and in the most extreme cases the cells are absent, as in worms presenting the “missing sections” phenotype, Figure 6.5.A and B. Incorrect localisation of the lateral hypodermal cells has a deleterious effect upon the cuticle secreted by them, which can be clearly seen when the worms are viewed by SEM, see 6.2.2.6.

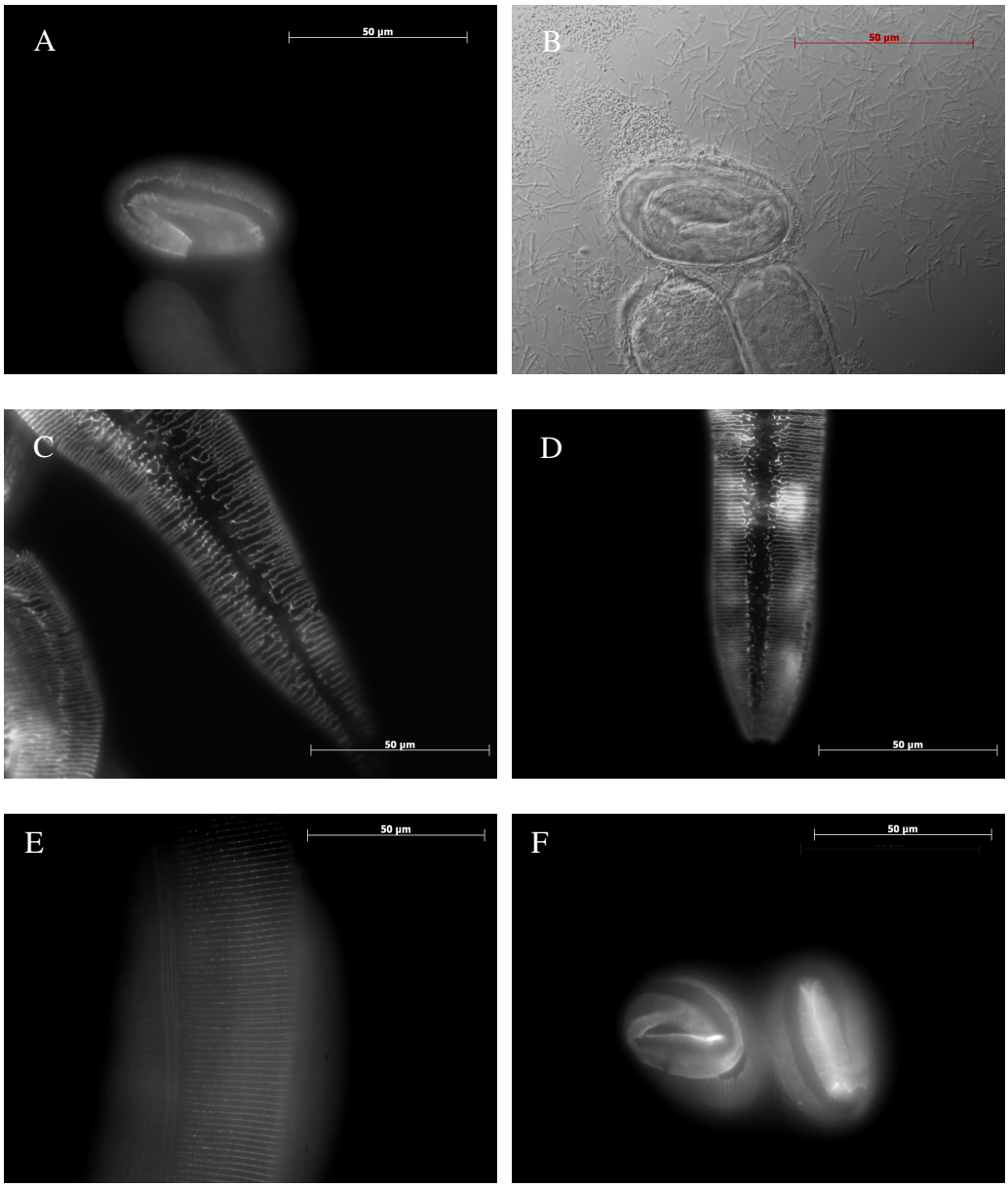

Figure 6.4: DPY-7 antibody staining of TP110 (*qsox-1(ka2)*) and N2 strains. (A) TP110 embryo showing DPY-7 staining of the annular furrows of the nematode. (B) DIC image of (A). (C and D) Disruption of the seam cell derived cuticle of the head and tail respectively. (E and F) N2 controls for larval stage and embryonic stage DPY-7 worms respectively.

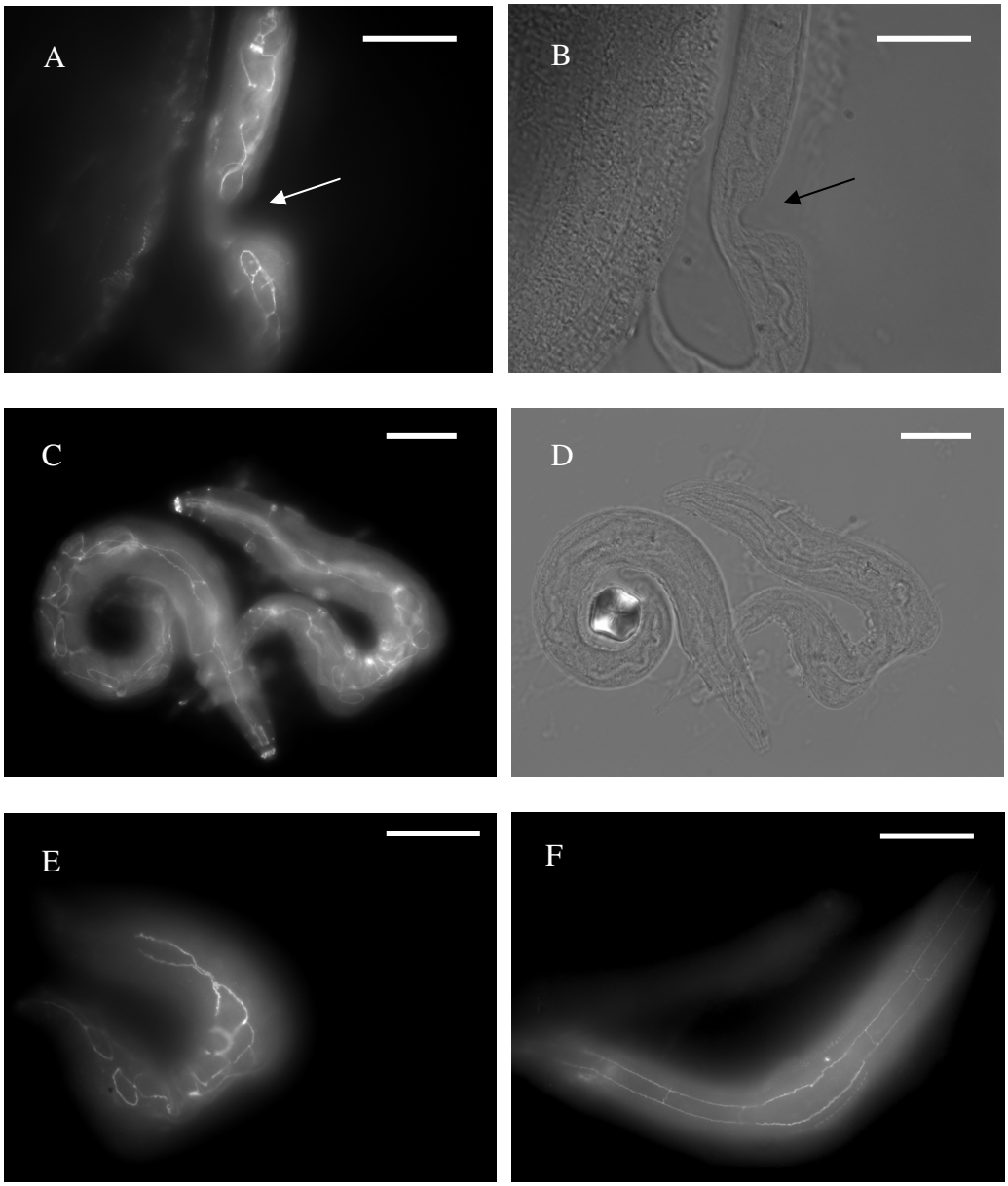

Figure 6.5: Seam cell specific staining using the MH27antibody and L1 stage TP70 (A) FITC image of nematode with characteristic missing section (white arrow). (B) DIC image of (A) (black arrow showing missing section). (C) Shows the severe disruption to the seam cell patterning, worsening towards the posterior of the animal. (D) DIC image of (C), with the left most nematode appearing to adopt wild type morphology, however the underlying seam cells are of an amorphous nature. (E) Magnification of right hand nematode from (C), illustrating the seam cell disruption. (F) Wild type L1 control showing the elongated regular patterning of wild type seam cell development. Scale bars represent 50µm

Cellular level disruptions are not uncommon with cuticular mutations and can be observed upon *pdi-3* RNAi treatment in a *dpy-18(e364)* mutant background. PDI-3 is associated with cuticle synthesis *via* its dual cuticle cross-linking activities; transglutaminase (TGase) activity, for the formation of bonds between glutamine and lysine; and protein disulphide isomerase activity, for the formation of disulphide linkages (Eschenlauer and Page, 2003). Similarly, *dpy-14(e188)* mutants demonstrate improperly fused seam cells caused by collagen mutations (Gallo *et al.,* 2006). Thus certain cuticle collagen mutations can have an effect upon cellular fate which may lead to morphology defects.

TP102 (qsox-2(tm1977)) stained with SQT-3

Staining of TP102 (*qsox-2(tm1977))* worms with the R584 serum returned wild type looking embryos and larva. SQT-3 being secreted into the annulae in a manner similar to R584 stained N2s. By hatching/elongation the embryos of N2 and TP102 worms had secreted the SQT-3 collagen into there respective annulae, Figure 6.6.

TP102 (qsox-2(tm1977)) stained with DPY-7

DPY-7 stained TP102 were wild type in appearance, showing the characteristic annular furrow localisation seen with DPY-7 stained N2 *C. elegans*, Figure 6.7.

TP102 (qsox-2(tm1977)) stained with MH27

MH27, like DPY-7 and SQT-3, returned regular wild type looking worms with no distinguishable deviation from similarly treated N2 controls. Pharyngeal seam cells appeared to be wild type. The hermaphrodite vulva maintained a wild type structure in TP102 worms, Figure 6.8. The male tail was not stained.

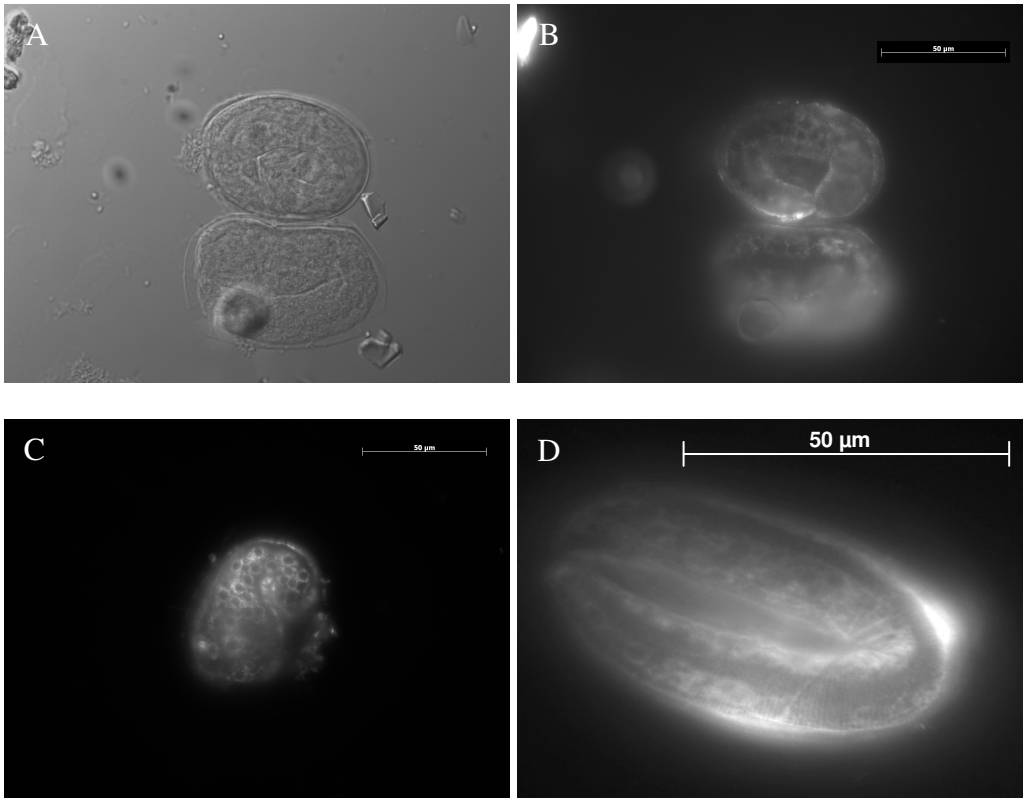

Figure 6.6: TP102 (*qsox-2(tm1977)*) antibody staining with SQT-3 poly-clonal antibody. (A) DIC image of TP102 mutant at 2/3-fold stage. (B) Corresponding FITC image of (A) showing the perinuclear SQT-3 localisation and weakly secreted localisation within the circumferential annular rings. Wild type for this stage. (C) 1.5-fold TP102 showing wild type distribution of SQT-3. (D) N2 elongated worm with some perinuclear SQT-3, most having been secreted into the annular rings by this stage of embryogenesis.

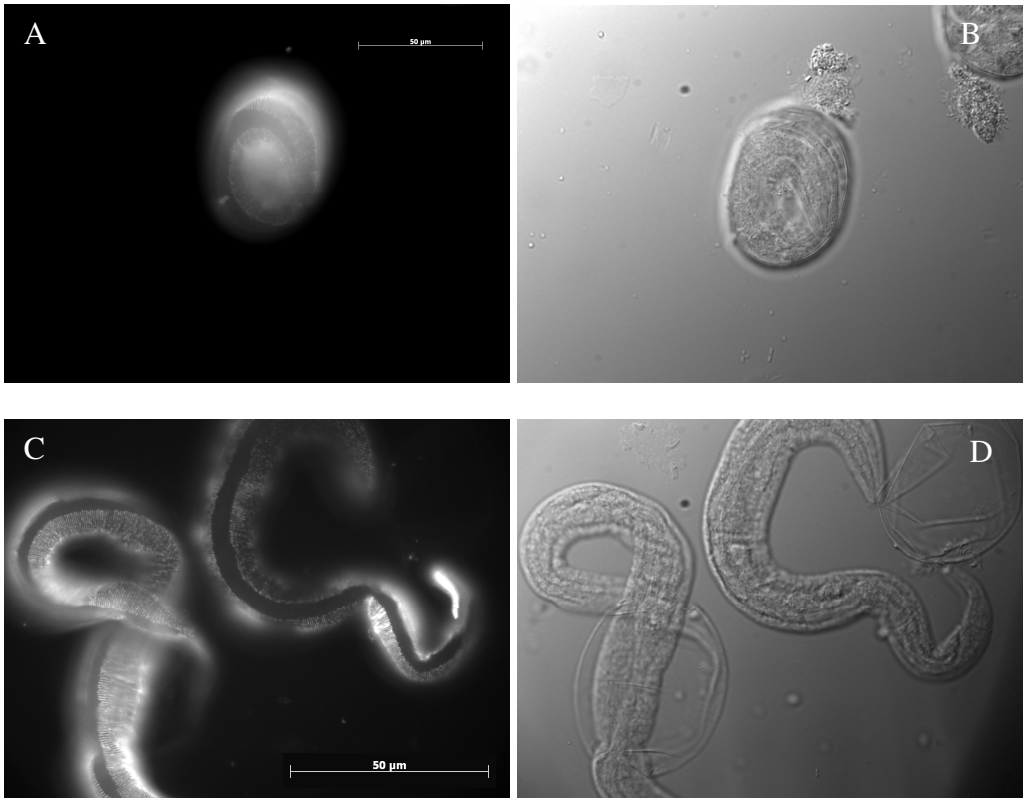

Figure 6.7: TP102 (*qsox-2 (tm1977)*) antibody staining with DPY-7 monoclonal antibody. (A) FITC image of an elongated embryo with a wild type DPY-7 localisation (B) Corresponding DIC image of (A). (C) Larval stage *C. elegans* similarly showing wild type DPY-7 distribution. (D) Corresponding DIC image of (C).

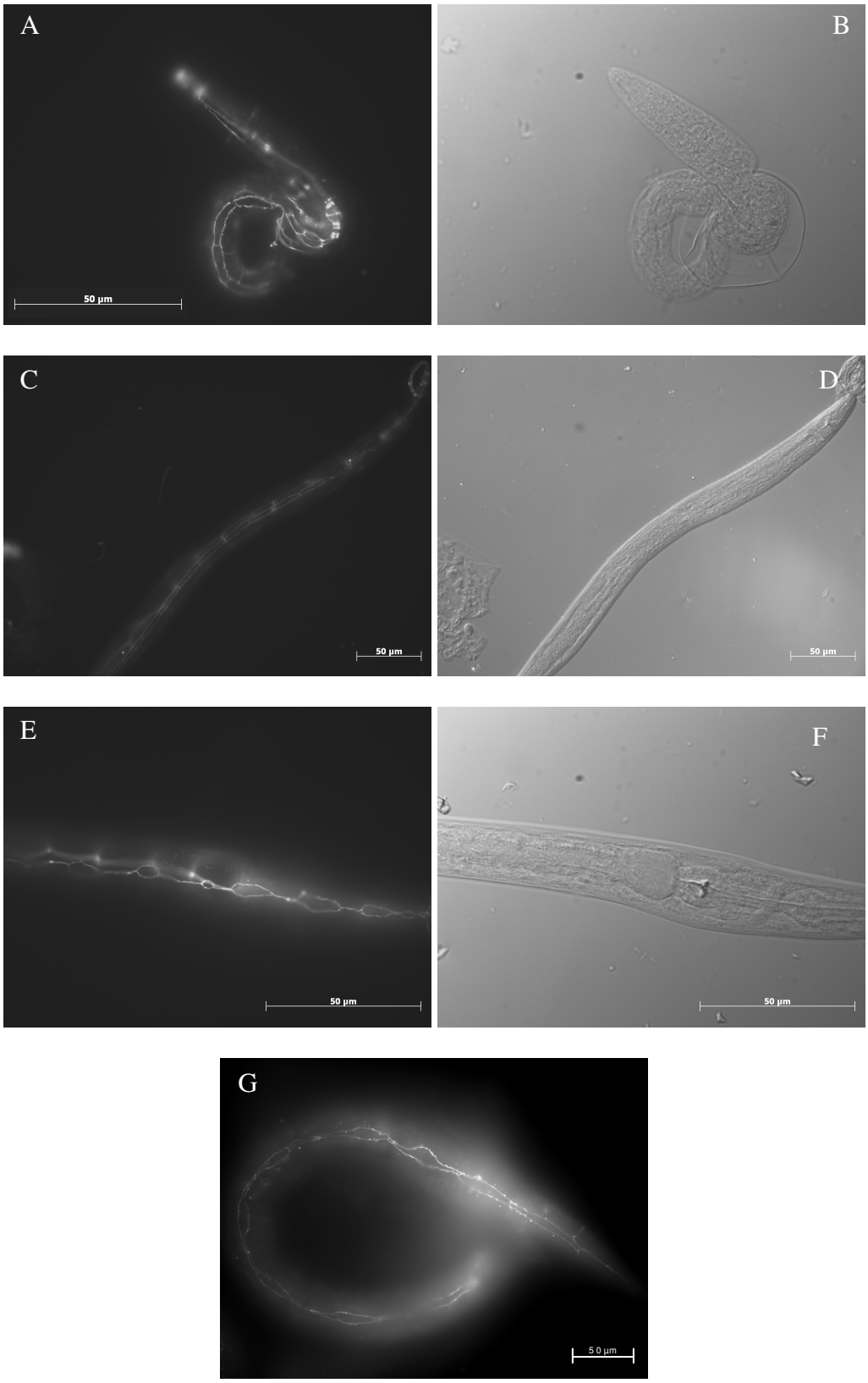

Figure 6.8: TP102 (*qsox-2(tm1977)*) antibody staining with MH27 monoclonal antibody. (A) FITC image of an L1 TP102 showing a wild type patterning of the seam cells along the lateral side of the worm. (B) Corresponding DIC image of (A), no gross morphological defects are evident. (C) FITC image of an L2 TP102 worm with wild type seam cell pattering, (D) corresponding DIC image of the same worm. (E) Head of an L2 TP102 worm showing no distortion to the seam cells, (F) corresponding DIC image of the same worm showing no pharyngeal disruption. (G) L2 N2 control.

6.2.2.6 SEM & TEM images of TP70

Scanning and transmission electron microscopy (SEM and TEM respectively) was used to visualise the cuticular morphology of the TP70 strain. The worms analysed were predominantly L1s: produced by bleaching gravid adults upon unseeded plates at 25ºC, and prepared for microscopy as per section 2.28.

SEMs showed that TP70 worms had severely disrupted cuticles, Figure 6.9. Evident were disrupted lateral alae which appeared either punctate, or, had a pulled/distorted appearance towards the dorsal or ventral surface of the worm. This was in accord with the previous MH27 immumo-localisations which showed scattered, distorted and irregular shaped seam cells, Figure 6.9. Phenocopy of previous RNAi data, see chapter 3, which highlighted an increase in girth of *C. elegans* targeted by *qsox-1* RNAi, was also apparent in these TP70 worms, Figure 6.9.E. The annular banding patterns could also be visualised, and although distorted still remained a discernable cuticular structure. Bleb like protrusions were also evident across the cuticle of the worm. TEM of TP70 showed detachment of the striated layer from the underlying cuticle layers, Figure 6.10, a feature that would lead to a loss of mechanical force transmission during alae formation, and based upon the hypothesis for alae formation proposed by Sapio, *et al* (2005), the alae would be mal formed and be drawn to either the dorsal or ventral surface of the worm, as noted in the SEM images of Figure 6.10. SEM and TEM were not performed upon *qsox-2(tm1977)* worms.

6.2.3 Functional characterisation of qsox-1(ka2) and qsox-2(tm1977) mutants

Swimming assays

An attempt was made to determine the effect of environmental redox balance upon the *qsox-1(ka2), qsox-2(tm1977), pdi-1(ka3)* and *pdi-3(ka1)* mutants by means of swimming assays (Larsen, 1993). Swimming assays involved the exposure of the target strain(s) of worms to a ranging concentration of oxidising or reducing environments, H_2O_2 and DTT respectively. The LD_{50} was then determined and compared relative to control N2 worms.

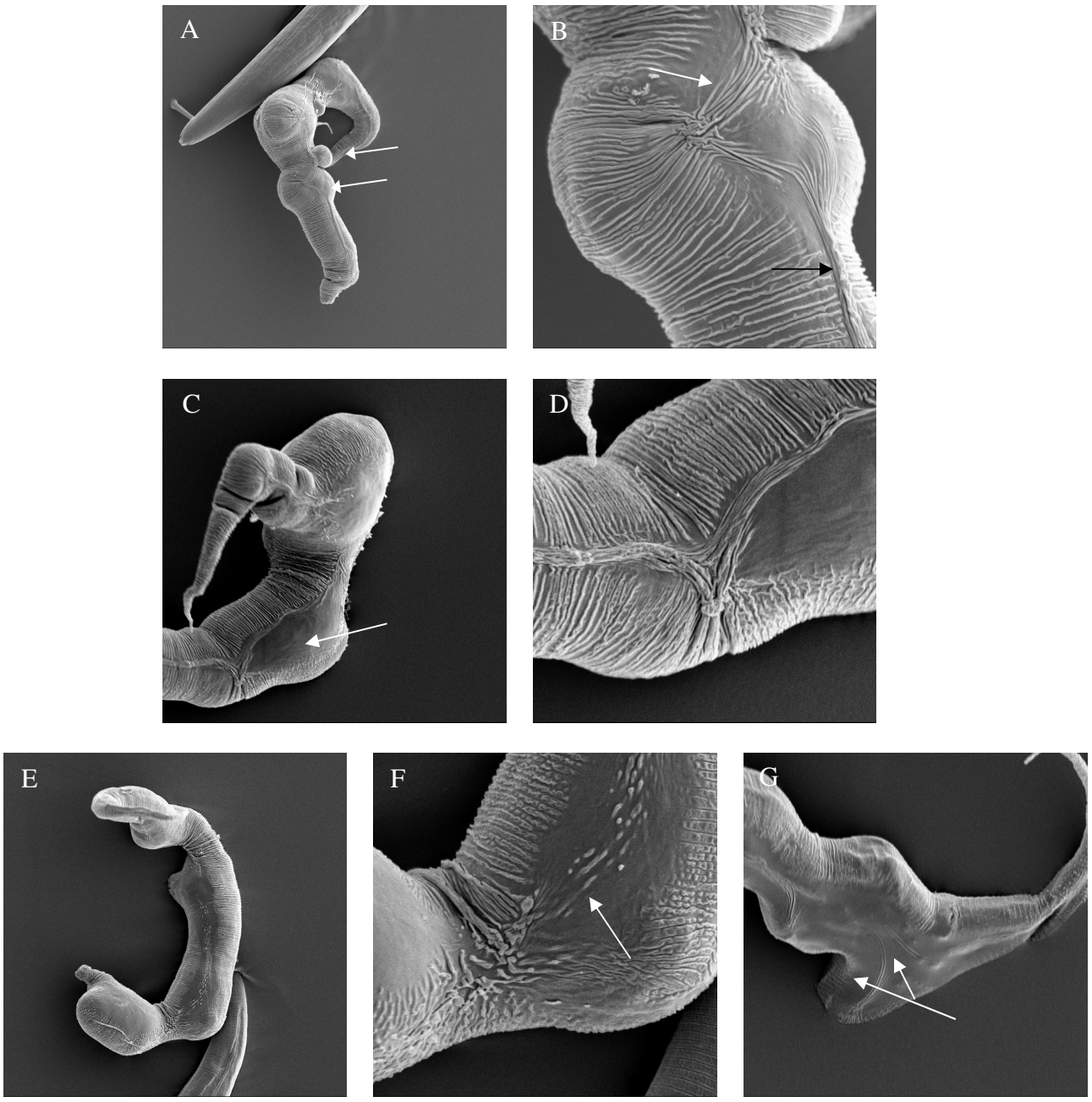

Figure 6.9: Scanning Electron Microscopy images of TP70 (A) Arrows show Bleb and characteristic alae disruption of early larval stage TP70. (Magnification 1100x). (B) Higher magnification (6000x) of (A). The white arrow illustrates the distortion of the alae; the black arrow illustrates a more wild type conformation. (C) Bulging of the cuticle that overlies the seam cells (Magnification 2000x). (D) Higher magnification of (C) (Magnification 5500x). (E) L1 Larva with distorted alae and large Bleb towards the anterior portion of the worm. (Magnification 1300x). (F) Higher magnification of (E). Arrow highlights the severity of the alae disruption. TP70 in this instance failing to secrete the lateral ridges at all, instead a fragmented dot like pattern can be seen (Magnification 6000x). (G) Posterior section of TP70 with characteristic seam cell secreted cuticle disruption. Arrow shows section of secreted alae that has been made by the underlying seam cells but due to the seam cells morphological distortion, fails to produce a wild type lateral alae. (Magnification 5500x).

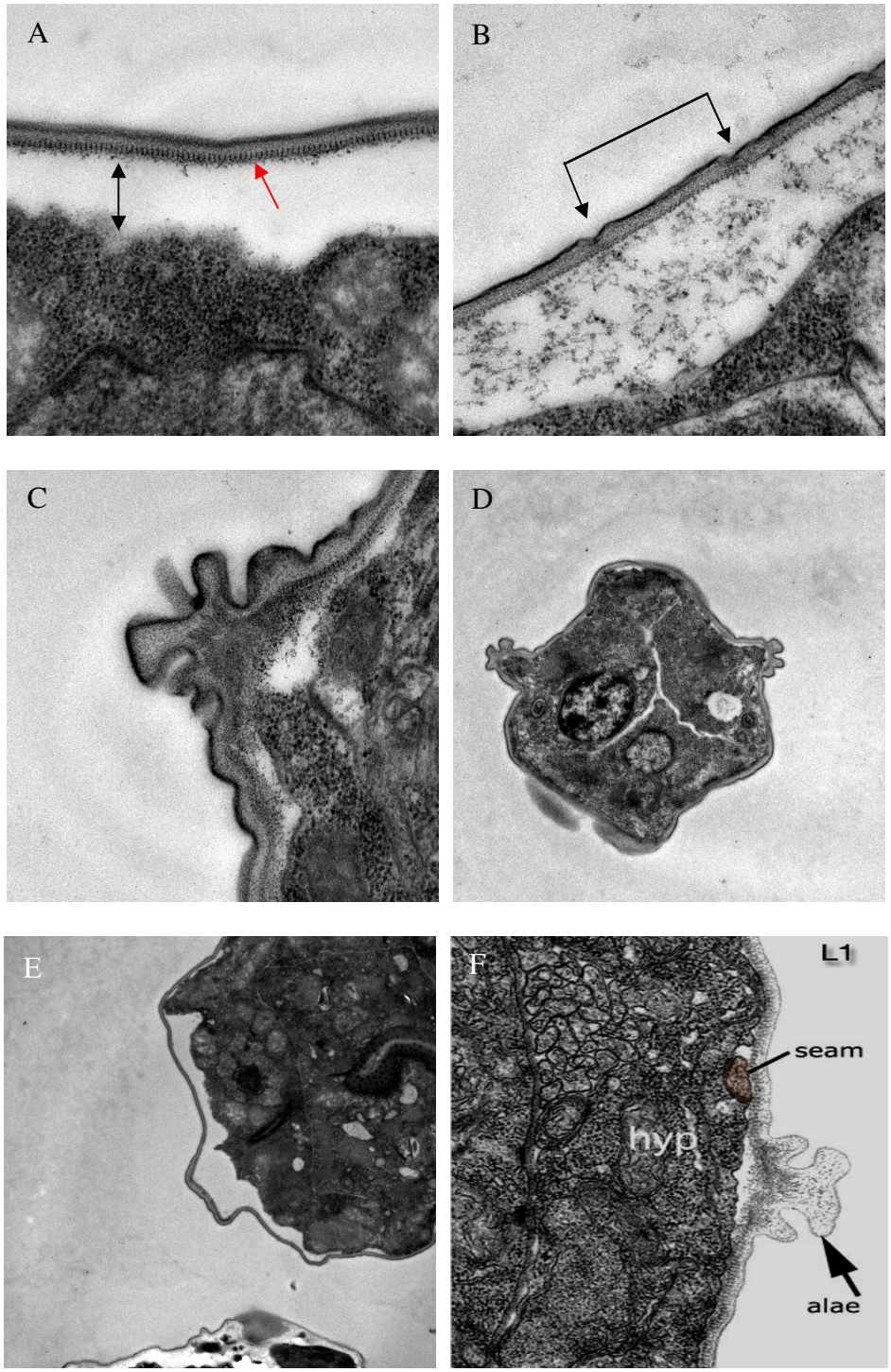

Figure 6.10: Transmission electron microscopy images of TP70: (A) L1 stage larva, separation of the striated layer (red arrow) from the underlying basal layer (black arrow) can be seen. (B) L1 showing separation of the striated layer across an annulus (black arrow). (C/D) Show the distortion of the typically three-foil mushroom shaped alae and overall morphological distortion. (E) Large area of detached cuticle from its underlying basal layer. (F) A wild type L1 with attached striated layer and wild type alae (image F was taken from www.wormatlas.org).

It was hypothesised that H_2O_2 would act to "recover" a lack of oxidative capacity associated with the loss of QSOX or PDI family members and that these oxidativley compromised lines would prove more susceptible to the reducing agent DTT than the N2 controls.

Staged larva (both L1 and L2) and mixed stage animals were tested and found to exhibit similar responses to environmental oxidation manipulation, therefore the results could be considered as applicable to all developmental stages of *C. elegans*. However, the dauer larva would be expected to have a higher $LD_{50,}$ with respect to H_2O_2 and DTT concentration, due to its lack of feeding and less permeable, thicker cuticle. Adults were not a focus of this experiment as their potential for cuticle generation is more limited than larva. The concentration range covered by both H_2O_2 and DTT was from zero (1xM9 only) to 50 mM as the LD_{50} for *C. elegans* was believed to lie within this range (Larsen, 1993). The actual LD_{50} of N2 worms for H_2O_2 was ~5 mM (n=150) and ~7 mM (n=116) for DTT. Young TP73 L4s were picked (35 per well in a 96 microtitre plate) into H_2O_2 (ranging from 0 mM to 50 mM) and incubated at 25ºC until they reached adulthood, when the cuticles of these worms were then viewed by UV microscopy. The resultant cuticles maintained their characteristic defects associated with TP73 and no "recovery" was noted. The more phenotypically distorted the TP73 worms were the more sensitive they were to environmental deviations in redox balance. LD_{50} being offset from ~5 mM (n=117), in the least disrupted worms, to ~2 mM (n=104) in those which had severely disrupted cuticles. This was determined by actively selecting the most and least severely distorted TP73 worms from a population, and exposing both batches to the same redox conditions, temperatures and exposure periods. This shift in LD50 was presumed to be caused by the severely distorted cuticles being more permeable than the more wild type cuticles.

TP70 worms treated with DTT ranging from 0mM to 50mM demonstrated little response to their environmental redox conditions. The LD_{50} remained between 6 mM and 8 mM (n=199) for the most severely disrupted and most wild type looking worms respectively. N2 LD_{50} for DTT is 7 mM (n=116). Similar results were defined with all strains which carried the *qsox-1(ka2)* deletion, including TP110.

TP102 (*qsox-2(tm1977))* worms showed a response similar to N2 worms, with regard to environmental redox conditions, with an LD_{50} for H_2O_2 of 5 mM (n=40) and LD_{50} of 6 mM (n=58) for DTT. TP67 (*pdi-1(ka3)*) had, like TP102 (*qsox-2(tm1977)),* wild type responses to the environmental redox conditions, with LD_{50} of 5 mM (n=100) and 6mM (n=75) for H_2O_2 and DTT respectively. TP66 (*pdi-3(ka1)*) also exhibited a wild type

response to H_2O_2 with an LD_{50} at 5 mM (n=50) but had an increased tolerance to the reducing DTT conditions, LD_{50} not occurring until a concentration of 8 mM (n=50) was reached.

6.2.3.1 Dichlorofluoureseine assays with mutant *qsox* and *pdi* containing strains

To determine the nascent oxidative capacity of *qsox-1, qsox-2, pdi-1* and *pdi-3,* H_2DCHFDA fluorescence assays (Harding *et al.,* 2003) were performed. Staged worms were used in these experiments to ensure that exposure to the fluorogenic probe matched the expression profile of the respective target gene. This meant that starved plates rich in arrested L1s were chunked out onto plates treated with tunicamycin, as per section 2.33.1, and incubated at 25ºC for between 15 to 20hrs. With this incubation period the target genes were within regions of peak expression when visualised. Expression profiles having previously been determined see chapter 5, (Page, 1997; Eschenlauer and Page, 2003).

qsox-1(ka2) containing strains, TP70, 73 and 110

An apparent reduction in oxidative capacity was noted in all strains containing the *qsox-1(ka2)* deletion, TP70, 73 and 110, following treatment with the flourogenic probe, Figure 6.11. The most severely disrupted TP70 and TP73 worms showed no greater reduction in fluorescence associated with their disrupted cuticular regions than was noted in TP110.

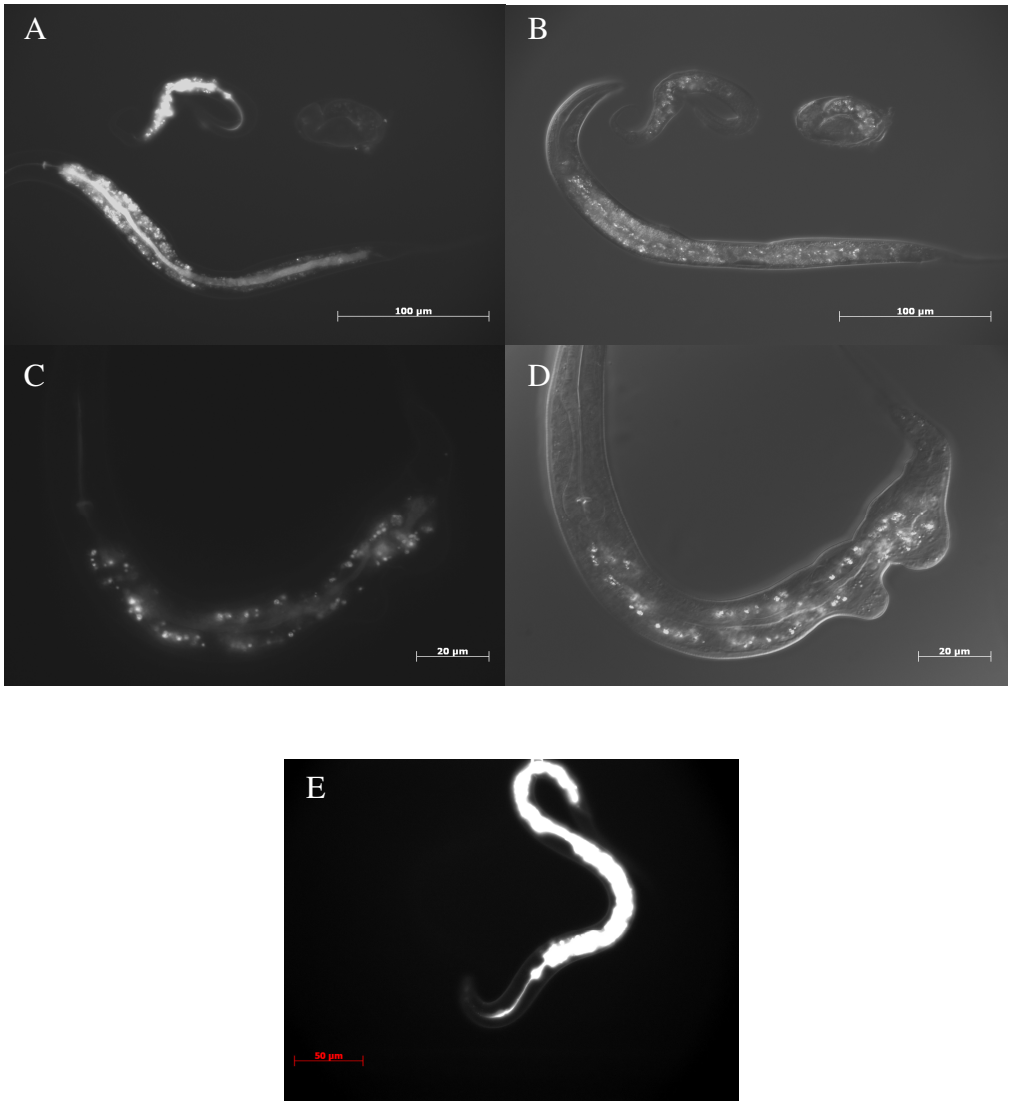

Figure 6.11: H_2DCHFDA fluorescence assay for TP70. (A-D) TP70 H_2DCHFDA treated worms; (A and C) viewed under UV light, (B and D) the corresponding DIC images. (E) N2 H_2DCHFDA treated control viewed under UV light. A reduction in fluorescence can be seen in the body of TP70. Also noted is a slight reduction in the pharyngeal region of the worm when compared with N2 worms. The reduction in fluorescence in TP70s does not correlate with the most severe regions of cuticular distortion.

TP102 (qsox-2(tm1977))

Spatial expression of *qsox-2* is predominantly pharyngeal and to a lesser extent hypodermal, as well as being detected in the male tail syncytium. The pharyngeal fluorescence appeared reduced and in some cases undetectable, Figure 6.12. Males were not examined.

TP67 (pdi-1(ka3))

TP67 worms demonstrated a reduced oxidative potential in regions associated with *pdi-1* expression. *pdi-1 lacZ* reporter constructs being strongly pharyngeal (Page, 1997), similar to *qsox-2*. These regions had the most evident reduction in fluorescence, Figure 6.13.A-D.

TP66 (pdi-3(ka1))

pdi-3 is expressed in the gut and hypodermis (Eschenlauer and Page, 2003), a corresponding reduction in fluorescence, compared with N2, was noted in these regions when the mutant strain TP66*(pdi-3(ka1))* was tested. The pharynx however maintained an approximately wild type level of fluorescence, Figure 6.13.E-H. Table 6-6 correlates both spatial expression profile and H_2DCHFDA response in the strains tested.

However, these are preliminary results and as such can not be deemed as conclusive by themselves: requiring further confirmation by other means to ensure that the apparent reductions noted in ROS production are genuine and specific. These follow up experiments would need to illustrate clearly a link between specific gene products and ROS production, this may prove easier to achieve by *in vitro* means, for example the O_2 electrode (or Clark electrode) assay which measures the electron flow to oxygen as a result of oxidative phosphorylation in turn producing H_2O_2, see diagram below.

$$O_2 + 2\ e^- + 2\ H_2O \rightarrow H_2O_2 + 2\ OH^-$$

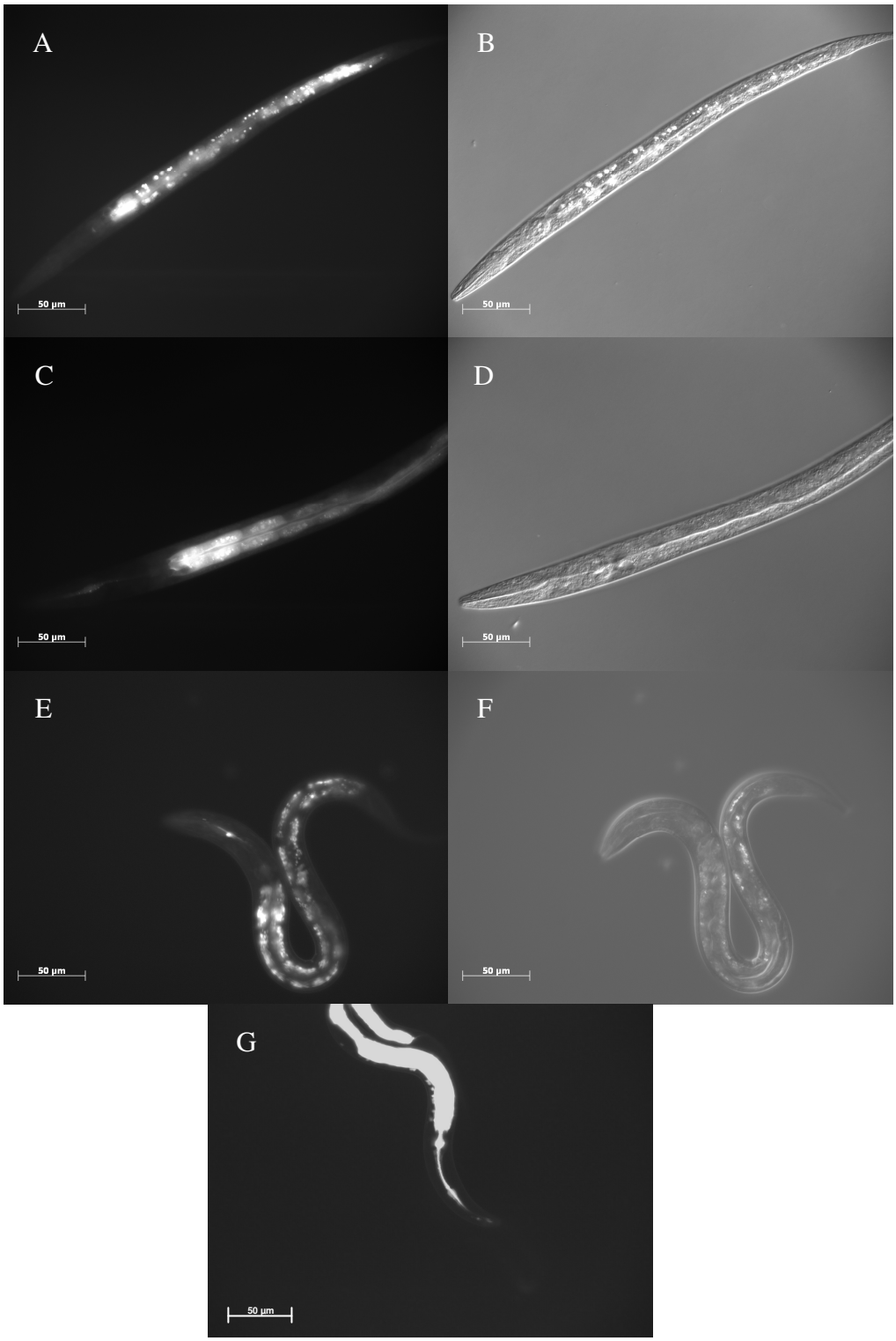

Figure 6.12: H_2DCHFDA fluorescence assay for TP102 (*qsox-2(tm1977)).* (A-F) TP102 H_2DCHFDA treated worms; (A, C and E) viewed under UV light, (B, D and F) the corresponding DIC images. (G) N2 H_2DCHFDA treated control viewed under UV light. A reduction in fluorescence can be seen in the pharyngeal regions of TP102 and also in the body of the worm when compared with N2 worms (G).

Figure 6.13: H_2DCHFDA fluorescence assay for TP67 (*pdi-1(ka3))* and TP66 (*pdi-3(ka1))*. (A-D) TP67 (*pdi-1(ka3))* H_2DCHFDA treated worms; (A and C) viewed under UV light, (B and D) the corresponding DIC images. (E-H) TP66 (*pdi-3(ka1))* H_2DCHFDA treated worms; (E and G) viewed under UV light, (F and H) the corresponding DIC images. (I) N2 H_2DCHFDA treated control viewed under UV light. (A-D) Illustrate the reduced fluorescence seen in the body, and complete ablation in the pharynx, of TP67 (*pdi-1(ka3))* worms. (E-H) TP66 (*pdi-3(ka1))* demonstrates a reduction of fluorescence in the body of the worm. Pharyngeal expression remains.

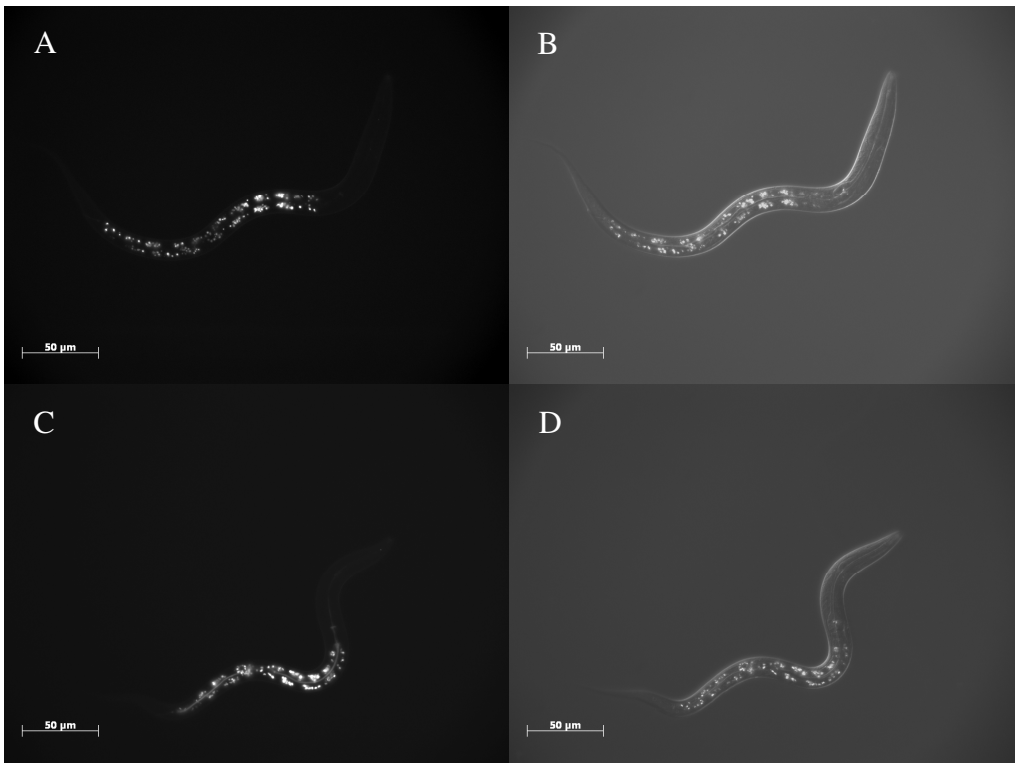

TP67
(pdi-1(ka3))

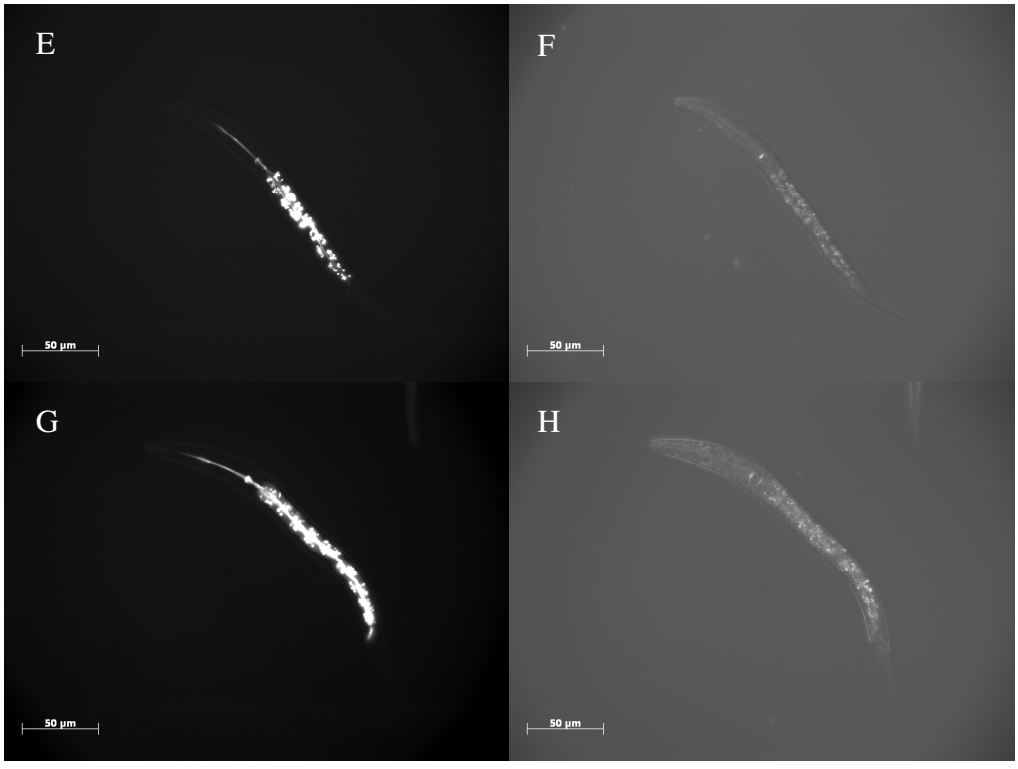

TP66
(pdi-3(ka1))

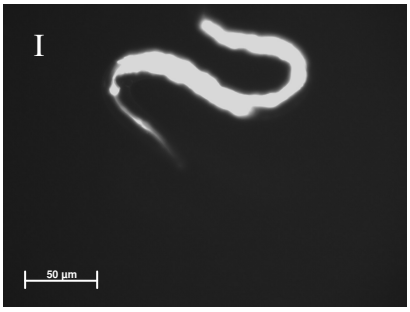

N2

Mutant allele	Spatial distribution of wild type gene	Effects noted upon treatment of mutant strain with H_2DCHFDA
qsox-1(ka2)	Body hyp (hyp7) Head hyp Seam cells Embryonic (undetermined cell types)	Reduction in body fluorescence. Pharyngeal fluorescence endures.
qsox-2(tm1977)	hyp7 Pharyngeal (strong) Seam cells Male tail syncytium	Notable reduction in pharyngeal fluorescence. Body fluorescence also diminished.
pdi-1(ka3)	hyp7 Pharyngeal (strong) (Page, 1997)	Notable reduction in pharyngeal fluorescence. Body fluorescence also diminished.
pdi-3(ka1)	Gut hyp7 (Eschenlauer and Page, 2003)	Body fluorescence reduced, pharyngeal fluorescence endures.

Table 6-6: Mutant alleles, their wild type localisation and effects noticed in worms containing said allele following H_2DCHFDA treatment and subsequent visualised by UV microscopy.

6.2.3.2 Western analysis of SQT-3 in *qsox* mutants.

A number of attempts were made to determine the effect that loss of QSOX enzymes had upon *in vivo* collagen assembly. Would the collagens be fully cross-linked; was there any developmental stage specific differences in the collagens of worms containing the mutations; would there be a reduced percentage of SQT-3 in the cuticle due to its improper deposition? In order to address these issues a Western blot approach using the SQT-3 R584 serum was attempted. The samples tested were whole worm extract and purified cuticle extracts of both mixed stage and synchronous populations, representing; early, (L1s); intermediate, (L3/L4); and late, (adult) stages of development. Samples were extracted then run on reducing SDS-PAGE gels, transferred to PVDF membrane, see section 2.33, and probed with the R584 anti-SQT-3 serum. To analyse the degree of disulphide bonding exhibited within SQT-3 complexes, varying concentrations of the reducing agent β-mercaptoethanol (500 mM, for strong reducing; 250 mM, for moderate reducing; and 5 mM, for weakly reducing) were used to reduce the extracts to their component/monomeric subunits: the hypothesis being that less disulphide bonding would equate to easier dissociation. Thus, strains which have compromised abilities for disulphide bond generation should have SQT-3 collagen complexes which revert to monomeric form at lower β-mercaptoethanol concentrations in comparison to N2 extracts. Attempts were made with mixed stage and synchronised worms for whole worm and cuticle only extracts in both *qsox-1(ka2)* and *qsox-2(tm1977)* deletion containing strains. These approaches all

proved inconclusive and the R584 antiserum was found to be unsuitable for Western analysis, as was also found by Novelli, *et al* (2006).

6.2.3.3 *qsox* and *pdi* RNAi in *qsox* mutant strains

All RNAi experiments were carried out at 15 and 25ºC (data shown represents the 25ºC set unless stated otherwise) with feeding constructs derived from the Kamath, *et al* (2003) feeding library. Each experiment was performed in triplicate.

qsox intrafamily RNAi

qsox-2 RNAi in qsox-1(ka2) mutant strains

With a *qsox-2* knockdown in a *qsox-1(ka2)* background, an increase in severity of the *qsox-1(ka2)* phenotype was evident. This included the presence of characteristic fluid filled blisters, as opposed to the large Bleb like structures seen in the TP70 strain, Figure 6.14.A-D. Of note was the lack of COL-19 structure in TP73 worms; inclusion bodies of improperly processed collagen were also apparent. RNAi of *qsox-2* in N2 worms produced no body morphology defects (Bmd) and only mild seam cell disruption was noted in the TP12 strain.

qsox-3 RNAi in qsox-1(ka2) mutant strain

RNAi of *qsox-3* in TP70 and 73 resulted in worms which had weakened cuticle and which often ruptured on the RNAi plate. This was an added effect not seen in TP70, TP73 or single knockdowns of *qsox-3*. The COL-19 banding pattern was also severely disrupted, particularly in the seam cell secreted regions, the overlying lateral alae also appeared distorted. RNAi of *qsox-3* in *TP110 (qsox-1(ka2))* worms did not generate severe Bmd mutants; however, the lateral alae were disrupted, Figure 6.14.E and F.

qsox-3 RNAi in TP102 (qsox-2(tm1977)) mutant strain

The TP102 (*qsox-2(tm1977))* worms subjected to RNAi of *qsox-3* showed no severe combined phenotype. The worms were noted as having four alae, but remained largely wild type in appearance. A sluggish phenotype was noted in accordance with the RNAi of *qsox-3,* Figure 6.13.G and H

Figure 6.14: Combined knockout and knockdown of *qsox* family members by targeted RNAi in *qsox* mutant strains. (A-D) TP110 (*qsox-1(ka2))* and TP73 following *qsox-2* RNAi. (E and F) TP110 (*qsox-1(ka2))* following *qsox-3* RNAi. (G and H) TP102 (*qsox-2(tm1977))* following *qsox-3* RNAi (A) The Bli phenotype associated with *qsox-2* knockdown in a TP110 (*qsox-1(ka2))* background, arrow. (B) The COL-19 pattern of a TP73 worm following RNAi of *qsox-2*, of note is the lack of discernable annular structures. (C) TP73 showing small blister, arrow, and the corresponding COL-19 pattern of the blistered region following *qsox-2* RNAi (D). (E) A disrupted punctate alae is evident in TP70 worms subject to *qsox-3* RNAi, arrows. (F) This is mirrored in TP110 (*qsox-1(ka2))* worms following RNAi of *qsox-3* (G) Four alae are noted in TP102 (*qsox-2(tm1977*)) worms which had been subject to *qsox-3* RNAi. Apart from this the worms appeared wild type. (H) Shows a wild type looking pharynx. LA denotes the lateral alae.

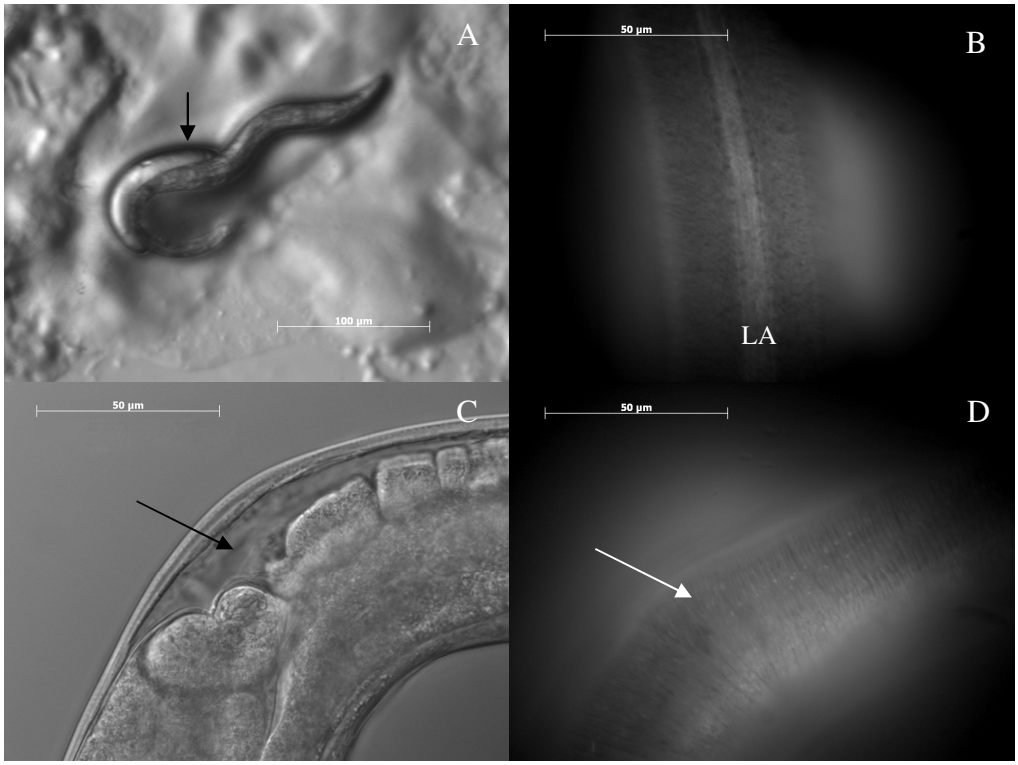
A
100 µm
B
50 µm
LA
C
50 µm
D
50 µm

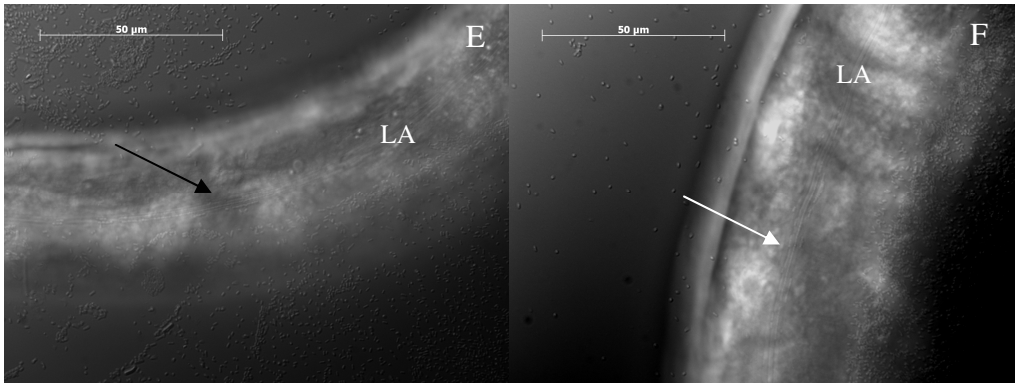
E
50 µm
LA
F
50 µm
LA

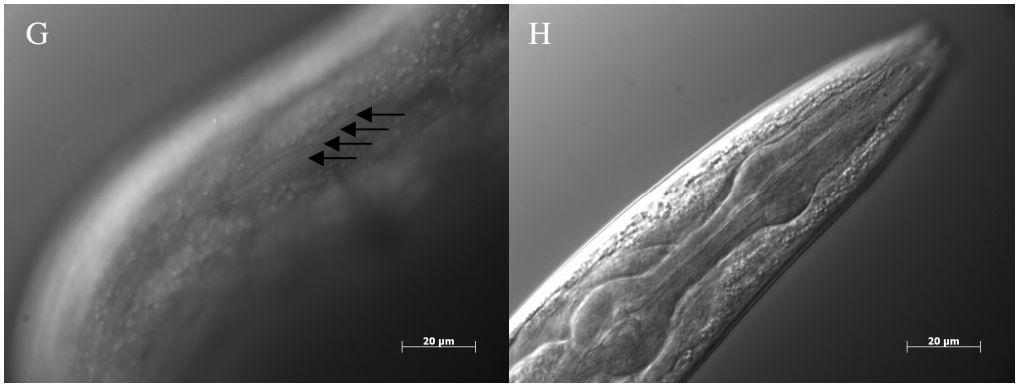
G
20 µm
H
20 µm

qsox/pdi RNAi

It was shown temporally that PDI enzymes and QSOX enzymes have overlapping spatial and temporal expression. To determine the affect loss of both *pdi* and *qsox* family members would have, RNAi of *pdi* genes in *qsox* mutant backgrounds were performed, see Table 6-7 and Table 6-8.

Strain	Gross morphological phenotype	Score (1-10)
TP70 *(ka2+ka6)*	As per Table 6-2	7
TP73 *(ka2+ka6+kaIs12)*		
TP110 *(qsox-1(ka2))*	Wild type	1
ka6	Same as TP70 and TP73	7
TP102 (qsox-2(tm1977))	Wild type	1
TP67 *(pdi-1(ka3))*	Wild type	1
TP68 *(pdi-2(tm0689))*	Severe Dpy (~200µm), Bmd, weak cuticle and lethal (Winter *et al.,* 2007).	10
TP66 *(pdi-3(ka1))*	Slightly Dpy	4
N2	Wild type	1

Table 6-7: Mutant strains, their gross morphological phenotypes and scores for the severity of the mutation.

Strain	RNAi	Phenotype	Score (1-10)
N2	*pdi-1*	Wild type	1
	pdi-2	Severe Dpy (~300µm), Bmd, do not rupture on RNAi plate	7
	pdi-3	Slight Dpy	3
TP70 and 73	*pdi-1*	Characteristic TP70/73 defects and annulae disruptions.	7
	pdi-2	Severe Dpy	10
	pdi-3	Dpy	8
TP110 (qsox-1(ka2))	*pdi-1*	Disrupted punctuate annulae and visible collagenous network underlying alae	4
	pdi-2	Severe Dpy (~220µm), more so than by RNAi of *pdi-2* alone.	9
	pdi-3	Disrupted alae and slight Dpy.	3
TP102 (qsox-2(tm1977))	*pdi-1*	Vacuolated pharynx evident.	4
	pdi-2	Severe Dpy (~300µm)	7
	pdi-3	Severely vacuolated pharynx and protruding vulva.	5
N2	*qsox-3 + pdi-1*	Long. L4s ~1000µm in length.	4
	qsox-3 + pdi-2	Weakened cuticles which can rupture on the RNAi plate.	8
	qsox-3 + pdi-3	Slight Dpy.	3

Table 6-8: The effects loss of *pdi* genes has on N2 worms, and the combined effect when members of both the *pdi* and *qsox* families are silenced. Scoring system based upon severity of gross morphological phenotype; with 1 being N2/wild type; and 10 the most severely disrupted knockout mutant, TP68 (*pdi-2(tm0689)*). Orange coloured cells illustrate a phenotype more severe than either constituent knockout alone, see table 6-7. White coloured cells denote no change in severity of the phenotype.

pdi-1, 2 and 3 RNAi in TP110 (qsox-1(ka2))

The RNAi of *pdi-1* in the *qsox-1(ka2)* mutant returned worms which had disrupted annulae. The individual annulus appeared interrupted and discontinuous around the circumference of the worm. A collagenous network of fibres was also visible above the lateral seam cells. Similar networks of fibres have been noted in other collagen processing mutants (Thein *et al.,* 2003), see Figure 6.15.B and C. The *pdi-1* loss-of-function mutant, TP67, is phenotypically wild type, see Table 6-7, thus the annular disruptions constitute an added phenotype not seen in either single knockout/down strain, see Table 6-8.

RNAi of *pdi-2* alone will produce: a strong dumpy phenotype; weakened cuticles, which burst during mounting onto microscope pads; irregular body morphology; and moult defects, Table 6-7. *pdi-2* RNAi performed in a TP110 (*qsox-1(ka2))* backgrounds resulted in worsening of these effects, Table 6-8 and Figure 6.15.D and E. The null *pdi-2(tm0689)* has a young adult length of 390µm which decreases to 200µm in mature adults (Winter *et al.,* 2007), under RNAi of *pdi-2* young adult *qsox-1(ka2)* measured approximately 220µm. By RNAi with the Kamath, *et al* (2003) feeding construct the *pdi-2* Dpy phenotype is not as severe as in the *pdi-2(tm0689)* null. Mature adult N2 worms average ~300µm following RNAi with this construct. Thus, the Dpy associated with *pdi-2* RNAi in *qsox-1(ka2*) worms can be attributed to the combined loss of both the *qsox* and *pdi* genes.

pdi-3 RNAi in a TP110 (*qsox-1(ka2))* background produced worms which were wild type, but which had weak alae disruptions and were, characteristic of the *pdi-3* RNAi, slightly Dpy , Table 6-7 and Table 6-8.

pdi-1, 2 and 3 RNAi in TP102 (qsox-2 (tm1977))

pdi-1 RNA mediated interference in TP102 (*qsox-2(tm1977))* worms produced sluggish, slow growing offspring with pharyngeal defects. The pharynx appeared abnormal, with the metacorpus and terminal bulb being distorted and vacuolated, Figure 6.15. The abnormal pharynx seen in these worms was dissimilar in appearance to the nuclei of the anterior pharynx, which are relatively easy to identify in L3 or L4 larvae by DIC microscopy (Ellis and Horvitz, 1991). Strains which contain the *pdi-1(ka3)* allele alone do not have pharyngeal defects, Table 6-7. These disruptions illustrated an added effect associated with loss of both *qsox-2* and *pdi-1* Table 6-8.

Figure 6.15: RNAi of the *pdi* family in a TP110 (*qsox-1(ka2)*) mutant background. (A-C) TP110 worms subject to *pdi-1* RNAi. (D and E) TP110 worms subject to *pdi-2* RNAi. (F and G) TP110 worms subject to *pdi-3* RNAi. (A) A wild type looking pharynx of a TP110 worm following *pdi-1* RNAi. (B) Interrupted annular rings can be seem in hyp7 secreted cuticle, insert is a zoomed picture of the same worm to more clearly demonstrate the disruption to the annular rings. (C) The white arrow points to the fibrous collagen network found underlying the lateral seam cells. (D and E) Demonstrate the Dpy animals seen following the RNAi of *pdi-2* in the TP110 mutant background. The average size of these Dpy adults is ~220µm. (F) TP110 worms which appear wild type following RNAi of *pdi-3*. (G) Higher power magnification reveals weak alae disruption.

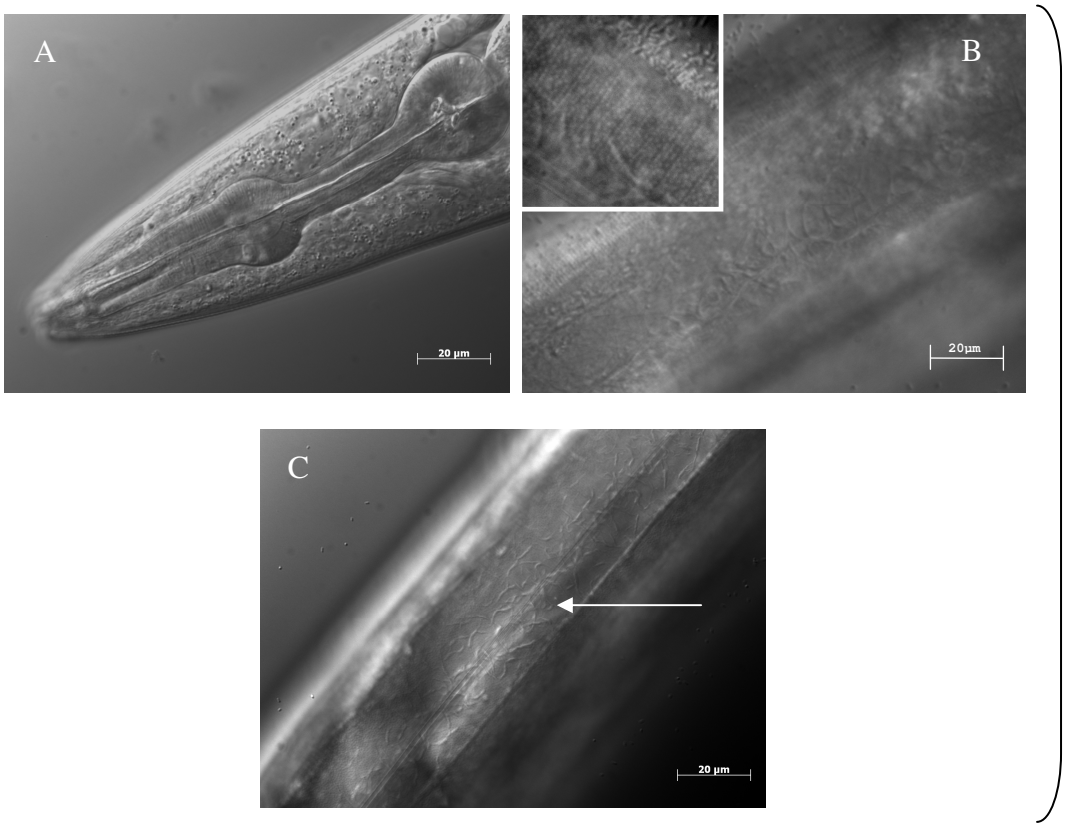

pdi-1 RNAi

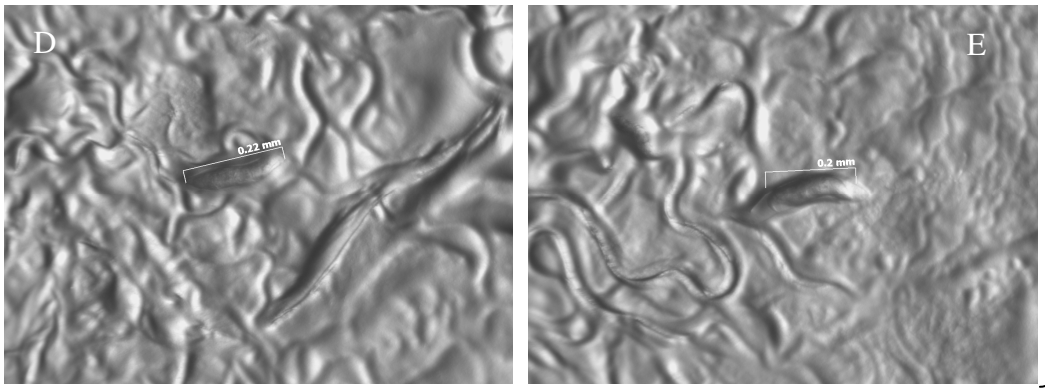

pdi-2 RNAi

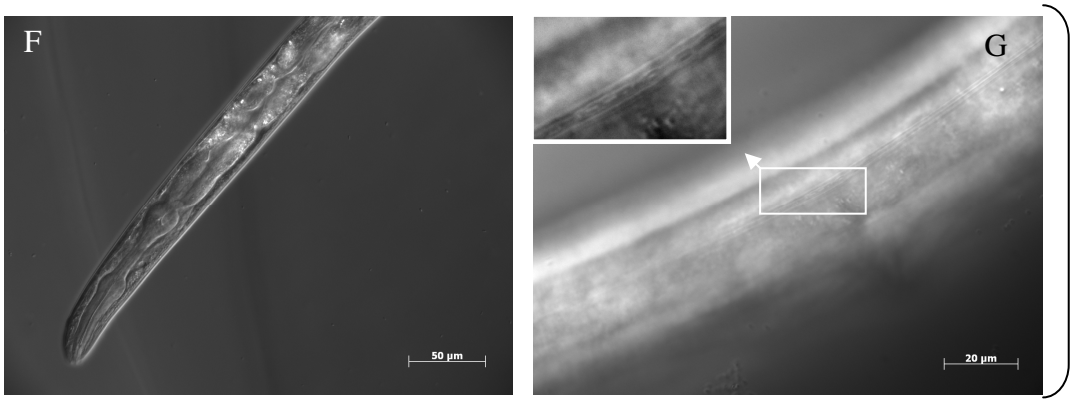

pdi-3 RNAi

Figure 6.16: RNAi of the *pdi* family in a TP102 (*qsox-2 (tm1977)*) mutant background. (A-B) TP102 worms subject to *pdi-1* RNAi (C-E) TP102 worms subject to *pdi-2* RNAi (F-G) TP102 worms subject to *pdi-3* RNAi. (A-B) Illustrate the abnormal phenotype associated with RNAi of *pdi-1* in a TP102 mutant background. Arrows point to the pharyngeal abnormalities. (C) A wild type pharynx of a *pdi-2* RNAi treated TP102 worm. (D) An overall Dpy phenotype was noted and can also be seen in (E). These worms measured ~350µm. RNAi of *pdi-3* produced worms which had pharyngeal defects similar to *pdi-1* and protruding vulvas, arrows in (F-G) respectively.

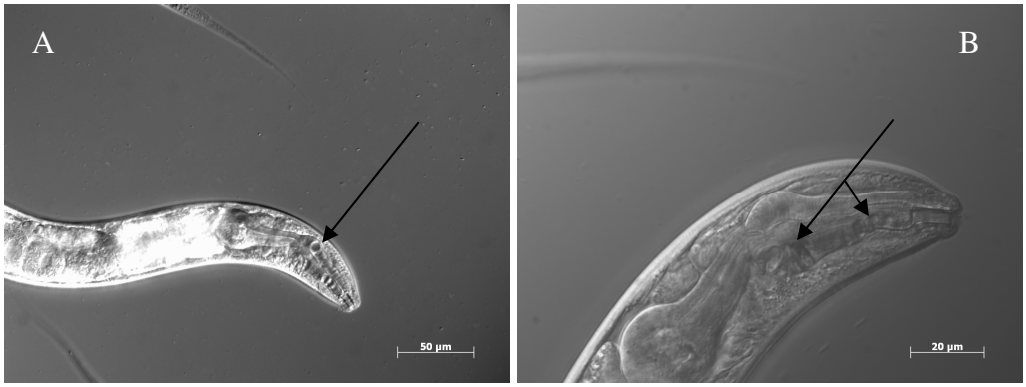

pdi-1 RNAi

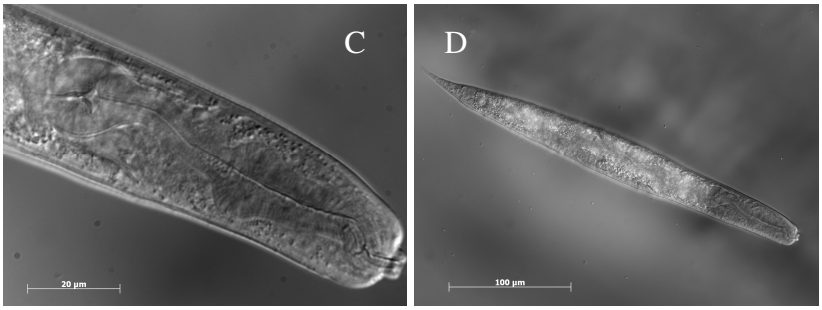

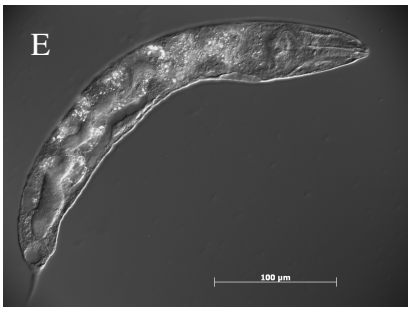

pdi-2 RNAi

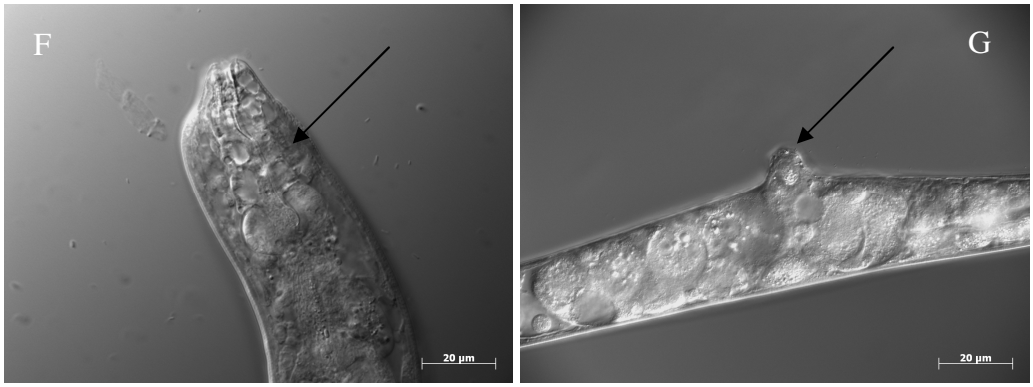

pdi-3 RNAi

pdi-2 produced the most severe phenotypes, as was expected. A Dpy phenotype was noted and attributed to the loss of *pdi-2,* as the Dpy phenotype was no more severe in the TP102 (*qsox-2(tm1977))* background than in similarly targeted N2 worms, Table 6-7 and Table 6-8.

TP66 *(pdi-3(ka1))* null mutants have a Dpy phenotype, with *pdi-3* RNAi in N2 backgrounds showing phenocopy, Table 6-7 and Table 6-8. Knockdowns in TP102 (*qsox-2(tm1977))* worms led to protruding vulvas and pharyngeal defects, Figure 6.16. As can be seen in, Table 6-8, this constitutes an added effect not attributed to the single loss of either *pdi-3* or *qsox-2.*

qsox-3 double RNAi with pdi-1, 2 or 3 in N2 worms

pdi-1 and *qsox-3* double feeding RNAi produced worms which had a Lon phenotype; characterised by the animal being longer and thinner than their wild type counter parts. The approximate length of L4 larvae is 620-650µm, *qsox-3/pdi-3* double RNAi L4 worms are approximately 1000µm in length, Figure 6.17. Such phenotypes have been attributed to; signalling defects, such as in *lon-1* mutants; collagen processing defects and in collagen mutants, such as *lon-3*. As can be seen form Table 6-7 and Table 6-8 this mutation is an added effect not associated with mutants/knockdowns of either of these genes singly. *pdi-2* and *qsox-3* double feeding RNAi lead to a weakening of the N2 cuticle, resulting in rupture of the worm on the growth plate. This was not a characteristic of the *pdi-2* RNAi alone, Table 6-7, nor was it seen with *qsox-3* RNAi in N2 worms, Table 6-8. TP68 worms do rupture on the growth plate and do have a weakened cuticle (Winter *et al.,* 2007), thus the combined loss of *qsox-3* and *pdi-2*, two hypodermally expressed genes which cycle coincidentally with the intermediate collagen group, produce phenocopy of the null TP68 strain. *pdi-3* and *qsox-3* double feeding RNAi showed no new combined phenotypes, Figure 6.17.

6.2.3.4 Protein expression attempts, proposed PDI association

Refolding assays were planned to determine the rate at which QSOX enzymes could reoxidise reduced thiols singly and in combination with PDI enzymes. Reduced avian PDI enzymes having been previously shown to be substrates for avian QSOX enzymes (Hoober *et al.,* 1999)

Figure 6.17: Double RNAi of the *pdi* and *qsox-3* family in an N2 background. (A-B) *pdi-1* and *qsox-3* double RNAi, scale bars represent 1mm (C-D) *pdi-2* and *qsox-3* double RNAi, scale bars represent 500µm (E-F) *pdi-3* and *qsox-3* double RNAi. (A-B) RNAi of *pdi-1* and *qsox-3* produce Lon (~1000µm) mutant animals, arrow highlights the characteristic L4 vulval precursor region. Wild type L4s measure approximately 650µm. (C-D) *pdi-2* and *qsox-3* RNAi produce worms which have weak cuticles and sometimes rupture on the growth plate, arrows. There was no added effect noted with *qsox-3* and *pdi-3* double RNAi, (E-F) show a wild type looking pharyngeal region and lateral alae respectively. (G) A Dpy phenotype was noted in *qsox-3/pdi-3* double RNAi adults, this adult measured ~830µm, scale bar represents 260µm. All RNAi experiments were carried out using the L4440 feeding vector derived from the Kamath, *et al* (2003) feeding library**.**

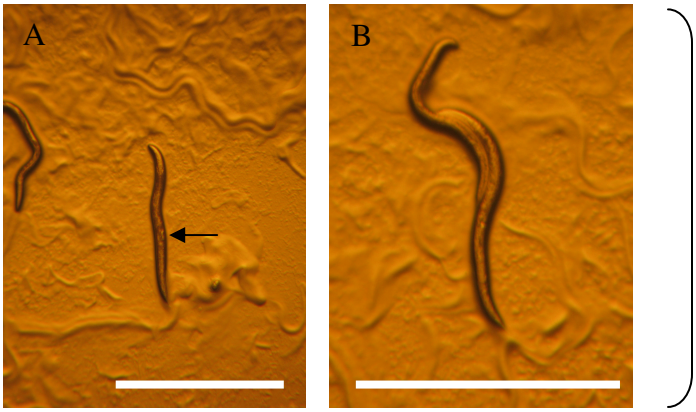

pdi-1 + qsox-3 double RNAi

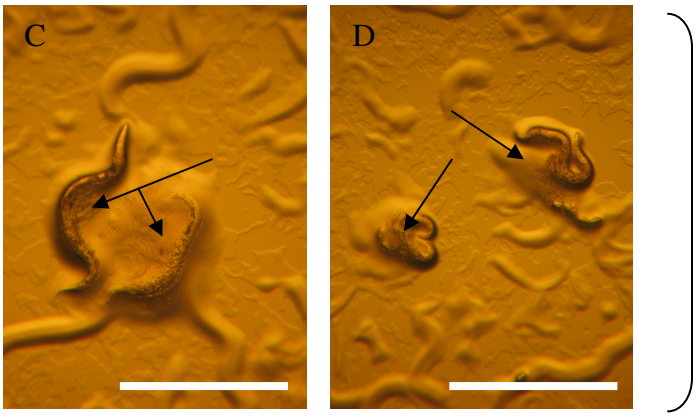

pdi-2 + qsox-3 double RNAi

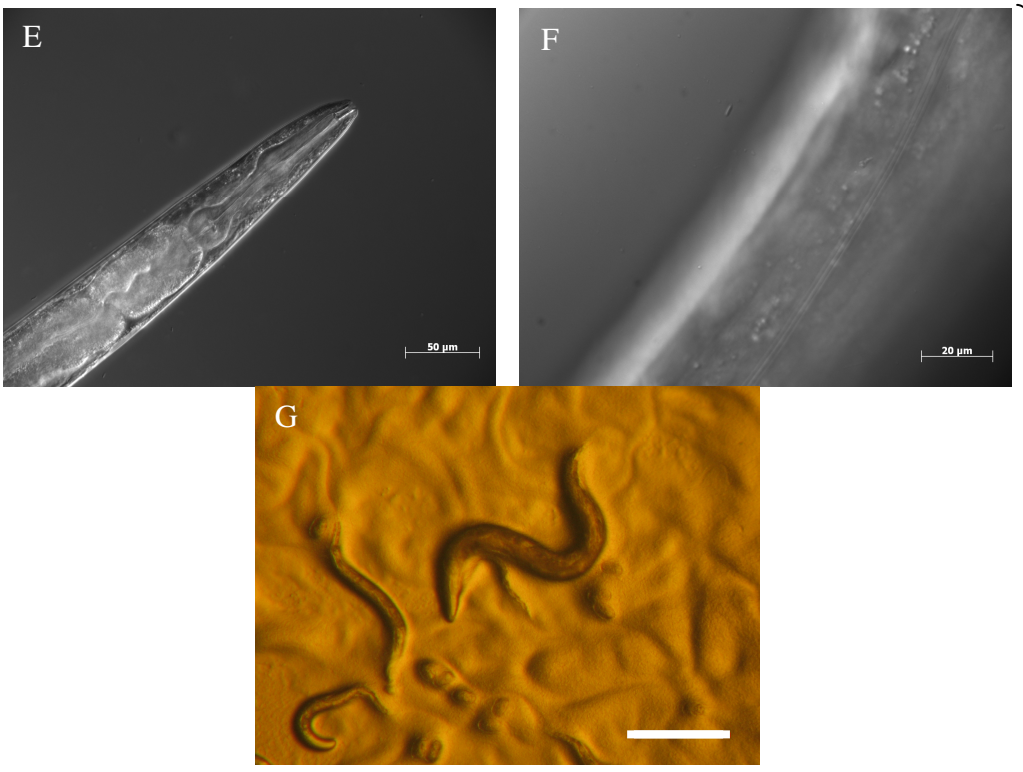

pdi-3 + qsox-3 double RNAi

The refolding assays involve the quantifiable *in vitro* refolding of a reduced substrate, RNase A, in the presence of cyclic CMP and either QSOX enzymes, PDI enzymes or combinations of both. This should determine the nascent ability of the PDI and QSOX enzymes to refold the reduced substrate and also determine whether in combination reduced PDI is a substrate for the QSOX enzymes.

As described in chapter 3, QSOX-1 and 2 have the wCghC motif that has been shown to be essential for TGase activity in PDI-3 (Blasko *et al.,* 2003). Although PDI-3 has two wCghC motifs, located within its *a* and *a'* domains, and QSOX-1 and 2 have only one each, located in their thioredoxin domain, it has been shown that one wCghC motif is sufficient for TGase activity (Blasko *et al.,* 2003). PDI-1 and PDI-2 have also been shown to have, albeit reduced by comparison to PDI-3, TGase activity (Eschenlauer and Page, 2003), both also contain two wCghC motifs. As the PDIs are the only known TGases found in the *C. elegans* genome to date, this functionality was also to be tested with the recombinant bacterially expressed QSOX enzymes.

Purified recombinant protein for PDI-1, PDI-2, PDI-3, QSOX-1, QSOX-2 and QSOX-3 were to be synthesised. The PDI enzymes had previously been cloned as a cDNA fragment into the HIS tag *E. coli* expression vector pET 15b. These clones had been expressed, purified and the protein produced and shown to be active (Eschenlauer and Page, 2003). The QSOX enzymes were cloned into pQE-30 and pQE-80L. pQE-80L, an IPTG inducible protein expression vector that incorporates an N-terminal HIS tag onto the recombinant protein, is used for highly toxic protein expression, with pQE-30 a more commonly used expression vector designed for high levels of expression. Following cloning of the *qsox* cDNA fragments and verification of their integrity within the pQE-30 vector, the constructs were transformed into BL21 (DE3) p*LYS*s cells and expression induced. No protein induction was noted with this combination of cells and expression vector at the standard expression conditions; inoculum cultures grown to OD of 0.6 at 37ºC with shaking before induction with IPTG at a final concentration of 1mM and grown for a further 4hrs. To improve the yield the standard growth conditions were altered. The expression temperature was dropped to 20ºC, booster shots of unstable antibiotics such as Ampicilin (100µg/ml) were given along with the 1mM IPTG (final), increased shaking and aeration and the induction phase lengthened to 16hrs or overnight. None of these changes affected the expression of any of the QSOX enzymes. Other cell types were used including, M15 cells, BL21 (DE3) cells and BL21 Star (DE3). No expression, at standard or altered expression conditions, was noted.

It was believed that the QSOX enzymes may have been toxic, which resulted in no detectable protein expression when visualised on SDS-PAGE coomassie stained gels with samples purified as per section 2.30.1. As such the coding fragments were sub-cloned into pQE-80L, a pQE-30 based vector which includes a *cis-lacIq* gene driving over expression of the *lac* repressor. Standard pQE-30 vectors contain a *trans-lacI* repressor gene present on a separate pREP4 plasmid. The inclusion of the *cis-lacIq* gene ensures strong suppression of the *lac* promoter pre-induction with IPTG. Suppression of protein expression prior to induction is particularly important for the stable propagation of expression constructs encoding "toxic" proteins[9]. The pQE-80L QSOX constructs were transformed into M15 cells, which also contain the pREP4 plasmid, and cultured as outlined above at both standard and altered growth conditions. No product was detectable by coomassie staining of a SDS-PAGE gel. BL21 (DE3) p*LYS*s cells were also tested, with the same result.

All cultures were purified following the methods outlined in section 2.32.1, both native and denaturing conditions were used in attempts to isolate any QSOX protein. Neither proved effectual, with no significant indication that the proteins were present. Each inoculum used to establish an expression culture was also tested by colony PCR prior to its use, thus ensuring that the coding constructs were present.

An auto-inducing technique outlined within Studier, (2005) demonstrated that the use of a non-inducing medium to establish the inoculum culture (that had been grown overnight to maximum cell density (or OD600 of approximately 10)) and subsequently used to inoculate an auto-inducing medium (which had been grown at 25ºC for 40hrs) proved efficient at amplifying difficult and insoluble proteins (Studier, 2005). The Studier method is based on amplification of BL21 (DE3) p*LYS*s cells transformed with the pQE-30 expression vector containing the protein coding sequence. This method may prove more successful for QSOX production in future studies.

6.2.3.5 TP70 *(qsox-1(ka2))* crossed with TP66 *(pdi-3(ka1))*

To further analyse the proposed association of *C. elegans* QSOX with *C. elegans* PDI, crosses between deletion mutants of both families were carried out. Stains containing the mutant alleles *qsox-1(ka2)* and *qsox-2(tm1977)* were to be crossed with the entire *pdi*

[9] http://www1.qiagen.com/Products/Protein/Expression/QIAexpressExpressionSystem/cis-repressedpQEvector.aspx?ShowInfo=1

family. However, difficulties arose following the initial cross of TP70 (*qsox-1(ka2))* with TP66 (*pdi-3(ka1)).*

TP66 *(pdi-3(ka1))* (*pdi-3* is located on autosome I) worms were crossed with N2 males and the subsequent heterozygous carrier males were then used in crosses with the backcrossed TP70 (*qsox-1(ka2))* strain (*qsox-1* is found upon the X chromosome). The resultant offspring were then cloned; genotyped, by single worm PCR using the deletion flanking backcross primers for both genes; and plates containing double heterozygous animals isolated. This plate was then sub-cloned by singly plating out approximately 50 of the double heterozygote parent's offspring. The offspring were allowed to egg lay and similarly genotyped. Resultant double homozygous offspring were then used to establish the new strain of worms, which shall be hence forth referred to as TP88.

TP88 worms were phenotypically unlike their progenitor TP70, exhibiting no visible cuticle distortions. Antibody staining with DPY-7, R584 anti-SQT-3 serum and MH27 illustrated a phenotypically wild type cuticular ECM. At this point it was proposed that the *pdi-3(ka1)* allele may have been acting as a suppressor to the *qsox-1(ka2)* allele. To determine if the suppression effect was genuine or if there was an epistatic mechanism responsible for the loss of the phenotypes, it was decided to separate the *pdi-3(ka1)* and *qsox-1(ka2)* alleles back out of TP88 into N2 backgrounds. This resulted in *pdi-3(ka1)* worms which reverted to their starting phenotypically wild type appearance and *qsox-1(ka2)* worms, which although genotypically homozygous for the deletion, were phenotypically wild type. Antibody staining performed on this revertant strain, which was termed TP110, illustrated seam cell cuticle disruption, at a much less severe level than had been noted previously in TP70 and wild type SQT-3 localisation which was paralleled by wild type MH27 staining, see Figure 6.18.

At this point there were two distinct populations of worms carrying the *qsox-1(ka2)* deletion mutant allele. One possessing the homozygous null genotype and the associated phenotypes that had been attributed to the loss of *qsox-1;* and another, which had the same *qsox-1* genotype but no phenotypes associated with loss of this gene. It was decided to further backcross the original TP70 strain of worms that possessed both the phenotypes and genotype with N2 worms to see if these properties separated or continued to be linked.

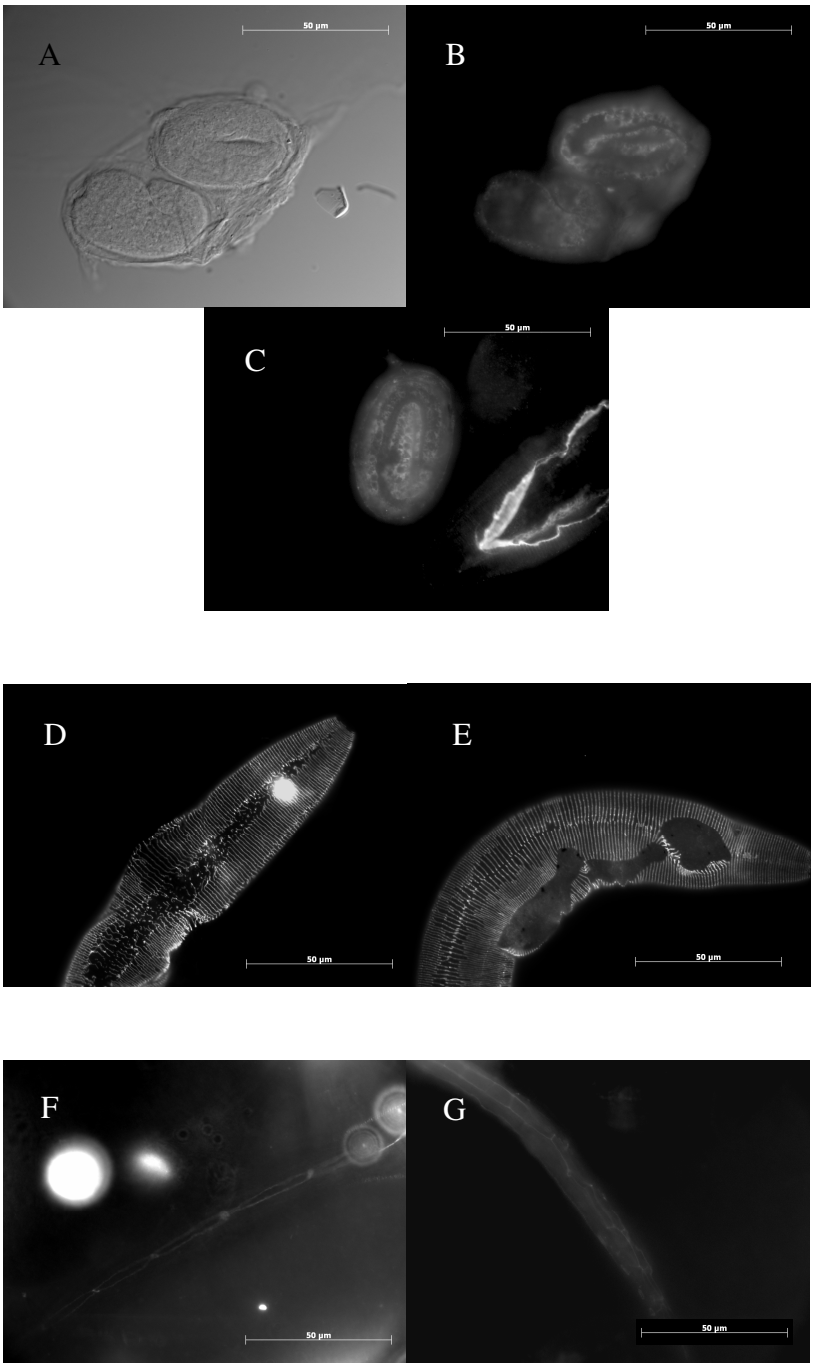

Figure 6.18: SQT-3, DPY-7 and MH27 antibody staining of segregated TP110. (A-C) SQT-3 antibody staining with the R584 serum, (D-E) DPY-7 staining and (F-G) MH27 seam cell staining. (A and B) 2-fold and 3-fold embryos illustrating a wild type expression profile for SQT-3. (C) An elongated worm which has begun to secrete SQT-3 into its ECM. (D and E) Mild seam cell DPY-7 disruption is still evident in the segregated TP110 (*qsox-1(ka2))* strain. (F and G) The seam cell disruption is not as severe as that which was originally attributed to *qsox-1(ka2)* see Figure 6.5.

A further four backcrosses, eight backcrosses in total, were performed and the phenotype and genotype did not separate. Each backcross was performed in a non-biased random selection manner, with no worms being chosen based upon their phenotype. Further scrutiny of these *qsox-1(ka2)* containing strains revealed that its genetic lesion was not the cause of the phenotypes, which had until this point, been attributed to the *qsox-1* null. This was concluded following segregation of the phenotype from the *qsox-1* locus, and resulted in a new strain of worms being produced which had all the phenotypes outlined in Table 6-2, and was genotypically wild type at the *qsox-1* locus. These worms were in effect another backcrossed cuticular mutant strain generated by the deletion screen, see chapter 4, in which to date the causative gene has yet to be determined and has been putatively given the strain name and allele designation TP111(*ka6)*. Further, there appeared to be no link between the genotype at the *qsox-1* locus and the severity of the mutation, as the phenotypes were consistent regardless of the genotype at the *qsox-1* locus. To fully confirm that *qsox-1* was not responsible for these mutations, rescue experiments were performed.

6.2.3.6 Rescues of *qsox-1(ka2)* with cosmid DNA and a genomic construct, and *qsox-2(tm1977)* with cosmid DNA

TP70 worms, which still associated the phenotype with the homozygous *qsox-1(ka2)* genotype, were subjected to rescue experiments by means of injection with two different rescue constructs. A genomic *qsox-1* clone driven by its own promoter (2007 bps upstream of the ATG start) which had been ligated into pPD95.81, a promoterless multi-synthetic intron GFP containing vector injected at concentrations of 20 µg/ml along with 10 µg/ml of the *dpy-7* marker and 180 µg/ml of pbluescript. The second rescue construct used the T10H10 cosmid. This was injected at concentrations of 1 µg/ml and 5 µg/ml with 10 µg/ml of the *dpy-7* marker and 150 µg/ml of pTAG vector into TP70 worms.

Neither of these constructs rescued the phenotypes associated with TP70. The constructs were shown to have been present by SWPCR, see Figure 6.19, using the backcross primers for *qsox-1*. This proved that it was not the loss of *qsox-1* which had led to the cuticle defects previously associated with the *qsox-1(ka2)* allele, but another linked gene. However, TP102 (*qsox-2(tm1977))* worms injected with F35G2 cosmid DNA, in the same manner described above, did rescue the associated *qsox-2* low brood size phenotype, with two rescue lines being generated.

6.2.3.7 *qsox-1* and *qsox-2* double knockout

TP110 worms in which *qsox-1(ka2)* had been segregated from the linked phenotype causing allele *ka6,* were crossed with TP102 (*qsox-2(tm1977))* to determine if combined knockout of these two wild type looking strains would produce any noticeable phenotype. The resulting strain, TP101, proved to be a lethal strain.

Individually plated out TP101 worms which were homozygous for the *qsox-1(ka2)* allele and heterozygous for *qsox-2(tm1977)*, failed to produce homozygotes at the *qsox-2* locus (n=288) when grown at 25ºC. When the temperature was moved to 15ºC, both alleles could become homozygous. The double homozygous progeny of parents which were homozygous for *qsox-1(ka2)*, heterozygous for *qsox-2(tm1977)* and which were grown at 15ºC, died as L1s, see Figure 6.20. The double homozygotes were left for prolonged periods, >48hrs at 15ºC, no further development past L1 was noted. Dead eggs were also observed. Animals which were *qsox-2(tm1977)* heterozygous and *qsox-1(ka2)* homozygous developed normally.

6.2.4 The segregated mutant allele ka6

Following the cross with TP66 (*pdi-3(ka1))* which lead to the segregation of the phenotype causing gene from the *qsox-1(ka2)* allele, the region around *qsox-1* was examined for candidate genes in which a mutation would lead to phenotypes such as those scored in the *ka6* strain.

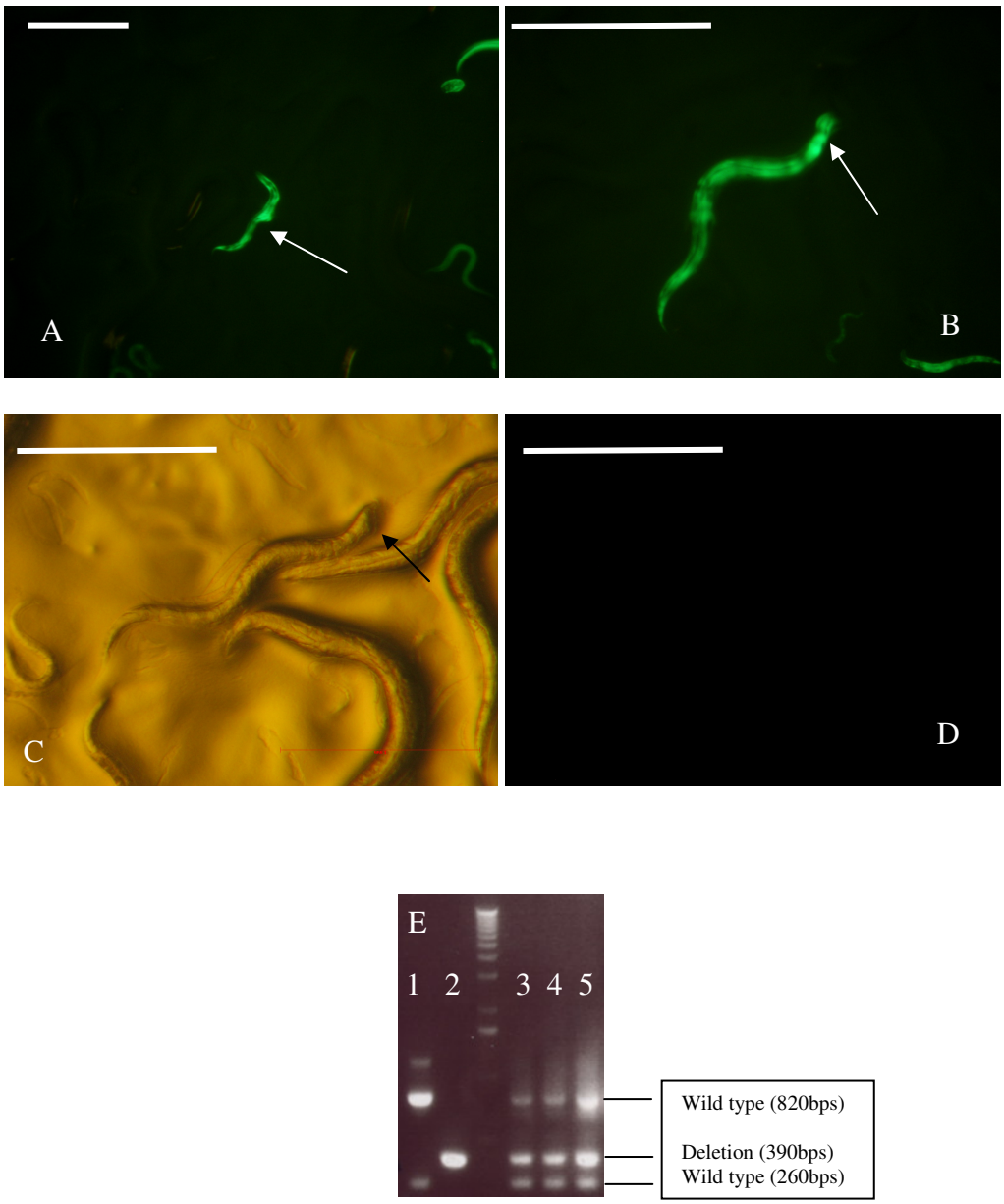

Figure 6.19: TP70 worms injected with T10H10 cosmid rescue construct along with the *dpy-7* GFP marker and SWPCR showing presence of the T10H10 cosmid in non-rescued worms. (A) L1 transgenic worm which is expressing the GFP marker, and shows no rescue of the phenotypes associated with the TP70 strain. Arrow highlights region of cuticular distortion. (B) L3 expressing the GFP marker but still displaying the distorted head phenotype, arrow. (C) Non rescued worm showing similar phenotype as (B) and no GFP signal (D). (E) (Lane 1) N2 control. (Lane 2) TP110 (*qsox-1(ka2)*) +ve control. (Lane 3-5) GFP +ve worms in which the phenotypes associated with TP70 were evident. All show presence of the transgenic cosmid T10H10 and no rescue of the TP70 phenotypes. DNA ladder is Invitrogens 1kb marker. Scale bar in (A) is 250µm. Scale bars in (B-D) are 300µm.

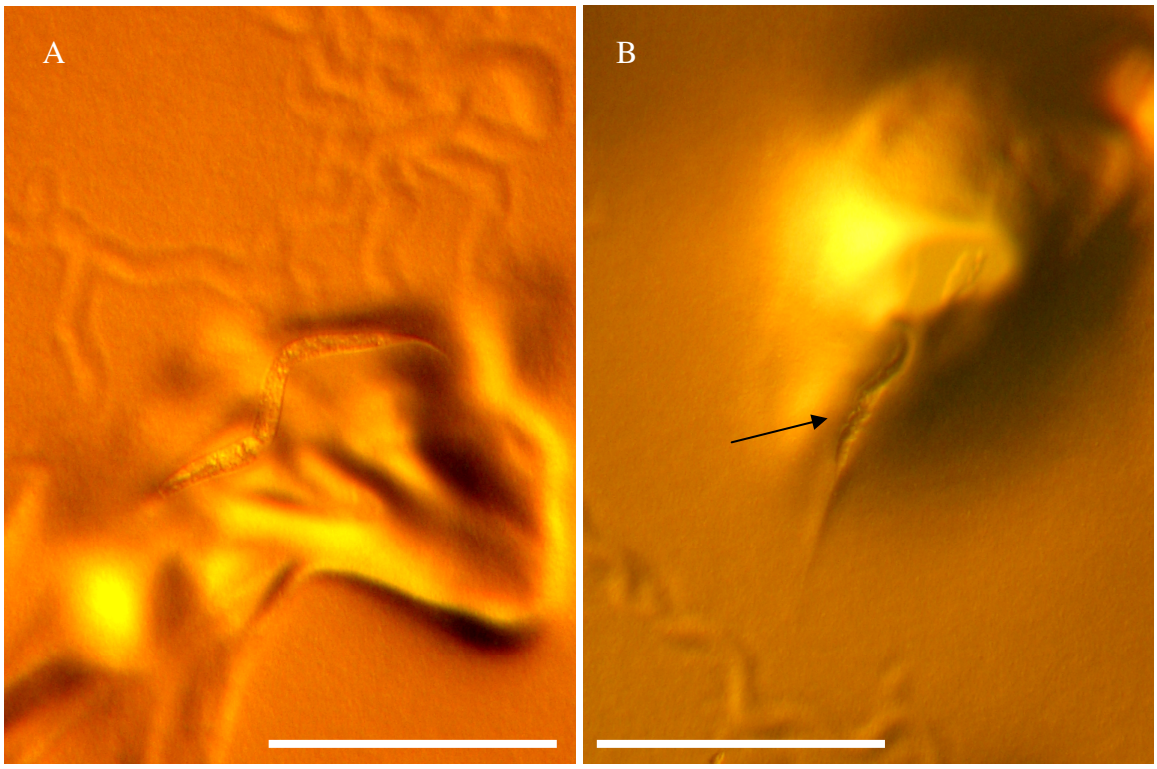

The *qsox-1* backcross primers used in these SWPCRs produce:

- 820bp wild type band.
- 390bp deletion band.
- 260bps wild type band.

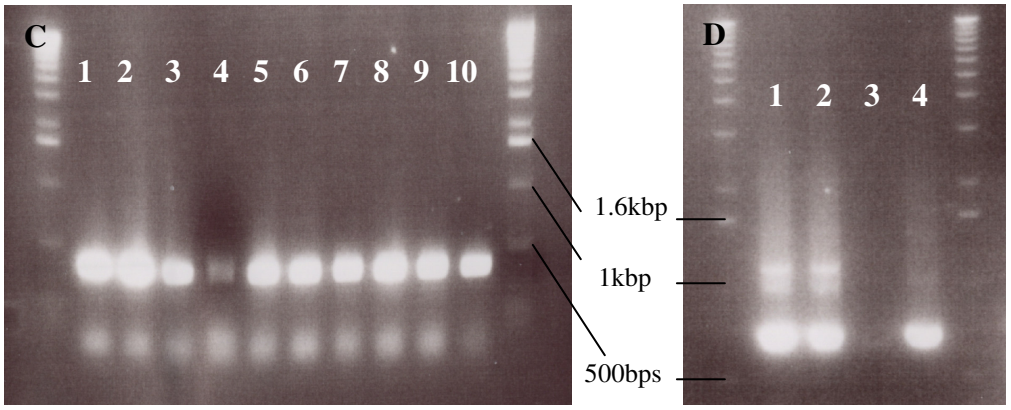

The *qsox-2* backcross primers used in these SWPCRs produce:

- 1.2kbp wild type band.
- 700bps deletion band.

Figure 6.20: TP101 larvae images and corresponding genotype. (A-B) Arrested TP101 larvae cloned out from a *qsox-1(ka2)* homozygous; *qsox-2(tm1977)* heterozygous parent which was grown at 15ºC. Morphological defects can be seen in (B) arrow. (C) Gel picture of SWPCR performed on the worms that produced the double homozygous strain using *qsox-1* backcross primers. All are homozygous at the *qsox-1* locus. (D) Gel picture of SWPCRs performed upon the progeny of a *qsox-1(ka2)* homozygous; *qsox-2(tm1977)* heterozygous parent using *qsox-2* backcross primers. (Lane 1 and Lane 2) *qsox-2(tm1977)* heterozygous animals which appeared phenotypically wild type and developed to adulthood. (Lane 3) SWPCR of the worm in image (A) PCR has failed. (Lane 4) SWPCR of the worm in image (B). This worm is genotypically double homozygous for *qsox-1(ka2)* and *qsox-2(tm1977).* Scale bar represents 300µm.

Based upon the backcrossing strategy used which passed the mutant alleles through N2 males back into N2 hermaphrodites, and the number of possible recombination events that could have taken place during these five rounds of backcrossing, it was concluded that the gene responsible for the scored phenotypes was linked to the *qsox-1* locus and was genetically nearby. As such, 500kbps of the upstream and 500kbps of the downstream genome were searched for possible candidate genes in which mutations could cause the phenotypes seen in *ka6*. This area covered a range of 4cM, approximately equating to 25 to 30 cosmids. Within this range possible candidate genes *rpl-11.2, gei-12* and *nhr-40* were uncovered; see Appendix C for specific details on each of these genes. Candidates were selected based upon phenocopy of the *ka6* strain and proximity to the *qsox-1* locus. Other genes not found upon the X-chromosome display similar phenotypes to the *ka6* strain, in particular 3′-Phosphoadenosine 5′-Phosphosulfate Synthase (*pps-1*). Mutant alleles of which closely mimicked the phenotypes seen within *ka6*; including the uncommon missing sections phenotype (Dejima *et al.,* 2006). *egl-19* mutants also exhibit similar morphological disruptions to those seen in the *ka6* strain (Lee *et al.,* 1997), see Appendix C.

To isolate the gene responsible for the phenotypes seen in the segregated strain a forward genetics approach of 2-point, followed by 3-point mapping would need to be employed.

6.3 Discussion

The aim of this chapter was to further characterise the members of the QSOX family and was reliant upon having deletion mutants in *qsox-1* and *qsox-2,* two of the three *C. elegans qsox* family members. From initial observations it appeared that the *qsox-1(ka2)* deletion caused pleiotropic mutations of the cuticular ECM, which was further supported by immunofluorescence and visualisation of the cuticle by SEM and TEM. These mutations of the ECM were later shown not to have been caused by a mutated *qsox-1* but were being caused by a linked, as yet unidentified, gene. The *qsox-1(ka2)* containing strain, TP110, did however show a reduced potential for oxidation and cuticle defects when combined with RNAi of the protein disulphide isomerases. Significant lethality was also evident in double knockouts of the pure *qsox-1(ka2)* allele with the *qsox-2(tm1977)* allele.

6.3.1 qsox-1(ka2) and ka6

As shown in chapter 5, the spatial and temporal expression profiles of *qsox-1* implied functionality associated with the synthesis of the cuticular ECM. This was borne out when the *qsox-1(ka2)* deletion mutant was isolated form a psoralen/UV mutagenised deletion library, chapter 4, in which pleiotropic cuticular mutations were evident. The genetic background was cleaned up by backcrossing homozygous deletion mutants through N2 males (*qsox-1* is located on the X-chromosome) back to N2 hermaphrodites four times, and the resulting strain was denoted TP70. Characterisation of TP70 revealed numerous cuticle defects; see Table 6-2, which were more penetrant in larval stages with 80% of larvae scoring positive for the associated mutants compared with 45% of adults at 15ºC. Embryonic lethality was also noted in the TP70 strain. Immunoflourescence of the TP70 strain with antibodies specific for cuticle collagens; DPY-7 and SQT-3, as well as the seam cell adherens junction specific antibody MH27, revealed that the TP70 strain was failing to secrete the essential cuticle collagen SQT-3 into the annulae of the cuticle and that the lateral hypodermal seam cells were misshapen, irregular and often missing in regions of severe cuticle disruption. The failure to secrete the essential SQT-3 collagen was of interest as *qsox-1* had previously been shown to coincide tightly with the temporal expression profile of *sqt-3,* see Figure 5.4*,* and was proposed as a possible substrate for QSOX-1, which this data was supporting. Western analysis of mutants containing the *qsox-1(ka2)* allele was attempted as a means of resolving aspects of the possible association using the same R584 anti-SQT-3 serum used for immunolocalisation. This serum however was not suitable for Western analysis, as was also reported by Novelli, *et al* (2006).

At this stage it appeared as though *qsox-1* was playing an essential role in the generation of a wild type cuticular ECM. This however turned out not to be the case.

Segregation of qsox-1(ka2) from ka6

Segregation of the *qsox-1(ka2)* allele from the as yet unknown mutant *ka6* occurred when TP70 was being crossed with TP66 (*pdi-3(ka1)).* This resulted in lines which had the phenotypes previously associated with the TP70 strain and which were wild type at the *qsox-1* locus. Similarly lines were produced, by crossing out the *qsox-1(ka2)* allele from the TP88 strain, which were genotypically homozygous for the *qsox-1(ka2)* mutation and did not have any evident phenotype. This wild type looking strain was denoted TP110.

The *ka6* allele is presumed to be located upon the X-chromosome and genetically near the *qsox-1* locus. Had the mutation been found upon one of *C. elegans* five autosomes the backcrossing strategy employed would have lead to segregation of the *ka6* and *qsox-1(ka2)* alleles during the initial rounds of backcrossing. It is impossible to work out the linkage distance between the *qsox-1* locus and the *ka6* allele with any certainty using the crossing data available. It can be concluded however that the mutant allele *ka6* was generated by the deletion screen mutagenesis procedure, and the region affected at the *ka6* locus is essential for wild type cuticular ECM synthesis. *ka6* mutants showed cellular level rearrangement of the cuticle secreting lateral seam cells which resulted in distorted lateral alae formation, see Figure 6.5 and Figure 6.10. The mechanism of lateral alae formation is not fully understood. Formation is reliant upon stage specific Zona Pellucida domain (ZP) cuticlin proteins; L1 alae formation requires, CUT-3 and CUT-5; and the dauer requires, CUT-1 and CUT-5 (Sapio *et al.,* 2005). Larvae which lack or have reduced *cut-1, cut-3* or *cut-5* function do not form a wild type alae and have an increased diameter. It was proposed that the alae formation is a result of a dorso-ventral shrinking of the internal layer of the lateral cuticle and the alae adopts its structure from the contracted internal layer (Sapio *et al.,* 2005). Following TEM of TP70 worms it was clear that the cuticle of the L1 animals was not of a wild type conformation, as the striated layer of these worms was dissociated from the underlying tissues. The striated layer may be acting as an anchorage of the cuticle to the underlying components, therefore, failure in this anchorage would result in a failure to transmit the contractile force associated with the formation of the stage specific lateral alae and may account for the defects seen in the *ka6* cuticle in these regions. Similarly it has been shown that in *sqt-3(e2117)* mutants, which are temperature sensitive lethal mutants and which fail to elongate during embryogenisis, also have striated layer defects. At 15ºC *sqt-3(e2117)* worms develop and elongate similarly to wild type worms. At 25ºC the worms elongate and then collapse to approximately their pre-elongated length (Priess and Hirsh, 1986). This effect has been attributed to the lack of a striated layer in the animals grown at 25ºC (Priess and Hirsh, 1986).

The contractual force which draws the lateral surfaces together above the seam cells is proposed as being driven by biochemical modifications such as cross-linking reactions with CUT-1, 3 and 5 being the potential substrates (Sapio *et al.,* 2005). The alae formed in L1 *ka6* worms does not conform to the wild type tri-foil mushroom shape, Figure 6.9 and Figure 6.10, a disruption which is reflected in the lateral hypodermal cells beneath. MH27 immunoflourescence showed that the seam cells were irregular and scattered across the lateral surface of the worm. In cases where the missing sections phenotype was evident, the

seam cells were not present at the corresponding missing portion of the nematode, Figure 6.5. The most extreme cases of cuticle disruption noted with the *ka6* allele did show an increased sensitivity to H_2O_2 with an $LD_{50,}$ decreased from 5 mM in N2 worms to 2 mM in the mutant strain. There was no difference noted in the response exhibited between *ka6* and N2s with regard to DTT treatment, as both had LD_{50s} of 7 mM. *C. elegans* are naturally susceptible to reactive oxygen species such as H_2O_2, a fact exploited in the killing of *C. elegans* by microbial pathogens (Chávez, 2007). The increased sensitivity seen in the *ka6* strain may have been due to the cuticle providing less of a barrier to the environment, as less severely distorted *ka6* animals showed a more wild type response.

The region responsible for the phenotypes noted in the *ka6* strain remains to be determined. Inferred from the phenotypes seen in the *ka6* strain, this unknown gene is likely to be one which is involved with cuticular synthesis or be a gene associated with the body musculature, see Appendix C.

TP110 (qsox-1(ka2))

When the *qsox-1(ka2)* allele was segregated from the *ka6* allele a phenotypically wild type strain remained. Immunofluorescence experiments revealed that the seam cell derived cuticle was, to a lesser extent than *ka6*, distorted, see Figure 6.18. The underlying seam cells which produced this cuticle however remained wild type with regard to presence and arrangement, as noted by the wild type staining with the MH27 seam cell specific antibody.

TP110 *(qsox-1(ka2))* worms in which *pdi* and other *qsox* family members were disrupted did exhibit phenotypic defects. TP110 (*qsox-1(ka2))* with *qsox-2* RNAi proved to be the most interesting of these associations, leading to the formation of adult specific blisters, see Figure 6.15. These were genuine fluid filled blisters, not the large Bleb structures seen in the *ka6* strain. A double knockout strain was made containing both the *qsox-1(ka2)* and *qsox-2(tm1977)* alleles. This strain proved to be L1 larval lethal, with double homozygotes only being produced at 15°C. It was noted that the double homozygous larvae exhibited some body morphology defects. This was an interesting development because it reaffirmed a dependence upon the QSOX family members for the production of viable larvae and cuticles. The Bli phenotype, in the knockdown worms, may have been an intermediary step towards lethality caused by reduced disulphide bonding within the cuticle, or by the lack of H_2O_2 production. Removing two highly expressed, hypodermal H_2O_2 producing enzymes would deplete the cellular concentrations of this ROS which may lead to a reduction in

tyrosine cross-linking of cuticular components by enzymes such as BLI-3 or HPX-1, an animal heam peroxidase of *C. elegans*. BLI-3 has been proposed as the main source of the H_2O_2 required for tysosyl cross-linking (Melanie Thein, personal communication). Knockdown of BLI-3 by RNAi causes blistering of the cuticle (Edens *et al.,* 2001) and some larval lethality, as only 76% of F1 embryos develop into larvae following *bli-3* RNAi (Melanie Thein, personal communication). Knockdown of *hpx-1* by RNAi in the mutant background *bli-3(n529)* causes 100% lethality; which is proposed to be due to the loss of peroxidases activity (Melanie Thein, personal communication). The H_2DCHFDA assay illustrated that both *qsox-1(ka2)* (all strains containing this allele including, TP70, 73 and 110) and *qsox-2(tm1977)* mutant strains had an apparent reduction in H_2O_2 production. This apparent reduction in H_2O_2 production of the double *qsox* mutant would appear to equate to loss of BLI-3 and HPX-1, with the knockdown of *qsox-2* in TP110 (*qsox-1(ka2)*), thereby producing a similar blistered cuticle as that found in N2s targeted by RNAi for *bli-3.* It is interesting to note that *bli-3* RNAi does not result in 100% lethality since the resulting combination would be the ablation of BLI-3 and any peroxidase activity dependent on its H_2O_2 donation. As has been proven to be lethal when *bli-3(n529)* animals are treated with *hpx-1* RNA. There are a few suggestions to explain the reduced level of lethality associated with *bli-3* knockout and knockdowns. These include that disruption may not be 100% effective, that some peroxidase function can occur in the absence of H_2O_2, or that there is an alternative source of H_2O_2. This latter suggestion is of interest as it has been shown that loss of QSOX enzymes depletes the ROS production, this goes someway to proposing the QSOX enzymes as a possible source of H_2O_2 which may be being utilised for tyrosyl cross-linking. However these results are preliminary and are in no way conclusive, further investigation into this matter is required.

Attempts were made to resolve whether *C. elegans* PDI was a substrate for *C. elegans* QSOX, as had previously been shown with avian PDI and QSOX enzymes. RNAi of the PDI family members in TP110 (*qsox-1(ka2))* mutants demonstrated additional phenotypes or more severe phenotypes than when N2 worms were similarly treated with the Kamath, *et al* (2003) *pdi* feeding library constructs. These include a punctate appearance of the annular ring in *pdi-1* targeted worms. Increased dumpiness of the *pdi-2* fed worms, to a level comparable with the most severe genetic knockouts (characteristically the *pdi-2* feeding RNAi worms did not give 100% phenocopy to the mutant strain with regard to the Dpy phenotype). *pdi-3* appeared to be the least involved with *qsox-1,* with weak disruption of the lateral alae the only noted new phenotype. The characteristic *pdi-3* weak Dpy phenotype was noted (Eschenlauer and Page, 2003) in worms targeted for *pdi-3* RNAi.

This data suggests that *qsox-1* was involved with PDI -1 and 2, facilitating the formation of the wild type cuticular ECM.

6.3.2 TP102 (qsox-2(tm1977))

qsox-2, in which expression had previously been shown to localise to the pharynx, hypodermis and male tail syncytium, see chapter 5, exhibited no cuticular ECM defects when mutated and its expression was constitutive throughout the life cycle of the worm. Viewed by DIC and following immunofluorescence with the DPY-7, SQT-3 and seam cell specific MH27 antibodies, the TP102 (*qsox-2(tm1977))* cuticles were wild type in apperance. An effect on fecundity was noted in the TP102 (*qsox-2(tm1977))* mutant strain. These worms showed little or no production of embryos at 25ºC and a significantly reduced production of embryos at 15ºC when compared with N2 worms. Effects which were rescued by injection of F35G2 cosmid DNA.

Interestingly, sulfhydryl oxidase expression has been found to be highly expressed in the male rat epididymis and seminal vesicles, where proposed functions include protecting spermatozoa from microbial or sulfhydryl degradation (Benayoun *et al.,* 2001; Tury *et al.,* 2006). Similarly *Drosophila melanogaster* CG17843, or dmQSOX2, has also been shown, by *in situ* hybridisation, to localise to the accessory glands of the male reproductive tract (Arbeitman *et al.,* 2004). The accessory gland consists of a lumen bordered by a single layer of secretory cells which produce the major components of the seminal fluid.

Targeting of the *pdi* family members in the TP102 (*qsox-2(tm1977))* mutant strain resulted in phenotypes not previously reported with loss of the respective genes singly. These included pharyngeal defects when *pdi-1* and *3* were silenced and vulval defects with *pdi-3*. Neither the mutant strains TP67 (*pdi-1(ka3))* or TP66 (*pdi-3(ka1))* exhibited such defects, nor have they been seen in N2 worms which had these genes silenced by RNAi. *pdi-2* RNAi in the TP102 (*qsox-2(tm1977))* strain had no added effects other than those attributable to the silenced genes singly. The vacuolated pharynx noted with the RNAi of *pdi-1* in TP102 (*qsox-2(tm1977))* worms could be attributed to the loss of two pharyngeal disulphide bond generating enzymes, both having been shown to localise to these regions (Page, 1997), see chapter 5, and both exhibiting an apparent reduction in ROS production in the pharynx when tested with H_2DCHFDA. Association has previously been shown between PDI and ERV/ALR homologues in the yeast *S. cerevisiae,* this association leads to the oxidation of reduced substrate thiols resulting in disulphide bond formation (Gross *et al.,* 2002; Thorpe *et al.,* 2002; Coppock and Thorpe, 2006; Gross *et al.,* 2006). Any such

association between *C. elegans* PDI and the ERV/ALR containing QSOX enzymes would have been highlighted by the RNase refolding assays.

A second deletion mutant allele for *qsox-2* became available toward the end of the project. This allele *ok1669* was obtained and noted to have a similar wild type gross morphological phenotype and fecundity as TP102 (*qsox-2(tm1977))*. The *ok1669* deletion was generated by treatment of N2s with EMS, and resulted in a 1711bp fragment being removed from the coding sequence. The deletion was generated by the Knockout consortium[10]. The effects noted by RNAi of *pdi* family members using TP102 (*qsox-2(tm1977))* were mirrored with the *qsox-2(ok1669)* containing strain. This strain had only been backcrossed once, and was therefore not included in the results section of this chapter.

qsox-3

RNAi of *qsox-3* in N2 worms exhibited a slow growth phenotype and disruption of the cuticle secreted by the seam cells. When *qsox-3* was silenced in TP110 (*qsox-1(ka2))* and TP102 (*qsox-2(tm1977))* backgrounds, seam cell derived cuticular defects were evident. The COL-19 patterning in these seam cell regions was amorphous and the alae punctate in nature. Double RNAi of *qsox-3* with the *pdi* family of enzymes illustrated weakened cuticles and a long (Lon) mutant phenotype. *pdi-1* and *qsox-3* RNAi resulted in Lon worms which at L4 were ~1000µm in length. Wild type L4 worms being ~650µm in length. Various classes of gene produce Lon animals when mutated/silenced which can encode structural (Suzuki *et al.,* 2002; Kamath *et al.,* 2003), proteolytic (Davis *et al.,* 2004) and signalling (Soete *et al.,* 2007) proteins. It is as yet unclear what was causing the Lon phenotype in these worms, however based upon the spatial and temporal expression profiles of these genes the affect is likely due to hypodermal cuticular protein missfolding or the aberrant incorporation of such structural proteins into the cuticular ECM.

pdi-2 and *qsox-3* double RNAi resulted in weakened cuticles. TP68 (*pdi-2(tm0689))* mutants alone show weakened cuticles which rupture during mounting onto standard 0.065% sodium azide agarose microscope pads. The knockdown of *pdi-2* by RNAi in N2 worms will produce less severe mutations than those seen in the knockout strain, and such RNAi worms do not rupture. In double knockdowns of *pdi-2* and *qsox-3* at 25ºC, adult worms were seen to rupture on the RNAi plate. This is proposed as a result of reduced

[10] www.celeganskoconsortium.omrf.org

cuticular strength and is attributable to the loss of both gene products in concert, as the combined effect is more severe than either singly.

pdi-3 and *qsox-3* double RNAi in N2s did not produce any significant deviations from singly targeted N2 worms. Perhaps these two proteins are functionally detached.

From the results noted with the combined knockouts of the *qsox* and *pdi* family it was interesting to propose that there was some interplay between the two families. These interactions could be determined by performing the RNase A refolding assays outlined in this chapter. Before these assays could be performed however a reliable expression method for the QSOX enzymes would need to be determined. The hypothesis is that the QSOX, enzymes, similar to Ero-1, are re-oxidising the reduced PDIs following their reduction in the process of disulphide bond generation, see Figure 6.21 which was adapted from (Chakravarthi *et al.,* 2006).

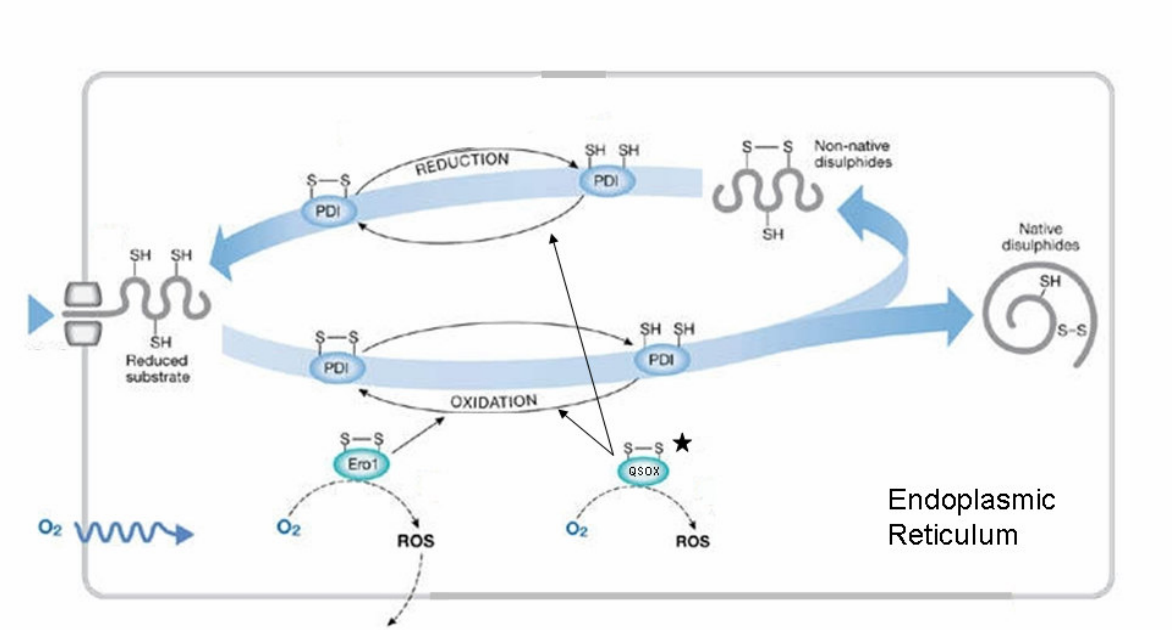

Figure 6.21: Disulphide bond generation by PDI and the proposed function of QSOX in re-oxidation of the reduced PDI. Star highlights QSOX. The ROS produced at this stage may then be utilised by the DUOX enzymes, BLI-3 or HPX-1, in tyrosyl cross-linking. Free accumulation of such ROS would prove damaging to the cell.

Chapter 7: *nas-36* and *37*, their functions in *C. elegans* and selected trichostrongylid parasites.

7.1 Introduction

In this chapter discussion will focus upon the *C. elegans* astacin metalloprotease family of enzymes, in particular those involved in the process of moulting. It was previously shown in chapter 3 that certain *nas* genes play important roles in all stages of *C. elegans* development; from the formation of a cuticular ECM, hatching from the eggshell and in the shedding of the cuticle. All of these stages having a corresponding *nas* gene in which a mutant causes failure to perform these tasks in a wild type manner.

This chapter will focus mainly upon the action of the group V (Mohrlen *et al.,* 2003) enzymes NAS-36 and 37 and their roles in moulting and exsheathment in *C. elegans* and the trichostrongylid parasites; *Teladorsagia circumcincta,* the most common parasitic nematode found in Britain and which infects sheep causing parasitic gastroenteritis*;* *Trichostrongylus colubriformis,* which infects sheep and cattle causing trichostrongylosis*;* *Trichostrongylus vitrinus,* infects sheep and similarly causes trichostrongylosis*; Cooperia oncophora,* infects cattle and causes cooperiosis*;* and *Haemonchus contortus,* which infects sheep and leads to anaemia, emaciation and can cause death. It had previously been shown that a 44kDa zinc metalloprotease component of *H. contortus* exsheathment fluid was responsible for ecdysis in self and other trichostrongylid parasites (Gamble *et al.,* 1989). It was an aim of this chapter to determine if such cross reactivity existed between the free-living *C. elegans* secretory moulting enzymes, NAS-36 and NAS-37, and the trichostrongylidae parasites. To investigate the potential for cross reaction of these *C. elegans* NAS enzymes refractile ring assays were performed, as outlined in (Gamble *et al.,* 1989) and (Ozerol and Silverma.Ph, 1972). These assays involved exposing chopped up and boiled L3(2M) trichostrongylid cuticles to purified recombinant NAS-36 and 37, and noting refractile ring formation. The refractile ring, which is a cuticular structure that forms invariably 20µm from the anterior of the worm, is the point at which the cuticle breaks down allowing the trapped L3 worm to escape the retained L2 cuticle sheath, freeing the infective stage larvae (Gamble *et al.,* 1989; Gamble *et al.,* 1989b).

7.2 Results

7.2.1 Characterisation of mutants

Deletion mutants, *nas-28(ka5), nas-36(tm1636)* and *nas-37(tm410)* were used to characterise the function of the respective gene. Allele *ok199,* a point mutation within the

coding sequence of *nas-37,* was also used. This point mutation lead to the generation of an opal stop codon at 600bp of transcript C17G1.6a and at 520bp of the splice variant transcript C17G1.6b. *tm410* contains a 429bp deletion which is found in both transcripts. The latter of these two alleles was favoured for the majority of experiments as the genotype could be determined by means of SWPCR. *nas-36(tm1636)* and *nas-37(tm410)* were generated by NBP Japan[11] and *nas-37(ok199)* was obtained from the CGC. For details on the *nas-28(ka5)* mutation see, chapter 4.2.3.

nas-37(tm410)

nas-37(tm410) was phenotypically identical to *ok199.* Both show moult defects at a penetrance of ~24% (n=301 and 233 respectively) at 25°C. As can be seen in, Figure 7.1, these phenotypes correspond to those noted with the RNAi experiments described in chapter 3. Hypodermal expression of *nas-37* implies a role in collagen maturation. From the mutant strain phenotypes this seems probable. Therefore it would appear that *nas-37* is involved with both collagen maturation, likely pro-collagen cleavage, and, is essential for ecdysis. However it must not be overlooked that the cuticular disruption noted with loss of *nas-37* may be a consequence of the associated impaired ecdysis.

nas-36(tm1636)

Phenotypically *nas-36(tm1636)* exhibited moulting defects, Figure 7.1, similar to the RNAi phenotype discovered in chapter 3. The occurrence of the phenotype was low, ~5% (n=148) at 25ºC. RNAi of *nas-36* appeared to produce a higher incidence of the Mlt phenotype, although exact counts were not made. This may be attributed to cross reactivity between *nas-36* with *nas-37*. The quad-alae and mild seam cell disruption noted by RNAi were also evident in *nas-36(tm1636)* mutants**.**

[11] http://shigen.lab.nig.ac.jp/c.elegans/index.jsp

Figure 7.1: *nas-37(tm410), nas-36(tm1636)* and *nas-28(ka5)* mutants. Cuticle defects in *nas-37* mutants. A DIC view of wild type (A) and *nas-37* (B) adults showing three-foil alae (slightly out of the plane of focus, left to right, arrowheads), but a network of fibres in deeper layers of the cuticle in *nas-37*. This network is not present in the wild type. The COL-19::GFP pattern of wild type (C) and *nas-37* (D) shows that the pattern is disrupted in the adult stages of *nas-37* mutants (arrowhead). DPY-7 collagen staining in the wild type (E) and *nas-37* (F) shows that the annuli are disrupted and do not laterally overlap in L4 stages of *nas-37* mutants, compared with the overlapping pattern in wild type L4s. Adapted from (Davis *et al.,* 2004). (G) *nas-36(tm1636)* adult exhibiting characteristic moult defect. In this case the constriction is over the vulva of the animal resulting in an egg laying defect. Arrow shows the constriction. (H and I) *nas-28(ka5)* elongated embryo and L1 stained with DPY-7 antibody, (J) *nas-28(ka5)* larva stained with MH27 seam cell specific antibody. *nas-28(ka5)* worms appear to have a wild type cuticle.

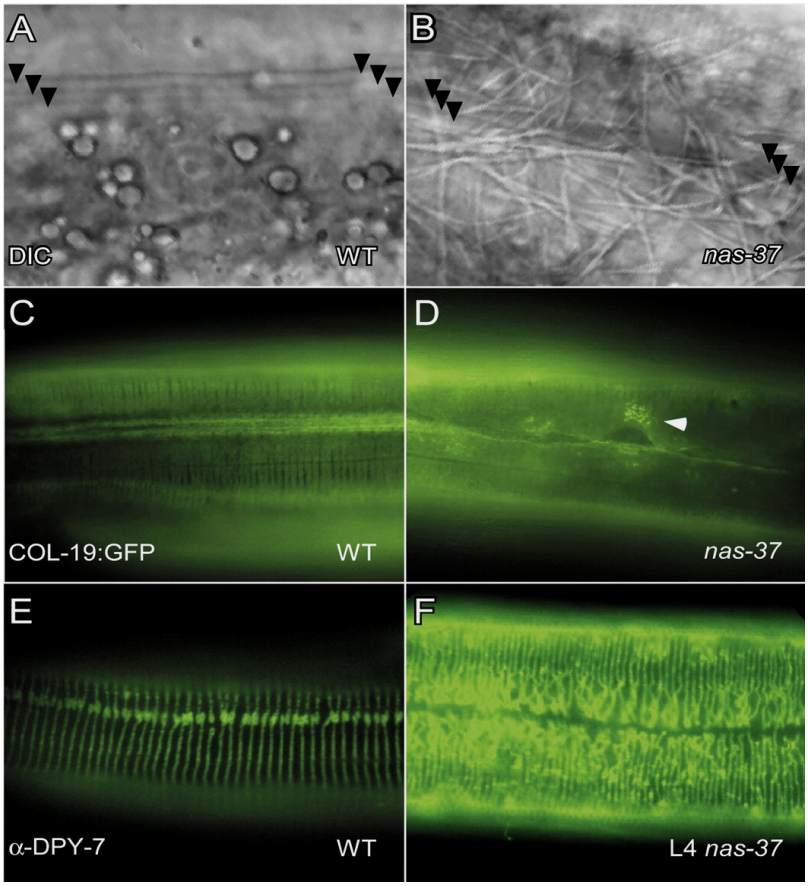

nas-37 (tm410)

Panel taken from (Davis *et al.*, 2004)

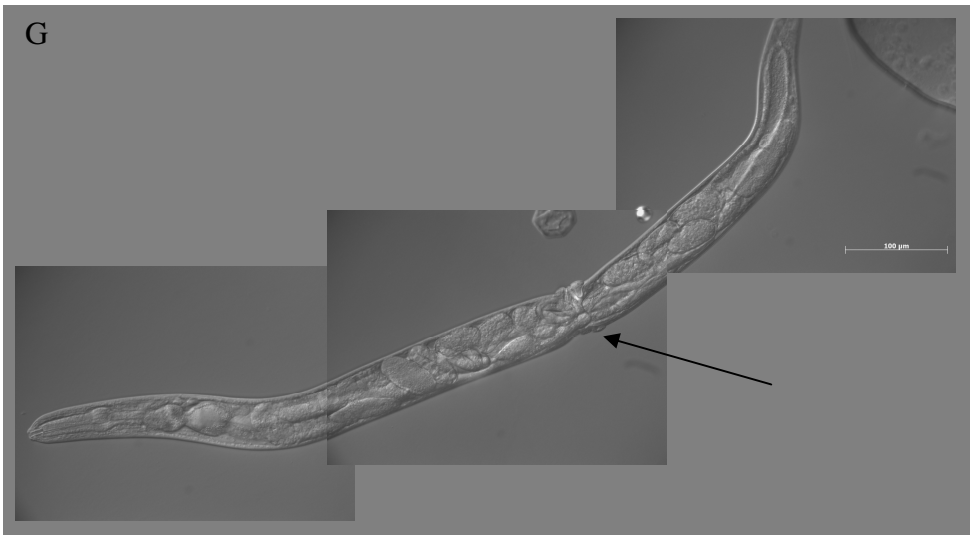

nas-36 (tm1636)

nas-28(ka5)

nas-28(ka5)

Phenotypically *nas-28(ka5)* appeared wild type, Figure 7.1. This was in contrast to the RNAi phenotype (severe Bmd) reported in chapter 3. *nas-28(ka5)* was backcrossed to N2s four times and at no stage was a Bmd evident. Antibody staining of *nas-28(ka5)* with the DPY-7 and MH27 antibodies demonstrated a wild type cuticle.

Scanning Electron Microscopy of ecdysis defective nas-37(tm410)

Scanning electron micrographs illustrating moult defective cuticles and denote the constrictive cuticular band found around the worm, Figure 7.2.

nas-36(tm1636) and nas-37(tm410) double mutant

Double mutants were made between *nas-36(tm1636)* and *nas-37(tm410)*. The new line generated was denoted TP93. TP93 had the same abundance of moult defective worms within a population grown a 25ºC as *nas-37(tm410)*, 24% (n=117). Therefore *nas-37* was emerging as the main astacin contributor towards moulting within *C. elegans*.

nas-37(tm410) and hch-1(ut110) double mutant

Crosses between the hatching defective strain *hch-1(ut110),* in which *nas-34* has been mutated by insertion of a Tc1 transposable element (Hishida *et al.,* 1996), and *nas-37(tm410)* were performed to determine if *nas-37* had any role in the process of hatching. The double mutant strain was denoted TP97. TP97 showed that *nas-34*, which had previously been suspected as involved with moulting, had no effect upon the moulting process, with the percentage of moult defective worms in a population of TP97 the same as in *nas-37(tm410)* worms.

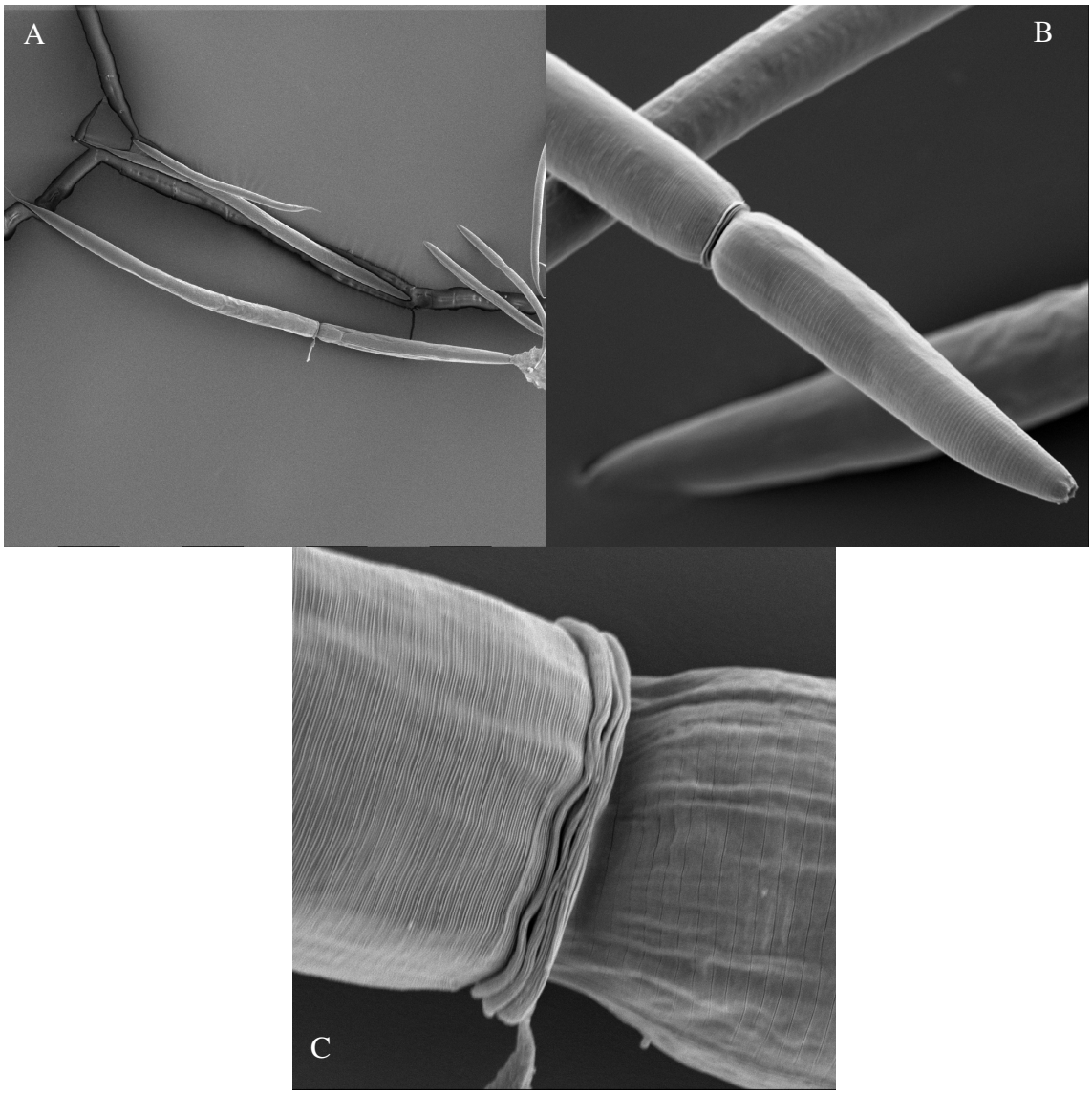

Figure 7.2: Scanning electron micrographs of *nas-37(tm410).* (A) Adult worm showing moult defect and retained cuticle (magnification x130). (B) Moult defect constriction around the anterior of the worm (magnification x 1.3k). (C) Improperly shed cuticle. Old retained cuticle to the left, new cuticle and head to the right (magnification x 3k).

A time course was established to ascertain the involvement of *nas-37* in hatching. Two OP50 seeded plates (each containing five adults from the strains listed in Table 7-1) were allowed to egg lay at 25ºC for 1hr. The adults were removed from the plates and the time course ran for 63hrs.

Strain and number of eggs scored	**% Hatched**			
	14hrs	**20hrs**	**39hrs** (~L3/L4 moult)	**63hrs** (>50hrs all hatched larvae should now be adult)
N2 (n=31)	97%	100%	100%	100%
hch-1(nas-34(ut110)) (n=54)	18%*	33%*	100%	100%
nas-36 (tm1636) (n=98)	95%	98%	98%	100%
nas-37(tm410) (n=55)	98%	98%	98%	100%
TP93 (n=54) *nas-36;nas-37*	78%	85%	95%	100%
TP97 (n=31) *nas-34/nas-37*	38%*	45%*	55%*	58%*

Table 7-1: Astacin mutants *nas-34, nas-36* and *nas-37* and their single and combined effects upon hatching times at 25ºC. By 11hrs at 25ºC N2 worms should have hatched (wormbook). Coloured cells denote <95% of the population having hatched. * Deviation significant following analysis by χ^2 with 1 degree of freedom.

An offset/delay in the hatching time for strains containing the *hch-1(ut110)* allele alone and in combination with *nas-37(tm410)* was noted. There is a dramatic jump from 33% to 100% hatching between 20 and 39hrs associated with the *hch-1(ut110)* strain. This could be attributed to the fact that *hch-1(ut110)* worms develop normally and remain trapped within an undigested proteinaceous shell. It is likely that within this period the eggshell has degraded sufficiently to allow the trapped L1 to hatch. The rate of development following hatching is unaffected in *hch-1(ut110)* worms.

An apparent hatching delay was noted for TP93 worms; however, these worms did not exhibit the characteristic *hch-1(ut110)* phenotype, instead TP93 worms appeared improperly developed within the eggshell. This delay was not a significant deviation form

the N2 hatching rate, thus neither *nas-36* nor *nas-37* were the predominant factors associated with hatching. TP97 strains exhibited both of these phenotypes, with both improperly developed larvae and wild type looking larvae trapped within an undigested eggshell.

It was concluded that *nas-37* is involved with hatching, given the significant added delay noted in the *hch-1(ut110)/nas-37(tm1977)* double mutant, and may have a role in embryogenesis, most likely in the formation of the L1 cuticle. No cuticle defects were evident in *hch-1(ut110)* worms. *nas-36(tm1636)/hch-1(ut110)* double mutants were not made; however, RNAi of *hch-1* in *nas-36(tm1636)* worms caused no detectable delay in hatching other than that noted by RNAi of *hch-1* in N2 worms.

Western analysis of nas-36(tm1636) and nas-37(tm410) mutants using R548 anti-SQT-3 antibody

Using the R584 anti-SQT-3 antibody, attempts were made to determine if *nas-36(tm1636)* and *nas-37(tm410)* showed improperly processed SQT-3 by Western blot analysis. As in chapter 6, these proved inconclusive due to the unsuitability of the antibody, for this application.

RNAi in nas-36(tm1636) and nas-37(tm410) backgrounds

With other astacin family members

Neither *nas-36(tm1636)* nor *nas-37(tm410)* showed increased incidence of the Mlt phenotype when subjected to RNAi of the astacin family members listed in Table 3-2.

nas-9 was of particular interest as its temporal expression profile was cyclical with the moults. *nas-9* RNAi caused no significant change in the moult defective phenotypes penetrance, in either *nas-36(tm1636)* or *nas-37(ok199)* and *(tm410).*

With the cuticlin encoding cut genes

The *cut* genes were analysed by RNAi in *nas-37(tm410)* backgrounds. The rationale for these experiments being that removal of particular CUT proteins would facilitate easier escape from the retained moult defective cuticle, see Table 7-2. All *cut* constructs listed in Table 7-2 were derived from the RNAi feeding library, except *cut-4.* Full-length *cut-4* was amplified from mixed stage genomic DNA, cloned into the L4440 double T7 feeding

vector and transformed into HT115 cells. All RNAi experiments were performed at 25ºC, in triplicate, except *cut-2* which was only tested twice.

RNAi	Number of moult defective worms over total number of worms in population after 40hrs at 25ºC			Average % incidences of moult defect
	I	II	III	
cut-1	7/39	23/71	34/125	27%*
cut-2	16/57	19/82	-	25%*
cut-3	7/29	6/37	23/79	24%
cut-4	5/18	20/64	25/83	30%*
cut-5	14/89	24/107	7/41	18%*
cut-6	14/90	9/48	23/93	20%*

Table 7-2: *cut* gene RNAi in *nas-37(tm410)* background. I, II and III represent the three different runs of the experiment. * Deviation not significant following analysis by χ^2 with 1 degree of freedom.

It is clear to see that the factor responsible for the constrictive ring found in moult defective worms was not attributable to a single *cut* gene or alternatively did not contain a cuticlin component. RNAi of *cut-2* was performed at a different time form the other *cut* genes, but was similarly found to not affect the incidence of moult defects noted in a *nas-37(tm410)* background. No moult defects were noted in N2 animals subjected to RNAi of these *cut* genes.

With C-terminal pro-collagen peptidases

dpy-31(e2770) worms were subjected to *nas-36* and *37* RNAi in an attempt to determine if either *nas-36* or *nas-37* had any C-terminal proteolytic activity directed toward SQT-3. *dpy-31(e2770)* animals when grown at 15ºC survive by having a weak residual C-terminal proteolytic activity (Novelli *et al.,* 2004), this weak activity is attributed to either residual NAS-35 activity, or redundancy with other astacin proteolytic enzymes. *nas-37* was a likely candidate for redundancy as it was shown to be involved with proteolytic cleavage of collagens, its expression is noted during embryogenesis, and it has 40% amino acid identity to *nas-35.* RNAi of *nas-36* and *37* showed no noticeable decrease in viability of *dpy-31(e2770)* worms at 15ºC, as viable offspring were still produced. Western analysis with the R584 anti-SQT-3 serum was also attempted upon these RNAi treated worm. No conclusive result could be made due to the unsuitable nature of the antibody for the Western blot procedure (Novelli *et al.,* 2006).

C. elegans cuticle degradation with Clostridium histolyticum type VII collagenase

The cuticles of *nas-37(tm410)* worms were prepared for proteolytic digestion as described in section 2.34. *nas-37(tm410)* worms were used as more moult defective worms could be isolated from a smaller sample size. Following digestion of isolated moult defective cuticles with *Clostridium histolyticum* type VII collagenase (2 mg/ml), the constrictive ring was still evident. Isolation of moult defective cuticles in the presence of 2% β-mercaptoethanol also produced cuticles that maintained their constrictive ring. This, in conjunction with the *cut* gene RNAi data, and the fact that the undigested constrictive ring was seen to contain a collagenous component, see Figure 3.11, suggests that the constriction contained both a collagenous component and a non-reducible cuticlin component. However from this data all that could be concluded was that loss of one particular cuticlin, or digestion of the collagenous component, was insufficient to degrade the constrictive ring. This may be demonstrating that the constrictive ring is comprised of more than one redundant cuticlin as well as having a collagenous component. More work will need to be done to characterise the exact components which make up this constrictive ring.

7.2.2 NAS protein expression and purification

NAS protein expression and rescue of nas-36(tm1636) and nas-37(tm410) phenotypes with in vivo expressed HIS tagged protein

NAS-36 and NAS-37 recombinant protein was required to perform certain key assays. Recombinant nematode astacin proteins have however proved difficult to express *in vitro,* and NAS-36 and NAS-37 were no exception.

E. coli expressed NAS proteins

The initial attempts to generate recombinant NAS-37 protein used *E. coli* cells transformed with the pWD100.4 construct, see section 2.29.3.2.1. Various cell lines were tested in attempts to improve yield: M15 pREP4, BL21(DE3) pLysS and BL21 Star(DE3) cells and all proved ineffectual at expressing recombinant NAS-37. However, using BL21(DE3) cells and the pWD100.4 construct some NAS-37 protein was synthesised and purified as per section 2.30.2. This protein was used in refractile ring assays with *H. contortus* at

10µg/ml, see section 2.35. The recombinant protein was found to be active and NAS-37 could be considered to, at least in part, be auto-regulatory. In an attempt to improve expression levels new constructs were generated. Two new constructs were made for both NAS-36 and 37. Full length constructs and constructs lacking the N-terminal pre-pro domain. These constructs were cloned into pQE-30 and expressed in all of the aforementioned cell lines. Purification by native and denaturing conditions, as per sections 2.30.4.1 and 2.30.4.3 respectively, were performed on cells transformed with these constructs and the fractions viewed on coomassie stained SDS PAGE gels. The lack of the pre-pro domain and use of a different IPTG inducible vector made no difference to the yield of protein produced, both constructs, for both genes, proved ineffectual at generating the recombinant proteins in any of the cell lines tested. The auto-induction method, previously discussed in section 6.2.3.4, (Studier, 2005) was also carried out by Dr. Gillian Stepek (University of Glasgow) in an attempt to improve the yield of the protein. Both the full length and pre-pro lacking constructs for NAS-36 and 37 were tested using this method. Neither produced any detectable levels of the target protein, following coomassie staining and anti-HIS probed Western blots.

From these experiments it was clear that neither NAS-36 nor NAS-37 were amenable to *E. coli* expression methods, and an *in vivo* method for expression was therefore considered.

In vivo expressed NAS proteins

In vivo expression of NAS-36 and 37 relied upon the generation of an expression vector containing a HIS tagged full-length genomic construct which was driven by its own promoter and which contained a 3′ UTR. In this case the 3′ UTR of *C. elegans unc-54* was used, see section 2.30.4 for details on the generation of the expression vector. The expression constructs were microinjected into their respective mutant lines as a rescue/HIS tagged protein construct along with the GFP DPY-7 marker. Full rescue of the associated moult defective phenotypes was noted in the injected lines, Figure 7.3 and Table 7-1. This confirmed the active nature of the protein and illustrated that the inclusion of the C-terminal HIS tag did not affect the activity of the protein.

Purification of in vivo expressed NAS proteins

The percentage of GFP positive progeny produced by rescue adults was high. Approximately 90% in *nas-37(tm410)* worms expressing the NAS-37 construct; and ~80% in *nas-36(tm1636)* worms expressing the NAS-36 construct.

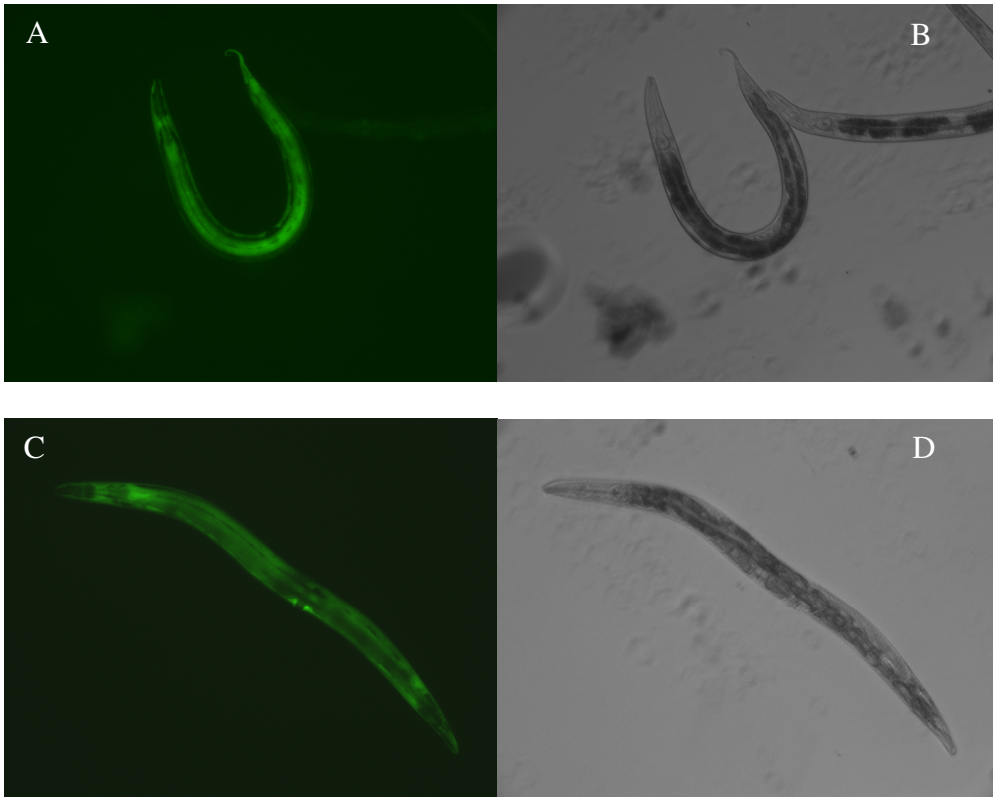

Figure 7.3: *nas-36(tm1636)* and *nas-37(tm410)* mutant strains injected with the respective rescue/protein expression construct. Microinjected mutants show no occurrence of their characteristic moult defects. (A-B) *nas-36(tm1663)* microinjected with the NAS-36 rescue/protein expression construct showing rescue of phenotype. (C-D) *nas-37(tm410)* microinjected with the NAS-37 rescue/protein expression construct showing rescue of phenotype.

Strain	Moult defective GFP +ve worms over Total GFP +ve worms grown at 25ºC	% moult defective
nas-37(tm410) injected with NAS-37 protein expression construct.	1/300	0.003%
nas-36(tm1663) injected with NAS-36 protein expression construct.	0/184	0%

Table 7-3: Rescue counts for mutant strains containing the respective protein expression construct.

15-20 GFP positive rescue worms were plated out on 30 large (9cm) plates and grown at 25ºC for 4 days to generate a large pool of mixed stage transformed worms. The cyclical nature of *nas-36* and *nas-37* expression meant that a large number of worms had to be screened in order to ensure sufficient quantities of the protein were recovered. Synchronous populations were tested, but owing to the extraction method, synchronicity proved difficult to maintain. Both native and denaturing conditions were utilised to extract the *in vivo* synthesised proteins, see section 2.30.4. The samples eluted from the pro-bond nickel columns were viewed on coomassie stained SDS-PAGE reducing gels and by Western blots probed with Invitrogens Anti-His(C-term) Antibody, Figure 7.4. Extraction of the HIS tagged NAS proteins using native conditions was the preferred method of extraction as it yielded active non-denatured protein. Bradford assays, section 2.31, determined that NAS-37 was extracted at 1.2 mg/ml and NAS-36 a concentration of 0.3 mg/ml.

7.2.3 Refractile ring assays

The infective stage in the life cycle of ruminant trichostrongyles is the L3. L3s remain sheathed by the previous L2 stage cuticle until the appropriate signals to exsheath are detected; the L2 cuticle then degrades releasing the infective L3. The L2 sheath protects the infective stage larvae from desiccation and allows for long incubation periods outside of the host. These sheathed L3 worms are designated L3(2M). In order that the L3(2M) nematode can escape the L2 cuticle an exsheathment event must occur. This is detectable by the formation of a refractile ring 20µm from the anterior tip of the nematode, Figure 7.5. In *H. contortus* this process of refractile ring formation was shown to be caused by a 44kDa Zn^{2+} metalloprotease (Gamble *et al.,* 1989). There are four consecutive steps associated with refractile ring formation in *H. contortus* (Ozerol and Silverma.Ph, 1972):

1) Formation of the first ring 20µm from the anterior tip of the worm, which may progress until the cap is completely removed, Figure 7.5.

2) Formation of a second ring 9µm from the anterior tip of the worm, progression may continue until this smaller cap is fully removed. Often shed caps show the formation of this second ring, Figure 7.5.

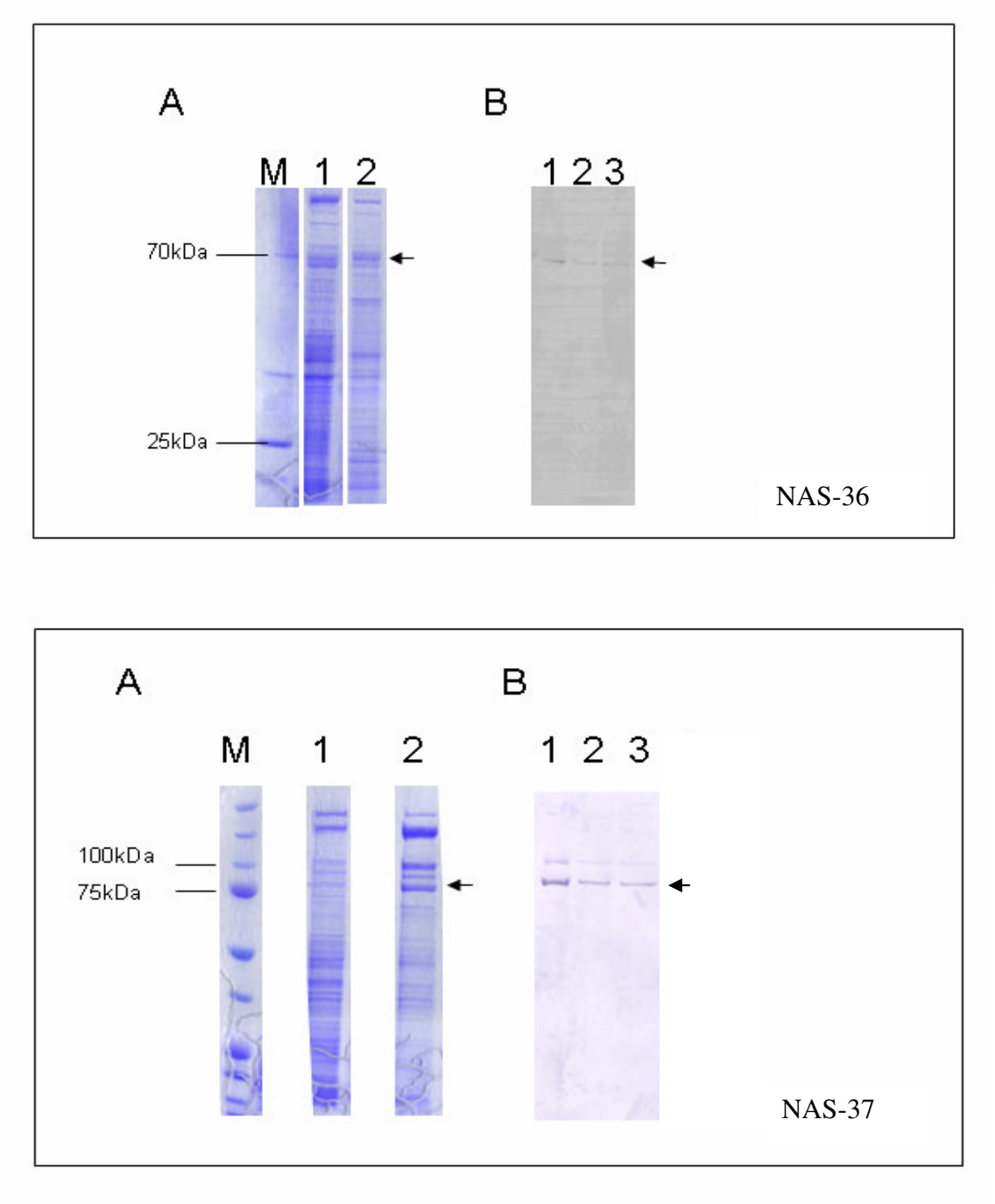

Figure 7.4: NAS protein extracted with Ni^{2+} affinity pro bond columns from *C. elegans* expressing NAS-36 and 37 HIS tagged protein constructs in *nas-36(tm1636)* and *nas-37(tm410)* mutant backgrounds respectively. (Top panel: A) Commassie stained SDS-PAGE gel showing 1 = flow through and 2 = elution fractions of protein extracted from worms expressing the NAS-36 protein construct. NAS-36 weighs 70kDa. (Top panel: B) 1,2 and 3 = Western blot of NAS-36 elution fractions probed with anti-HIS antibody showing detection of NAS-36. (Bottom panel: A) Commassie stained SDS-PAGE gel showing 1 = flow through and 2 = elution fraction of protein extracted from worms expressing the NAS-37 protein constuct. NAS-37 weighs 76kDa. (Bottom panel: B) 1,2 and 3 = Western blot of NAS-37 elution fractions probed with the same anti-HIS antibody showing detection of NAS-37. Arrows indicate the bands of interest and M = marker lanes.

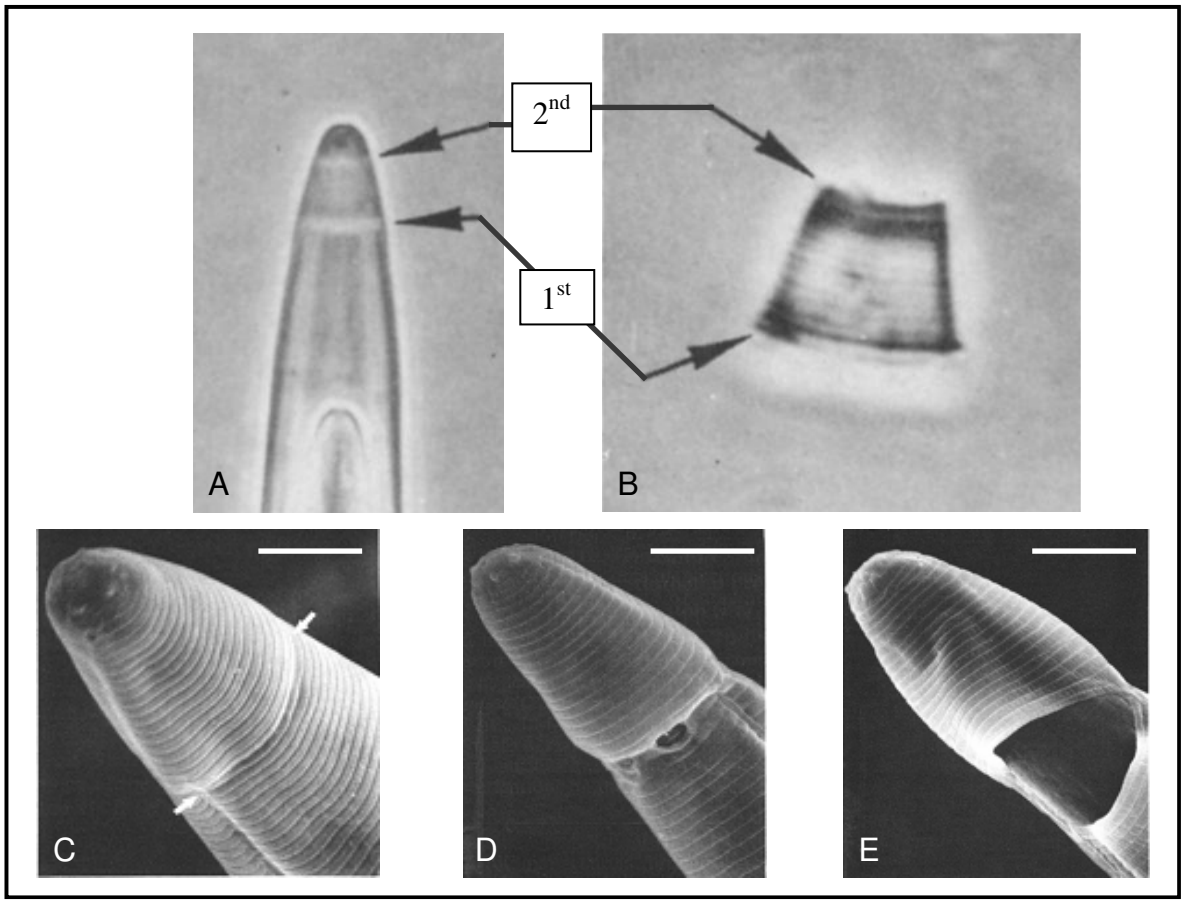

Figure 7.5: Light and scanning electron microscopy of L3(2M) *H. contortus* refractile ring formation and moulting. (A) *H. contortus* L3(2M) cuticle formation of first and second refractile rings, magnification x450. (B) Shed cuticle tip showing separation of cuticle at both refractile rings, magnification x860. (A-B) Adapted from (Ozerol and Silverma.Ph, 1972) (C) Arrows show depression in the cuticle at point of refractile ring formation. (D) Holes appear at the ring region. (E) Large hole evident in the L2 cuticle, and the L3 *H. contortus* can be seen beneath. (C-E) Adapted from (Gamble *et al.,* 1989b), scale bar represents 10µm.

3) The cuticle posterior to the 20µm ring is affected by the exsheathment fluids, becoming transparent and softer.

4) Finally the anterior of the cuticle fully collapses and loss of normal morphology is noted. This occurs when cuticles have been exposed to exsheathment fluids for ≥ 48hrs.

These consecutive steps only occur in animals that have been exposed to exsheathment fluids. Isolated L3(2M) larval cuticles can be maintained in dH_2O for over a month at temperatures ranging from -15 to 60ºC with no refractile ring formation being noted. Those cuticles which were maintained at 38 and 60ºC softened and narrowed following a one month incubation (Ozerol and Silverma.Ph, 1972). This demonstrates that any specific refractile ring formation noted could be attributed to the substance added to the isolated L3(2M) cuticles, as refractile ring formation could not occur spontaneously.

Exsheathment fluid of *H. contortus* has been shown to cause formation of refractile rings in various trichostrongyles including *O. ostertagi*, *C. oncophora* and *H. placei* (Gamble *et al.,* 1989). Our hypothesis was that the machinery involved with the moulting process was conserved across the trichostrongyle parasites; our aim was to determine if the *C. elegans* machinery was similar to that of the parasites.

Haemonchus contortus refractile ring formation with bacterially expressed C. elegans NAS-37

A concentration of 10 µg/ml NAS-37, which had been expressed from the pWD100.4 construct in BL21(DE3) *E. coli*, was exposed to isolated L3(2M) cuticles for 1hr at 37ºC. This resulted in the formation of a refractile ring 20µm from the anterior tip of the parasites, see Figure 7.6, illustrating that there was a shared function between *C. elegans* Zn^{2+} metalloprotease moulting enzyme NAS-37, and the process of L3(2M) refractile ring formation in the parasite *H. contortus*. As *H. contortus* exsheathment fluid also caused refractile rings to form in other trichostrongylid parasites NAS-37 was tested for similar cross reactivity. NAS-36 was likewise tested on *H. contortus* and the other trichostrongylid parasites; however, *in vivo C. elegans* expressed NAS-36 and 37 were used for these experiments due to the difficulties of expressing NAS proteins in *E. coli*.

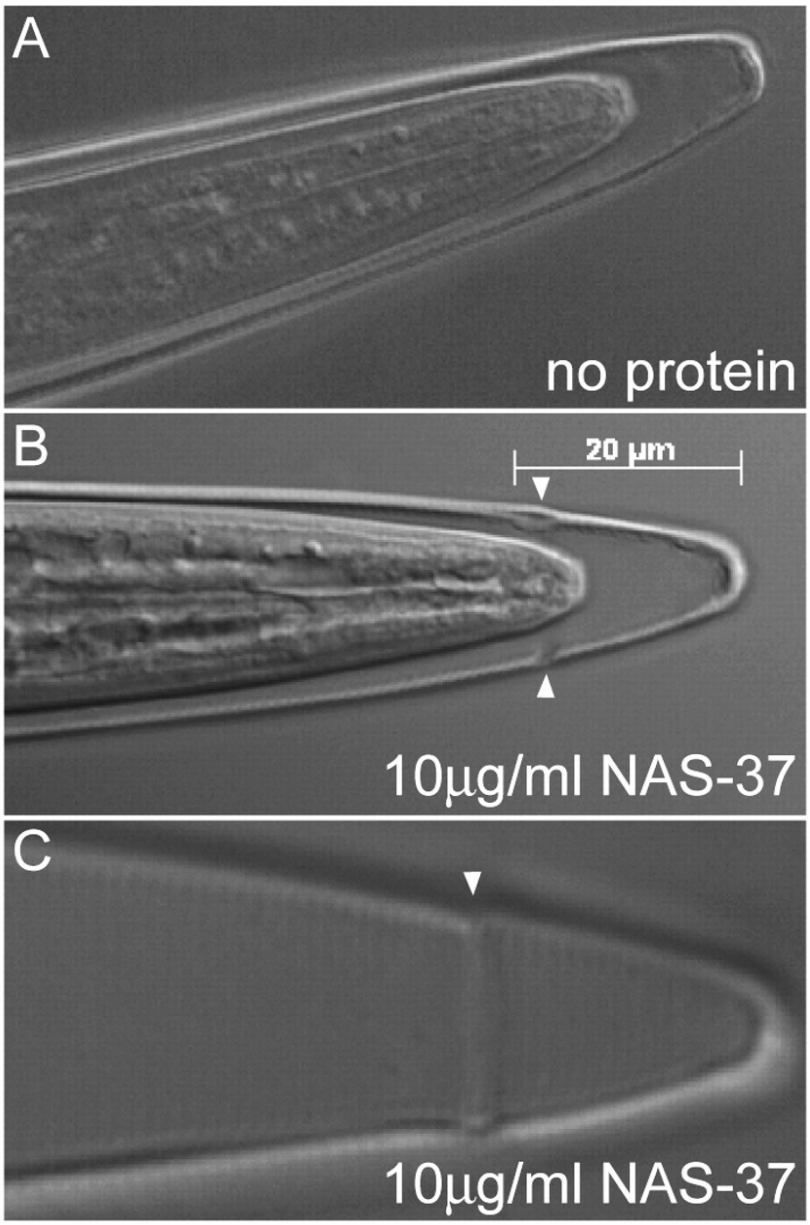

Figure 7.6: NAS-37 induces refractile ring formation in isolated *H. contortus* L3(2M) cuticles. A DIC view of isolated *H. contortus* L3(2M) cuticles incubated with no protein (A) or 10 µg/ml of *E. coli* expressed and purified NAS-37 protein (B-C) shows that NAS-37 can induce refractile ring formation (arrowheads), 20µm distal to the anterior tip.

In vivo expressed NAS-36 and NAS-37 mediated refractile ring formation in a range of trichostrongylid parasites

In vivo expressed NAS-36 and NAS-37 extracted from transgenic *C. elegans* was exposed to the following trichostrongylid parasites, a gift from Dr John Gilliard (University of Glasgow) and refractile ring formation noted, see Table 7-4 and Figure 7.7.

Parasite	NAS-36		NAS-37		Control	
	10µg/ml protein	Protein + 10mM chelating agent	10µg/ml protein	Protein + 10mM chelating agent	No Protein	BSA 10µg/ml
Haemonchus contortus	+	-	+	-	-	-
Teladorsagia circumcincta	+/-	-	+	-	-	-
Trichostrongylus colubriformis	-	-	-	-	-	-
Trichostrongylus vitrinus	-	-	+	-	-	-
Cooperia oncophora	+/-	-	+/-	-	-	-

Table 7-4: Parasites exposed to *C. elegans in vivo* expressed NAS-36 and NAS-37 and the effects noted on refractile ring formation. + denotes occurance of refractile ring, – denotes no refractile ring formation noted. +/- denotes low levels of refractile ring formation (less that 10% of exposed sheaths exhibiting refractile rings).Chelating agent used was 1,10-phenanthroline at a final concentrations of 10mM.

It was clear that both NAS-36 and NAS-37 had cross reactivity with isolated L3(2M) trichostrongylid cuticles from various species. NAS-37 inducing refractile ring formation more efficiently than NAS-36. This was particularly notable with *H. contortus* where after a 1hr incubation at 37ºC the isolated cuticle treated with NAS-37 (10 µg/ml) formed both the first and second refractile rings, and treatment with NAS-36 (10 µg/ml) resulted in formation of only the first 20µm ring, Figure 7.7.

Adding the metal chelating agents EDTA or 1,10-phenanthroline ablated functionality of the Zn^{2+} metalloproteases. 10 mM (final) of 1,10-phenanthroline exhibited a 100% inhibition of refractile ring formation in *H. contortus* for both NAS-36 and NAS-37. This is a similar finding to that reported by Gamble *et al*, (1989) in which a reported 100% reduction in refractile ring formation was noted using the same concentration of 1,10-phenanthroline on isolated cuticles exposed to an unknown 44kDa metalloprotease.

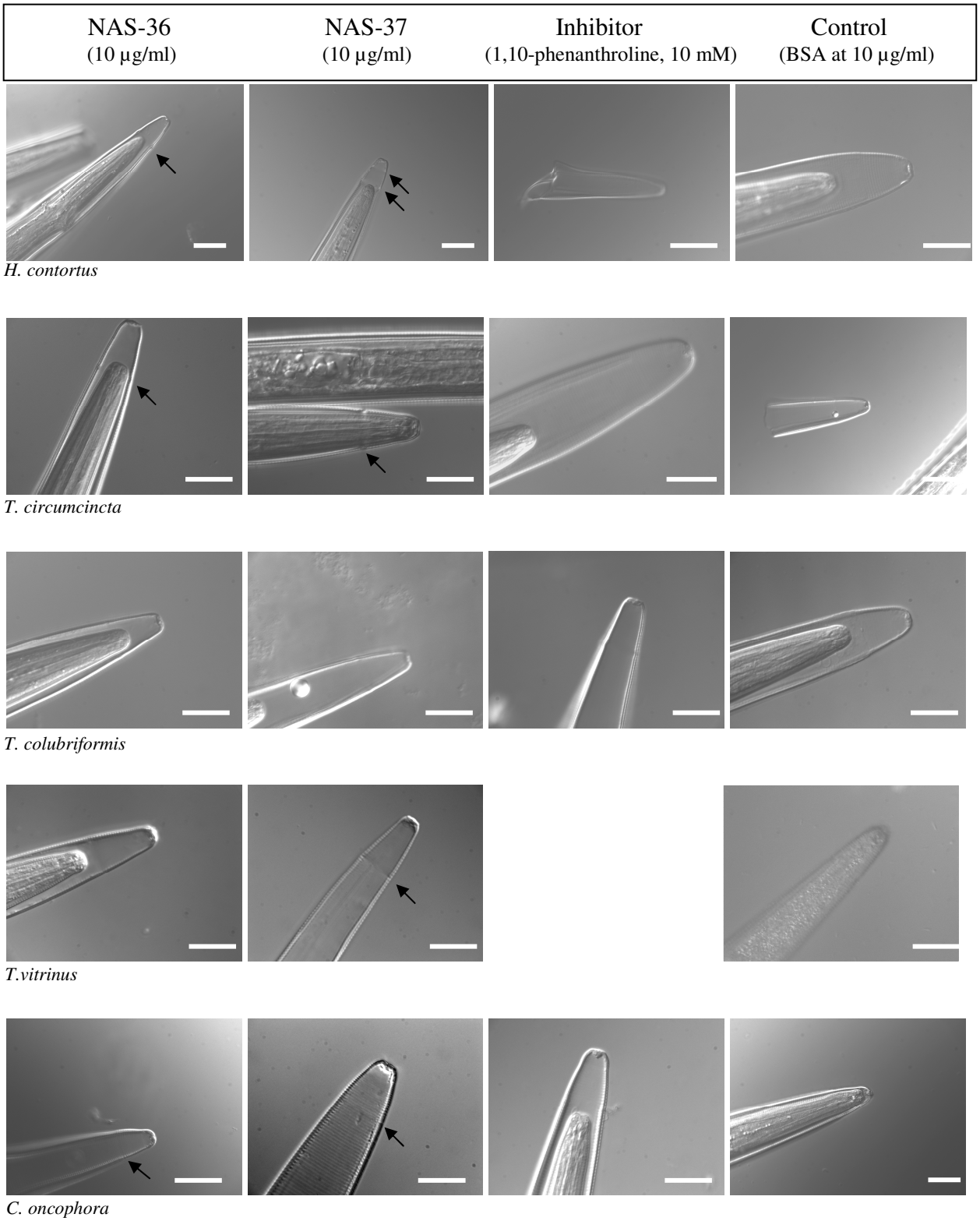

Figure 7.7: Refractile ring assays for NAS-36 and NAS-37 upon selected ruminant trichostrongylids. *H. contortus* forms refractile rings with treatment of both NAS-36 and NAS-37, as does *T. circumcincta* and *C. oncophora*, *T. vitrinus* forms refractile rings in the presence of NAS-37 but not NAS-36 and *T. colubriformis* does not form refractile rings in the presence of either NAS protein. All incubations were carried out at 37ºC for 1hr. The chelating agent used was 1,10-phenanthroline at 10 mM final concentration. Scale bars represent 20µm.

Digestion of isolated cuticles, for each of the above parasites, was performed using either sodium hypochlorite (two volumes of 4 M NaOH to three volumes 10-20% ClNaO) or *Clostridium histolyticum* type VII collagenase (2 mg/ml) for 1hr at 37ºC. This ruled out non-specific digestion of the cuticle as the causative agent for refractile ring formation, an overall thinning and softening of the cuticle was however noted. Isolated cuticles were also exposed to whole protein extracts from N2 worms, prepared and purified in an identical manner to that used for the extraction of NAS-36 and NAS-37 from transgenic *C. elegans*; no refractile ring formation was noted. As isolated parasite cuticles alone could not form refractile rings (Ozerol and Silverma.Ph, 1972), and no specific structures were formed following digestion with either hypochlorite or collagenase digestion, refractile ring formation could be attributed to the specific activity of the NAS enzymes upon the isolated parasite cuticles.

7.2.4 Parasitic homologs of nas genes

Database searches revealed that orthologs of *nas-37* exist in EST databases derived from several parasitic nematodes, including *Brugia malayi, Strongyloides ratti* (GenBank BI741990) and *Meloidogyne chitwoodi* (GenBank CB831257). Of these, the most complete gene sequence is found in the genome sequence of *B. malayi* (Davis *et al.,* 2004). Two fragments which possibly represent a single gene, (TIGR *Brugia malayi* whole genome shotgun sequence contigs 1132528 and 1133899) were orthologous to *C. elegans nas-37*. The splice sites of *C. elegans nas-37* were conserved for four out of five introns in the *B. malayi* ortholog, Figure 7.8, whereas only one out of five of *C. elegans nas-37* splice sites were conserved in the closely related *hch-1* gene. Splice sites were predicted based upon *C. elegans* consensus splice site signals (Blumenthal and Steward, 1997). Thus, it would appear that the NAS-37 protease is conserved in parasitic nematodes.

Attempts were made to close the gap between contigs 1133899 (which contains the astacin zinc binding and Met-turn domain) and 1132528 by PCR. No product was returned with extension periods ranging from 1-10 minutes using primers designed to amplify across the intervening gap, Figure 7.8. Splice leader PCR was also performed in an attempt to determine the 5′ end of the 1133899 contig. An approximately 1.6kbp product was returned using the SL1 consensus Fwd primer with its reciprocal contig based Rev primer, blue arrow in Figure 7.8. *C. elegans nas-37* is similarly SL1 processed. All PCRs were performed using *B. malayi* genomic DNA.

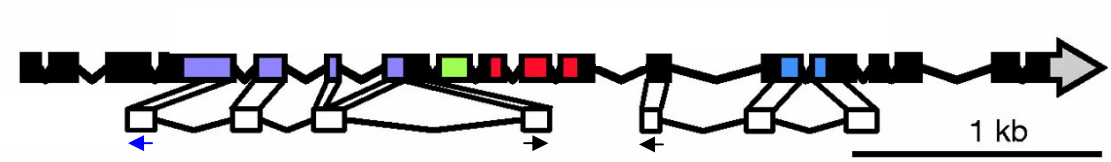

Figure 7.8: Diagrammatic representation of *B. malayi* contigs 1133899 (left) and 1132528 (right) overlaid upon genomic schematic of *nas-37* showing intron-exon boundary conservation. White boxed regions of the contig sequences are 75% identical to the NAS-37 sequence. The purple shading denotes the Astacin domain, green the EGF domain, red the CUB domain, and blue the Thrombospondin domian Arrows denote primers designed for SL-PCR (blue arrow) and gap filling PCR (black arrows). Adapted from (Davis *et al.,* 2004)

... ***H E*** x x ***H*** x x ***G F*** x ***H E*** x x ***R*** x ***D R D*** ..... ***S*** x ***M H Y*** **… (Consensus motifs)**
..G I V A ***H E*** V L ***H*** A L ***G*** L W ***H E*** Q S ***R*** S ***D R D*** ..... ***S*** L ***M H Y*** .... *(C. elegans nas-37)*
..G I V S ***H E*** T L ***H*** A L ***G*** L W ***H E*** Q S ***R*** D ***D R D*** ..... ***S*** V ***M H Y*** .... *(B. malayi ortholog)*

1 2

Figure 7.9: Conserved Astacin domain (1) and Met-turn (2) of putative *B. malayi nas-37* ortholog. Both of theses domains are features of the nematode astacins, and both are found in the 1133899 contig illustrated in Figure 7.8 above. Residues in bold and italic are conserved between the consensus, *C. elegans* and *B. malayi* sequences.

Amino acid identity between the contigs and NAS-37 is ~ 75% across the conserved intron-exon boundaries. 85% and 80% conservation is noted within the astacin zinc binding and Met-turn domains respectively, Figure 7.9, characteristic features of the NAS family.

Other *B. malayi* orthologs to the *C. elegans nas* genes have been found by Dr Gillian Stepek (University of Glasgow). These include a very high sequence identity ortholog of *nas-35*, an ortholog of *nas-36* and a C-terminal portion of *nas-38*. *H. contortus* orthologs of *nas-35(dpy-31)* (70% identity for both isoforms), *nas-36* (63% identity) and *nas-38* (56% identity) have also been found. These are all currently being cloned and sequenced, with the aim of generating orthologous rescue constructs and noting if *C. elegans* mutations can be rescued by the corresponding parasitic genes. This is of great interest as such genes could become possible anthelmintic targets for drug studies.

7.3 Discussion

It was clear that *nas-36* and *nas-37* encoded proteins were both involved with the process of ecdysis in *C. elegans,* with *nas-37* mutants proving to illicit a more penetrant moult defect than the *nas-36* mutant. NAS-36 and NAS-37 also have functions in processing of ECM cuticular collagens with *nas-37* also appearing to have further proteolytic roles in hatching. Functional conservation of ecdysis between free-living *C. elegans* and trichostrongylid parasites was also determined, with NAS-36 and NAS-37 able to induce refractile ring formation in L3(2M) isolated trichostrongylid cuticles.

7.3.1 Cuticle defects associated with loss of nas-28, 36 and 37.

Severe body morphology defects and cuticle defects have been noted in strains containing mutant nematode astacins, most notably *nas-35* (Novelli *et al.,* 2004). Of the mutants investigated in this chapter, no severe body morphology defects were evident.

Following RNAi *nas-28* was proposed as being essential for the generation of a normal body structure. When a deletion mutant was made for this gene, see chapter 4 for details, no such defects were noted. It would thus appear that the *nas-28* RNAi was not specific to *nas-28* alone and perhaps similar genes were also being targeted. As such *nas-28* was not investigated further in this study.

A deletion mutant was made in *nas-36* by the NBP Japan[12] and given the allele designation *nas-36(tm1636).* This mutant illustrated weak seam cell disruptions of the cuticular ECM, but most notable was a moult defective phenotype. These phenotypes were similar to those noted in *nas-37(tm410)* and *ok199* mutants. The main difference being that the moult defect associated with loss of *nas-37* (both alleles) was approximately five times more penetrant than those of *nas-36(tm1636)* which had 5% Mlt compaired to the 24% Mlt for *nas-37(tm410)* at 25ºC. The seam cell disruptions noted for *nas-36(tm1636)* and *37(tm410)* proposed a role for them in collagen biosynthesis. Spatial and temporal expression pattern analysis showed *nas-37* to have a hypodermal pattern and be expressed during each life cycle stage concurrent with early collagen synthesis. This expression profile supports a role for *nas-37* in cuticle collagen maturation. *nas-36* has a temporal expression profile consistent with intermediate collagen synthesis and is also spatially expressed in embryos and at each subsequent larval stage. No adult expression was noted for *nas-36*.

The amorphous networks of collagen fibres underlying the lateral alae noted in the alleles *ox199* and *tm410* of *nas-37* and *nas-36(tm1636)* supported their association with collagen maturation. Such phenotypes are consistent with previously characterised cuticular mutants (Thein *et al.,* 2003). It must not be over looked however that these disruptions to the cuticle collagens may be an artifact of the improper ecdysis process caused by loss of *nas-36* or *nas-37.*

7.3.2 Hatching time course

Since an embryonic expression profile was evident for both *nas-36* and *nas-37* a role in hatching was investigated. *nas-36(tm1636), nas-37(tm410)* and *hch-1(ut110)* were used to determine the effect loss of proteolytic *nas* genes had upon hatching, see Table 7-1. The *hch-1(ut110)* mutant had been previously shown to delay hatching by up to 11hrs at 25ºC (Hishida *et al.,* 1996) which was confirmed in these experiments. *nas-36(tm1636)* and *nas-37(tm410)* mutant strains appeared to have a wild type hatching response; however, when a double knockout of theses genes was generated the embryos appeared mutant within the eggshell. When double mutant knockouts were made between *nas-37(tm410)* and *hch-1(ut110)* severe delays in hatching and some developmental defects were noted. 55% of eggs laid hatched after 39hrs, and of the eggs which did not hatch a mix of *hch-1* like trapped L1s and embryogenesis defective worms were present. The embryogenesis

[12] http://shigen.lab.nig.ac.jp/c.elegans/index.jsp

defective worms were not characteristically vermiform within the eggshell, and those worms which exhibited the *hch-1* phenotype showed greater delays in hatching than *hch-1(ut110)* mutants. Post-hatch these worms developed throughout the remaining larval stages in a wild type manner and rate, becoming adults approximately 40hrs after hatching at 25ºC. *nas-36(tm1636)* and *hch-1(ut110)* double mutants were not made; but, by RNAi of *hch-1* in a *nas-36(tm1636)* background no further delay in hatching beyond that noted with the RNAi of *hch-1* in N2 worms was evident. The delay associated with the *nas-36(tm1636)* and *nas-37(tm410)* double mutant strain was not attributed to failure in degrading the proteinaceous eggshell, but to failures in embryogenesis. Supported by the fact that this strain did not have the characteristic *hch-1* phenotype of trapped L1s within an undigested eggshell; instead, they developed slower than wild type, taking up to 63hrs post lay to hatch. Thus there appeared to be a role in embryogenesis for both *nas-36* and *nas-37,* most likely in the formation of the L1 cuticle, with *nas-37* also having a role in digestion of the proteinaceous eggshell.

7.3.3 Where do the NAS enzymes fit into the moulting cascade?

Frand *et al* (2005) proposed a model for moulting in *C. elegans*, see Figure 7.10, which demonstrated the multistage nature of the moulting process and the position of the *nas* genes within this gene cascade. The exact cue for moulting in *C. elegans* however remains to be determined. The model proposed by Frand *et al* (2005) illustrates the involvement of endocrine cues for moulting based upon the identification of signalling components that when silenced produced moult defects. These putative signalling peptides include; MLT-8, which contains features consistent with peptide hormones; PAN-1, which contains an N-terminal secretory signal and glycosylaton site; and QUA-1, which contains a C-terminal Hint domain (Frand *et al.,* 2005; Hao *et al.,* 2006). It was also proposed that the production of such hormones was being controlled by angiotensin converting enzyme I (ACN-1). *C. elegans* ACN-1 lacks the proteolytic Zn^{2+} co-ordinating residues of human ACE-1 and as such is believed to be non proteolytic, human ACE-1 is a peptide protease which cleaves angiontensin I to angiotensin II. As there is no proteolytic functionality associated with *C. elegans* ACN-1 it is thought to be involved with the maturation or secretion of hormones (Brooks *et al.,* 2003; Frand *et al.,* 2005).

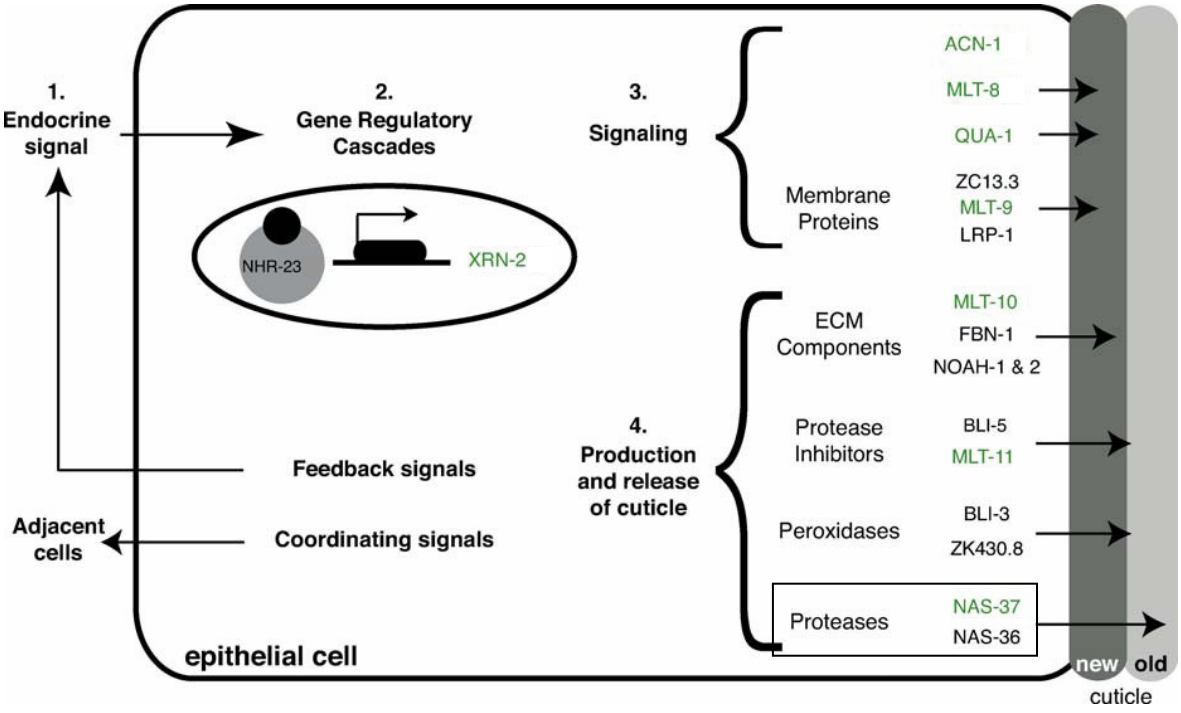

Figure 7.10: A model for moulting of *C. elegans*. (1) Endocrine and possibly neuroendocrine cues trigger moulting, stimulating epithelial cells to remodel the exoskeleton near the end of each larval stage. (2) Endocrine cues involving NHRs alter gene expression. NHR-23 directly or indirectly activates expression of multiple genes involved with moulting, *mlt-8, mlt-9, mlt-10, mlt-11, acn-1*, and *nas-37* in the hypodermis. *xrn-2,* in the pharyngeal myoepithelium, is also activated. (3) Factors such as MLT-8 and ACN-1 amplify the signal to moult. (4) Extracellular matrix proteins, and secreted enzymes, NAS-36 and 37 (boxed), associate with cuticle generation and degredation. The state of moulting is transmitted to the surrounding tissues, and self, by coordinating and feedback signals respectivley. Taken from (Frand *et al.,* 2005).

In cholesterol free media *C. elegans* also exhibit moult defects (Entchev and Kurzchalia, 2005), thus the hormones which were proposed as controlling the moult process could be sterol based, requiring cholesterol to be synthesised correctly, as with QUA-1 (Hao *et al.,* 2006b). Secreted signals are expected to provide feedback on the moult status to endocrine regulators. QUA-1 is a possible candidate for this activity and it may amplify an ecdysis cue, signal neighbouring tissues or provide feedback regarding the moult status (Frand *et al.,* 2005).

Environmental cues such as CO_2 concentration, pH, agitation and temperature (Sciacca *et al.,* 2002) have been identified as inducing exsheathment in ruminant parasites. Entomopathogenic parasites have different cues from ruminant/mammalian parasites. For example agitation of a substrate containing the insect parasite *Steinernema carpocapsae* will induce exsheathment. *Heterorhabditis bacteriophora* another entomopathegenic parasite does not respond to agitation, but will exsheath following prolonged incubation (64 days) (Campbell and Gaugler, 1991). Entemopathogenic parasites do not react to mammalian parasitic nematode exsheathment cues (Campbell and Gaugler, 1991). Thus, specific cues have evolved for specific parasite species to suit there infective strategy and

target. Gaugler *et al* (1989) described two behavioural strategies for host-finding in entemopathegenic parasites, hunters and ambushers. These strategies are employed by other classes of parasite outside entomopathegenic species; hunter parasites, such as *Ancylostoma caninum* which become active and exsheath at breath CO_2 concentrations to seek there host; and ambush parasites, such as *H. contortus*, which exsheath only at the significantly higher internal CO_2 concentrations. This illustrates that numerous specific cues have evolved for exsheathment/moulting in parasitic nematodes based upon the host's behaviour and the parasite's mode of infection; but, the machinery of exsheathment appears to remain constant across the parasitic and free-living nematodes.

7.3.4 Determination of refractile ring composition

It was concluded that the refractile ring which forms during the process of moulting at the point of cuticle degradation contained both a cuticlin and collagenous component. This was determined by collagenase digestion of Mlt defective worms as well as SDS soluble protein extraction (with and without 2% β-mercaptoethanol). Following both the extraction of all SDS soluble proteins and digestion with collagenase the refractile ring remained. This remaining component was likely to be a cross linked non-collagenous component, probably cuticlin. Inclusion of 2% β-mercaptoethanol in the ST buffer used to extract the cuticles, see section 2.37, also led to a cuticle which maintained the constrictive ring, further evidence supporting the presence of cuticlin in the constrictive ring of moult defective cuticles. Individual *cut* genes were silenced by RNAi in a *nas-37(tm410)* background to attempt to remove the refractile ring cuticlin component and hence facilitate easier escape from the cuticle. This did not occur, leading to the belief that there was not one specific CUT component of the refractile ring or that RNAi of the *cut* gene family was not sufficient to remove functionality of the targeted gene. Knockouts in the *cut* gene family members or use of CUT specific antibodies would prove useful in fully defining the composition of this constrictive ring.

7.3.5 NAS-36 and NAS-37 can induce refractile ring formation in trichostrongylid cuticles

In vivo expressed NAS-36 and NAS-37 caused the formation of refractile rings in isolated L3(2M) trichostrongylid cuticles. NAS-37 induced refractile ring formation in a wider range of trichostrongyles and in a higher proportion of the isolated sheaths tested, when compared with a similar concentration of NAS-36. This activity of *C. elegans* ecdysis

enzymes on parasitic refractile ring formation demonstrates a conservation of the mechanism for moulting between divergent species. It is possible that this mechanism arose in a common ancestor which pre-dated the divergence of parasitic and free-living nematodes and its importance to the organism has lead to the conservation of the process and the proteins involved with it. Also of note is the conservation of collagens between parasitic and free-living nematodes (Shamansky *et al.,* 1989; Johnstone *et al.,* 1996; Fu *et al.,* 2005), see chapter 1, and this may correlate with conservation of enzymes required to process/cleave such structural components. High levels of conservation between parasitic and free-living nematodes, with respect to cuticular genes, should facilitate the exchange of genes between both species e.g. rescue of *C. elegans* cuticular defect phenotypes with parasitic gene orthologs.

As previously shown, a Zn^{2+} metalloprotease is responsible for exsheathment in *H. contortus* parasites (Gamble *et al.,* 1989). We show here that the *C. elegans* Zn^{2+} metalloproteases NAS-36 and NAS-37 can substitute for the *H. contortus* exsheathment fluid and drive refractile ring formation. NAS-36 and 37 were also shown to cross react, like the *H. contortus* exsheathment fluid, with other trichostrongylid cuticles, see Table 7-4. As such these *C. elegans* enzymes, or the parasitic orthologues which remain to be determined, could be considered as possible drug targets, as conservation of genes associated with moulting in non-ecdysozoan species is poor.

Chapter 8: General Discussion.

8.1 Discussion

The aim of this thesis was to investigate two gene families, the quiescence sulfhdryl oxidases and the nematode astacins, and define their involvement with cuticle biosynthesis and degradation. This relied upon the generation and use of deletion mutants in key members of these gene families.

8.2 Deletion mutant generation

A deletion library of psoralen-UV mutagenised worms was constructed. These worms were screened using the poison primer approach for small deletion detection, with deletion strains produced for *qsox-1* and *nas-28*. Strains carrying the *qsox-1* deletion mutant allele were a key resource for this project.

8.3 Quiescence sulfhydryl oxidases and cuticle collagen biosynthesis

All *qsox* genes encode an N-terminal thioredoxin domain and a C-terminal ERV1/ALR domain, which communicate between one another in the shuttling of reducing equivalents from the target protein to the final acceptor molecule O_2, that in turn generates a reactive oxygen species by product (Thorpe *et al.,* 2002):

$$2P\text{-}SH + O_2 \longrightarrow P\text{-}S\text{-}S\text{-}P + H_2O_2$$

These domains if separated are substrates for one another and will co-operate in the oxidation of reduced thiols (Raje and Thorpe, 2003; Coppock and Thorpe, 2006), re-enforcing the advantage of unifying these co-operative domains in one protein. We have shown that the QSOX enzymes are expressed in collagen secreting cells at times concurrent with collagen synthesis and that certain *qsox* family members are essential for viability.

qsox-1

qsox-1 was associated with seam cells regions and was found to be involved in cuticle collagen biosynthesis. Evidence for such activity includes the facts that *qsox-1* is expressed in the lateral hypodermal seam cells coincidentally with intermediate collagen synthesis,

and that the TP110 (*qsox-1(ka2)*) mutant strain exhibits seam cell cuticular disruptions when viewed by immunofluorescence. *qsox-1(ka2)* mutants also exhibited an apparent reduction in H_2O_2 production. On the basis of the intermediate expression profile of *qsox-1* and the lack of disruption noted in the patterns of DPY-7 (an early expressed collagen) the cuticular collagen substrates of QSOX-1 are likely to be the intermediate collagens, such as SQT-3 a highly expressed larval transcript.

qsox-2

The *qsox-2* mutant did not exhibit severe disruptions of cuticular collagen patterning and only mild disruption was noted in lateral seam cell secreted regions. The mutant strain carrying the *qsox-2(tm1977)* deletion allele did however exhibit reduced fecundity, particularly at higher temperatures, implicating a role for *qsox-2* in zygote development. This theory was supported by *qsox-2* expression having been noted within the male tail hypodermis. Orthologous QSOX enzymes have been shown to associate with regions of sperm production in *Drosophila* and vertebrates (Arbeitman *et al.,* 2004; Thorpe and Coppock, 2007) proposing probable functions in; protecting spermatozoa from microbial or sulfhydryl degradation by production of ROS, or in production of seminal fluid components (Ostrowski and Kistler, 1980; Benayoun *et al.,* 2001). Regions associated with the constitutively expressed *qsox-2,* most notably the pharynx, appeared to exhibit reduced H_2O_2 production in *qsox-2* mutant strains. Pharyngeal defects were noted in *qsox-2(tm1977)* mutants in which *pdi-1* or *pdi-3* had been knocked-down. *pdi-1* is noted for strong pharyngeal expression (Page, 1997) and *pdi-3* has been shown to be important in cuticle formation, but only in certain mutant backgrounds (Eschenlauer and Page, 2003). These pharyngeal defects and expression profiles implied a role for *qsox-2* in pharyngeal development; however, other possible roles were examined, see following.

qsox-3

A deletion mutant was not available for *qsox-3*; however, following RNAi in N2 backgrounds an Unc/Gro phenotype was evident (Kamath *et al.,* 2003; Simmer *et al.,* 2003). Orthologous QSOX enzymes have been shown to localise to rat and guinea pig central nervous systems, and have been proposed to be involved with neuronal migration (Amiot *et al.,* 2004; Mairet-Coello *et al.,* 2005); however, since RNAi is ineffective within neuronal tissues such a proposed functionality for *qsox-3* could not be determined. RNAi targeting of *qsox-3* also resulted in seam cell cuticular collagen disruptions in the TP12

strain, indicating a role for *qsox-3* in lateral hypodermal collagen synthesis. Evidence further supporting an involvement of *qsox-3* with seam cell cuticle biosynthesis included expression profiles which demonstrated lateral hypodermal expression concurrent with intermediate collagen synthesis, the intermediate collagens are therefore the likely collagenous substrates of *qsox-3*.

QSOX produced H_2O_2: the effects and uses of

Although disulphide bond generation is a key facet of QSOX activity, the accompanying production of H_2O_2 and its use, may prove of similar importance as continual accumulation of H_2O_2 within the cell would ultimately become lethal. It has been proposed that such ROS may have a role as anti-microbial agents, when in conjunction with extracellular peroxidases (Ostrowski and Kistler, 1980; Benayoun *et al.,* 2001; Coppock and Thorpe, 2006). This is an interesting proposal as *qsox-2* was constitutively expressed in the pharynx, and could conceivably have an anti-microbial role through secretion of H_2O_2 into the pharyngeal lumen. In addition to the effect as an anti-microbial agent H_2O_2 production, as a by product of disulphide bond generation, could be considered as a source of oxidative stress.

Oxidative stress has been implicated in the death of beta cells during progression of type II diabetes (Araki *et al.,* 2003). In diabetes the body can no longer control the blood glucose concentration which can lead to it becoming significantly higher than normal. This elevated blood sugar level is mirrored by an increase in H_2O_2 concentration which is responsible for death of the beta cells. However, the QSOX enzymes have been largely overlooked as a source of this H_2O_2 production. In cases of high blood glucose levels expression of insulin from the pancreas would be up regulated, termed hyperinsulinemia. In hyperinsulinemia there is a significant demand for QSOX1 and 2, which have been shown to strongly localise to the pancreas during hyperinsulinemia (Thorpe *et al.,* 2002). Each mature insulin molecule requires the generation of three disulphide bonds to be folded correctly. Generation of each disulphide bond produces one molecule of H_2O_2 leading to the elevation of the nascent H_2O_2 concentration. This in turn further damages the beta cells ultimately leading to their death. Hyperinsulinemia is not the only condition in which higher than typical H_2O_2 concentrations prove damaging to tissues. Damage to muscle cells (cardiac and striated) of Duchenne muscular dystrophy (DMD) sufferers can be in part attributed to elevated levels of H_2O_2 (Whitehead *et al.,* 2006; Jackson *et al.,* 2007). In MDX mice (which lack dystrophin, the protein missing in DMD sufferers)

heightened levels of H_2O_2 leads to increased damage to muscle cells following tetanus (Whitehead *et al.,* 2006). The source of this ROS was originally believed to be leakage from the mitochondrial electron transport chain but recent research has cast significant doubt on this theory, and a more complex association of mechanical and metabolic cues upon various subcellular sites is being considered (Whitehead *et al.,* 2006; Allen, 2007; Jackson *et al.,* 2007). Increased levels of H_2O_2 are currently thought to be caused by; activation of stretch activated Ca^{2+} channels, which open following stretch induced damage to the muscle; and up regulation of NADPH-oxidase activity within the muscle (Whitehead *et al.,* 2006). The mechanism for this up regulation is not know at this time; however, it is proposed that NADPH-oxidase may be regulated by dystrophin, its associated membrane proteins or other cytoskeletal structures and as such its function may be altered in dystrophic muscle leading to increased ROS production (Whitehead *et al.,* 2006). These observations are of interest as BLI-3 is the only known NADPH-oxidase found in the genome of *C. elegans* and it has been shown to be expressed within the body wall, but not the pharyngeal, muscles (Edens *et al.,* 2001). *qsox-2*, a constitutively expressed QSOX enzyme, is expressed in pharyngeal muscle where its production of H_2O_2 may be associated with the inflammatory repair response in muscle damaged by the continual pumping of the pharynx. However, no pharyngeal pumping defects were evident in the *qsox-2(tm1977)* mutant. Pharyngeal muscle is bi-nucleated, a similar structure to that of cardiac muscle.

Combined knockouts of qsox-1 and 2 are lethal

The essential nature of the QSOX enzymes was confirmed in the double knockout strain *qsox-1(ka2); qsox-2(tm1977).* The loss of *qsox-1* and *qsox-2* caused larval lethality and cuticle defects, which may be in part attributed to the reduced levels of H_2O_2 produced in these strains. This proposal is supported by the fact that apparent reduction in fluorescence was noted in H_2DCHFDA treated TP110 (*qsox-1(ka2)*) and TP102 (*qsox-2(tm1977)*) strains, and that *qsox-2* RNAi targeted TP110 (*qsox-1(ka2)*) worms were Bli. The Bli phenotype noted is similar to that seen in N2 worms with RNAi targeting of *bli-3* or *hpx-1*, such worms having a compromised ability to generate di- and tri-tyrosyl cross-links of the cuticle collagens, causing a blistered appearance (Edens *et al.,* 2001). RNAi knockdown of both *bli-3* and *hpx-1* have proved to be 100% lethal and is hypothesised to be due to their inability to form di- and tri- tyrosyl cross-links (Edens *et al.,* 2001). The NADPH-oxidase domain of BLI-3 was presumed to be responsible for the production of the H_2O_2 utilised by the peroxidase domains of BLI-3 and HPX-1 in tyrosyl cross-linking (Melanie

Thein University of Glasgow, unpublished work). It was therefore proposed that the Bli phenotype noted with *qsox-2* RNAi targeted TP110 (*qsox-1(ka2)*) worms was an intermediary between the wild type *qsox-1* and *qsox-2* mutants and the lethality of the *qsox* double mutant, with both of these phenotypes being attributed to a reduced ability to generate H_2O_2 in cuticle synthesising cell types. The work shown here goes some way to proposing QSOX enzyme produced H_2O_2 as being important in cuticle collagen synthesis, but other roles/associations can not be overlooked. Further work is required to determine the source of the H_2O_2 used in tyrosyl cross-linking and whether QSOX is a contributer.

Proposed association of QSOX with protein disulphide isomerases in C. elegans

The functional association between *qsox* and *pdi* families in *C. elegans* was investigated by RNAi. Association between the two gene families was shown by an increased severity of the mutant phenotypes associated with the combined silencing of QSOX and PDI enzymes. The proposed association was that of QSOX re-oxidising the reduced PDI enzymes; PDI itself being reduced following the generation of disulphide bonds. QSOX and PDI association has previously been shown in an avian model with reduced PDI acting as a substrate of QSOX (Hoober *et al.,* 1999). RNase A refolding assays were planned as a method to highlight any such association between these two gene families; however, recombinant QSOX enzymes could not be produced.

From this and the previously discussed actions attributed to the QSOX enzymes it is clear that QSOX proteins represent multifunctional enzymes which have many possible involvements and associations with processes such as cuticle collagen maturation, zygote production and possible anti-microbial activity. Of these potential functions the association with the PDI family and possible TGase activity, see section 8.5.1.1, may prove enlightening with regard to the process of cuticle formation.

8.4 Two subgroup V nematode astacins and their involvement with cuticle degradation in *C. elegans* and trichostrongyle parasites

From RNAi screening of the *nas* gene family *nas-36* and *37* proved to be interesting candidates for investigation. Both NAS-36 and NAS-37 were shown to be involved not

only with moulting in *C. elegans,* specifically in the process of ecdysis, but with exsheathment in trichostrongylid parasites.

nas-36 and 37 mutants

Mutations within *nas-36* and *37* led to improper ecdysis and moult defective worms, implicating NAS-36 and NAS-37 in the process of moulting in *C. elegans*. Spatial expression of these *nas* genes associated them with points of cuticle attachment and degradation. Hatching defects were also evident in worms which contained the *nas-37(tm410)* deletion mutation, this effect was examined by generating a double mutant between *nas-37(tm410)* and the hatching defective strain *hch-1(ut110).* Hatching delays in excess of those noted in *hch-1(ut110)* mutants alone were scored in this double mutant strain, thus eggshell degradation was also proposed as a function of NAS-37. This claim was further supported following examination of the *nas-37* embryonic expression profile. Similar embryogenic expression was noted for *nas-36* and delays in hatching were evident in *nas-36(tm1636); nas-37(tm410)* double mutants. These delays were not attributed to a failure in eggshell degradation but to a failure in embryogenesis, most likely in the formation of the L1 cuticle, as embryos did not appear vermiform within the eggshell. Thus an apparent role in embryogenesis was also discernable for NAS-36 and NAS-37.

Examination of *nas-36(tm1636)* and *nas-37(tm410)* mutant cuticles revealed networks of fibres consistent with improper collagen maturation. With *nas-37* having been shown to be expressed in hypodermal cells at times associated with production of early collagens (Davis *et al.,* 2004), such as DPY-7, and *nas-36* having been shown to be expressed in hypodermal cells (Suzuki *et al.,* 2004) at times concurrent with intermediate collagens, such as SQT-3, a role in collagen maturation may also be envisaged for NAS-36 and 37. However it must not be overlooked that these disruptions to the cuticle may prove to be artifacts, caused by the improper ecdysis in the *nas-36(tm1636)* and *nas-37(tm410)* mutants.

NAS-36 and 37 can induce exsheathment of L3(2M) trichostrongyle nematodes

When L3(2M) trichostrongylid parasite cuticles were exposed to NAS-36 and NAS-37 refractile rings were formed. Since these samples were chopped and boiled prior to the addition of the *C. elegans* enzymes it could be concluded that the ring formation is

undeniably derived from the activity of NAS-36 and NAS-37. NAS-37 induced refractile ring formation in more of the trichostrongylid species tested and at a higher penetrance, when compared, like for like, with NAS-36. Such observations demonstrate that the mechanisms associated with the process of exsheathment and moulting have been conserved across the free-living and parasitic (trichostrongylus) nematodes of clade V, and may extend further as orthologs for *nas-36* and *nas-37* have been found in the diverse clade III parasitic nematode species *B. malayi*, see Figure 8.1.

Caenorhabditis elegans as a model for parasitic nematodes

C. elegans has been used as a model organism in developmental biology for sometime, and is becoming a powerful tool for parasitology research. One of the main advantages in using *C. elegans* as a model for parasites is its eases of *in vitro* culture. Certain parasites do have model laboratory hosts, *Brugia malayi* for example can be maintained within mice, but for many species such hosts are not available precluding them from straight forward *in vitro* culturing.

A brief phylogenetic analysis of the phylum Nematoda has given rise to a cladogram with five distinct clades numbered I-V (Blaxter, 1998), Figure 8.1 adapted from (Gilleard, 2004). From this analysis *C. elegans* was placed within clade V along side the veterinary important parasite species trichostrongylidae. Also found within clade V are the human hookworm species *Necator* and *Ancylostoma.*

From such a cladogram it can be assumed that members of distinct clades will be less conserved than members of the same clade, as such clade V members will probably have a reduced conservation with members of clade III. This would appear to be the case with comparative analysis of the *B. malayi* genome with *C. elegans* revealing little conservation of local synteny (Ghedin, 2007). However, rescue experiments using *B. malayi* orthologues of *C. elegans pdi-2* have complemented the *C. elegans pdi-2(tm689)* mutant strain (Dr A. Winter University of Glasgow, personal communication). This is the only known example of a *B. malayi* orthologue rescuing a *C. elegans* mutant, and as such cross clade transgenic rescues would need to be considered in a case by case manner.

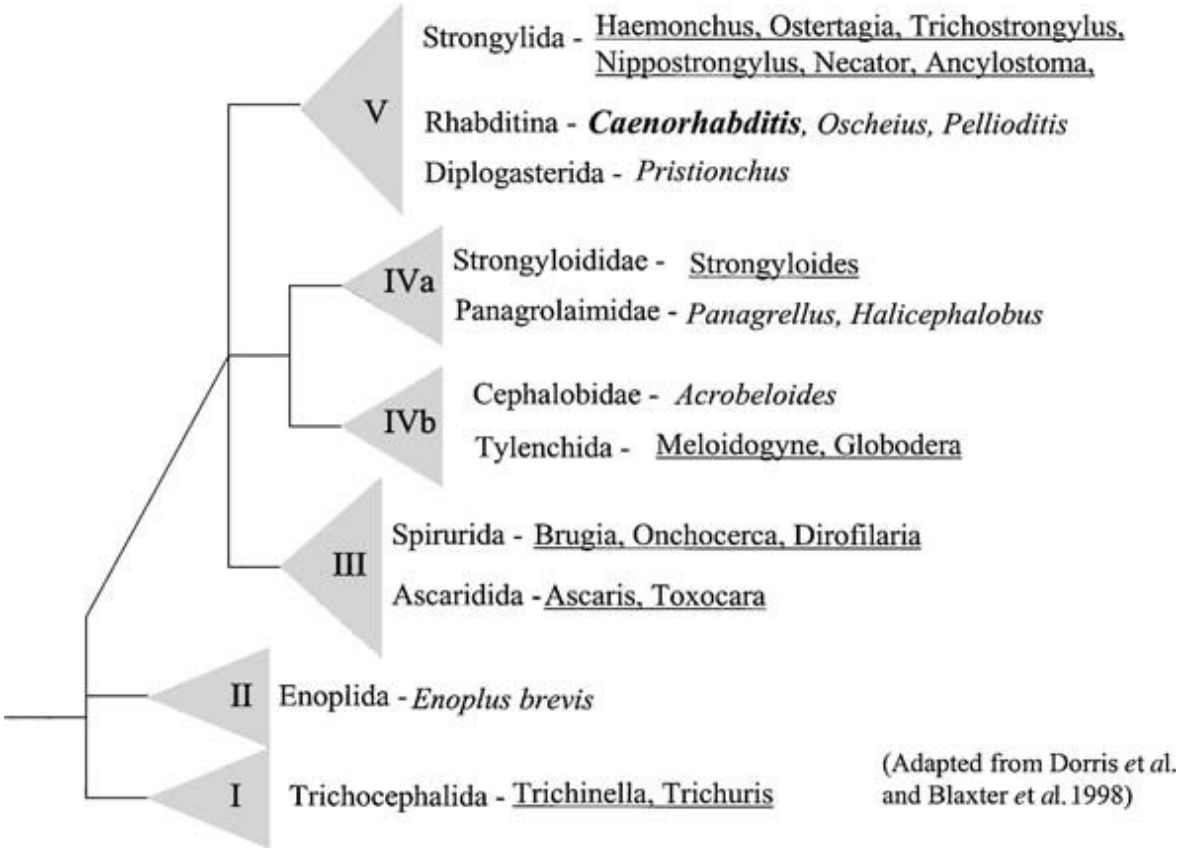

Figure 8.1: Schematic phylogenetic tree showing the evolutionary relationships of some nematode species. It is adapted from (Dorris *et al.,* 1999) and is based on small subunit rDNA sequence (Blaxter *et al.,* 1998b). The genera that are underlined are parasitic nematodes and the genera shown in italics are free-living nematodes that have been subject to evolutionary development studies and comparative analysis with *C. elegans.*

Due to the relative ease of transgenic line establishment in *C. elegans,* orthologous reporter constructs have been applied to localise many parasitic nematode genes in *C. elegans*. Such orthologous reporter constructs can yield key information about that particular genes functionality; however, it is important that the reporter construct generated contains all of the necessary reporter elements to ensure that ectopic expression is eliminated (Gilleard, 2004). Since orthologous parasitic reporter elements can be expressed in *C. elegans* it follows that full length coding sequences should be similarly amenable to expression within *C. elegans*.

Expression of recombinant parasitic proteins *in vitro* has not always yielded active protein (De Maere *et al.,* 2005), This may be due to inappropriate folding and/or glycosolation of the target protein (Murray *et al.,* 2007). Several reports of using *C. elegans* as an expression medium to produce active protein are present in the literature (Kwa *et al.,* 1995; Redmond *et al.,* 2001; Britton and Murray, 2002; Kampkotter *et al.,* 2003; Murray *et al.,* 2007). The use of *C. elegans* as an expression system for parasitic genes thus provides

a significant tool for *in vivo* analysis of parasitic genes in an easily culturable system. Gilleard, (2004) reviewed several approaches for analysis of parasitic targets using *C. elegans* as an expression system. Of which the expression of a parasite gene to rescue a *C. elegans* RNAi phenotype would appear to be a powerful and elegant means of target protein analysis, and one in which several problematic issues which arise with *trans*-expression and rescue using a parasitic gene in *C. elegans* can be overcome. The RNAi approach is reliant upon the fact that a higher degree of sequence homology is required for dsRNA to interfere with an endogenous transcript than exists, in general, between *C. elegans* and parasitic species. Thus RNAi can be administered to a transgenic *C. elegans* line expressing the parasitic gene with no effect upon the orthologs expression, however knockdown of the endogenous *C. elegans* transcript will occur. This would allow for the relatively easy study of lethal/essential genes rescued by orthologous parasitic *cis*-expressed transcripts, as was achieved by Britton & Murray (2002) in which the *C. elegans* cathepsin-L protease, 99.7% lethal by RNAi, was rescued by its *H. contortus* orthologue, resulting in 2.1% lethality. With the availability of the *C. elegans* RNAi library (Kamath *et al.,* 2003), and the ease of generation of RNAi constructs not found within the library, any parasitic gene which has a *C. elegans* orthologue could be studied using this RNAi based method.

RNAi within parasites is a subject beyond the scope of this discussion. However, if a reliable/suitable system is to be found it would prove of immense importance and could become a powerful system allowing the identification of possible parasite control targets. However, although RNAi seems to be possible in some nematodes, *H. contortus* (Geldhof *et al.,* 2006; Kotze and Bagnall, 2006) and *T. colubriformis* (Issa *et al.,* 2005) among others, caution must be exercised when interpreting such experiments. It is of significance that the effects noted can be specifically attributed to reduction in target gene transcription and not the non-specific toxic effects of dsRNA, or effects caused by the delivery procedure (Knox *et al.,* 2007). Of note is that a general cross species/clade method for RNAi in parasites would appear unlikely given the differences noted within particular species. For example, siRNA would appear to mediate a specific effect upon *T. colubriformis* but the longer dsRNA does not, the complete opposite from what is noted in *C. elegans.* Also, several genes which are key for RNAi in *C. elegans* have not been found in the genomes of some parasites; *rde-4,* which is associated with the generation of siRNA in *C. elegans*; *rde-2,* which is required for the functional silencing of chromosomal loci by transgenes and functions downstream of *rde-1* in the RNAi pathway; and *sid-2* and *rsd-2,* which are involved with the uptake and spreading of dsRNA have not been found within

the genomes of *H. contortus* or *B. malayi* (Zawadzki *et al.,* 2006; Knox *et al.,* 2007). Thus it would appear that a tailored approach may be required for each parasitic species.

Nematode astacins as possible drug targets

The *C. elegans* NAS enzymes have been shown to be involved in the degradation of structural components and cleavage of cuticular collagens, with mutants exhibiting moult, hatching and cuticular defects (Hishida *et al.,* 1996; Davis *et al.,* 2004; Novelli *et al.,* 2004). As such these specific enzymes could become novel anti-nematode drug targets.

To my knowledge, there currently are no known specific natural inhibitors of astacin metalloproteases. We have shown that non-specific chelating agents such as EDTA or 1,10 phenanthroline (both at 10 µM final), will completely inhibit NAS enzyme activity, see Table 7-4. Bond and Beynon (1995) noted that reducing agents such as cysteine and glutathione can also inhibit astacin metalloproteases *in vitro* at concentrations of 1 mM and above, with such inhibition thought to be caused by the non-specific chelation of the metal ligand or by the reduction of the enzyme's disulphide bonds. Tissue inhibitors of metalloendoproteases (TIMPs) do not inhibit the activity of astacin metalloproteases nor do the inhibitors of serine, cysteine, or aspartic proteinases (e.g. PMSF, 3,4-dichloroisocoumarin, iodoacetate, E-64, leupeptin, pepstatin), or by angiotensin I-converting enzyme inhibitors such as captopril or thiorphan (Bond and Beynon, 1995). This apparent lack of specific inhibition of astacin metalloproteases could turn out to be a distinct advantage as this promotes the astacin domain as a specific target region for drug development, and these potential drugs should have little cross reactivity with the endogenous metalloproteases.

Isolating genes which have essential functions in the process of moulting enables detection of gene products only found in Ecdysozoans. This means that if drugs could be found which specifically targets the astacin motif of the NAS enzymes there is likely to be little cross reactivity with the endogenous matrix metalloproteases of the host. As astacin metalloproteases NAS-36 and NAS-37 are essential for proper ecdysis, it is a remote possibility that they will be conserved within mammals. Due also to the cross reactivity of NAS-36 and NAS-37 with parasite cuticles, and that orthologues of both exist within parasitic genomes, they represent attractive prospects for the development of specific non-host targeting anti-nematode drugs. A difficulty which may arise in drug development is the impermeable nature of the cuticle. However, previous studies using metallo- and

cysteine-peptidase inhibitors in *Onchocerca volvulus* have shown that intact cuticles can be permeated by peptidase inhibitors (Lustigman, 1993).

The current effective anti-nematode drugs in use today target cytoskeletal components (benzimidazol) and ion channels (avermectins), which are not specific to the nematode and can prove to be toxic to the host species and humans (Barkwell and Shields, 1997; Kalivas, 1999; Neff *et al.,* 2004). With resistance to such drugs becoming increasingly common (Dent *et al.,* 2000; Leathwick *et al.,* 2001) new drug targets should be explored. Given the well established use of insect-pesticide controls which specifically target the processes of moulting and tegument synthesis with bisacyldhydrazines and acylureas respectively (Dhadialla *et al.,* 1998; Cohen, 2001), NAS-36 and particularly NAS-37 are valid candidates for drug development with *C. elegans,* a proven candidate in which to perform such a study.

8.5 Future prospects

8.5.1 QSOX

8.5.1.1 RNase A refolding and TGase activity assays

The RNAi data of chapter 6 regarding targeting of *pdi* family members in *qsox* mutant backgrounds suggested that QSOX and PDI enzymes were co-operating to facilitate the formation of the wild type cuticular ECM. To further investigate the nature of any such association refolding assays should be performed. Recombinant PDI and QSOX enzymes would be tested for there ability to re-oxidise the reduced thiols of the substrate RNase A singly and in combination. This would highlight any involvement between the families, and determine the nascent rate at which QSOX enzymes generate disulphide bonds in reduced di-thiols. The experimental procedures for these assays are outlined within Hoober *et al* (1999) and Eschenlauer *et al* (2002). Such assays could not be performed for inclusion within this thesis as recombinant QSOX could not be produced. As a possible means around this problem the auto-induction protocol within Studier, (2005) could be employed. If this yielded no detectable or insufficient amounts of protein, *in vivo* expression of the protein, using the previously described pAB-1 vector, could be performed.

Recombinant QSOX enzymes could also be tested to determine if they possessed any latent TGase activity as QSOX-1 and 2 both contain the essential wCghC TGase active site

motif within their thioredoxin domains. It has been shown that strict adherence to this motif is required for TGase functionality, as mutation of the second cysteine in this motif result in total loss of TGase activity within *C. elegans* PDI-3 (Blasko *et al.,* 2003). Similarly, within each of the thioredoxin domains of PDI-3 there is only one histidine residue (located within the TGase motif), that when removed also ablates the TGase function (Blasko *et al.,* 2003). QSOX-1 and 2, like PDI-3, contain only one histidine residue within their thioredoxin domain which resides within the TGase motif. The thioredoxin domains of the PDIs and QSOX-1 and 2 are closely related to those of human and *E. coli* thoiredoxins, which also exhibit TGase activity (Lee *et al.,* 1993). If QSOX-1 or 2 were shown to exhibit TGase activity this would be of great interest as *C. elegans* do not contain any designated TGase enzymes, PDI-3 being the closest homologue to mammalian ERp60 (Blasko *et al.,* 2003; Eschenlauer and Page, 2003). This may also highlight an additional cross-linking activity for the multi-functional QSOX enzymes.

8.5.1.2 TP111 *(ka6)* mutant gene determination

It is clear from the results in section 6.2.3.6, that *qsox-1* is not the locus responsible for the associated phenotypes of the TP70 strain. The determination of the unknown gene mutated within the TP111 *(ka6)* mutant strain would however be of interest due to the association of the *ka6* allele with cuticle formation. To achieve this, two and three point mapping would be a suitable strategy. However, performing a series of RNAi experiments, targeting the candidate genes mentioned within Appendix C in the TP111 *(ka6)* mutant background would be a prudent first step prior to undertaking such a mapping strategy.

8.5.1.3 Cuticle collagen Western blotting

Development of a monoclonal antibody directed towards a collagen, such as SQT-3, which could be used in Western blot analysis would be a worth while endeavour. Such an antibody could be utilised to yield many interesting results regarding the state (degree of disulphide bonding exhibited between the target collagen and its partner collagens, or whether the target collagen is found in predominantly a monomeric, dimeric or trimeric form) of the target collagen within the cuticle of various mutant strains.

8.5.2 NAS

8.5.2.1 Pro-Collagen C-peptidase (PCP) activity of NAS-36 and NAS-37.

As it was not shown here whether NAS-36 or NAS-37 had any PCP activity this point could be investigated through exposure of baculovirus expressed SQT-3 constructs, which have TY tags incorporated upstream and downstream of the C-terminal cleavage site, to recombinant NAS-36 and NAS-37 and noting the cleavage products by Western blot analysis using the anti-TY antibody. With the TY tags being incorporated upstream and downstream of the SQT-3 C-terminal proteolytic cleavage site, if cleavage did occur following addition of either NAS-36 or 37, the products when resolved and probed with anti-TY antibody would illustrate a notably larger product for the upstream construct than the downstream construct. If no cleavage occurred there would be a single large uncleaved product irrespective of the construct used. Such experiments would be controlled by the inclusion of DPY-31/NAS-35 the proven C-terminal proteolytic enzyme of SQT-3 (Novelli *et al.,* 2004).

8.5.2.2 Test NAS proteins on a wider range of trichostrongylid parasites

It would be interesting to note the effects of NAS-36 and particularly NAS-37 in a wider range of trichostrongylid parasites, one such interesting candidate species would be *Ostertagia ostertagi*. *O. Ostertagi* worms infect cattle and cause damage to the stomach wall as they mature from larvae to adult stages, leading to a loss in productivity throughout the life of the animal. Of note however is that combined infections of *O.ostertagi* and *T. vitrinus* lead to greater lethality than by infection with only one of these worm species. NAS-37 was shown to elicit exsheathment in *T. vitrinus* and if it proved so in *O. ostertagi* too, this would be a significant result.

8.5.2.3 Cloning of parasitic orthologues for use as rescue constructs

Currently orthologues of key astacins, such as *nas-34, 35, 36* and *37* are being cloned and sequenced from parasitic species by Dr G. Stepek (University of Glasgow), with a view to generating orthologous rescue constructs for *C. elegans* mutants. Orthologues of these astacins have been isolated in *B. malayi* (clade III) and *H. contortus* (clade V) and are being sequenced using combinations of SL-PCR, 5′and 3′ RACE-PCR. It is of particular relevance to the work covered in chapter 7 that orthologues of *nas-36* and *37* should be isolated, cloned and tested for there ability to rescue the corresponding *C. elegans* mutants,

particularly those of *H. contortus*. If reliable techniques were developed for RNAi within parasitic species targets such as *nas-36* and *nas-37* would prove of interest, most notably to determine if knockdown of these orthologues would compromise the ability of the parasite to exsheath.

8.5.2.4 Drug development

Libraries of metalloprotease inhibitors, or new astacin directed metalloprotease inhibitor compounds could be screened against wild type *C. elegans,* selecting those compounds which are cuticle permeable and which elicit moult defects in the worm.

C. elegans strains *nas-36(tm1636), nas-37(tm410)* or the double mutant could be manipulated to express parasitic orthologues of these respective *nas* genes. The resulting transgenic worms could then be scored for recovery of the characteristic moult defective phenotype associated with loss of NAS-36 or NAS-37, and the previous moult defect inducing compounds would be retested in a pseudo-parasitic manner. This method would surmount the difficulties associated with *in vitro* culture of certain parasitic species while still allowing relative *in vivo* analysis of the target parasite protein(s). Such an approach could ultimately yield possible anti-nematode drugs. Obviously candidates generated in this manner would then need to be revalidated *in vivo* upon the actual parasitic species.

.

Appendices.

Appendix A: F56C11.3, a possible *C. elegans* ortholog of yeast Erv1p.

A.1 The quiescin-sulfhydryl oxidase in *C. elegans*

C. elegans has been shown to contain three QSOX enzymes. However, based upon domain similarities to the QSOX group, one other sulfhydryl oxidase was proposed as a QSOX family member. This was shown however not to be the case.

A.2 F56C11.3 is not a QSOX

F56C11.3 was initially proposed as a QSOX family member due to its possessing the FAD binding domain, ERV1/ALR. *qsox-1, qsox-2* and all splice variants of *qsox-3* have this FAD binding domain and an N-terminal thioredoxin domain which contains a CxxC motif. This motif can be more stringently classified in QSOX proteins as wCgxC. An identical motif can be found in *C. elegans* PDI a/a′ thioredoxin domains (Thorpe *et al.,* 2002). The wCgxC motif is not present in F56C11.3 as there is no N-terminal thioredoxin domain. Also lacking in F56C11.3 is a signal peptide. Both of which are prerequisites for QSOX classification.

The predicted sequence of F56C11.3 was for a 486bp coding and 1455bp genomic sequence encoding a 161 residue ERV1/ALR containing protein. This polypeptide was believed to be either a mis-prediction, unconfirmed prediction made by wormbase, or that splice variant(s) containing the missing thioredoxin domain were present.

SL-PCR of F56C11.3

Splice leader PCR was carried out using mixed stage N2 cDNA with combinations of; SL1, SL2, F56C11.3 Fwd (gene specific sense) and F56C11.3 Rev (gene specific antisense) primers. The results of which can be seen in Figure A.1. Lane 1 shows the product generated from a combination of SL1 and gene specific antisense primer, illustrating that the gene product of F56C11.3 is *trans*-spliced with SL1 splice leader sequence, and amplifies the predicted ~500bp sequence. Lane 2 shows no product for SL1 and the gene specific sense primer. Lanes 3 and 4 show no product from the combinations of SL2 primer, with antisense and sense gene primers respectively. Thus the predicted size of 486bp for F56C11.3 coding sequence was accurate, and a splice variant product which included the thioredoxin domain was unlikely, given the mixed stage nature of the cDNA sample used.

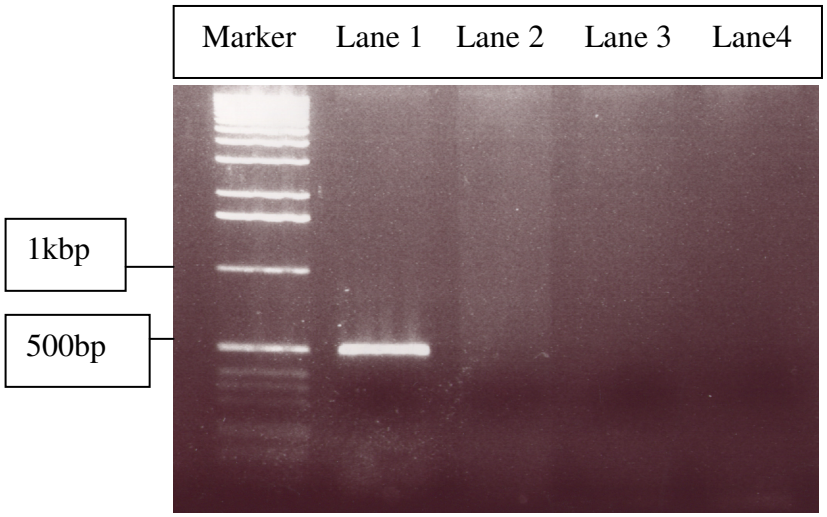

Figure A.1: SL PCR of F56C11.3 from mixed stage *C.elegans* cDNA. (Lane 1) shows the product when SL1 and F56C11.3 REV. Illustrating that F56C11.3 is SL1 *trans*-spliced and that the proposed 486bp fragment is valid. (Lane 2) shows no product from SL1 and F56C11.3 gene specific sense primers. (Lanes 3) shows SL2 primer with F56C11.3 antisense primer. (Lane 4) shows SL2 primer with F56C11.3 sense primer. No product is produced by either of the SL2 PCRs. Marker is a 1kb marker from Invitrogen.

The use of cDNA in determining the size of the product, and the fact that the F56C11.3 transcript had been *trans*-spliced indicated that F56C11.3 was not a *pseudo* gene and was a genuine ERV1/ALR containing peptide distinct from the QSOX family.

In silico analysis of F56C11.3

F56C11.3 has two CxxC motifs and a C-terminal ERV1/ALR domain. The most N-terminal CxxC lies out with the ERV1/ALR domain; the second is within the ERV1/ALR domain proximal to the FAD binding region. This second C-terminal CxxC motif is termed the proximal disulphide. BLASTP searches for F56C11.3 highlighted homologues in mosquito (*Aedes aegypti*), yeast (*S. cerevisiae*), and human. Those of interest contained similar domain and motif arrangements to F56C11.3: an ERV1/ALR domain prefixed by an N-terminal CxxC motif respectively. F56C11.3 shares 50% amino acid identity to *A. aegypti* (Q16FJ5), 45% amino acid identity to *S. cerevisiae* (Erv1p) and 39% amino acid identity to human ALR (HsALR). All contain an ERV1/ALR domain with a CxxC proximal disulphide and an N-terminal CxxC lying out with the ERV1/ALR domain. HsALR contains a signal peptide, 85% probability at position 24/25, where as F56C11.3, Q16FJ5 and Erv1p all lack a signal peptide. Erv2p, 35% amino acid identity to F56C11.3, also contains a signal peptide, 87% probability at position 34/35. The peptides were analysed using Signal P, an *in silico* means of predicting the presence and cleavage position of the signal peptide. Signal P has been shown to be the most reliable of *in silico* signal peptide prediction tools with 78.1% accuracy of prediction (Zhang and Henzel, 2004). ERV2p and ERV1p do not share high sequence homology (~20% over the most highly conserved C-terminal region), either between each other, or with other proteins found in the genome of *S. cerevisiae* (Gerber *et al.,* 2001). However, they do share a similar tertiary structure. Figure A.2 shows the predicted structure for ERV2p, ERV1p, and F56C11.3. Modelling was performed using, 3Djigsaw[13], an online tertiary structure prediction tool, and visualised with RASMOL v2.6. The tertiary structure of ERV2p has previously been crystallised to a resolution of 1.5 Å (Gross *et al.,* 2002). The structure given for ERV2p by 3Djigsaw agrees with the crystallised structure. ERV2p is dissimilar to ERV1p in that the N-terminal CxxC of ERV1p is not conserved in ERV2p, ERV2p having a CgC motif found C-terminally to the ERV1/ALR domain. The CgC motif has been shown to be associated with dimer formation, and in the shuttling of reducing equivalents (Hofhaus *et al.,* 2003). It is proposed that this C-terminal CgC, and the N-terminal CxxC, share functional similarities.

[13] www.bmm.icnet.uk/servers/3djigsaw/

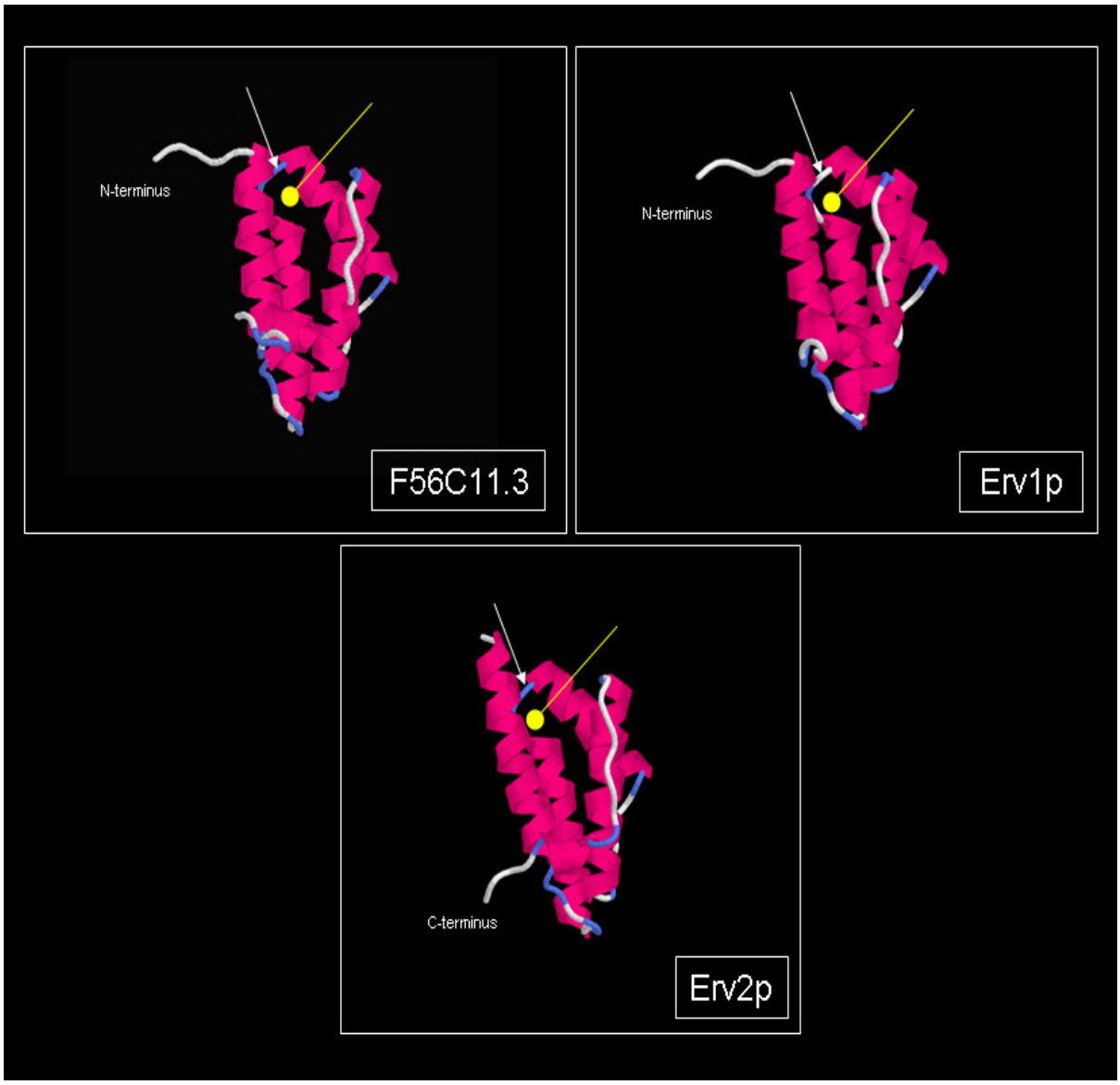

Figure A.2: Structural predictions of F56C11.3, ERV1p and ERV2p. White arrows denote the proximal disulphides location. Yellow arrows denote the FAD binding pocket. The conserved CxxC of F56C11.3 and ERV1p lie on their respective N-terminal extensions. The CgG of ERV2p is found on its C-terminal extension. Predictions made using 3Djigsaw and visualised with RASMOL v2.6

It can be seen from the predicted structures that there are similarities between ERV1p and F56C11.3. Of note is the maintenance of the conserved proximal disulphide cysteine residues (white arrows in Figure A.2) and there location in proximity to the FAD binding core (yellow arrows in Figure A.2). Based upon this structural conservation, and high amino acid identity between F56C11.3 and ERV1p (45%) it is interesting to postulate that they have similar functions, and similar degrees of dependence upon specific residues. Namely the CxxC motif located N-terminally to the ERV1/ALR domain.

RNAi of F56C11.3

Targeted RNAi of F56C11.3, utilising the RNAi feeding library construct (Kamath *et al.,* 2003) in TP12 and N2 backgrounds at both 20ºC and 25ºC, returned a wild type cuticle both with respect to gross morphology and COL-19 patterning. There were no seam cell distortions; overlying alae appeared normal and the annular rings were intact when viewed by DIC and UV microscopy, Figure A.3.

Localisation of F56C11.3

Lines expressing the F56C11.3 promoter tagged to a GFP reporter construct have been generated by the Genome BC *C. elegans* Gene Expression Consortium[14]. Based upon there two lines the localisation of F56C11.3 could be proposed. To be confirmed, three lines in total would need to be generated and checked for overlapping expression profile.

F56C11.3 has been proposed as localising to the pharynx and to body wall muscle, in larva and adults respectively. Expression has also been noted during embryogenesis, in undetermined cell types, and in the muscles of the adult vulva, Figure A.4.

[14] http://elegans.bcgsc.ca/home/ge_consortium.html

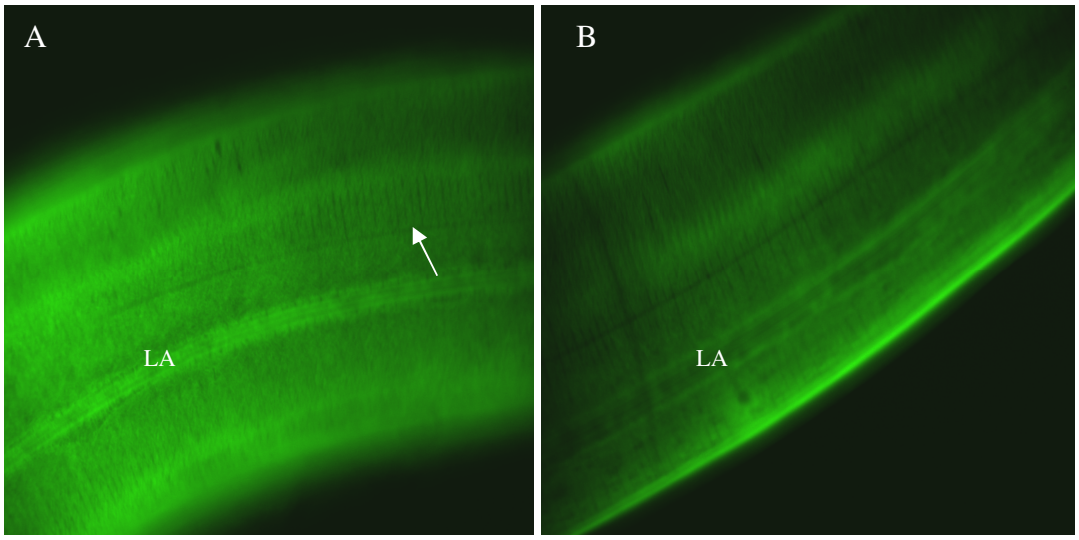

Figure A.3: F56C11.3 RNAi in TP12 background. RNAi carried out at 25ºC. (A/B) Following targeted RNAi the body cuticle was wild type. Regular patterning can be seen in both the lateral alae (LA) and the annular rings (white arrow).

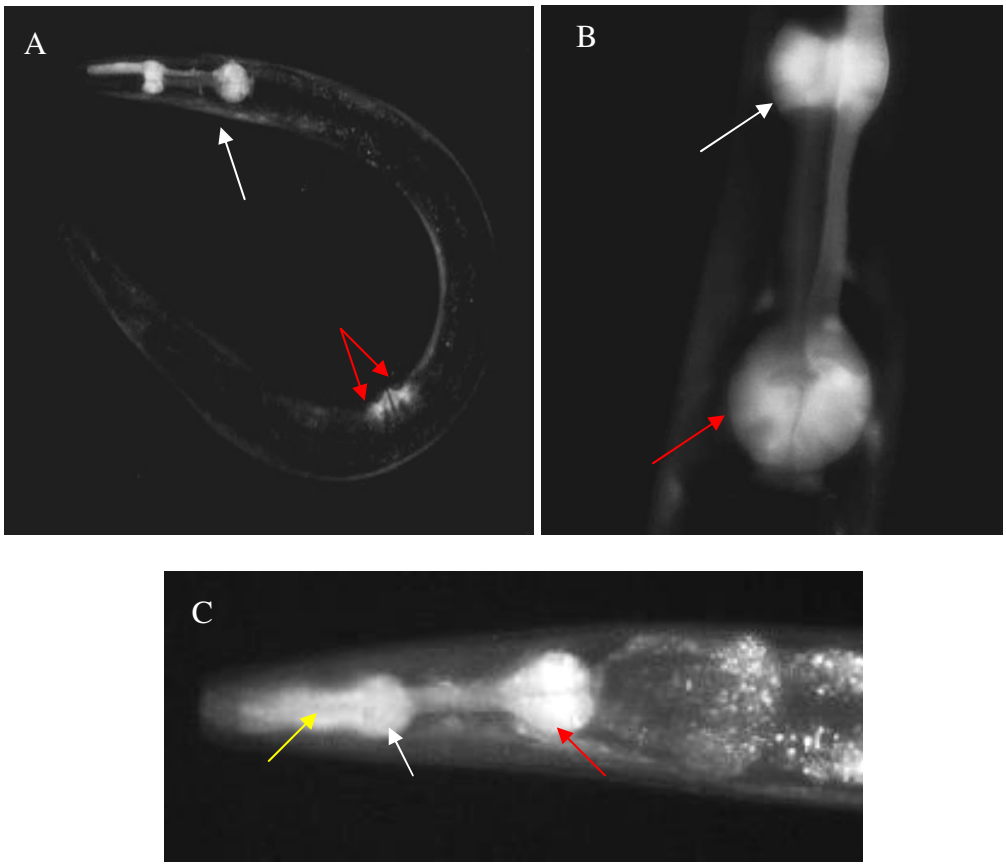

Figure A.4: Worms expressing a GFP reporter constructs for F56C11.3. Constructs made, and pictures taken, by the Genome BC Gene Expression Consortium. (A) Illustrates an adult hermaphrodite expressing F56C11.3 in both the pharynx (white arrow) and the vulval muscle cells (red arrow). (B) Shows GFP staining of the pharynx. Both the metacorpus (white arrow) and the terminal bulb (red arrow) show F56C11.3 expression. (C) Shows similar staining of the metacorpus (white arrow) and the terminal bulb (red arrow) as in (B) with added staining in the procorpus and channels (yellow arrow).

The *C. elegans* pharynx is a cuticle lined structure composed of type IV collagen (Graham *et al.,* 1997). The cuticular structure of the pharynx differs from the body cuticle in that it is not layered, instead adopting a basal membrane structure (Graham *et al.,* 1997). The pharynx is comprised of at least four distinct cuticular constituents, from anterior to posterior; the bridging cuticle, flaps, channels, sieve and the grinder. The grinder cuticle exhibits specialisations for its location with thickening and kerotinisation at points of stress. These cuticles, unlike body cuticle, are secreted in part by the underlying cell types, notably the muscle cells and pharyngeal epithelial cells (Avery, 1997; Hao *et al.,* 2006).

Localisation of F56C11.3 was also noted in the vulva muscle of adult nematodes, a noted site for production of the type IV collagen *emb-9* (Graham *et al.,* 1997). *qsox-2* has also been shown to localise to the pharynx muscle cells at all stages of development, the male tail hypodermis and to the dorso-ventral hypodermal cells, see chapters 5 and 6.

A.3 Discussion

F56C11.3, initially proposed as a QSOX enzyme, is more closely related to yeast Erv1p than to any other *C. elegans* QSOX enzyme.

F56C11.3 yeast Erv1p homologue

Splice leader PCR analysis using mixed stage N2 cDNA, with the splice leader consensus primers and F56C11.3 antisense primer, amplified a product of ~500bps, which had been *trans*-spliced with the 22 nucleotide SL1 sequence. Size determined by comparison with a known size standard. This confirmed the prediction made by wormbase, and targets F56C11.3 as a unique *C. elegans* gene consisting of only an ERV1/ALR domain with no other discernable domains. Of note was the lack of a signal peptide, and N-terminal thioredoxin domain, which are considered prerequisites for classification as a QSOX family member. These moieties were initially hypothesised to be present either as a splice variant, or that the prediction of this genes sequence had not been complete. Neither of these events was the case as no splice variants were detected and the prediction bore true. It could be concluded therefore that F56C11.3 is in fact not a QSOX family member, more closely resembling *S. cerevisiae* Erv1p. Yeast Erv1p shares a similar domain structure to F56C11.3 and conservation of an N-terminal CxxC motif out with the ERV1/ALR domain. The tertiary structure predictions of F56C11.3 and Erv1p made by 3Djigsaw, Figure A.2, showed conservation of the proximal disulphides within the FAD binding pocket and

similarly positioned N-terminal CxxC motifs in F56C11.3 and Erv1p. F56C11.3 and Erv1p also share structural similarities with Erv2p which does not contain an N-terminal CxxC but has a functionally similar CgC C-terminal domain (Hofhaus *et al.,* 2003). The conserved N-terminal cysteines have been shown in yeast to be in redox communication with the proximal disulphide in the ERV1/ALR domain, and are essential for the *in vivo* activity of the protein Erv1p (Hofhaus *et al.,* 2003). The N-terminal CxxC motif has also been shown to be involved in dimer formation in yeast Erv1p (Lee *et al.,* 2000; Gross *et al.,* 2002; Hofhaus *et al.,* 2003). This may be a functionality maintained in the *C. elegans* F56C11.3 N-terminal CxxC.

Feeding RNAi of F56C11.3 returned wild type worms, with respect to their COL-19 arrangement and gross morphological phenotype. It would thus appear that F56C11.3 is not involved with the generation of cuticle components secreted from the body hypodermal cells of *C. elegans,* or that there is redundancy between F56C11.3 and an as yet unknown protein (ERO-1 for example).

From lines generated by the Genome BC *C. elegans* Gene Expression Consortium, the spatial expression profile of F56C11.3 could be postulated as localising to; the pharynx and body wall muscle, of larva and adults, and vulval muscle cells in adults Figure A.4. The pharynx muscle cells have been reported as sites of production of the type IV collagens that line the pharynx (Avery, 1997; Hao *et al.,* 2006).

Organisms that lack QSOX enzymes (yeast) associate thioredoxin containing proteins, PDIs/thioredoxins, with ERV1/ALR homologs. PDI-1 associates with Erv1p in the yeast *S. cerevisiae* with the resulting effect of thiol reduction and subsequent generation of disulphide bonds (Gross *et al.,* 2002; Thorpe *et al.,* 2002; Coppock and Thorpe, 2006; Gross *et al.,* 2006). It is interesting to propose F56C11.3 as a partner protein associating with a PDI/thioredoxin containing protein, leading to co-operative disulphide bond generation in *C. elegans* collagens of the pharynx. Further to this PDI-1 has also been localised to the pharynx of *C. elegans* (Page, 1997) at the same developmental stages as F56C11.3. No association has been shown between F56C11.3 and PDI-1 at this point, and the association itself remains purely speculative. Further work into this, or any association would need to be performed to draw any such conclusions.

A further role for F56C11.3, which similarly would need investigation, is that F56C11.3 may be acting as an anti-microbial agent within the pharynx of the worm. F56C11.3 which still retains the potential for production of the ROS H_2O_2 may be so doing in the pharynx to

neutralise any ingested pathogens or bacteria in general. A similar model for oxidant/antioxidant response has been noted in *C. elegans* intestinal cells following of the colonisation of the intestinal lumen with the bacteria *Enterococcus faecalis* (Chávez, 2007).

Appendix B: Structural predictions for the QSOX enzymes.

B.1 Proposed structure of the QSOX family of enzymes based upon prediction by 3Djigsaw

Tertiary structure predictions were made for each of the QSOX enzymes using 3Djigsaw[15] and the output visualised using RASMOL v2.6. From these predictions it was noted that each of the QSOX enzymes contained both a thioredoxin like and ERV/ALR like fold. Full length polypeptides could not be visualised, as such the protein sequences were split in two, one portion containing the thioredoxin domain and a second portion containing the ERV/ALR. The structural predictions were based upon previously crystallised structures of thioredoxin proteins, Erv2p and human ALR. Of note in these unconfirmed structural predictions was the conservation of the N-terminal thioredoxin domain CxxC motifs, FigureB.1. The C-terminal ERV/ALR domains of QSOX-2 and 3 failed to produce any convincing structures. QSOX-1 however, produced an ERV/ALR domain which appeared similar to Erv2p.

These structures are based upon predictions using related previously crystallised proteins as a template and as such may not reflect the final structure of the enzymes *in vivo*. To resolve there actual structure each of the QSOX enzymes would need to be crystallised and undergo X-ray diffusion crystallography.

[15] www.bmm.icnet.uk/servers/3djigsaw/

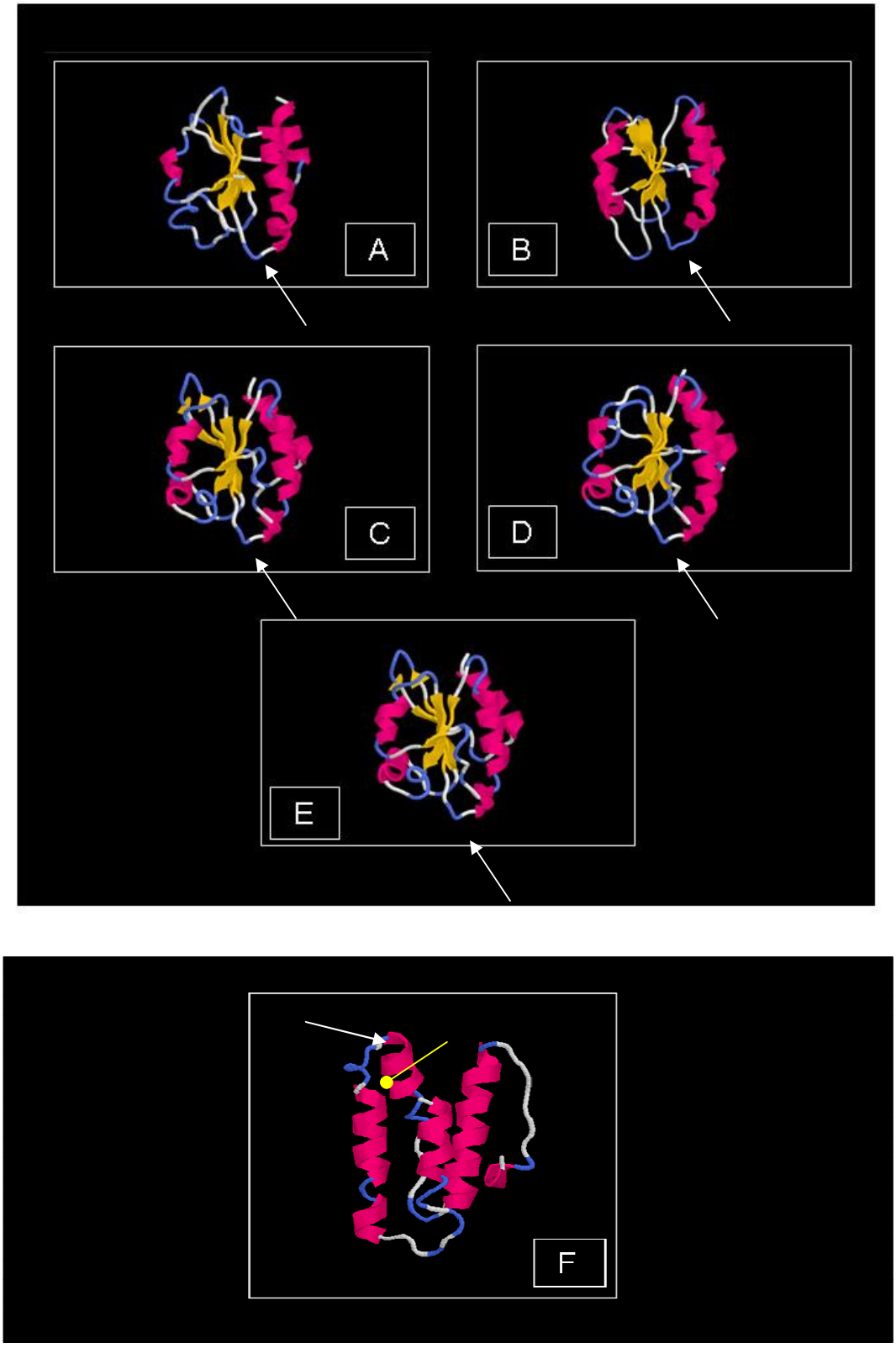

Figure B.1: Structural predictions for QSOX enzymes. (A) QSOX-1 thioredoxin domain (B) QSOX-2 thioredoxin domin (C-E) QSOX-3 thioredoxin domain, splice variants a, b and c respectively. (F) QSOX-1 ERV/ALR domain. Conserved CxxC motifs are highlighted by arrows in (A-E). (F) ERV/ALR domain of QSOX-1 white arrow shows the CxxC motif, and the yellow arrow shows the FAD binding pocket.

Appendix C: The *ka6* mutant allele.

C.1 ka6 candidate genes which lie within a 4cM range of *qsox-1*

Following are a list of genes found within 500kbps downstream and 500kbps upstream of *qsox-1* which also share RNAi/mutant phenotypes coincidental with those scored in the *ka6* strain. The genes listed here are a cursory overview of the immediate surrounding region centred upon the *qsox-1* locus, and should not be considered as a definitive list of candidate genes, a wider range than 4cM may need to be considered and mapped to determine the actual causative gene. Included are screen dumps (adapted from wrombase.org) for each gene, illustrating information such as expression profile and genomic location.

Gene Summary for rpl-11.2

Specify a gene using a gene name (unc-26), a predicted gene id (R13A5.9), or a protein ID (CE02711) rpl-11.2

[identification][location][function][expression][gene ontology][alleles][similarities][reagents][bibliography]

Identification

IDs:

CGC name	Sequence name	Other name(s)	WB Gene ID	Version
rpl-11.2 - (*Ribosomal Protein, Large subunit*)	F07D10.1	XC860 (inferred automatically) NM_076012 (inferred automatically)	WBGene00004423	1

Concise Description: rpl-11.2 encodes a large ribosomal subunit L11 protein; by homology, RPL-11.2 is predicted to function in protein biosynthesis. [details]

NCBI KOGs*: 60S ribosomal protein L11 [KOG0397]

Species: *Caenorhabditis elegans*

NCBI: [AceView: XC860] [RefSeq: NM_076012]

Gene model(s):

Gene Model	Status	Nucleotides (coding/transcript)	Protein	Amino Acids
F07D10.1.1 [1, 2, 3]	confirmed by cDNA(s)	591/992 bp	WP:CE07033	196 aa
F07D10.1.2 [1, 2, 3]	confirmed by cDNA(s)	591/872 bp	WP:CE07033	196 aa

⊞ Footnotes

Location

Interpolated Genetic Position: X:-15.99

Genomic Position: X:2242740..2241742 bp

Genomic Environs:

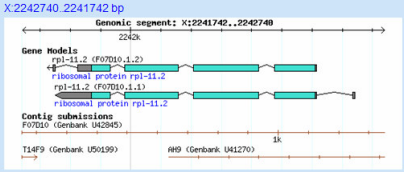

Expression

Anatomic expression pattern:

Larval Expression: pharynx; intestine; anal depressor muscle; Reproductive System; developing vulva; body wall muscle; hypodermis; Nervous System; nerve ring; head neurons; unidentified cells in head; unidentified cells in tail ;Adult Expression: pharynx; intestine; anal depressor muscle; body wall muscle; hypodermis; Nervous System; nerve ring; head neurons; unidentified cells in .. [Details: Expr:5672]

Function

Pre-WormBase information: Orthologous to yeast (S.cerevisiae) ribosomal protein rpl11 using blastP

Definitions of abbreviations used in the text.

RNAi Phenotype(s):

Primary targets* (RNAi experiments whose top identity in the genome is to rpl-11.2)

Phenotype	Observed (specific:nonspecific) / total experiments [1]	Cited in
larval arrest (Lva)	2 (0:2) / 2	Rual JF 2004, Simmer F 2003
slow growth (Gro)	2 (2:0) / 4	Maciejowski J 2005
pleiotropic defects severe early emb (Emb)	1 (1:0) / 2	Sonnichsen B 2005
maternal sterile (Ste)	1 (1:0) / 3	Sonnichsen B 2005
larval lethal (Lvl)	1 (0:1) / 1	Rual JF 2004
transgene subcellular localization abnormal	1 (1:0) / 1	Nollen EAA 2004

View all 10 RNAi experiments that target rpl-11.2

Secondary targets* (rpl-11.2 is a secondary target of the following RNAi experiments)

Phenotype	Observed (specific:nonspecific) / total experiments [1]	Cited in
embryonic lethal (Emb)	3 (0:0) / 3	Simmer F 2003, Piano F 2002, Sonnichsen B 2005
maternal sterile (Ste)	2 (0:0) / 3	Rual JF 2004, Piano F 2002
sterile progeny (Stp)	2 (0:0) / 2	Simmer F 2003, Piano F 2002
slow growth (Gro)	2 (0:0) / 4	Simmer F 2003, Piano F 2002
pleiotropic defects severe early emb (Emb)	1 (0:0) / 2	Sonnichsen B 2005
protruding vulva (Pvl)	1 (0:0) / 1	Simmer F 2003

View all 10 RNAi experiments that target rpl-11.2

rpl-11.2 encodes L11, a protein found within the large ribosomal subunit. Its functionality, which was conferred by homology, is predicted as being involved with protein biosynthesis. *rpl-11.2* is located at genetic position X:-15.99 and genomic position X:2242740..2241742 bp. *qsox-1* lies upstream at genetic position X:-15.85 and genomic position: X:2294743..2298144 bp, at a distance of ~0.14cM.

Phenotypes associated with RNAi of *rpl-11.2* in N2 strains included; pleiotropic embryonic defects, larval lethality and sterility (Maciejowski *et al.,* 2005). The expression profile of *rpl-11.2* highlights the hypodermis, pharynx, body wall muscle and unidentified head and tail cells (Maciejowski *et al.,* 2005) (Genome BC Gene Expression Consortium). RNAi phenotypes and an expression profile such as this highlighted *rpl-11.2* as a possible gene in which a mutation could account for the phenotypes seen in *ka6* worms.

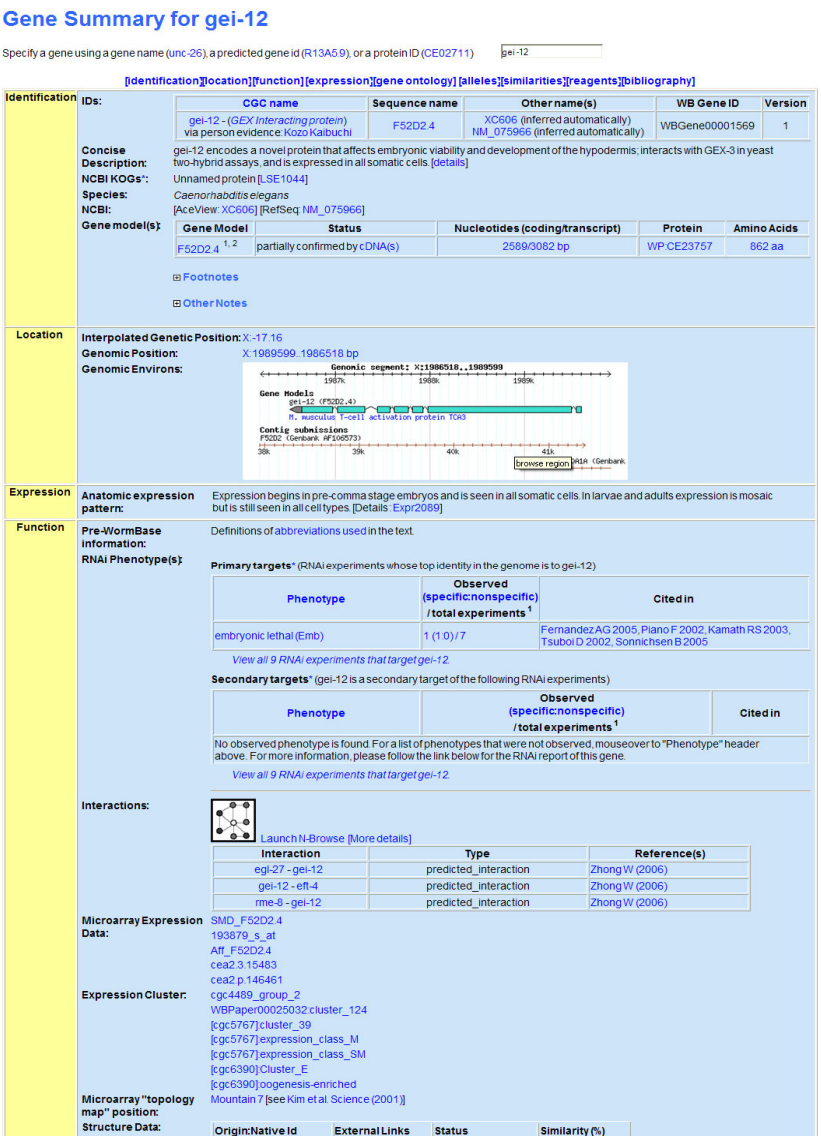

Gene Summary for gei-12

Specify a gene using a gene name (unc-26), a predicted gene id (R13A5.9), or a protein ID (CE02711) gei-12

[identification] [location] [function] [expression] [gene ontology] [alleles] [similarities] [reagents] [bibliography]

Identification

IDs:

CGC name	Sequence name	Other name(s)	WB Gene ID	Version
gei-12 - (*GEX Interacting protein*) via person evidence Kozo Kaibuchi	F52D2.4	XC606 (inferred automatically) NM_075966 (inferred automatically)	WBGene00001569	1

Concise Description: gei-12 encodes a novel protein that affects embryonic viability and development of the hypodermis; interacts with GEX-3 in yeast two-hybrid assays, and is expressed in all somatic cells. [details]

NCBI KOGs*: Unnamed protein [LSE1044]

Species: *Caenorhabditis elegans*

NCBI: [AceView: XC606] [RefSeq: NM_075966]

Gene model(s):

Gene Model	Status	Nucleotides (coding/transcript)	Protein	Amino Acids
F52D2.4 [1, 2]	partially confirmed by cDNA(s)	2589/3082 bp	WP:CE23757	862 aa

Footnotes

Other Notes

Location

Interpolated Genetic Position: X:-17.16

Genomic Position: X:1989599..1986518 bp

Genomic Environs:

Expression

Anatomic expression pattern: Expression begins in pre-comma stage embryos and is seen in all somatic cells. In larvae and adults expression is mosaic but is still seen in all cell types. [Details: Expr2089]

Function

Pre-WormBase information: Definitions of abbreviations used in the text.

RNAi Phenotype(s):

Primary targets* (RNAi experiments whose top identity in the genome is to gei-12)

Phenotype	Observed (specific:nonspecific) / total experiments [1]	Cited in
embryonic lethal (Emb)	1 (1:0) / 7	Fernandez AG 2005, Piano F 2002, Kamath RS 2003, Tsuboi D 2002, Sonnichsen B 2005

View all 9 RNAi experiments that target gei-12.

Secondary targets* (gei-12 is a secondary target of the following RNAi experiments)

Phenotype	Observed (specific:nonspecific) / total experiments [1]	Cited in
No observed phenotype is found. For a list of phenotypes that were not observed, mouseover to "Phenotype" header above. For more information, please follow the link below for the RNAi report of this gene.		

View all 9 RNAi experiments that target gei-12.

Interactions: Launch N-Browse [More details]

Interaction	Type	Reference(s)
egl-27 - gei-12	predicted_interaction	Zhong W (2006)
gei-12 - eft-4	predicted_interaction	Zhong W (2006)
rme-8 - gei-12	predicted_interaction	Zhong W (2006)

Microarray Expression Data: SMD_F52D2.4, 193879_s_at, Aff_F52D2.4, cea2.3.15483, cea2.p.146461

Expression Cluster: cgc4489_group_2, WBPaper00025032:cluster_124, [cgc5767]:cluster_39, [cgc5767]:expression_class_M, [cgc5767]:expression_class_SM, [cgc6390]:Cluster_E, [cgc6390]:oogenesis-enriched

Microarray "topology map" position: Mountain 7 [see Kim et al. Science (2001)]

Structure Data:

Origin:Native Id	External Links	Status	Similarity (%)

gei-12 encodes a novel protein that affects embryonic viability and development of the hypodermis; interacts with GEX-3 in yeast two-hybrid assays, and is expressed in all somatic cells.

gei-12 is located at genetic position: X:-17.16 which relates to genomic position: X:1989599..1986518 bp; ~2cM downstream of *qsox-1*. *gei-12* has been shown to associate with the essential gene *gex-3* (Tsuboi et al., 2002) . Mutations in *gex-3* cause embryonic lethality and hypodermal defects, shown by MH27 antibody staining (Soto *et al.,* 2002). *gei-12* RNAi also shows hypodermal defects, embryonic lethality and has been shown to be involved with hypodermal morphogenesis along with *gex-3* (Tsuboi *et al.,* 2002).

Based upon the morphological effects, disrupted seam cell localisation, and proximity with *qsox-1, gei-12* was also highlighted as a possible candidate gene in which a mutation could be responsible for the phenotypes scored in *ka6* animals.

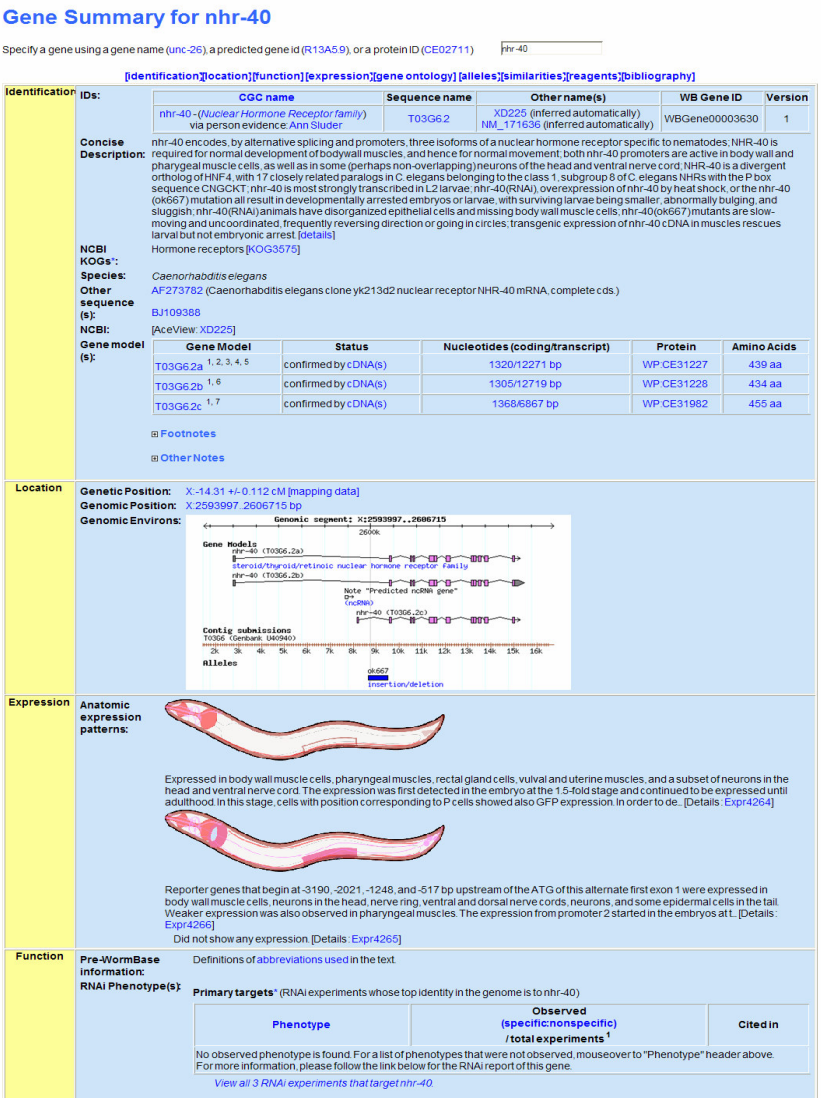

Gene Summary for nhr-40

Specify a gene using a gene name (unc-26), a predicted gene id (R13A5.9), or a protein ID (CE02711) nhr-40

[identification] [location] [function] [expression] [gene ontology] [alleles] [similarities] [reagents] [bibliography]

Identification

IDs:

CGC name	Sequence name	Other name(s)	WB Gene ID	Version
nhr-40 - (*Nuclear Hormone Receptor family*) via person evidence: Ann Sluder	T03G6.2	XD225 (inferred automatically) NM_171636 (inferred automatically)	WBGene00003630	1

Concise Description: nhr-40 encodes, by alternative splicing and promoters, three isoforms of a nuclear hormone receptor specific to nematodes; NHR-40 is required for normal development of bodywall muscles, and hence for normal movement; both nhr-40 promoters are active in body wall and pharygeal muscle cells, as well as in some (perhaps non-overlapping) neurons of the head and ventral nerve cord; NHR-40 is a divergent ortholog of HNF4, with 17 closely related paralogs in C. elegans belonging to the class 1, subgroup 8 of C. elegans NHRs with the P box sequence CNGCKT; nhr-40 is most strongly transcribed in L2 larvae; nhr-40(RNAi) overexpression of nhr-40 by heat shock, or the nhr-40 (ok667) mutation all result in developmentally arrested embryos or larvae, with surviving larvae being smaller, abnormally bulging, and sluggish; nhr-40(RNAi) animals have disorganized epithelial cells and missing body wall muscle cells; nhr-40(ok667) mutants are slow-moving and uncoordinated, frequently reversing direction or going in circles; transgenic expression of nhr-40 cDNA in muscles rescues larval but not embryonic arrest [details]

NCBI KOGs*: Hormone receptors [KOG3575]

Species: *Caenorhabditis elegans*

Other sequence (s): AF273782 (Caenorhabditis elegans clone yk213d2 nuclear receptor NHR-40 mRNA, complete cds.)

BJ109388

NCBI: [AceView: XD225]

Gene model (s):

Gene Model	Status	Nucleotides (coding/transcript)	Protein	Amino Acids
T03G6.2a [1, 2, 3, 4, 5]	confirmed by cDNA(s)	1320/12271 bp	WP:CE31227	439 aa
T03G6.2b [1, 6]	confirmed by cDNA(s)	1305/12719 bp	WP:CE31228	434 aa
T03G6.2c [1, 7]	confirmed by cDNA(s)	1368/6867 bp	WP:CE31982	455 aa

Footnotes

Other Notes

Location

Genetic Position: X:-14.31 +/- 0.112 cM [mapping data]

Genomic Position: X:2593997..2606715 bp

Genomic Environs:

Expression

Anatomic expression patterns:

Expressed in body wall muscle cells, pharyngeal muscles, rectal gland cells, vulval and uterine muscles, and a subset of neurons in the head and ventral nerve cord. The expression was first detected in the embryo at the 1.5-fold stage and continued to be expressed until adulthood. In this stage, cells with position corresponding to P cells showed also GFP expression. In order to de.. [Details: Expr4264]

Reporter genes that begin at -3190, -2021, -1248, and -517 bp upstream of the ATG of this alternate first exon 1 were expressed in body wall muscle cells, neurons in the head, nerve ring, ventral and dorsal nerve cords, neurons, and some epidermal cells in the tail. Weaker expression was also observed in pharyngeal muscles. The expression from promoter 2 started in the embryos at t.. [Details: Expr4266]

Did not show any expression [Details: Expr4265]

Function

Pre-WormBase information: Definitions of abbreviations used in the text.

RNAi Phenotype(s):

Primary targets* (RNAi experiments whose top identity in the genome is to nhr-40)

Phenotype	Observed (specific:nonspecific) / total experiments [1]	Cited in
No observed phenotype is found. For a list of phenotypes that were not observed, mouseover to "Phenotype" header above. For more information, please follow the link below for the RNAi report of this gene.		

View all 3 RNAi experiments that target nhr-40.

The NHR (nuclear hormone receptor) family has undergone extensive diversification in nematodes resulting in an expansive group which shares homology with vertebrate and insect NHRs.

nhr-40 is located at genetic position: X:-14.31 +/- 0.112 cM, genomic position: X:2593997..2606715 bp which translates to ~2cM upstream of the *qsox-1* locus. RNAi or knockout of *nhr-40* leads to phenocopy of the *ka6* strain, with larvae exhibiting severe body morphology defects (Brozova *et al.,* 2006). Phalloidin staining of *nhr-40(rb840)* worms demonstrated a disruption of the cytoskeleton of the worms body wall muscle which corresponded to regions of cuticle distortions (Brozova *et al.,* 2006). This agrees with the distortions seen in the alae of *ka6* worms, which was, in-part, hypothesised as being caused by a failure of the worms to contract correctly.

As can be seen in the report above, screen dump from wormbase.org, expression of *nhr-40* is noted in the pharynx and body wall muscles.

C.2 *ka6* candidate genes which lie out with a 4cM range of *qsox-1*

Searches of the X-chromosome, using the wormbase phenotype search applet, and the scored phenotypes associated with the segregated mutant strain uncovered several possible candidates.

dpy-23: Which encodes an adaptin: specifically, it encodes an ortholog of the *mu2* subunit of adaptor protein complex 2 (AP-2). During embryogenesis, DPY-23 is expressed in most if not all cells. After hatching, expression is prominent in neurons, while other regions of the body have less expression Genetic Position: X:-7.79 +/- 0.025cM Genomic Position: X:4389338..4393768bp.

lam-2: Extracellular matrix glycoprotein Laminin subunits alpha and gamma. Genetic Position: X:-1.82 Genomic Position: X:7151090..7144823bp.

nmy-1: Which encodes a class II non-muscle myosin heavy chain related to *Drosophila mellanogaster* zipper, which plays a role in several aspects of embryonic morphogenesis; in *C. elegans*, NMY-1 is required for embryonic elongation and establishment of normal body morphology. Expression of *nmy-1* is noted in embryos in undetermined cells and neuronaly in larval and adult worms.
Genetic Position: X:-12.67 +/- 0.003cM Genomic Position: X:2909547..2918027bp.

cut-5: CUT-5 is involved with the formation of the lateral alae and dorso-ventral shrinking in both dauer and L1 larvae (Sapio *et al.,* 2005). Expression of *cut-5* is localised to the seam cells in embryos (3-fold) and in dauer larvae. Genetic Position: X:1.92 +/- 0.015 cM Genomic Position: X:10338119..10333944bp

Of these candidate genes *nmy-1* mutants produce strong phenocopy of the *ka6* mutant larvae. NMY-1 has been shown to be involved with elongation of larvae during embryogenesis through involvement in the *let-502/mel-11* pathway and to function with *mlc-4/rMLC* to regulate the contractile process of elongation (Piekny *et al.,* 2003b).

C.3 *ka6* candidate genes out with the X-chromosome

Phenotype searches were performed across the entire genome to check for genes which showed phenocopy to the *ka6* strain. Among the genes found two in particular exhibited strong phenocopy, *pps-1*, which is involved with sulfation of biomolecules (Dejima *et al.,* 2006) and *egl-19*, a voltage gated Ca^{2+} channel (Jospin *et al.,* 2002)

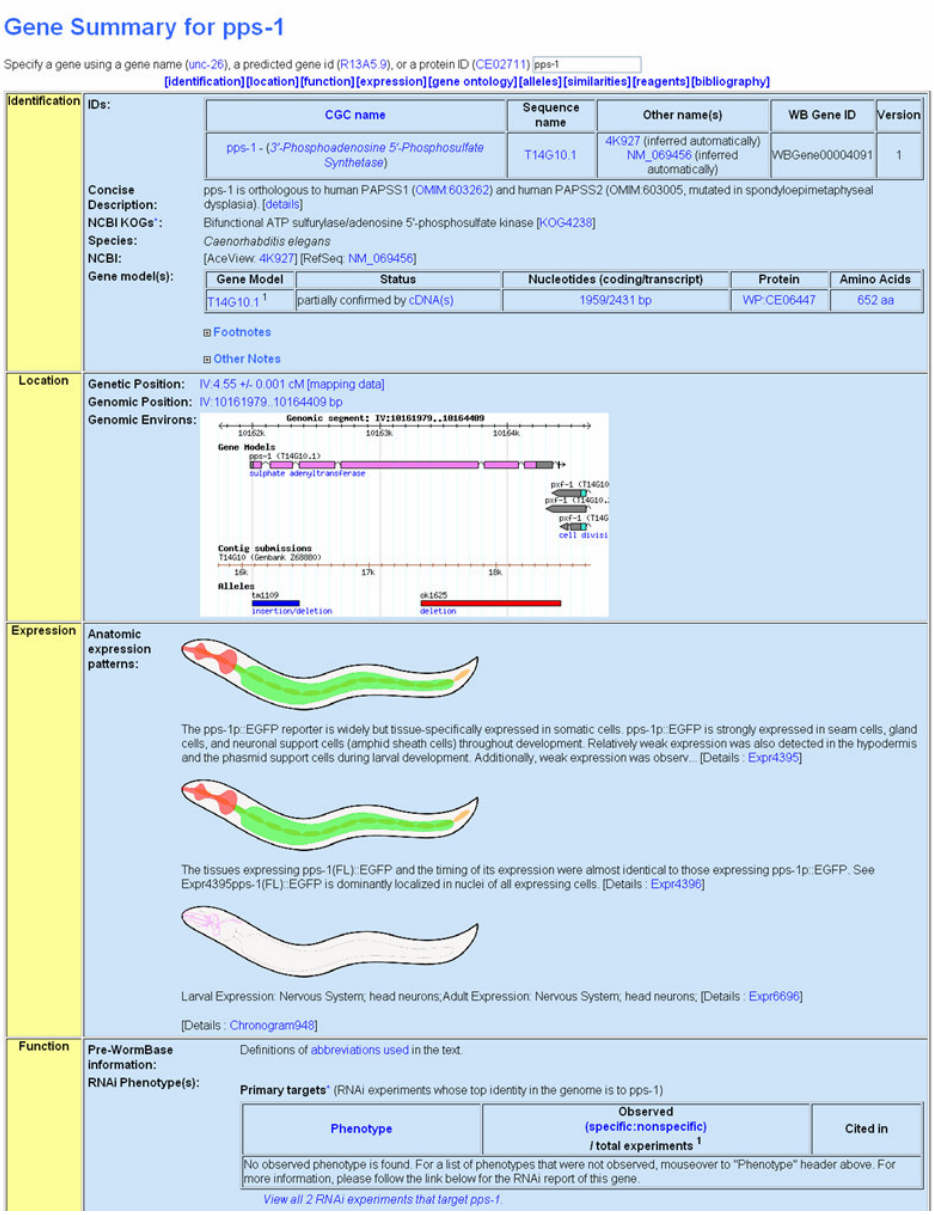

Gene Summary for pps-1

Specify a gene using a gene name (unc-26), a predicted gene id (R13A5.9), or a protein ID (CE02711) pps-1

[identification] [location] [function] [expression] [gene ontology] [alleles] [similarities] [reagents] [bibliography]

Identification

IDs:

CGC name	Sequence name	Other name(s)	WB Gene ID	Version
pps-1 - (*3'-Phosphoadenosine 5'-Phosphosulfate Synthetase*)	T14G10.1	4K927 (inferred automatically) NM_069456 (inferred automatically)	WBGene00004091	1

Concise Description: pps-1 is orthologous to human PAPSS1 (OMIM:603262) and human PAPSS2 (OMIM:603005, mutated in spondyloepimetaphyseal dysplasia). [details]

NCBI KOGs*: Bifunctional ATP sulfurylase/adenosine 5'-phosphosulfate kinase [KOG4238]

Species: *Caenorhabditis elegans*

NCBI: [AceView: 4K927] [RefSeq: NM_069456]

Gene model(s):

Gene Model	Status	Nucleotides (coding/transcript)	Protein	Amino Acids
T14G10.1 [1]	partially confirmed by cDNA(s)	1959/2431 bp	WP:CE06447	652 aa

Footnotes

Other Notes

Location

Genetic Position: IV:4.55 +/- 0.001 cM [mapping data]

Genomic Position: IV:10161979..10164409 bp

Genomic Environs:

Expression

Anatomic expression patterns:

The pps-1p::EGFP reporter is widely but tissue-specifically expressed in somatic cells. pps-1p::EGFP is strongly expressed in seam cells, gland cells, and neuronal support cells (amphid sheath cells) throughout development. Relatively weak expression was also detected in the hypodermis and the phasmid support cells during larval development. Additionally, weak expression was observ... [Details : Expr4395]

The tissues expressing pps-1(FL)::EGFP and the timing of its expression were almost identical to those expressing pps-1p::EGFP. See Expr4395pps-1(FL)::EGFP is dominantly localized in nuclei of all expressing cells. [Details : Expr4396]

Larval Expression: Nervous System; head neurons;Adult Expression: Nervous System; head neurons; [Details : Expr6696]

[Details : Chronogram948]

Function

Pre-WormBase information: Definitions of abbreviations used in the text.

RNAi Phenotype(s):

Primary targets* (RNAi experiments whose top identity in the genome is to pps-1)

Phenotype	Observed (specific:nonspecific) / total experiments [1]	Cited in
No observed phenotype is found. For a list of phenotypes that were not observed, mouseover to "Phenotype" header above. For more information, please follow the link below for the RNAi report of this gene.		

View all 2 RNAi experiments that target pps-1.

pps-1 RNAi was found to mimic the uncommon missing sections phenotype scored in *ka6* worms. Similar head distortions were also noted in *pps-1* RNAi treated animals (Dejima *et al.,* 2006). *pps-1* is located on autosome IV. The expression profile of *pps-1* is consistent with a role in cuticle biomolecule cross-linking. Phalloidin staining also shows distortion of the cytoskeleton of RNAi treated worms (Dejima *et al.,* 2006).

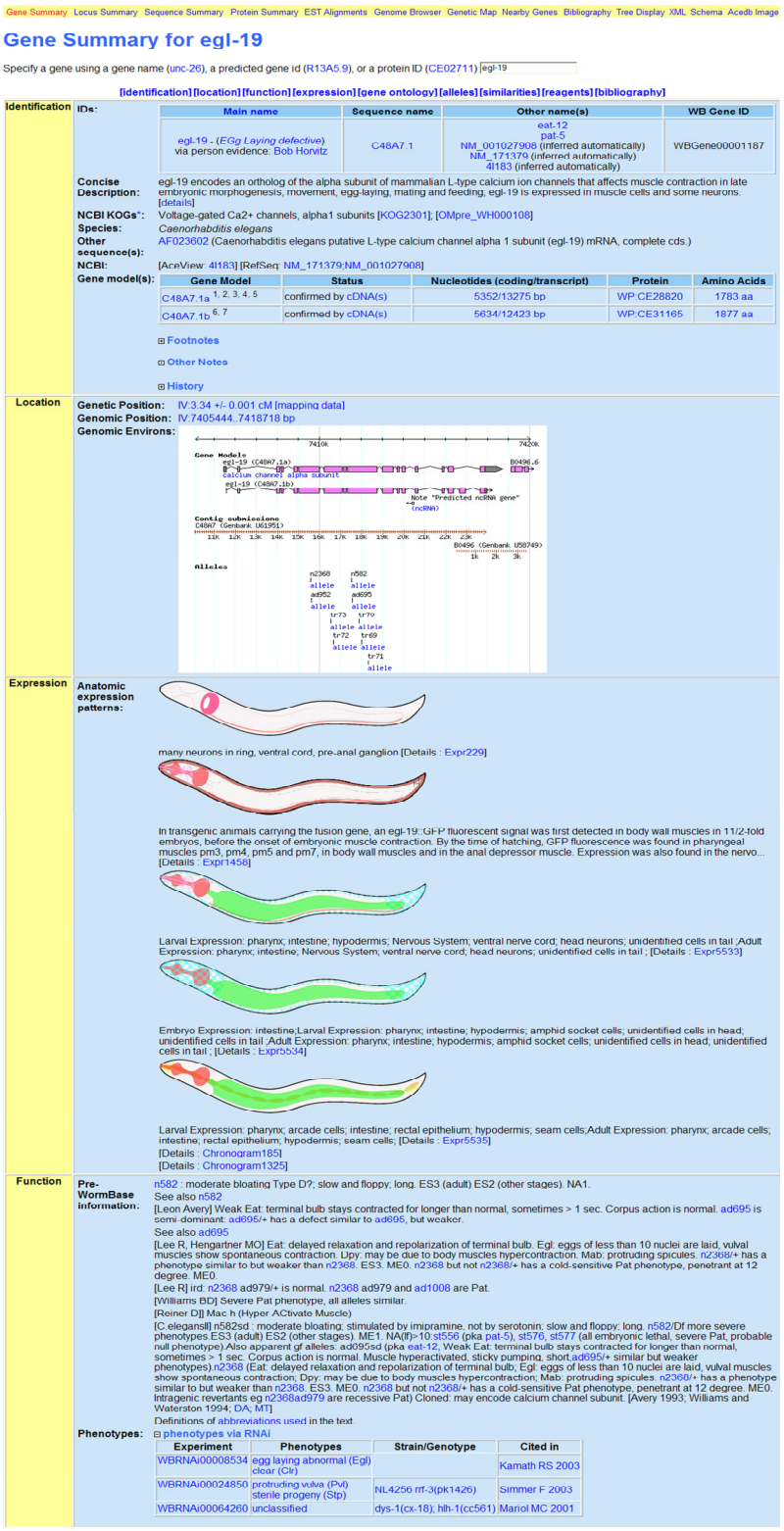

Gene Summary Locus Summary Sequence Summary Protein Summary EST Alignments Genome Browser Genetic Map Nearby Genes Bibliography Tree Display XML Schema Acedb Image

Gene Summary for egl-19

Specify a gene using a gene name (unc-26), a predicted gene id (R13A5.9), or a protein ID (CE02711) egl-19

[identification] [location] [function] [expression] [gene ontology] [alleles] [similarities] [reagents] [bibliography]

Identification

IDs:

Main name	Sequence name	Other name(s)	WB Gene ID
egl-19 - (*EGg Laying defective*) via person evidence: Bob Horvitz	C48A7.1	eat-12 pat-5 NM_001027908 (inferred automatically) NM_171379 (inferred automatically) 4l183 (inferred automatically)	WBGene00001187

Concise Description: egl-19 encodes an ortholog of the alpha subunit of mammalian L-type calcium ion channels that affects muscle contraction in late embryonic morphogenesis, movement, egg-laying, mating and feeding. egl-19 is expressed in muscle cells and some neurons. [details]

NCBI KOGs*: Voltage-gated Ca2+ channels, alpha1 subunits [KOG2301]; [OMpre_WH000108]

Species: *Caenorhabditis elegans*

Other sequence(s): AF023602 (Caenorhabditis elegans putative L-type calcium channel alpha 1 subunit (egl-19) mRNA, complete cds.)

NCBI: [AceView: 4l183] [RefSeq: NM_171379;NM_001027908]

Gene model(s):

Gene Model	Status	Nucleotides (coding/transcript)	Protein	Amino Acids
C48A7.1a [1, 2, 3, 4, 5]	confirmed by cDNA(s)	5352/13275 bp	WP:CE28820	1783 aa
C48A7.1b [6, 7]	confirmed by cDNA(s)	5634/12423 bp	WP:CE31165	1877 aa

Footnotes

Other Notes

History

Location

Genetic Position: IV:3.34 +/- 0.001 cM [mapping data]

Genomic Position: IV:7405444..7418718 bp

Genomic Environs:

Expression

Anatomic expression patterns:

many neurons in ring, ventral cord, pre-anal ganglion [Details : Expr229]

In transgenic animals carrying the fusion gene, an egl-19::GFP fluorescent signal was first detected in body wall muscles in 1 1/2-fold embryos, before the onset of embryonic muscle contraction. By the time of hatching, GFP fluorescence was found in pharyngeal muscles pm3, pm4, pm5 and pm7, in body wall muscles and in the anal depressor muscle. Expression was also found in the nervo... [Details : Expr1458]

Larval Expression: pharynx; intestine; hypodermis; Nervous System; ventral nerve cord; head neurons; unidentified cells in tail ;Adult Expression: pharynx; intestine; Nervous System; ventral nerve cord; head neurons; unidentified cells in tail ; [Details : Expr5533]

Embryo Expression: intestine;Larval Expression: pharynx; intestine; hypodermis; amphid socket cells; unidentified cells in head; unidentified cells in tail ;Adult Expression: pharynx; intestine; hypodermis; amphid socket cells; unidentified cells in head; unidentified cells in tail ; [Details : Expr5534]

Larval Expression: pharynx; arcade cells; intestine; rectal epithelium; hypodermis; seam cells;Adult Expression: pharynx; arcade cells; intestine; rectal epithelium; hypodermis; seam cells; [Details : Expr5535]

[Details : Chronogram185]

[Details : Chronogram1325]

Function

Pre-WormBase information:

n582 : moderate bloating Type D?; slow and floppy; long. ES3 (adult) ES2 (other stages). NA1.
See also n582
[Leon Avery] Weak Eat: terminal bulb stays contracted for longer than normal, sometimes > 1 sec. Corpus action is normal. ad695 is semi-dominant: ad695/+ has a defect similar to ad695, but weaker.
See also ad695
[Lee R, Hengartner MO] Eat: delayed relaxation and repolarization of terminal bulb. Egl: eggs of less than 10 nuclei are laid, vulval muscles show spontaneous contraction. Dpy: may be due to body muscles hypercontraction. Mab: protruding spicules. n2368/+ has a phenotype similar to but weaker than n2368. ES3. ME0. n2368 but not n2368/+ has a cold-sensitive Pat phenotype, penetrant at 12 degree. ME0.
[Lee R] ird: n2368 ad979/+ is normal. n2368 ad979 and ad1008 are Pat.
[Williams BD] Severe Pat phenotype, all alleles similar.
[Reiner DJ] Mac h (Hyper ACtivate Muscle)
[C. elegans] n582sd : moderate bloating; stimulated by imipramine, not by serotonin; slow and floppy; long. n582/Df more severe phenotypes.ES3 (adult) ES2 (other stages). ME1. NA(lf)>10:st556 (pka pat-5), st576, st577 (all embryonic lethal, severe Pat, probable null phenotype).Also apparent gf alleles: ad095sd (pka eat-12, Weak Eat: terminal bulb stays contracted for longer than normal, sometimes > 1 sec. Corpus action is normal. Muscle hyperactivated, sticky pumping, short.ad695/+ similar but weaker phenotypes).n2368 [Eat: delayed relaxation and repolarization of terminal bulb; Egl: eggs of less than 10 nuclei are laid, vulval muscles show spontaneous contraction; Dpy: may be due to body muscles hypercontraction; Mab: protruding spicules. n2368/+ has a phenotype similar to but weaker than n2368. ES3. ME0. n2368 but not n2368/+ has a cold-sensitive Pat phenotype, penetrant at 12 degree. ME0. Intragenic revertants eg n2368ad979 are recessive Pat) Cloned: may encode calcium channel subunit. [Avery 1993; Williams and Waterston 1994; DA; MT]
Definitions of abbreviations used in the text

Phenotypes: phenotypes via RNAi

Experiment	Phenotypes	Strain/Genotype	Cited in
WBRNAi00008534	egg laying abnormal (Egl) clear (Clr)		Kamath RS 2003
WBRNAi00024850	protruding vulva (Pvl) sterile progeny (Stp)	NL4256 rrf-3(pk1426)	Simmer F 2003
WBRNAi00064260	unclassified	dys-1(cx-18); hih-1(cc561)	Mariol MC 2001

egl-19 mutants also exhibit similar morphological disruptions to those seen in the *ka6* strain (Lee *et al.*, 1997). *egl-19* is located on chromosome IV and is postulated as encoding a voltage-activated L-type Ca^{2+} channel which controls body wall muscle formation. *egl-19* mutations *ad980* and *ad991* result in *C. elegans* with variable bulging larvae and occasionally produce arrested 2-fold embryos (Jospin *et al.*, 2002), both characteristics of the segregated mutant strain.

C.4 Summary

From this initial *in silico* analysis of the immediate surrounding region of *qsox-1* and genome wide phenotype searches, candidates that may be responsible for the *ka6* phenotypes were postulated. The genes highlighted share common features of hypodermal expression and a functionality of either protein biosynthesis or are involved with cellular arrangement. *nhr-40* does not show hypodermal expression but is still required for wild type cuticular ECM development of larval *C. elegans* (Brozova *et al.,* 2006). Other family members such as *nhr-23*, have been shown to be involved with cuticle formation through collagen expression level control (Kostrouchova *et al.,* 2001). *nmy-1* does not show hypodermal expression but has a role in collagen and cuticlin based cuticle development, inferred from mutant phenotype, and involvement in larval development (Piekny *et al.,* 2003b). *egl-19*, although hypodermally expressed, does not affect body morphology by cuticle protein modification instead through muscle paralysis or excessive contraction can cause the cuticular ECM to malform.

There are many other genes in which mutations could lead to the phenotypes seen in *ka6* nematodes; therefore, 2-point and 3-point mapping would need to be performed to assign the causative gene responsible for the phenotypes scored in *ka6* animals. However, before mapping was to begin it would prove interesting to perform RNAi with the genes listed here on *ka6* mutants to examine if any association existed.

References.

Adams, J. C. (2001). Thrombospondins: Multifunctional regulators of cell interactions. *Annual Review Of Cell And Developmental Biology* **17**, 25-51.

Aguinaldo, A. M. A., Turbeville, J. M., Linford, L. S., Rivera, M. C., Garey, J. R., Raff, R. A. and Lake, J. A. (1997). Evidence for a clade of nematodes, arthropods and other moulting animals. *Nature* **387**, 489-493.

Allen, I. W. a. D. G. (2007). The role of reactive oxygen species in the hearst of dystrophin deficient mdx mice. *Am j Physiol Heart Circ Physiol*.

Altun, Z. F. a. H., D. H. (2005). Handbook of *C. elegans* Anatomy. *Worm Atlas* http://www.wormatlas.org/handbook/contents.htm.

Amiot, C., Musard, J. F., Hadjiyiassemis, M., Jouvenot, M., Fellmann, D., Risold, P. Y. and Adami, P. (2004). Expression of the secreted FAD-dependent sulfydryl oxidase (QSOX) in the guinea pig central nervous system. *Molecular Brain Research* **125**, 13-21.

Annunen, P., Koivunen, P. and Kivirikko, K. I. (1999). Cloning of the α subunit of prolyl 4-hydroxylase from *Drosophila* and expression and characterization of the corresponding enzyme tetramer with some unique properties. *Journal of Biological Chemistry* **274**, 6790-6796.

Annunen, P., Helaakoski, T., Myllyharju, J., Veijola, J., Pihlajaniemi, T. and Kivirikko, K. I. (1997). Cloning of the human prolyl 4-hydroxylase α subunit isoform α(II) and characterization of the type II enzyme tetramer. The α(I) and α(II) subunits do not form a mixed $\alpha(I)\alpha(II)\beta_2$ tetramer. *Journal of Biological Chemistry* **272**, 17342-17348.

Appella, E., Weber, I. T. and Blasi, F. (1988). Structure And Function Of Epidermal Growth Factor-Like Regions In Proteins. *Febs Letters* **231**, 1-4.

Araki, E., Oyadomari, S. and Mori, M. (2003). Impact of endoplasmic reticulum stress pathway on pancreatic beta-cells and diabetes mellitus. *Experimental Biology And Medicine* **228**, 1213-1217.

Arbeitman, M. N., Fleming, A. A., Siegal, M. L., Null, B. H. and Baker, B. S. (2004). A genomic analysis of *Drosophila* somatic sexual differentiation and its regulation. *Development* **131**, 2007-2021.

Asahina, M., Ishihara, T., Jindra, M., Kohara, Y., Katsura, I. and Hirose, S. (2000). The conserved nuclear receptor Ftz-F1 is required for embryogenesis, moulting and reproduction in *Caenorhabditis elegans*. *Genes to Cells* **5**, 711-723.

Avery, L. (1997). Feeding and Defication: Cold harbour springs.

Barkwell, R. and Shields, S. (1997). Deaths associated with ivermectin treatment of scabies. *Lancet* **349**, 1144-1145.

Benayoun, B., Esnard-Feve, A., Castella, S., Courty, Y. and Esnard, F. (2001). Rat seminal vesicle FAD-dependent sulfhydryl oxidase - Biochemical characterization and molecular cloning of a member of the new sulfhydryl oxidase/quiescin Q6 gene family. *Journal Of Biological Chemistry* **276**, 13830-13837.

Bisoffi, M. and Betschart, B. (1996). Identification and sequence comparison of a cuticular collagen of *Brugia pahangi*. *Parasitology* **113**, 145-155.

Blasko, B., Madi, A. and Fesus, L. (2003). Thioredoxin motif of *Caenorhabditis elegans* PDI-3 provides Cys and His catalytic residues for transglutaminase activity. *Biochemical And Biophysical Research Communications* **303**, 1142-1147.

Blaxter, M. (1998). *Caenorhabditis elegans* is a nematode. *Science* **282**, 2041-2046.

Blaxter, M. L., De Ley, P., Garey, J. R., Liu, L. X., Scheldeman, P., Vierstraete, A., Vanfleteren, J. R., Mackey, L. Y., Dorris, M., Frisse, L. M. et al. (1998b). A molecular evolutionary framework for the phylum Nematoda. *Nature* **392**, 71-75.

Blumenthal, T. and Steward, K. (1997). RNA processing and gene structure. *In, C. elegans II, (Riddle, D. L., Blumenthal, T., Meyer, B. J., Priess, J. R., eds)* **Cold Spring Harbour Laboratory Press, Cold Spring Harbour, NY**, pp. 117-145.

Blumenthal, T., Evans, D., Link, C. D., Guffanti, A., Lawson, D., Thierry-Mieg, J., Thierry-Mieg, D., Chiu, W. L., Duke, K., Kiraly, M. et al. (2002). A global analysis of *Caenorhabditis elegans* operons. *Nature* **417**, 851-854.

Bode, W., Gomisruth, F. X. and Stockler, W. (1993). Astacins, serralysins, snake-venom and matrix metalloproteinases exhibit identical zinc-binding environments (Hexxhxxgxxh and Met-Turn) and topologies and should be grouped into a common family, The Metzincins. *Febs Letters* **331**, 134-140.

Bond, J. S. and Beynon, R. J. (1995). The Astacin Family Of Metalloendopeptidases. *Protein Science* **4**, 1247-1261.

Bork, P. (1991). Complement Components Clr/Cls, Bone Morphogenic Protein-1 and *Xenopus-Laevis* Developmentally Regulated Protein Uvs.2 Share Common Repeats. *Febs Letters* **282**, 9-12.

Bork, P. and Beckmann, G. (1993). The Cub Domain - A Widespread Module In Developmentally-Regulated Proteins. *Journal Of Molecular Biology* **231**, 539-545.

Bornstein, P. (2003). Covalent cross-links in collagen: a personal account of their discovery. *Matrix Biology* **22**, 385-391.

Brenner, S. (1974). The genetics of *Caenorhabditis elegans*. *Genetics* **77**, 71-94.

Britton, C. and Murray, L. (2002). A cathepsin L protease essential for *Caenorhabditis elegans* embryogenesis is functionally conserved in parasitic nematodes. *Molecular and Biochemical Parasitology* **122**, 21-33.

Britton, C. and Murray, L. (2006). Using *Caenorhabditis elegans* for functional analysis of genes of parasitic nematodes. *International Journal For Parasitology* **36**, 651-659.

Brooks, D. R., Appleford, P. J., Murray, L. and Isaac, R. E. (2003). An essential role in molting and morphogenesis of *Caenorhabditis elegans* for ACN-1, a novel member of the angiotensin-converting enzyme family that lacks a metallopeptidase active site. *Journal Of Biological Chemistry* **278**, 52340-52346.

Brozova, E., Simeckova, K., Kostrouch, Z., Rall, J. E. and Kostrouchova, M. (2006). NHR-40, a *Caenorhabditis elegans* supplementary nuclear receptor, regulates embryonic and early larval development. *Mechanisms Of Development* **123**, 689-701.

Brubacher, J. L. and Bols, N. C. (2001). Chemically de-acetylated 2 ',7 '-dichlorodihydrofluorescein diacetate as a probe of respiratory burst activity in mononuclear phagocytes. *Journal Of Immunological Methods* **251**, 81-91.

Bullerjahn, A. M. E. and Riddle, D. L. (1988). Fine-Structure Genetics Of *ama-1*, An Essential Gene Encoding The Amanitin-Binding Subunit Of RNA Polymerase-II In *Caenorhabditis elegans*. *Genetics* **120**, 423-434.

Campbell, L. R. and Gaugler, R. (1991). Mechanisms For Exsheathment Of Entomopathogenic Nematodes. *International Journal For Parasitology* **21**, 219-224.

Cariello, L., Velasco, P. T., Wilson, J., Parameswaran, K. N., Karush, F. and Lorand, L. (1990). Probing the transglutaminase-mediated, post-translational modification of proteins during development. *Biochemistry* **29**, 5103-5108.

Chakravarthi, S., Jessop, C. E. and Bulleid, N. J. (2006). The role of glutathione in disulphide bond formation and endoplasmic-reticulum-generated oxidative stress. *Embo Reports* **7**, 271-275.

Chalfie, M., Tu, Y., Euskirchen, G., Ward, W. W. and Prasher, D. C. (1994). Green fluorescent protein as a marker for gene expression. *Science* **263**, 802-805.

Chandrashekar, R., Devarajan, E. and Mehta, K. (2002). *Dirofilaria immitis*: further characterization of the transglutaminase enzyme and its role in larval molting. *Parasitology Research* **88**, 185-191.

Chandrashekar, R., Tsuji, N., Morales, T., Ozols, V. and Mehta, K. (1998). An ERp60-like protein from the filarial parasite *Dirofilaria immitis* has both transglutaminase and protein disulfide isomerase activity. *Proceedings of the National Academy of Sciences of the United States of America* **95**, 531-536.

Chávez, V. A. M.-S., Arash Maadani, Luis Alberto Vega and Danielle A. Garsin. (2007). Oxidative stress enzymes are required for DAF-16 mediated immunity due to generation of reactive oxygen species by *Caenorhabditis elegans*. *Genetics* **vol167**, 1567-1577.

Chen, X. D., Fisher, L. W., Robey, P. G. and Young, M. F. (2004). The small leucine-rich proteoglycan biglycan modulates BMP-4-induced osteoblast differentiation. *Faseb Journal* **18**, 948-958.

Cohen, E. (2001). Chitin synthesis and inhibition: a revisit. *Pest Management Science* **57**, 946-950.

Consortium. (1998). Genome sequence of the nematode *C. elegans*: a platform for investigating biology. *Science* **282**, 2012-2018.

Coppock, D. L. and Thorpe, C. (2006). Multidomain flavin-dependent sulfhydryl oxidases. *Antioxidants & Redox Signaling* **8**, 300-311.

Costa, M., Draper, B. W. and Priess, J. R. (1997). The role of actin filaments in patterning the *Caenorhabditis elegans* cuticle. *Developmental Biology* **184**, 373-384.

Cox, G. N. (1992). Molecular and biochemical aspects of nematode cuticle collagens. *Journal of Parasitology* **78**, 1-15.

Cox, G. N., Kusch, M. and Edgar, R. S. (1981). Cuticle of *Caenorhabditis elegans*: its isolation and partial characterisation. *Journal of Cell Biology* **90**, 7-17.

Cox, G. N., Staprans, S. and Edgar, R. S. (1981b). The cuticle of *Caenorhabditis elegans* II. Stage-specific changes in ultrastructure and protein composition during postembryonic development. *Developmental Biology* **86**, 456-470.

Cox, G. N., Kusch, M., Denevi, K. and Edgar, R. S. (1981c). Temporal regulation of cuticle synthesis during development of *Caenorhabditis elegans*. *Developmental Biology* **84**, 277-285.

Craig, H., Isaac, R. E. and Brooks, D. R. (2007). Unravelling the moulting degradome: new opportunities for chemotherapy? *Trends In Parasitology* **23**, 248-253.

Davies, K. G., Fargette, M., Balla, G., Daudi, A., Duponnois, R., Gowen, S. R., Mateille, T., Phillips, M. S., Sawadogo, S., Trivino, C. et al. (2001). Cuticle heterogeneity as exhibited by Pasteuria spore attachment is not linked to the phylogeny of parthenogenetic root-knot nematodes (*Meloidogyne spp.*). *Parasitology* **122**, 111-120.

Davis, M. W., Birnie, A. J., Chan, A. C., Page, A. P. and Jorgensen, E. M. (2004). A conserved metalloprotease mediates ecdysis in *Caenorhabditis elegans*. *Development* **131**, 6001-6008.

De Maere, V., Vercauteren, I., Geldhof, P., Gevaert, K., Vercruysse, J. and Claerebout, E. (2005). Molecular analysis of astacin-like metalloproteases of *Ostertagia ostertagi. Parasitology* **130**, 89-98.

Dejima, K., Seko, A., Yamashita, K., Gengyo-Ando, K., Mitani, S., Izumikawa, T., Kitagawa, H., Sugahara, K., Mizuguchi, S. and Nomura, K. (2006). Essential roles of 3 '-phosphoadenosine 5 '-phoshosulfate synthase in embryonic and larval development of the nematode *Caenorhabditis elegans*. *Journal Of Biological Chemistry* **281**, 11431-11440.

Dent, J. A., Smith, M. M., Vassilatis, D. K. and Avery, L. (2000). The genetics of ivermectin resistance in *Caenorhabditis elegans*. *Proceedings Of The National Academy Of Sciences Of The United States Of America* **97**, 2674-2679.

Dhadialla, T. S., Carlson, G. R. and Le, D. P. (1998). New insecticides with ecdysteroidal and juvenile hormone activity. *Annual Review Of Entomology* **43**, 545-569.

Doolittle, R. F., Feng, D. F. and Johnson, M. S. (1984). Computer-based characterization of epidermal growth-factor precursor. *Nature* **307**, 558-560.

Dorris, M., De Ley, P. and Blaxter, M. L. (1999). Molecular analysis of nematode diversity and the evolution of parasitism. *Parasitology Today* **15**, 188-193.

Edens, W. A., Sharling, L., Cheng, G. J., Shapira, R., Kinkade, J. M., Lee, T., Edens, H. A., Tang, X. X., Sullards, C., Flaherty, D. B. et al. (2001). Tyrosine cross-linking of extracellular matrix is catalyzed by Duox, a multidomain oxidase/peroxidase with homology to the phagocyte oxidase subunit gp91 *phox*. *Journal of Cell Biology* **154**, 879-891.

Ellis, R. E. and Horvitz, H. R. (1991). Two *C. elegans* genes control the programmed deaths of specific cells in the pharynx. *Development* **112**, 591-603.

Engel, J. and Prockop, D. J. (1991). The zipper-like folding of collagen triple helices and the effects of mutations that disrupt the zipper. *Annual Review of Biophysics and Biophysical Chemistry* **20**, 137- 152.

Entchev, E. V. and Kurzchalia, T. V. (2005). Requirement of sterols in the life cycle of the nematode *Caenorhabditis elegans*. *Seminars In Cell & Developmental Biology* **16**, 175-182.

Eschenlauer, S. C. P. and Page, A. P. (2003). The *Caenorhabditis elegans* ERp60 homolog PDI-3 has disulphide isomerase and transglutaminase-like cross-linking activity and is involved in the maintainance of body morphology. *Journal of Biological Chemistry*, 4227-4237.

Fetterer, R. H. and Rhoads, M. L. (1990). Tyrosine-derived cross-linking amino acids in the sheath of *Haemonchus contortus* infective larvae. *Journal of Parasitology* **76**, 619-624.

Fetterer, R. H., Rhoads, M. L. and Urban, J. F. (1993). Synthesis of tyrosine-derived cross-links in *Ascaris suum* cuticular proteins. *Journal of Parasitology* **79**, 160-166.

Fire, A. (1992). Histochemical techniques for locating *Escherichia coli* β-galactosidase activity in transgenic organisms. *Genetic Analysis-Biomolecular Engineering* **9**, 151-158.

Fire, A., White Harrison, S. and Dixon, D. (1990). A modular set of *lacZ* fusion vectors for studying gene expression in *Caenorhabditis elegans*. *Gene* **93**, 189-198.

Fire, A., Xu, S. Q., Montgomery, M. K., Kostas, S. A., Driver, S. E. and Mello, C. C. (1998). Potent and specific genetic interference by double-stranded RNA in *Caenorhabditis elegans*. *Nature* **391**, 806-811.

Frand, A. R., Cuozzo, J. W. and Kaiser, C. A. (2000). Pathways for protein disulphide bond formation. *Trends In Cell Biology* **10**, 203-210.

Frand, A. R., Russel, S. and Ruvkun, G. (2005). Functional genomic analysis of *C. elegans* molting. *Plos Biology* **3**, 1719-1733.

Friedman, L., Higgin, J. J., Moulder, G., Barstead, R., Raines, R. T. and Kimble, J. (2000). Prolyl 4-hydroxylase is required for viability and morphogenesis in *Caenorhabditis elegans*. *Proceedings of the National Academy of Sciences of the United States of America* **97**, 4736-4741.

Fu, B. Q., Liu, M. Y., Kapel, C. M. O., Meng, X. P., Lu, Q., Wu, X. P., Chen, Q. J. and Boireau, P. (2005). Molecular cloning of a cDNA encoding a putative cuticle collagen of *Trichinella spiralis*. *Veterinary Parasitology* **132**, 31-35.

Fujimoto, D. (1975). Occurrence of dityrosine in cuticlin, a structural protein from *Ascaris* cuticle. *Comparative Biochemistry And Physiology B-Biochemistry & Molecular Biology* **51**, 205-207.

Fujimoto, D., Horiuchi, K. and Hirama, M. (1981). Isotrityrosine, a new crosslinking amino acid isolated from *Ascaris* cuticle collagen. *Biochemical and Biophysical Research Communications* **99**, 637-643.

Gallo, M., Mah, A. K., Johnsen, R. C., Rose, A. M. and Baillie, D. L. (2006). *Caenorhabditis elegans dpy-14*: an essential collagen gene with unique expression

profile and physiological roles in early development. *Molecular Genetics And Genomics* **275**, 527-539.

Gamble, H. R., Lichtenfels, J. R. and Purcell, J. P. (1989b). Light and scanning electron-microscopy of the ecdysis of *Haemonchus contortus* infective larvae. *Journal Of Parasitology* **75**, 303-307.

Gamble, H. R., Purcell, J. P. and Fetterer, R. H. (1989). Purification of a 44 kilodalton protease which mediates the ecdysis of infective *Haemonchus contortus* larvae. *Molecular And Biochemical Parasitology* **33**, 49-58.

Garciacastineiras, S., Dillon, J. and Spector, A. (1978). Detection of bityrosine in cataractous human lens protein. *Science* **199**, 897-899.

Gaugler, R., McGuire, T. and Campbell, J. (1989). Genetic-Variability Among Strains Of The Entomopathogenic Nematode Steinernema-Feltiae. *Journal Of Nematology* **21**, 247-253.

Geldhof, P., Murray, L., Couthier, A., Gilleard, J. S., McLauchlan, G., Knox, D. P. and Britton, C. (2006). Testing the efficacy of RNA interference in *Haemonchus contortus*. *International Journal For Parasitology* **36**, 801-810.

Geldhof, P., Vercauteren, I., Knox, D., Demaere, V., Van Zeveren, A., Berx, G., Vercruysse, J. and Claerebout, E. (2003). Protein disulphide isomerase of *Ostertagia ostertagi*: an excretory-secretory product of L4 and adult worms? *International Journal for Parasitology* **33**, 129-136.

Gelse, K., Poschl, E. and Aigner, T. (2003). Collagens - structure, function, and biosynthesis. *Advanced Drug Delivery Reviews* **55**, 1531-1546.

Gerber, J., Muhlenhoff, U., Hofhaus, G., Lill, R. and Lisowsky, T. (2001). Yeast Erv2p is the first microsomal FAD-linked sulfhydryl oxidase of the Erv1p/Alrp protein family. *Journal Of Biological Chemistry* **276**, 23486-23491.

Ghedin, E. W., S.Spiro, D. Elisabet Caler, Qi Zhao, Jonathan Crabtree, Jonathan E. Allen, Arthur L. Delcher, David B. Guiliano, Diego Miranda-Saavedra,Samuel V. Angiuoli, Todd Creasy, Paolo Amedeo, Brian Haas, Najib M. El-Sayed,et al. (2007). Draft Genome of the Filarial Nematode Parasite *Brugia malayi*. *Science* **317**, 1756-1760.

Gilleard, J. S. (2004). The use of *Caenorhabditis elegans* in parasitic nematode research. *Parasitology* **128**, S49-S70.

Gissendanner, C. R. and Sluder, A. E. (2000). *nhr-25*, the *Caenorhabditis elegans* ortholog of *ftz-f1*, is required for epidermal and somatic gonad development. *Developmental Biology* **221**, 259-272.

Goicoechea, S., Pallero, M. A., Eggleton, P., Michalak, M. and Murphy-Ullrich, J. E. (2002). The anti-adhesive activity of thrombospondin is mediated by the N-terminal domain of cell surface calreticulin. *Journal Of Biological Chemistry* **277**, 37219-37228.

Gomisruth, F. X., Stocker, W., Huber, R., Zwilling, R. and Bode, W. (1993). Refined 1.8 angstrom X-Ray crystal-structure of astacin, a zinc-endopeptidase from the crayfish *Astacus astacus* L - structure determination, refinement, molecular-structure and comparison with thermolysin. *Journal Of Molecular Biology* **229**, 945-968.

Gönczy, P., Echeverri, C., Oegema, K., Coulson, A. R., Jones, S. J. M., Copley, R. R., Duperon, J., Oegema, J., Brehm, M., Cassin, E. et al. (2000). Functional genomic analysis of cell division in *C. elegans* using RNAi of genes on chromosome III. *Nature* **408**, 331-336.

Graham, P. L., Johnson, J. J., Wang, S. R., Sibley, M. H., Gupta, M. C. and Kramer, J. M. (1997). Type IV collagen is detectable in most, but not all, basement membranes of *Caenorhabditis elegans* and assembles on tissues that do not express it. *Journal of Cell Biology* **137**, 1171-1183.

Gray, L. J., Curtis, R. H. and Jones, J. T. (2001). Characterisation of a collagen gene subfamily from the potato cyst nematode Globodera pallida. *Gene* **263**, 67-75.

Greenberg, C. S., Birckbichler, P. J. and Rice, R. H. (1991). Transglutaminases - multifunctional cross-linking enzymes that stabilize tissues. *FASEB Journal* **5**, 3071-3077.

Griffin, M., Casadio, R. and Bergamini, C. M. (2002). Transglutaminases: Nature's biological glues. *Biochemical Journal* **368**, 377-396.

Gross, E., Sevier, C. S., Vala, A., Kaiser, C. A. and Fass, D. (2002). A new FAD-binding fold and intersubunit disulfide shuttle in the thiol oxidase Erv2p. *Nature Structural Biology* **9**, 61-67.

Gross, E., Sevier, C. S., Heldman, N., Vitu, E., Bentzur, M., Kaiser, C. A., Thorpe, C. and Fass, D. (2006). Generating disulfides enzymatically: Reaction products and electron acceptors of the endoplasmic reticulum thiol oxidase Ero1p. *Proceedings Of The National Academy Of Sciences Of The United States Of America* **103**, 299-304.

Guiliano, D. B., Hong, X. Q., McKerrow, J. H., Blaxter, M. L., Oksov, Y., Liu, J., Ghedin, E. and Lustigman, S. (2004). A gene family of cathepsin L-like proteases of filarial nematodes are associated with larval molting and cuticle and eggshell remodeling. *Molecular and Biochemical Parasitology* **136**, 227-242.

Guo, X. D., Johnson, J. J. and Kramer, J. M. (1991). Embryonic lethality caused by mutations in basement membrane collagen of *C. elegans*. *Nature* **349**, 707-709.

Gupta, M. C., Graham, P. L. and Kramer, J. M. (1997). Characterization of α1(IV) collagen mutations in *Caenorhabditis elegans* and the effects of α 1 and α 2(IV) mutations on type IV collagen distribution. *Journal of Cell Biology* **137**, 1185-1196.

Hanna-Rose, W. and Han, M. (1999). COG-2, a Sox domain protein necessary for establishing a functional vulval-uterine connection in *Caenorhabditis elegans*. *Development* **126**, 169-179.

Hao, L. M., Johnsen, R., Lauter, G., Baillie, D. and Burglin, T. R. (2006). Comprehensive analysis of gene expression patterns of hedgehog-related genes. *BMC Genomics* **7**.

Hao, L. M., Mukherjee, K., Liegeois, S., Baillie, D., Labouesse, M. and Burglin, T. R. (2006b). The hedgehog-related gene *qua-1* is required for molting in *Caenorhabditis elegans*. *Developmental Dynamics* **235**, 1469-1481.

Harding, H. P., Zhang, Y. H., Zeng, H. Q., Novoa, I., Lu, P. D., Calfon, M., Sadri, N., Yun, C., Popko, B., Paules, R. et al. (2003). An integrated stress response regulates amino acid metabolism and resistance to oxidative stress. *Molecular Cell* **11**, 619-633.

Hartigan, N., Garrigue-Antar, L. and Kadler, K. E. (2003). Bone morphogenetic protein-1 (BMP-1) - Identification of the minimal domain structure for procollagen C-proteinase activity. *Journal Of Biological Chemistry* **278**, 18045-18049.

Hashmi, S., Tawe, W. and Lustigman, S. (2001). *Caenorhabditis elegans* and the study of gene function in parasites. *Trends in Parasitology* **17**, 387-393.

Hashmi, S., Zhang, J., Oksov, Y. and Lustigman, S. (2004). The *Caenorhabditis elegans* cathepsin Z-like cysteine protease, Ce-CPZ-1, has a multifunctional role during the worms' development. *Journal Of Biological Chemistry* **279**, 6035-6045.

Hashmi, S., Britton, C., Liu, J., Guiliano, D. B., Oksov, Y. and Lustigman, S. (2002). Cathepsin L is essential for embryogenesis and development of *Caenorhabditis elegans*. *Journal Of Biological Chemistry* **277**, 3477-3486.

Hawdon, J. M., Datu, B. and Crowell, M. (2003). Molecular cloning of a novel multidomain Kunitz-type proteinase inhibitor from the hookworm *Ancylostoma caninum*. *Journal Of Parasitology* **89**, 402-407.

Heim, R., Cubitt, A. B. and Tsien, R. Y. (1995). Improved green fluorescence. *Nature* **373**, 663-664.

Helaakoski, T., Annunen, P., Vuori, K., Macneil, I. A., Pihlajaniemi, T. and Kivirikko, K. I. (1995). Cloning, baculovirus expression, and characterization of a

second mouse prolyl 4-hydroxylase α subunit isoform: formation of an $\alpha_2\beta_2$ tetramer with the protein disulfide isomerase/β subunit. *Proceedings of the National Academy of Sciences of the United States of America* **92**, 4427-4431.

Hill, K. L., Harfe, B. D., Dobbins, C. A. and L'Hernault, S. W. (2000). *dpy-18* encodes an α-subunit of prolyl 4-hydroxylase in *Caenorhabditis elegans*. *Genetics* **155**, 1139-1148.

Hishida, R., Ishihara, T., Kondo, K. and Katsura, I. (1996). *hch-1*, a gene required for normal hatching and normal migration of a neuroblast in *C. elegans*, encodes a protein related to TOLLOID and BMP-1. *EMBO Journal* **15**, 4111-4122.

Hofhaus, G., Lee, J. E., Tews, I., Rosenberg, B. and Lisowsky, T. (2003). The N-terminal cysteine pair of yeast sulfhydryl oxidase Erv1p is essential for *in vivo* activity and interacts with the primary redox centre. *European Journal Of Biochemistry* **270**, 1528-1535.

Holmgren, A. (1989). Thioredoxin And Glutaredoxin Systems. *Journal Of Biological Chemistry* **264**, 13963-13966.

Hoober, K. L., Joneja, B., White, H. B. and Thorpe, C. (1996). A sulfhydryl oxidase from chicken egg white. *Journal Of Biological Chemistry* **271**, 30510-30516.

Hoober, K. L., Sheasley, S. L., Gilbert, H. F. and Thorpe, C. (1999). Sulfhydryl oxidase from egg white - A facile catalyst for disulfide bond formation in proteins and peptides. *Journal Of Biological Chemistry* **274**, 22147-22150.

Hoober, K. L., Glynn, N. M., Burnside, J., Coppock, D. L. and Thorpe, C. (1999b). Homology between egg white sulfhydryl oxidase and quiescin Q6 defines a new class of flavin-linked sulfhydryl oxidases. *Journal Of Biological Chemistry* **274**, 31759-31762.

Issa, Z., Grant, W. N., Stasiuk, S. and Shoemaker, C. B. (2005). Development of methods for RNA interference in the sheep gastrointestinal parasite, *Trichostrongylus colubriformis*. *International Journal For Parasitology* **35**, 935-940.

Jackson, M. J., Pye, D. and Palomero, J. (2007). The production of reactive oxygen and nitrogen species by skeletal muscle. *Journal Of Applied Physiology* **102**, 1664-1670.

Janolino, V. G. and Swaisgood, H. E. (1975). Isolation and characterization of sulfhydryl oxidase from bovine milk. *Journal Of Biological Chemistry* **250**, 2532-2538.

Jenkins, C. L., Bretscher, L. E., Guzei, I. A. and Raines, R. T. (2003). Effect of 3-hydroxyproline residues on collagen stability. *Journal Of The American Chemical Society* **125**, 6422-6427.

Jiang, M., Ryu, J., Kiraly, M., Duke, K., Reinke, V. and Kim, S. K. (2001). Genome-wide analysis of developmental and sex-regulated gene expression profiles in *Caenorhabditis elegans*. *Proceedings Of The National Academy Of Sciences Of The United States Of America* **98**, 218-223.

John, D. C. A., Grant, M. E. and Bulleid, N. J. (1993). Cell-free synthesis and assembly of prolyl 4-hydroxylase: the role of the β-subunit (PDI) in preventing misfolding and aggregation of the α-subunit. *EMBO Journal* **12**, 1587-1595.

Johnston, W. L., Krizus, A. and Dennis, J. W. (2006). The eggshell is required for meiotic fidelity, polar-body extrusion and polarization of the *C. elegans* embryo. *BMC Biology* **4**.

Johnstone, I. L. (2000). Cuticle collagen genes: expression in *Caenorhabditis elegans*. *Trends in Genetics* **16**, 21-27.

Johnstone, I. L. and Barry, J. D. (1996). Temporal reiteration of a precise gene expression pattern during nematode development. *EMBO Journal* **15**, 3633-3639.

Johnstone, I. L., Shafi, Y., Majeed, A. and Barry, J. D. (1996b). Cuticular collagen genes from the parasitic nematode *Ostertagia circumcincta*. *Molecular and Biochemical Parasitology* **80**, 103-112.

Jospin, M., Jacquemond, V., Mariol, M. C., Segalat, L. and Allard, B. (2002). The L-type voltage-dependent Ca2+ channel EGL-19 controls body wall muscle,function in *Caenorhabditis elegans*. *Journal Of Cell Biology* **159**, 337-347.

Kalivas, J. (1999). Is ivermectin safe for humans? *International Journal Of Dermatology* **38**, 235-236.

Kamath, R. S., Martinez-Campos, M., Zipperlen, P., Fraser, A. G. and Ahringer, J. (2000). Effectiveness of specific RNA-mediated interference through ingested double-stranded RNA in *Caenorhabditis elegans*. *Genome Biology* **2**, 1-10.

Kamath, R. S., Fraser, A. G., Dong, Y., Poulin, G., Durbin, R., Gotta, M., Kanapin, A., Le Bot, N., Moreno, S., Sohrmann, M. et al. (2003). Systematic functional analysis of the *Caenorhabditis elegans* genome using RNAi. *Nature* **421**, 231-237.

Kampkotter, A., Volkmann, T. E., de Castro, S. H., Leiers, B., Klotz, L. O., Johnson, T. E., Link, C. D. and Henkle-Duhrsen, K. (2003). Functional analysis of the glutathione S-transferase 3 from *Onchocerca volvulus* (*Ov*-GST-3): A parasite GST confers increased resistance to oxidative stress in *Caenorhabditis elegans*. *Journal Of Molecular Biology* **325**, 25-37.

Khoshnoodi, J., Cartailler, J. P., Alvares, K., Veis, A. and Hudson, B. G. (2006). Molecular recognition in the assembly of collagens: Terminal noncollagenous domains are key recognition modules in the formation of triple helical protomers. *Journal Of Biological Chemistry* **281**, 38117-38121.

Kim, S. K., Lund, J., Kiraly, M., Duke, K., Jiang, M., Stuart, J. M., Eizinger, A., Wylie, B. N. and Davidson, G. S. (2001). A gene expression map for *Caenorhabditis elegans*. *Science* **293**, 2087-2092.

Kingston, B. I. (1991). Nematode collagen genes. *Parasitology Today* **7**, 11-15.

Kingston, I. B., Wainwright, S. M. and Cooper, D. (1989). Comparison of collagen gene sequences in *Ascaris suum* and *Caenorhabditis elegans*. *Molecular and Biochemical Parasitology* **37**, 137-146.

Kinoshita, H., Sakiyama, H., Tokunaga, K., Imajohohmi, S., Hamada, Y., Isono, K. and Sakiyama, S. (1989). Complete Primary Structure Of A Calcium-Dependent Serine Proteinase Capable Of Degrading Extracellular-Matrix Proteins. *FEBS Letters* **250**, 411-415.

Kivirikko, K. I. and Pihlajaniemi, T. (1998). Collagen hydroxylases and the protein disulfide isomerase subunit of prolyl 4-hydroxylases. *Advances in Enzymology and Related Areas of Molecular Biology* **72**, 325-400.

Kivirikko, K. I. and Myllyharju, J. (1998b). Prolyl 4-hydroxylases and their protein disulfide isomerase subunit. *Matrix Biology* **16**, 357-368.

Kivirikko, K. I., Myllylä, R. and Pihlajaniemi, T. (1992). Hydroxylation of proline and lysine residues in collagens and other animal and plant proteins. *In, Post translational modification of proteins (Harding, J.J. and Crabe, M. J. C., eds)* **CRC Press, Boca Raton**, pp. 1-51.

Knox, D. P., Geldhof, P., Visser, A. and Britton, C. (2007). RNA interference in parasitic nematodes of animals: a reality check? *Trends In Parasitology* **23**, 105-107.

Ko, F. C. F. and Chow, K. L. (2002). A novel thioredoxin-like protein encoded by the *C. elegans dpy-11* gene is required for body and sensory organ morphogenesis. *Development* **129**, 1185-1194.

Koltai, H., Chejanovsky, N., Raccah, B. and Spiegel, Y. (1997). The first isolated collagen gene of the root-knot nematode *Meloidogyne javanica* is developmentally regulated. *Gene* **196**, 191-199.

Kostrouchova, M., Krause, M., Kostrouch, Z. and Rall, J. E. (2001). Nuclear hormone receptor CHR3 is a critical regulator of all four larval molts of the nematode *Caenorhabditis elegans*. *Proceedings of the National Academy of Sciences of the United States of America* **98**, 7360-7365.

Kotze, A. C. and Bagnall, N. H. (2006). RNA interference in *Haemonchus contortus*: Suppression of beta-tubulin gene expression in L3, L4 and adult worms *in vitro*. *Molecular And Biochemical Parasitology* **145**, 101-110.

Kramer, J. M. (1994). Genetic-analysis of extracellular-matrix in *C. elegans*. *Annual Review of Genetics* **28**, 95-116.

Kramer, J. M. (1994b). Structures and functions of collagens in *Caenorhabditis elegans*. *FASEB Journal* **8**, 329-336.

Kramer, J. M. (1997). Extracellular matrix. *In, C. elegans II, (Riddle, D. L., Blumenthal, T., Meyer, B. J., Priess, J. R., eds)* **Cold Spring Harbour Laboratory Press, Cold Spring Harbour, NY**, pp. 471-500.

Kramer, J. M. and Johnson, J. J. (1993). Analysis of mutations in the s*qt-1* and *rol-6* collagen genes of *Caenorhabditis elegans*. *Genetics* **135**, 1035-1045.

Kramer, J. M., Cox, G. N. and Hirsh, D. (1985). Expression of the *Caenorhabditis elegans* collagen genes *col-1* and *col-2* is developmentally regulated. *Journal of Biological Chemistry* **260**, 1945-1951.

Krause, M. (1995). *Caenorhabditis elegans*: modern biological analysis of an organism. *Methods in Cell Biology* **Vol 48**, 483–512.

Kress, H., Jarrin, A., Thuroff, E., Saunders, R., Weise, C., Schmidt am Busch, M., Knapp, E. W., Wedde, M. and Vilcinskas, A. (2004). A Kunitz type protease inhibitor related protein is synthesized in *Drosophila* prepupal salivary glands and released into the moulting fluid during pupation. *Insect Biochemistry And Molecular Biology* **34**, 855-869.

Kurzchalia, T. V. and Ward, S. (2003). Why do worms need cholesterol? *Nature Cell Biology* **5**, 684-688.

Kwa, M. S. G., Veenstra, J. G., Vandijk, M. and Roos, M. H. (1995). β-tubulin genes from the parasitic nematode *Haemonchus contortus* modulate drug resistance in *Caenorhabditis elegans*. *Journal of Molecular Biology* **246**, 500-510.

Lam, G. T., Jiang, C. A. and Thummel, C. S. (1997). Coordination of larval and prepupal gene expression by the DHR3 orphan receptor during *Drosophila* metamorphosis. *Development* **124**, 1757-1769.

Lamberg, A., Helaakoski, T., Myllyharju, J., Peltonen, S., Notbohm, H., Pihlajaniemi, T. and Kivirikko, K. I. (1996). Characterization of human type III collagen expressed in a baculovirus system. Production of a protein with a stable triple helix requires coexpression with the two types of recombinant prolyl 4-hydroxylase subunit. *Journal of Biological Chemistry* **271**, 11988- 11995.

Larsen, P. L. (1993). Aging and resistance to oxidative damage in *Caenorhabditis elegans*. *Proceedings Of The National Academy Of Sciences Of The United States Of America* **90**, 8905-8909.

Lassandro, F., Sebastiano, M., Zei, F. and Bazzicalupo, P. (1994). The role of dityrosine formation in the cross-linking of *cut-2*, the product of a second cuticlin gene of *Caenorhabditis elegans*. *Molecular and Biochemical Parasitology* **65**, 147-159.

Leathwick, D. M., Pomroy, W. E. and Heath, A. C. G. (2001). Anthelmintic resistance in New Zealand. *New Zealand Veterinary Journal* **49**, 227-235.

Lee, J. E., Hofhaus, G. and Lisowsky, T. (2000). Erv1p from *Saccharomyces cerevisiae* is a FAD-linked sulfhydryl oxidase. *Febs Letters* **477**, 62-66.

Lee, K. N., Arnold, S. A., Birckbichler, P. J., Patterson, M. K., Fraij, B. M., Takeuchi, Y. and Carter, H. A. (1993). Site-directed mutagenesis of human tissue transglutaminase - Cys-277 is essential for transglutaminase activity but not for Gtpase activity. *Biochimica Et Biophysica Acta* **1202**, 1-6.

Lee, R. Y. N., Lobel, L., Hengartner, M., Horvitz, H. R. and Avery, L. (1997). Mutations in the alpha 1 subunit of an L-type voltage-activated Ca2+ channel cause myotonia in *Caenorhabditis elegans*. *Embo Journal* **16**, 6066-6076.

Lee, S. S., Lee, R. Y. N., Fraser, A. G., Kamath, R. S., Ahringer, J. and Ruvkun, G. (2003). A systematic RNAi screen identifies a critical role for mitochondria in *C. elegans* longevity. *Nature Genetics* **33**, 40-48.

Levy, A. D., Yang, J. and Kramer, J. M. (1993). Molecular and genetic analyses of the *Caenorhabditis elegans dpy-2* and *dpy-10* collagen genes: a variety of molecular alterations affect organismal morphology. *Molecular Biology of the Cell* **4**, 803-817.

Li, S. W., Sieron, A. L., Fertala, A., Hojima, Y., Arnold, W. V. and Prockop, D. J. (1996). The C-proteinase that processes procollagens to fibrillar collagens is identical to the protein previously identified as bone morphogenic protein-1. *Proceedings of the National Academy of Sciences of the United States of America* **93**, 5127-5130.

Lipkind, G. M., Zhou, A. and Steiner, D. F. (1998). A model for the structure of the P domains in the subtilisin-like prohormone convertases. *Proceedings Of The National Academy Of Sciences Of The United States Of America* **95**, 7310-7315.

Liu, Z. C., Kirch, S. and Ambros, V. (1995). The *Caenorhabditis elegans* heterochronic gene pathway controls stage-specific transcription of collagen genes. *Development* **121**, 2471-2478.

Lustigman, S. (1993). Molting, enzymes and new targets for chemotherapy of *Onchocerca volvulus*. *Parasitology Today* **9**, 294-297.

Lustigman, S., Brotman, B., Huima, T., Castelhano, A. L., Singh, R. N., Mehta, K. and Prince, A. M. (1995). Transglutaminase-catalyzed reaction is important for molting of *Onchocera volvulus* third-stage larvae. *AntimicrobiaL Agents and Chemotherapy* **39**, 1913-1919.

Maciejowski, J., Ahn, J. H., Cipriani, P. G., Killian, D. J., Chaudhary, A. L., Lee, J. I., Voutev, R., Johnsen, R. C., Baillie, D. L., Gunsalus, K. C. et al. (2005). Autosomal genes of autosomal/X-linked duplicated gene pairs and germ-line proliferation in *Caenorhabditis elegans*. *Genetics* **169**, 1997-2011.

Maeda, I., Kohara, Y., Yamamoto, M. and Sugimoto, A. (2001). Large-scale analysis of gene function in *Caenorhabditis elegans* by high-throughput RNAi. *Current Biology* **11**, 171-176.

Mairet-Coello, G., Tury, A., Fellmann, D., Risold, P. Y. and Griffond, B. (2005). Ontogenesis of the sulfhydryl oxidase QSOX expression in rat brain. *Journal Of Comparative Neurology* **484**, 403-417.

Massey, V. (1994). Activation Of Molecular-Oxygen By Flavins And Flavoproteins. *Journal Of Biological Chemistry* **269**, 22459-22462.

Matsui, M., Oshima, M., Oshima, H., Takaku, K., Maruyama, T., Yodoi, J. and Taketo, M. M. (1996). Early embryonic lethality caused by targeted disruption of the mouse thioredoxin gene. *Developmental Biology* **178**, 179-185.

Matsuki, M., Yamashita, F., Ishida-Yamamoto, A., Yamada, K., Kinoshita, C., Fushiki, S., Ueda, E., Morishima, Y., Tabata, K., Yasuno, H. et al. (1998). Defective stratum corneum and early neonatal death in mice lacking the gene for transglutaminase 1 (keratinocyte transglutaminase). *Proceedings Of The National Academy Of Sciences Of The United States Of America* **95**, 1044-1049.

Matyash, V., Geier, C., Henske, A., Mukherjee, S., Hirsh, D., Thiele, C., Grant, B., Maxfield, F. R. and Kurzchalia, T. V. (2001). Distribution and transport of cholesterol in Caenorhabditis elegans. *Molecular Biology Of The Cell* **12**, 1725-1736.

Mazzorana, M., Cogne, S., Goldschmidt, D. and Aubert-Foucher, E. (2001). Collagenous sequence governs the trimeric assembly of collagen XII. *Journal of Biological Chemistry* **276**, 27989-27998.

McElwee, J. J., Schuster, E., Blanc, E., Thomas, J. H. and Gems, D. (2004). Shared transcriptional signature in *Caenorhabditis elegans* dauer larvae and long-lived *daf-*

2 mutants implicates detoxification system in longevity assurance. *Journal Of Biological Chemistry* **279**, 44533-44543.

McLaughlin, S. H. and Bulleid, N. J. (1998). Molecular recognition in procollagen chain assembly. *Matrix Biology* **16**, 369-377.

McMahon, L., Muriel, J. M., Roberts, B., Quinn, M. and Johnstone, I. L. (2003). Two sets of interacting collagens form functionally distinct sub-structures within the *C. elegans* extracellular matrix. *Molecular Biology of the Cell* **14**, 1366-1378.

Mehta, K., Rao, U. R., Vickery, A. C. and Birckbichler, P. J. (1990). Significance of transglutaminase-catalyzed reactions in growth and development of filarial parasite, *Brugia malayi*. *Biochemical and Biophysical Research Communications* **173**, 1051-1057.

Mehta, K., Rao, U. R., Vickery, A. C. and Fesus, L. (1992). Identification of a novel transglutaminase from the filarial parasite *Brugia malayi* and its role in growth and development. *Molecular and Biochemical Parasitology* **53**, 1-15.

Mei, D., Woo, W. M. and Chisholm, A. D. (2004). The cytoskeleton and epidermal morphogenesis in *C. elegans*. *Experimental Cell Research* **301**, 84-90.

Mello, C. and Fire, A. (1995). DNA transformation. *In, Methods in cell biology volume 48, Caenorhabditis elegans: modern biological analysis of an organism (Epstein, H. F. and Shakes, D. C., eds), Academic Press, San Diego*, pp. 451-482.

Mello, C. C., Kramer, J. M., Stinchcomb, D. and Ambros, V. (1991). Efficient gene transfer in *C. elegans*: extrachromosomal maintenance and integration of transforming sequences. *EMBO Journal* **10**, 3959- 3970.

Merris, M., Wadsworth, W. G., Khamrai, U., Bittman, R., Chitwood, D. J. and Lenard, J. (2003). Sterol effects and sites of sterol accumulation in *Caenorhabditis elegans*: developmental requirement for 4 alpha-methyl sterols. *Journal Of Lipid Research* **44**, 172-181.

Merriweather, A., Guenzler, V., Brenner, M. and Unnasch, T. R. (2001). Characterization and expression of enzymatically active recombinant filarial prolyl 4-hydroxylase. *Molecular and Biochemical Parasitology* **116**, 185-197.

Milstone, A. M., Harrison, L. M., Bungiro, R. D., Kuzmic, P. and Cappello, M. (2000). A broad spectrum Kunitz type serine protease inhibitor secreted by the hookworm *Ancylostoma ceylanicum*. *Journal of Biological Chemistry* **275**, 29391-29399.

Mohler, W. A., Simske, J. S., Williams-Masson, E. M., Hardin, J. D. and White, J. G. (1998). Dynamics and ultrastructure of developmental cell fusions in the *Caenorhabditis elegans* hypodermis. *Current Biology* **8**, 1087-1090.

Mohrlen, F., Hutter, H. and Zwilling, R. (2003). The astacin protein family in *Caenorhabditis elegans*. *European Journal Of Biochemistry* **270**, 4909-4920.

Mooijaart, S. P., Brandt, B. W., Baldal, E. A., Pijpe, J., Kuningas, M., Beekman, M., Zwaan, B. J., Slagboom, P. E., Westendorp, R. G. J. and van Heemst, D. (2005). *C. elegans* DAF-12, Nuclear Hormone Receptors and human longevity and disease at old age. **4**, 351.

Murray, L., Geldhof, P., Clark, D., Knox, D. P. and Britton, C. (2007). Expression and purification of an active cysteine protease of *Haemonchus contortus* using *Caenorhabditis elegans*. *International Journal For Parasitology* **37**, 1117-1125.

Myllyharju, J. and Kivirikko, K. I. (2001). Collagens and collagen-related diseases. *Annals of Medicine* **33**, 7-21.

Myllyharju, J. and Kivirikko, K. I. (2004). Collagens, modifying enzymes and their mutations in humans, flies and worms. *Trends in Genetics* **20**, 33-43.

Myllyharju, J., Kukkola, L., Winter, A. D. and Page, A. P. (2002). The exoskeleton collagens in *Caenorhabditis elegans* are modified by prolyl 4-hydroxylase with unique combinations of subunits. *Journal of Biological Chemistry* **277**, 29187-29196.

Nagai, N., Hosokawa, M., Itohara, S., Adachi, E., Matsushita, T., Hokawa, N. and Nagata, K. (2000). Embryonic lethality of molecular chaperone Hsp47 knockout

mice is associated with defects in collagen biosynthesis. *Journal of Cell Biology* **150**, 1499-1505.

Neff, M. W., Robertson, K. R., Wong, A. K., Safra, N., Broman, K. W., Slatkin, M., Mealey, K. L. and Pedersen, N. C. (2004). Breed distribution and history of canine *mdr1-1* Delta, a pharmacogenetic mutation that marks the emergence of breeds from the collie lineage. *Proceedings Of The National Academy Of Sciences Of The United States Of America* **101**, 11725-11730.

Newman, A. P., Inoue, T., Wang, M. and Sternberg, P. W. (2000). The *Caenorhabditis elegans* heterochronic gene *lin-29* coordinates the vulval-uterine-epidermal connections. **10**, 1479.

Nguyen, C. Q., Hall, D. H., Yang, Y. and Fitch, D. H. A. (1999). Morphogenesis of the *Caenorhabditis elegans* male tail tip. *Developmental Biology* **207**, 86-106.

Nishiwaki, K. and Miwa, J. (1998). Mutations in genes encoding extracellular matrix proteins suppress the *emb-5* gastrulation defect in *Caenorhabditis elegans*. *Molecular And General Genetics* **259**, 2-12.

Norman, K. R. and Moerman, D. G. (2000). The *let-268* locus of *Caenorhabditis elegans* encodes a procollagen lysyl hydroxylase that is essential for type IV collagen secretion. *Developmental Biology* **227**, 690-705.

Novelli, J., Ahmed, S. and Hodgkin, J. (2004). Gene interactions in *Caenorhabditis elegans* define DPY-31 as a candidate procollagen C-proteinase and SQT-3/ROL-4 as its predicted major target. *Genetics* **168**, 1259-1273.

Novelli, J., Page, A. P. and Hodgkin, J. (2006). The C terminus of collagen SQT-3 has complex and essential functions in nematode collagen assembly. *Genetics* **172**, 2253-2267.

Nyström, J., Shen, Z., Aili, M., Flemming, A. J., Leroi, A. and Tuck, S. (2002). Increased or decreased levels of *Caenorhabditis elegans lon-3*, a gene encoding a collagen, cause reciprocal changes in body length. *Genetics* **161**, 83-97.

Ostrowski, M. C. and Kistler, W. S. (1980). Properties Of A Flavoprotein Sulfhydryl Oxidase From Rat Seminal-Vesicle Secretion. *Biochemistry* **19**, 2639-2645.

Ozerol, N. H. and Silverma.Ph. (1972). Exsheathment phenomenon in infective-stage larvae of *Haemonchus contortus*. *Journal Of Parasitology* **58**, 34-&.

Page, A. P. (1997). Cyclophilin and protein disulphide isomerase genes are co-transcribed in a functionally related manner in *Caenorhabditis elegans*. *DNA and Cell Biology* **16**, 1335-1343.

Page, A. P. and Winter, A. D. (2003). Enzymes involved in the biogenesis of the nematode cuticle. In *Advances In Parasitology*, vol. **53**, pp. 85-148.

Page, A. P., MacNiven, K. and Hengartner, M. O. (1996). Cloning and biochemical characterization of the cyclophilin homologues from the free-living nematode *Caenorhabditis elegans*. *Biochemical Journal* **317**, 179-185.

Page, A. P., McCormack, G. and Birnie, A. J. (2006). Biosynthesis and enzymology of the *Caenorhabditis elegans* cuticle: Identification and characterization of a novel serine protease inhibitor. *International Journal For Parasitology* **36**, 681-689.

Pan, T. L., Groger, H., Schmid, V. and Spring, J. (1998). A toxin homology domain in an astacin-like metalloproteinase of the jellyfish Podocoryne carnea with a dual role in digestion and development. *Development Genes And Evolution* **208**, 259-266.

Parise, G. and Bazzicalupo, P. (1997). Assembly of nematode cuticle: role of hydrophobic interactions in *cut-2* cross-linking. *Biochimica et Biophysica Acta-Protein Structure and Molecular Enzymology* **1337**, 295-301.

Parkinson, J., Mitreva, M., Whitton, C., Thomson, M., Daub, J., Martin, J., Schmid, R., Hall, N., Barrell, B., Waterston, R. H. et al. (2004). A transcriptomic analysis of the phylum Nematoda. *Nature Genetics* **36**, 1259-1267.

Pennington, M. W., Lanigan, M. D., Kalman, K., Mahnir, V. M., Rauer, H., McVaugh, C. T., Behm, D., Donaldson, D., Chandy, K. G., Kem, W. R. et al.

(1999). Role of disulfide bonds in the structure and potassium channel blocking activity of ShK toxin. *Biochemistry* **38**, 14549-14558.

Peters, K., McDowall, J. and Rose, A. M. (1991). Mutations in the *bli-4* (I) locus of *Caenorhabditis elegans* disrupt both adult cuticle and early larval development. *Genetics* **129**, 95-102.

Pfleider.G, Zwilling, R. and Sonnebor.Hh. (1967). Zur Evolution Der Endopeptidasen.3. Eine Protease Vom Molekulargewicht 11000 Und Eine Trypsinahnliche Fraktion Aud Astacus Fluviatilis Fabr. *Hoppe-Seylers Zeitschrift Fur Physiologische Chemie* **348**, 13&19.

Piekny, A. J. and Mains, P. E. (2003). Squeezing an Egg into a Worm: *C. elegans* Embryonic Morphogenesis. **3**, 1370.

Piekny, A. J., Johnson, J. L. F., Cham, G. D. and Mains, P. E. (2003b). The *Caenorhabditis elegans* nonmuscle myosin genes *nmy-1* and *nmy-2* function as redundant components of the let-502/Rho-binding kinase and mel-11/myosin phosphatase pathway during embryonic morphogenesis. *Development* **130**, 5695-5704.

Podbilewicz, B. and White, J. G. (1994). Cell fusions in the developing epithelia of *C. elegans*. *Developmental Biology* **161**, 408-424.

Poole, C. B., Jin, J. M. and McReynolds, L. A. (2003). Cloning and biochemical characterization of blisterase, a subtilisin-like convertase from the filarial parasite, *Onchocerca volvulus*. *Journal Of Biological Chemistry* **278**, 36183-36190.

Pothof, J., van Haaften, G., Thijssen, K., Kamath, R. S., Fraser, A. G., Ahringer, J., Plasterk, R. H. A. and Tijsterman, M. (2003). Identification of genes that protect the *C. elegans* genome against mutations by genome-wide RNAi. *Genes & Development* **17**, 443-448.

Priess, J. R. and Hirsh, D. I. (1986). *Caenorhabditis elegans* morphogenesis: the role of the cytoskeleton in elongation of the embryo. *Developmental Biology* **117**, 156-173.

Prockop, D. J., Sieron, A. L. and Li, S. W. (1998). Procollagen N-proteinase and procollagen C-proteinase. Two unusual metalloproteinases that are essential for procollagen processing probably have important roles in development and cell signaling. *Matrix Biology* **16**, 399-408.

Radom, J., Colin, D., Thiebault, F., Dognin-Bergeret, M., Mairet-Coello, G., Esnard-Feve, A., Fellmann, D. and Jouvenot, M. (2006). Identification and expression of a new splicing variant of FAD-sulfhydryl oxidase in adult rat brain. *Biochimica Et Biophysica Acta-Gene Structure And Expression* **1759**, 225-233.

Raje, S. and Thorpe, C. (2003). Inter-domain redox communication in flavoenzymes of the quiescin/sulfhydryl oxidase family: Role of a thioredoxin domain in disulfide bond formation. *Biochemistry* **42**, 4560-4568.

Rao, U. R., Mehta, K., Subrahmanyam, D. and Vickery, A. C. (1991). *Brugia malayi* and *Acanthocheilonema viteae*: antifilarial activity of transglutaminase inhibitors *in vitro*. *Antimicrobial Agents and Chemotherapy* **35**, 2219-2224.

Rawlings, N. D. and Barrett, A. J. (1995). Evolutionary families of metallopeptidases. In *Proteolytic Enzymes: Aspartic And Metallo Peptidases*, vol. 248, pp. 183-228.

Redmond, D. L., Clucas, C., Johnstone, I. L. and Knox, D. P. (2001). Expression of *Haemonchus contortus* pepsinogen in *Caenorhabditis elegans*. *Molecular and Biochemical Parasitology* **112**, 125-131.

Richer, J. K., Hunt, W. G., Sakanari, J. A. and Grieve, R. B. (1993). *Dirofilaria immitis* - effect of fluoromethyl ketone cysteine protease inhibitors on the 3rd-stage to 4th-stage moult. *Experimental Parasitology* **76**, 221-231.

Rogalski, T. M. and Riddle, D. L. (1988). A *Caenorhabditis elegans* RNA Polymerase-II gene, *ama-1*-IV, and nearby essential genes. *Genetics* **118**, 61-74.

Sakura, S. and Fujimoto, D. (1984). Absorption and fluorescence study of tyrosine-derived crosslinking amino-acids from collagen. *Photochemistry and Photobiology* **40**, 731-734.

Sambrook, J., Fritsch, E. F. and Maniatis, T. (1989). Molecular cloning: a laboratory manual. **Cold Spring Harbour Laboratory Press, Cold Spring Harbour, NY**.

Sapio, M. R., Hilliard, M. A., Cermola, M., Favre, R. and Bazzicalupo, P. (2005). The Zona Pellucida domain containing proteins, CUT-1, CUT-3 and CUT-5, play essential roles in the development of the larval alae in *Caenorhabditis elegans*. *Developmental Biology* **282**, 231-245.

Savage, C., Das, P., Finelli, A. L., Townsend, S. R., Sun, C. Y., Baird, S. E. and Padgett, R. W. (1996). *Caenorhabditis elegans* genes *sma2, sma-3,* and *sma-4* define a conserved family of transforming growth factor beta pathway components. *Proceedings Of The National Academy Of Sciences Of The United States Of America* **93**, 790-794.

Savage, D. (2005). TGF-ß Signaling. [http://www.wormbook.org/chapters/www_tgfbsignal/tgfbsignal.html].

Sciacca, J., Forbes, W. M., Ashton, F. T., Lombardini, E., Gamble, H. R. and Schad, G. A. (2002). Response to carbon dioxide by the infective larvae of three species of parasitic nematodes. *Parasitology International* **51**, 53-62.

Scott, A. L., Yenbutr, P., Eisinger, S. W. and Raghavan, N. (1995). Molecular cloning of the cuticular collagen gene *Bmcol-2* from *Brugia malayi*. *Molecular and Biochemical Parasitology* **70**, 221-225.

Sebastiano, M., Lassandro, F. and Bazzicalupo, P. (1991). *cut-1* a *Caenorhabditis elegans* gene coding for a dauer-specific noncollagenous component of the cuticle. *Developmental Biology* **146**, 519-530.

Selkirk, M. E., Nielsen, L., Kelly, C., Partono, F., Sayers, G. and Maizels, R. M. (1989). Identification, synthesis and immunogenicity of cuticular collagens from the filarial nematodes *Brugia malayi* and *Brugia pahangi*. *Molecular and Biochemical Parasitology* **32**, 229-246.

Sevier, C. S. and Kaiser, C. A. (2006). Disulfide transfer between two conserved cysteine pairs imparts selectivity to protein oxidation by Ero1. *Molecular Biology Of The Cell* **17**, 2256-2266.

Sevier, C. S., Cuozzo, J. W., Vala, A., Aslund, F. and Kaiser, C. A. (2001). A flavoprotein oxidase defines a new endoplasmic reticulum pathway for biosynthetic disulphide bond formation. *Nature Cell Biology* **3**, 874-882.

Shamansky, M. L., Pratt, P., Boisvenue, R. J. and Cox, G. N. (1989). Cuticle collagen genes of *Haemonchus contortus* and *Caenorhabditis elegans* are highly conserved. *Molecular and Biochemical Parasitology* **37**, 73-86.

Shaw, L. M. and Olsen, B. R. (1991). FACIT collagens: diverse molecular bridges in extracellular matrices. *Trends in Biochemical Sciences* **16**, 191-194.

Silhankova, M., Jindra, M. and Asahina, M. (2005). Nuclear receptor NHR-25 is required for cell-shape dynamics during epidermal differentiation in *Caenorhabditis elegans*. *Journal Of Cell Science* **118**, 223-232.

Simmer, F., Moorman, C., van der Linden, A. M., Kuijk, E., van den Berghe, P. V. E., Kamath, R. S., Fraser, A. G., Ahringer, J. and Plasterk, R. H. A. (2003). Genome-wide RNAi of *C. elegans* using the hypersensitive *rrf-3* strain reveals novel gene functions. *Plos Biology* **1**, 77-84.

Singh, N. and Sulston, J. E. (1978). Some observations on molting in *C. elegans*. *Nematologica* **24**, 63-71.

Singh, R. N. and Mehta, K. (1994). Purification and characterization of a novel transglutaminase from filarial nematode *Brugia malayi*. *European Journal of Biochemistry* **225**, 625-634.

Singh, R. N., Chandrashekar, R. and Mehta, K. (1995). Purification and partial characterization of a transglutaminase from dog filarial parasite, *Dirofilaria immitis*. *International Journal of Biochemistry & Cell Biology* **27**, 1285-1291.

Sluder, A. E., Mathews, S. W., Hough, D., Yin, V. P. and Maina, C. V. (1999). The nuclear receptor superfamily has undergone extensive proliferation and diversification in nematodes. *Genome Research* **9**, 103-120.

Smith, K. F., Nolan, K. F., Reid, K. B. M. and Perkins, S. J. (1991). Neutron and X-Ray-scattering studies on the human-complement protein properdin provide an analysis of the thrombospondin repeat. *Biochemistry* **30**, 8000-8008.

Soete, G., Betist, M. C. and Korswagen, H. C. (2007). Regulation of *Caenorhabditis elegans* body size and male tail development by the novel gene *lon-8*. *BMC Developmental Biology* **7**, 1-13.

Sonnichsen, B., Koski, L. B., Walsh, A., Marschall, P., Neumann, B., Brehm, M., Alleaume, A. M., Artelt, J., Bettencourt, P., Cassin, E. et al. (2005). Full-genome RNAi profiling of early embryogenesis in *Caenorhabditis elegans*. *Nature* **434**, 462-469.

Soto, M. C., Qadota, H., Kasuya, K., Inoue, M., Tsuboi, D., Mello, C. C. and Kaibuchi, K. (2002). The GEX-2 and GEX-3 proteins are required for tissue morphogenesis and cell migrations in *C. elegans*. *Genes and Development* **16**, 620-632.

Standley, S., Roche, K. W., McCallum, J., Sans, N. and Wenthold, R. J. (2000). PDZ domain suppression of an ER retention signal in NMDA receptor NR1 splice variants. *Neuron* **28**, 887-898.

Stoscheck, C. M. (1990). Quantitation Of Protein. *Methods In Enzymology* **182**, 50-68.

Studier, F. W. (2005). Protein production by auto-induction in high-density shaking cultures. *Protein Expression And Purification* **41**, 207-234.

Sulston, J. and Hodgkin, J. (1988). Methods. *"The Nematode Caenorhabditis elegans." Wood WB and the Community of C. elegans Researchers (eds), Cold Spring Harbor Laboratory.*, 587-606.

Sulston, J. E. and Horvitz, H. R. (1977). Post-embryonic cell lineages of the nematode *Caenorhabditis elegans*. *Developmental Biology* **56**, 110-156.

Sulston, J. E., Schierenberg, E., White, J. G. and Thomson, J. N. (1983). The embryonic cell lineage of the nematode *Caenorhabditis elegans*. *Developmental Biology* **100**, 64-119.

Sutherlin, M. E. and Emmons, S. W. (1994). Selective lineage specification by *mab-19* during *Caenorhabditis elegans* male peripheral sense organ development. *Genetics* **138**, 675-688.

Suzuki, M., Sagoh, N., Iwasaki, H., Inoue, H. and Takahashi, K. (2004). Metalloproteases with EGF, CUB, and thrombospondin-1 domains function in molting of Caenorhabditis elegans. *Biological Chemistry* **385**, 565-568.

Suzuki, Y., Morris, G. A., Han, M. and Wood, W. B. (2002). A cuticle collagen encoded by the *lon-3* gene may be a target of TGF-beta signaling in determining *Caenorhabditis elegans* body shape. *Genetics* **162**, 1631-1639.

Swan, K. A., Curtis, D. E., McKusick, K. B., Voinov, A. V., Mapa, F. A. and Cancilla, M. R. (2002). High-throughput gene mapping in *Caenorhabditis elegans*. *Genome Research* **12**, 1100-1105.

Tabara, H., Grishok, A. and Mello, C. C. (1998). RNAi in *C. elegans*: soaking in the genome sequence. *Science* **282**, 430-431.

Takahara, K., Lyons, G. E. and Greenspan, D. S. (1994). Bone morphogenetic protein-1 and a mammalian tolloid homolog (mTld) are encoded by alternatively spliced transcripts which are differentially expressed in some tissues. *Journal of Biological Chemistry* **269**, 32572-32578.

Takaluoma, K., Hyry, M., Lantto, J., Sormunen, R., Bank, R. A., Kivirikko, K. I., Myllyharju, J. and Soininen, R. (2007). Tissue-specific changes in the

hydroxylysine content and cross-links of collagens and alterations in fibril morphology in lysyl hydroxylase 1 knock-out mice. *Journal Of Biological Chemistry* **282**, 6588-6596.

Thacker, C. and Rose, A. M. (2000). A look at the *Caenorhabditis elegans* kex2/subtilisin-like proprotein convertase family. *Bioessays* **22**, 545-553.

Thacker, C., Srayko, M. and Rose, A. M. (2000b). Mutational analysis of *bli-4/kpc-4* reveals critical residues required for proprotein convertase function in *C. elegans*. *Gene* **252**, 15-25.

Thacker, C., Peters, K., Srayko, M. and Rose, A. M. (1995). The *bli-4* locus of *Caenorhabditis elegans* encodes structurally distinct kex2/subtilisin-like endoproteases essential for early development and adult morphology. *Genes & Development* **9**, 956-971.

Thein, M. C., McCormack, G., Winter, A. D., Johnstone, I. L., Shoemaker, C. B. and Page, A. P. (2003). The *Caenorhabditis elegans* exoskeleton collagen COL-19: an adult-specific marker for collagen modification, assembly and the analysis of organismal morphology. *Developmental Dynamics* **226**, 523-39.

Thorpe, C. and Coppock, D. L. (2007). Generating disulfides in multicellular organisms: Emerging roles for a new flavoprotein family. *Journal Of Biological Chemistry* **282**, 13929-13933.

Thorpe, C., Hoober, K. L., Raje, S., Glynn, N. M., Burnside, J., Turi, G. K. and Coppock, D. L. (2002). Sulfhydryl oxidases: emerging catalysts of protein disulfide bond formation in eukaryotes. *Archives Of Biochemistry And Biophysics* **405**, 1-12.

Tian, G., Xiang, S., Noiva, R., Lennarz, W. J. and Schindelin, H. (2006). The crystal structure of yeast protein disulfide isomerase suggests cooperativity between its active sites. *Cell* **124**, 61-73.

Timmons, L., Court, D. L. and Fire, A. (2001). Ingestion of bacterially expressed dRNAs can produce specific and potent genetic interference in *Caenorhabditis elegans*. *Gene* **263**, 103-112.

Tsuboi, D., Qadota, H., Kasuya, K., Amano, M. and Kaibuchi, K. (2002). Isolation of the interacting molecules with GEX-3 by a novel functional screening. *Biochemical And Biophysical Research Communications* **292**, 697-701.

Tury, A., Mairet-Coello, G., Poncet, F., Jacquemard, C., Risold, P. Y., Fellmann, D. and Griffond, B. (2004). QSOX sulfhydryl oxidase in rat adenohypophysis: localization and regulation by estrogens. *Journal Of Endocrinology* **183**, 353-363.

Tury, A., Mairet-Coello, G., Esnard-Feve, A., Benayoun, B., Risold, P. Y., Griffond, B. and Fellmann, D. (2006). Cell-specific localization of the sulphydryl oxidase QSOX in rat peripheral tissues. *Cell And Tissue Research* **323**, 91-103.

Unsold, C., Pappano, W. N., Imamura, Y., Steiglitz, B. M. and Greenspan, D. S. (2002). Biosynthetic processing of the pro-alpha 1(V)(2)pro-alpha 2(V) collagen heterotrimer by bone morphogenetic protein-1 and furin-like proprotein convertases. *Journal Of Biological Chemistry* **277**, 5596-5602.

Vandereycken, W., Engler, J. D., Vanmontagu, M. and Gheysen, G. (1994). Identification and analysis of a cuticular collages-encoding gene from the plant-parasitic nematode *Meloidogyne Incognita*. *Gene* **151**, 237-242.

Veijola, J., Pihlajaniemi, T. and Kivirikko, K. I. (1996). Co-expression of the α subunit of human prolyl 4-hydroxylase with BiP polypeptide in insect cells leads to the formation of soluble and insoluble complexes. Soluble α subunit-BiP complexes have no prolyl 4-hydroxylase activity. *Biochemical Journal* **315**, 613-618.

Veijola, J., Koivunen, P., Annunen, P., Pihlajaniemi, T. and Kivirikko, K. (1994). Cloning, baculovirus expression, and characterization of the α subunit of prolyl 4-hydroxylase from the nematode *Caenorhabditis elegans.* This α subunit forms an active αβ dimer with the human protein disulfide isomerase/β subunit. *Journal of Biological Chemistry* **269**, 26746-26753.

Veijola, J., Annunen, P., Koivunen, P., Page, A. P., Philajaniemi, T. and Kivirikko, K. I. (1996b). Baculovirus expression of two protein disulphide isomerase isoforms from *Caenorhabditis elegans* and characterisation of prolyl 4-hydroxylases containing one of these polypeptides as their β subunit. *Biochemical Journal* **317**, 721-729.

Vogtli, M., Elke, C., Imhof, M. O. and Lezzi, M. (1998). High level transactivation by the ecdysone receptor complex at the core recognition motif. *Nucleic Acids Research* **26**, 2407-2414.

Vuori, K., Pihlajaniemi, T., Myllylä, R. and Kivirikko, K. I. (1992). Site-directed mutagenesis of human protein disulfide isomerase: effect on the assembly, activity and endoplasmic reticulum retention of human prolyl 4-hydroxylase in *Spodoptera frugiperda* insect cells. *EMBO Journal* **11**, 4213-4217.

Vuori, K., Pihlajaniemi, T., Marttila, M. and Kivirikko, K. I. (1992). Characterization of the human prolyl 4-hydroxylase tetramer and its multifunctional protein disulfide isomerase subunit synthesized in a baculovirus expression system. *Proceedings of the National Academy of Sciences of the United States of America* **89**, 7467-7470.

Walmsley, A. R., Batten, M. R., Lad, U. and Bulleid, N. J. (1999). Intracellular retention of procollagen within the endoplasmic reticulum is mediated by prolyl 4-hydroxylase. *Journal of Biological Chemistry* **274**, 14884-14892.

White, J. (1988). The anatomy. *In, The nematode Caenorhabditis elegans (Wood, W. B., ed)* **Cold Spring Harbour Laboratory Press, Cold Spring Harbour, NY**, pp. 81-122.

White, K. P., Hurban, P., Watanabe, T. and Hogness, D. S. (1997). Coordination of *Drosophila* metamorphosis by two ecdysone-induced nuclear receptors. *Science* **276**, 114-117.

Whitehead, N. P., Yeung, E. W. and Allen, D. G. (2006). Muscle damage in *mdx* (dystrophic) mice: Role of calcium and reactive oxygen species. *Clinical And Experimental Pharmacology And Physiology* **33**, 657-662.

Wilson, W. R., Tuan, R. S., Shepley, K. J., Freedman, D. O., Greene, B. M., Awadzi, K. and Unnasch, T. R. (1994). The *Onchocerca volvulus* homolog of the multifunctional polypeptide protein disulfide isomerase. *Molecular and Biochemical Parasitology* **68**, 103-117.

Winter, A. D. and Page, A. P. (2000). Prolyl 4-hydroxylase is an essential procollagen-modifying enzyme required for exoskeleton formation and the maintenance of body shape in the nematode *Caenorhabditis elegans*. *Molecular and Cellular Biology* **20**, 4084-4093.

Winter, A. D., Myllyharju, J. and Page, A. P. (2003). A hypodermally expressed prolyl 4-hydroxylase from the filarial nematode *Brugia malayi* is soluble and active in the absence of protein disulphide isomerase. *Journal of Biological Chemistry* **278**, 2554-62.

Winter, A. D., McCormack, G. and Page, A. P. (2007). Protein disulfide isomerase activity is essential for viability and extracellular matrix formation in the nematode *Caenorhabditis elegans*. *Developmental Biology* **308**, 449-461.

Winter, A. D., Eschenlauer, S. C. P., McCormack, G. and Page, A. P. (2007b). Loss of secretory pathway FK506-binding proteins results in cold-sensitive lethality and associate extracellular matrix defects in the nematode *Caenorhabditis elegans*. *Journal Of Biological Chemistry* **282**, 12813-12821.

Winter, A. D., Keskiaho, K., Kukkola, L., McCormack, G., Felix, M.-A., Myllyharju, J. and Page, A. P. (2007c). Differences in collagen prolyl 4-hydroxylase assembly between two *Caenorhabditis nematode* species despite high amino acid sequence identity of the enzyme subunits. **26**, 382.

Winter, J., Klappa, P., Freedman, R. B., Lilie, H. and Rudolph, R. (2002). Catalytic activity and chaperone function of human protein-disulfide isomerase are required

for the efficient refolding of proinsulin. *Journal Of Biological Chemistry* **277**, 310-317.

Wood. (1988). The nematode *Caenorhabditis elegans*. *Cold Spring Harbor Laboratory Press*, p 509.

Yang, J. and Kramer, J. M. (1994). *In vitro* mutagenesis of *Caenorhabditis elegans* cuticle collagens identifies a potential subtilisin-like protease cleavage site and demonstrates that carboxyl domain disulfide bonding is required for normal function but not assembly. *Molecular and Cellular Biology* **14**, 2722-2730.

Yang, J. and Kramer, J. M. (1999). Proteolytic processing of *Caenorhabditis elegans* SQT-1 cuticle collagen is inhibited in right roller mutants whereas cross-linking is inhibited in left roller mutants. *Journal of Biological Chemistry* **274**, 32744-32749.

Yochem, J., Gu, T. and Han, M. (1998). A new marker for mosaic analysis in *Caenorhabditis elegans* indicates a fusion between hyp6 and hyp7, two major components of the hypodermis. *Genetics* **149**, 1323-1334.

Yochem, J., Tuck, S., Greenwald, I. and Han, M. (1999). A gp330/megalin-related protein is required in the major epidermis of *Caenorhabditis elegans* for completion of molting. *Development* **126**, 597-606.

Zawadzki, J. L., Presidente, P. J. A., Meeusen, E. N. and De Veer, M. J. (2006). RNAi in *Haemonchus contortus*: a potential method for target validation. *Trends In Parasitology* **22**, 495-499.

Zhang, H. and Emmons, S. W. (2002). *Caenorhabditis elegans unc-37/groucho* interacts genetically with components of the transcriptional mediator complex. *Genetics* **160**, 799-803.

Zhang, Z. M. and Henzel, W. J. (2004). Signal peptide prediction based on analysis of experimentally verified cleavage sites. *Protein Science* **13**, 2819-2824.

Zimmerman, C. M. and Padgett, R. W. (2000). Transforming growth factor beta signaling mediators and modulators. *Gene* **249**, 17-30.